Effects of hypothyroidism on pancreatic islet development and tissue insulin signalling pathways in the ovine fetus

Shelley Elizabeth Harris

A thesis submitted to Oxford Brookes University in partial fulfilment of the requirements of the award of Doctor of Philosophy

July 2016

OXFORD BROOKES UNIVERSITY

ABSTRACT

Thyroid hormones are important regulators of fetal growth and maturation, although their mechanism of action and interactions with other hormones are unclear. The overall aim of the project was to elucidate the effects of hypothyroidism on the growth and development of the sheep fetus in late gestation. Specifically, the project investigated the extent to which the changes in fetal growth induced by thyroid hormone deficiency were mediated by changes in pancreatic islet development and insulin signalling in fetal tissues. In nineteen twin-bearing pregnant ewes at 105-110 days of gestation (dGA; term~145dGA) and under general anaesthesia, one fetus was thyroidectomised, while the other was sham-operated. At either 129 or 143dGA, umbilical blood samples and a variety of fetal tissues were collected after euthanasia.

Hypothyroidism *in utero* did not affect fetal bodyweight but impaired skeletal growth and led to disproportionate patterns of organ growth. A 30-40% increase in pancreatic β-cell mass was observed in the thyroid deficient fetuses, compared to sham controls, and this was associated with increased plasma insulin and leptin concentrations. In studies using isolated fetal ovine pancreatic islets, β-cell proliferation *in vitro* was inhibited by T3 in a dose-dependent manner but was stimulated by the highest dose of insulin. Pancreatic β-cell proliferation was inhibited at low, and stimulated at high, leptin concentrations. Perirenal adipose tissue was enlarged in the hypothyroid fetuses due to an increase in the proportion of unilocular adipocytes, characteristic of white adipose tissue. The greater relative unilocular adipocyte mass was caused by hyperplasia in association with upregulation of the insulin signalling pathway. Kidneys of hypothyroid fetuses had no apparent changes in glomerular or tubular structure, but a greater water content may have accounted for the increased kidney mass seen in the thyroid deficient fetuses, compared to sham controls. No changes in insulin signalling or sodium transporter expression were seen in the kidneys of the hypothyroid fetuses.

This research demonstrates that the thyroid hormones are required in the ovine fetus during late gestation for the normal development of the endocrine pancreas, adipose tissue and kidney. Alterations in organ development in response to hypothyroidism may have short and long term consequences for carbohydrate metabolism, obesity and renal function.

ACKNOWLEDGEMENTS

Undergoing the PhD and writing the thesis have largely been positive experiences, and for that I have a lot of people to thank for their invaluable support. I am extremely thankful to Dr Alison Forhead for her continued encouragement and support throughout her supervision. I have become a better scientist and researcher through her guidance, both in and out of the laboratory. Thank you for all of the opportunities and for helping me get to this amazing achievement, needless to say, I could not have done any of this without you and your enthusiasm.

Grateful thanks also go to Dr David Meredith for his encouragement, helpful discussions and constructive advice. A big thank you goes to the technical staff at the Department of Neuroscience, Development and Physiology at the University of Cambridge for all of the animal work and the collection of samples, and to Prof Abby Fowden for her encouragement and helpful critique. I am indebted to Prof Sean Limesand for allowing me to work under his wing at the University of Arizona. It was an experience I will never forget and that goes down to the friendliness and enthusiasm of Sean and his research team. I would also like to thank the support of the Postdoctoral Training Tutors and the staff within the Department of Biological and Medical sciences at Oxford Brookes University for all the help over the duration of my studies, especially Dr Ryan Pink for his help with the molecular biology aspects of the project.

To my close friends, Lucy, Kit, Aelwyn, Leah and Katie, thank you for being there in the beginnings of my scientific journey. It has been so important to have you all in my life when the going gets tough. The support of my family has been invaluable throughout my PhD journey. Thank you to my Mum, Dad and big brother Stuart, for the continued love and support and for never letting me forget that I can achieve my dreams. I love you all and I couldn't have got this far without you. Last, but by no means least, a huge thank you to my partner and best friend, Tom, for his encouragement, love and support throughout the PhD. Thank you listening to me moan about failed results, commuting and funding, and for keeping me sane and happy. This experience would not have been the same without you by my side.

CONTRIBUTIONS TO THE THESIS

Work presented in this thesis was carried out at Oxford Brookes University between September 2013 and September 2016. The thesis, and publications and presentations arising, represent my own work with the following contributions:

With the exception of Chapter 4, all animal husbandry, surgical and post mortem procedures (Section 2.1) and all processing steps for tissue collection and wax embedding (Section 2.3.1), were conducted by staff within the Department of Physiology, Development and Neuroscience at the University of Cambridge, before experimental work began at Oxford Brookes University.

Analysis of plasma concentrations of leptin, IGF-I and IGF-II (Sections 2.2.4 and 2.2.5) were carried out by Dr Dominique Blache at the School of Animal Biology, University of Western Australia.

In Chapter 4, animal husbandry and surgical procedures (Sections 4.2.1 and 4.2.2) were carried out by Prof Sean Limesand at the Department of Animal Sciences, University of Arizona, Tucson, Arizona, USA. Analysis of glucose stimulated insulin secretion (Section 4.2.5) was carried out in collaboration with Miss Amy Kelly in the Limesand lab.

Wax sectioning, staining and stereological measurements of the fetal kidney in Chapter 6 was carried out by Oxford Brookes University undergraduate student Mona Hasim while under supervision by myself.

TABLE OF CONTENTS

LIST OF FIGURES

LIST OF TABLES

LIST OF EQUATIONS

LIST OF ABBREVIATIONS

ACTH	Adrenocorticotropic hormone
Akt	Protein kinase B
ANOVA	Analysis of variance
AT_1R	Angiotensin II receptor type 1
AT_2R	Angiotensin II receptor type 2
ARX	Aristaless-related homeobox gene
Au	Arbitrary units
BAT	Brown adipose tissue
BCA	Bicinchoninic acid
BrdU	5-bromo-2-deoxyuridine
BSA	Bovine serum albumin
C/EBP	CCAAT/enhancer-binding protein
C_T	Threshold cycle
Cu^{2+}	Copper (II) ion
CV	Coefficient of variation
D1	Type I 5'-deiodinase
D2	Type II 5'-deiodinase
D3	Type III 5-deiodinase
DAB	3,3'-diaminobenzidine
DAPI	4',6-diamidino-2-phenylindole
dGA	Days of gestation

dH_2O	Distilled water
DPX	Distyrene plasticizer xylene
DTT	Dithiothreitol
ECL	Enhanced chemiluminescence
EdU	5-ethynyl-2’-deoxyuride
ELISA	Enzyme-linked immunosorbent assay
ENaC	Epithelial sodium ion channel
FAM	Carboxyfluorescein
FOXA2	Forkhead box A2
FOXO1	Forkhead box O1
GAPDH	Glyceraldehyde 3-phosphate dehydrogenase
GATA4	GATA binding protein 4
GOI	Gene of interest
GLUT2	Glucose transporter 2
GLUT4	Glucose transporter 4
GSIS	Glucose stimulated insulin secretion
H&E	Haematoxylin and eosin
HPT	Hypothalamus-pituitary-thyroid
HRP	Horseradish peroxidase
IGF	Insulin-like growth factor
^{125}I	Iodine-125 isotope
IGFBP	Insulin-like growth factor binding protein
IGF-IR	IGF-I receptor
IgG	Immunoglobulin G
IMS	Industrial methylated spirits
InsR	Insulin receptor
IRS	Insulin receptor substrate
IUGR	Intrauterine growth restriction
KLF	Kruppel-Like factors

KRB	Krebs ringer buffer
MAFA	V-maf avian musculoaponeurotic fibrosarcoma oncogene homolog a
MAFB	V-maf avian musculoaponeurotic fibrosarcoma oncogene homolog b
MAPK	Mitogen-activated protein kinase
MCT8	Monocarboxylate transporter 8
MCT10	Monocarboxylate transporter 10
ML	Multilocular adipocyte
mTOR	Mammalian target of rapamycin
Myf5	Myogenic factor-5
Na^+	Sodium ion
Na^+/K^+ ATPase	Sodium-potassium adenosine triphosphatase
Ngn3	Neurogenin 3
NKX2-2	NK2 homeobox-2
NKX6-1	NK6 homeobox-1
OATPs	Organic anion transporters
PAT	Perirenal adipose tissue
PAX	Paired box gene
PBS	Phosphate buffered saline
PCNA	Proliferating cell nuclear antigen
PDK	Phosphoinositide-dependent kinase
PDX1	Pancreatic duodenal homeobox factor 1
PEPCK	Phosphoenol-pyruvate carboxykinase
PI3K	Phosphatidylinositide 3-kinase
PIP2	Phosphatidylinositol-4,5-bisphosphate
PIP3	Phosphatidylinositol-3,4,5-trisphosphate
PPARγ	Peroxisome proliferator-activated receptor gamma
PPRE	Peroxisome proliferator response element

PRDM16	Positive regulatory domain containing-16
qRT-PCR	Real-time reverse transcription polymerase chain reaction
RAS	Renin-angiotensin system
RIA	Radioimmunoassay
RPL13a	Ribosomal protein L13a
rT3	Reverse T3
RXR	Retinoid X receptor
S6K	S6 kinase
SDS	Sodium dodecyl sulphate
SDS-PAGE	Sodium dodecyl sulphate polyacrylamide gel electrophoresis
SEM	Standard error of the mean
SREBP-1	Sterol regulatory element-binding transcription factor 1
SURS	Systematic uniform random sampling
T3	Triiodothyronine
T4	Thyroxine
T3S	Sulphated T3
T4S	Sulphated T4
TBP	TATA-box binding protein
TBST	Tris buffered saline with Tween-20
TMB	3,3’-5,5’-tetramethylbenzidine
TRα	Thyroid hormone receptor alpha
TRβ	Thyroid hormone receptor beta
TRE	Thyroid hormone-response element
TRH	Thyrotropin-releasing hormone
TSH	Thyroid stimulating hormone
TX	Thyroidectomised
UCP1	Uncoupling protein 1

UL	Unilocular adipocytes
WAT	White adipose tissue
ZFP423	Zinc finger protein-423

PUBLICATIONS AND PRESENTATIONS ARISING FROM THE THESIS

Harris SE, De Blasio MJ, Wooding FBP, Fowden AL, Meredith D and Forhead AJ. (2014). Effect of hypothyroidism on pancreatic β-cell mass and circulating insulin concentration in ovine fetuses. *Fetal and Neonatal Society annual meeting, St. Vincent, Italy*. **Oral communication**.

Harris SE. (2015). Effects of hypothyroidism on pancreatic islet cell development and insulin signalling pathways in the ovine fetus. *Research Student Symposium, Faculty of Health and Life Sciences, Oxford Brookes University*. **Oral communication.**

Harris SE, De Blasio MJ, Wooding FBP, Fowden AL, Meredith D and Forhead AJ. (2015). Effect of hypothyroidism on pancreatic β-cell mass and circulating insulin concentration in the ovine fetus. *Endocrine Abstracts 38*, P433. *Society for Endocrinology BES, Edinburgh, UK.* **Poster presentation, shortlisted for the SfE Junior Poster Prize**.

Harris SE, Kelly A, Davis MA, Anderson M, Forhead AJ and Limesand SD. (2015). Hormonal control of β-cell proliferation in fetal ovine pancreatic islets *in vitro*. *Endocrine Abstracts* 38, P140. *Society for Endocrinology BES, Edinburgh, UK.* **Poster presentation.**

Harris SE. (2016). Hormonal control of β-cell proliferation in fetal ovine pancreatic islets *in vitro*. *Research Student Symposium, Faculty of Health and Life Sciences, Oxford Brookes University*. **Poster presentation.**

Harris SE, De Blasio MJ, Wooding FBP, Fowden AL, Blache D, Meredith D and Forhead AJ. (2016). Hypothyroidism induces hyperplasia of unilocular adipocytes in perirenal adipose tissue of the ovine fetus. *Fetal and Neonatal Society annual meeting, Cambridge, UK*. **Oral communication**.

Harris SE, De Blasio MJ, Wooding FBP, Fowden AL, Blache D, Meredith D and Forhead AJ. (2016). Hypothyroidism induces hyperplasia of unilocular adipocytes in perirenal adipose tissue of the ovine fetus. *Endocrine Abstracts 44*, P235. *Society for Endocrinology BES, Brighton, UK.* **Poster presentation.**

Harris SE, De Blasio MJ, Davis MA, Kelly AC, Wooding FBP, Blache D, Meredith D, Anderson MJ, Fowden AL, Limesand SW, and Forhead AJ. (2016). Developmental

control of pancreatic β-cell proliferation by thyroid hormones, insulin and leptin in the ovine fetus. *Journal of Physiology.* **In Review.**

Harris SE, De Blasio MJ, Wooding FBP, Blache D, Meredith D, Fowden AL, Forhead AJ. (2016). Hypothyroidism induces hyperplasia of unilocular adipocytes in perirenal adipose tissue of the ovine fetus. *Paper in review with co-authors*.

1. INTRODUCTION

1.1 Fetal growth and maturation

Late gestation is a critical period for the control of fetal growth, development and maturation. A multitude of factors regulate fetal growth including maternal nutrition, placental function and the supply of nutrients and oxygen. Changes in the environment *in utero* can lead to permanent changes in the structure of organs, such as the kidney and heart, and in the activity of key metabolic pathways in fetal tissues. In experimental animals, restricting nutrient supply or oxygen availability leads to intrauterine growth restriction (IUGR) and impairments of cardiovascular, metabolic and endocrine function in the short and longer term (Sferruzzi-Perri *et al.*, 2013).

In humans, growth restricted infants have significantly higher rates of morbidity and mortality in the neonatal period compared to those of average size, and are at greater risk of developing diseases such as diabetes, obesity and heart disease in adulthood (Barker *et al.*, 1989; Hales & Barker, 2001). Homeostatic adaptations to perturbations *in utero* are mediated, in part, by hormones produced by the fetus. Hormones have the ability to control the fate of nutrients delivered to the fetus and therefore have an important role in matching nutrient supply to fetal growth and metabolism. During the perinatal period, hormones are also important in the stimulation of maturation processes in the fetus, which are necessary for survival after birth.

The thyroid hormones are responsible for growth and maturation in many fetal organs during late gestation, such as the heart, lungs, brain and muscle (Ansari *et al.*, 2000; Lanham *et al.*, 2011; Chattergoon *et al.*, 2012a). There is limited knowledge however, on the role thyroid hormones on the growth and maturation of organs such as the pancreas, adipose tissue and kidney. Additionally, insulin is a potent growth factor in the fetus and the insulin signalling pathway has been proposed to be an important growth stimulus *in utero*, but their interactions with the thyroid hormones in late gestation are unknown.

1.2 Thyroid hormones

Thyroid hormones, thyroxine (T4) and triiodothyronine (T3), are tyrosine-based lipid-soluble hormones produced by the follicular cells of the thyroid gland. Thyroxine is synthesised entirely in the follicular cells, and is a pro-hormone for active T3. The biological activity of the thyroid hormones is determined primarily by the intracellular concentration of T3 available to bind to its nuclear receptor. This, in turn, depends on a) circulating concentrations of T3 and T4, b) the presence of transporters regulating the cellular uptake of thyroid hormones and c) the activities of the deiodinase enzymes that metabolise thyroid hormones to more or less active substances (Forhead & Fowden, 2014).

1.2.1 The hypothalamic-pituitary-thyroid (HPT) axis

The paraventricular nucleus of the hypothalamus maintains the circulating levels of the thyroid hormones by the production of thyrotropin-releasing hormone (TRH); TRH, in turn, stimulates thyrotrophs in the anterior pituitary gland to produce thyroid stimulating hormone (TSH). Pituitary TSH stimulates the thyroid gland to produce T4 and T3. A large proportion of the T3 in circulation is derived from deiodination of T4 in peripheral organs by the actions of deiodinase enzymes (Senese *et al.*, 2014). In sheep and primates, the HPT undergoes maturation *in utero,* compared to rodents, in which the majority of maturation occurs postnatally (Kapoor *et al.*, 2006).

Pituitary TSH is detectable in the human fetus at 8 to 10 weeks of gestation (where term is 40 weeks) and the circulating concentration remains low until around 18 weeks of gestation when it increases rapidly (Blackburn, 2003a; Kapoor *et al.*, 2006). In sheep fetuses, TSH can be detected from 50 days of gestation (dGA; term ~145dGA) and also increases towards term (Fisher & Polk, 1989). Plasma T4 levels are low at mid-gestation and gradually increase and plateau towards full term (Figure 1.1). Plasma T3 levels, however, remain low until a surge just before birth as the conversion from T4 to T3 increases (Polk *et al.*, 1989; Blackburn, 2003a; Hillman *et al.*, 2012).

1.2.2 Thyroid hormone transport

The active sites of deiodinase and thyroid hormone receptors are intracellular and for thyroid hormone metabolism and action to take place, the hormone must be transported into the cell. Thyroid hormone is transported into the cell by membrane transporters such as monocarboxylate transporters 8 and 10 (MCT8, MCT10), organic anion transporters (OATP) and L-type amino acid transporters (Visser *et al.*, 2008; Loubière *et al.*, 2010). The membrane transporter MCT8 is specific to thyroid hormones, and in MCT8-deficient mice, thyroid hormone levels in the brain are markedly decreased (Trajkovic *et al.*, 2007).

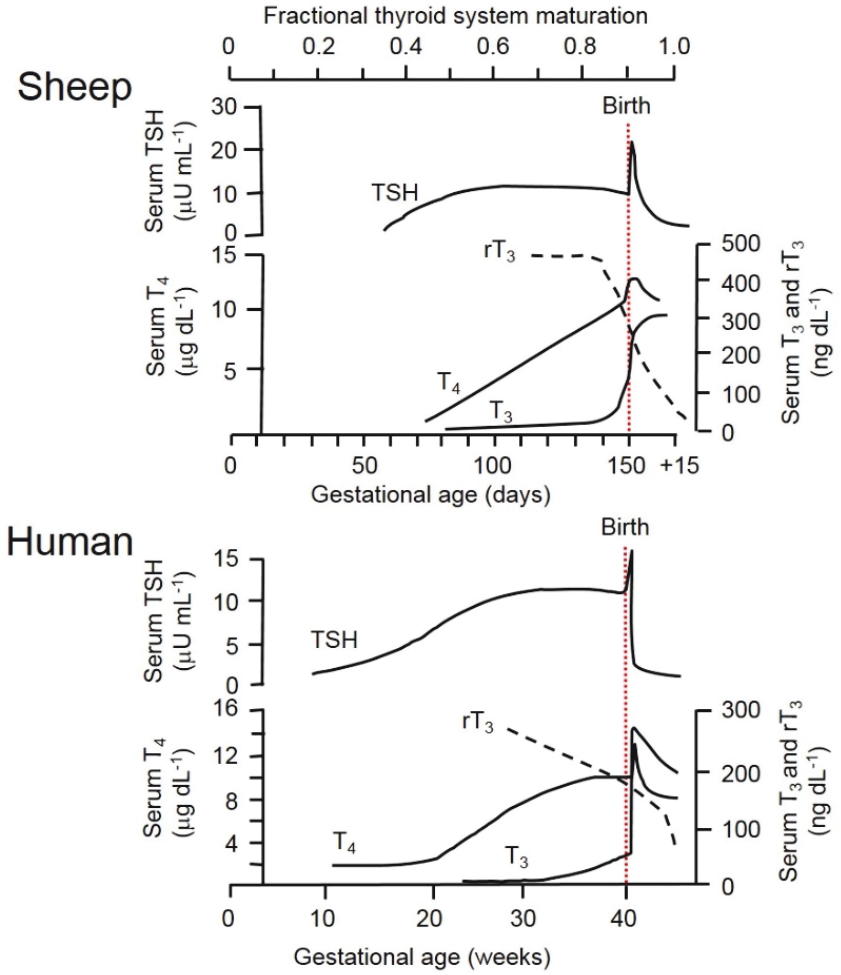

Figure 1.1. Development of thyroid function in the human and sheep fetus. Fetal serum levels of thyroid stimulating hormone (TSH), thyroxine (T4), triiodothyronine (T3) and reverse T3 (rT3) are shown relative to the fraction of thyroid system maturation and show similarities between the species. Adapted from Fisher and Polk. (1989).

Placental transfer of thyroid hormones can contribute to thyroid hormone levels in fetal circulation, depending on species. In humans, cellular uptake of T3 and T4 by the placenta is critical for thyroid hormone action, within the organ itself and for thyroid hormone transport to the fetus (Loubière *et al.*, 2010). In the human placenta, mRNA and protein expression of MCT8 and MCT10 are present from 6 weeks of gestation and increase with gestation from 15 weeks onwards (Loubière *et al.*, 2010). Intrauterine growth restriction of the human fetus is associated with a reduction in MCT8 and MCT10 protein in the placenta, thus compromising thyroid hormone transport to the fetus (Loubière *et al.*, 2010).

Little is known about the developmental expression of thyroid hormone transporters in fetal life. At 30 weeks of gestation, *MCT8* mutation in the human fetus leads to deficiencies in brain maturation, myelination and expression of neuronal proteins (López-Espíndola *et al.*, 2014). It has recently been identified that MCT8 can interact with MCT10 to regulate fetal thyroid hormone availability, as mouse models of genetic knockouts for both transporters have a less severe phenotype than MCT8 knockout alone and have normal serum T4 levels (Müller *et al.*, 2014).

1.2.3 Thyroid hormone metabolism

Deiodinase enzymes are important in the regulation of cellular T3 levels. Once T4 enters the cell, it can be deiodinated by the activities of type I 5'-deiodinase (D1) and type II 5'-deiodinase (D2) into the active form of T3. Inactivation of T4 to reverse T3 (rT3), and of T3 to T2, is mediated by type III 5'-deiodinase (D3), as illustrated by Figure 1.2 (Gereben *et al.*, 2008; Brent, 2012).

In the fetus, the deiodinases regulate thyroid hormone metabolism during development in a tissue specific manner (Gereben *et al.*, 2008). The conversion of T4 to T3 by D1 in the fetal liver is the major source of circulating T3 and D1 is also found present in other tissues, such as the kidney and pituitary (Polk, 1995). The brain and brown adipose tissue primarily express D2, where it is responsible for the generation of local concentrations of T3. The inactivating deiodinase D3 is highly expressed in the uterus and placenta

where it has a key role in regulating placental transfer of thyroid hormones and limiting exposure of the fetus to maternal T3 and T4 (Forhead & Fowden, 2014).

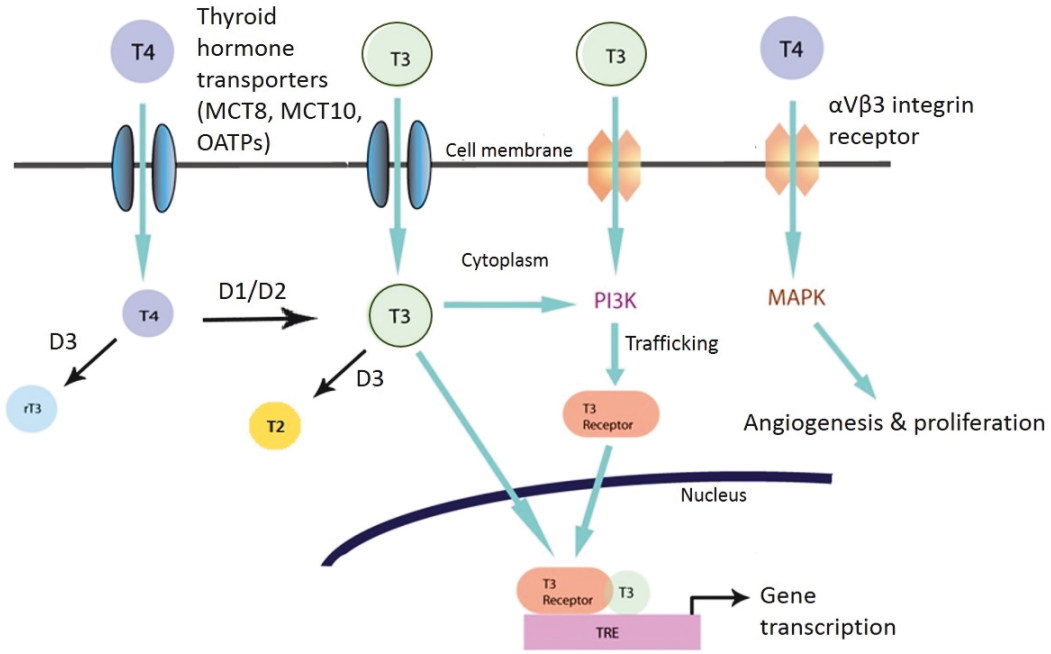

Figure 1.2. Thyroid hormone transport and cellular metabolism. T3 and T4 are transported into the cell cytoplasm. T4 is deiodinated to T3 or rT3 by the deiodinase enzymes. When bound to its receptor, T3 regulates transcription of genes in the nucleus via the thyroid hormone-response element (TRE). Transportation of T3 via the integrin receptor on the cell surface promotes trafficking of the receptor into the nucleus by activation of phosphatidylinositide 3-kinase (PI3K) and T4 activates the mitogen-activated protein kinases (MAPK) pathway.

As well as deiodination, sulphation of the hydroxyl group is another important pathway of metabolism for the thyroid hormones (Figure 1.3), especially in the fetus (Visser, 1994). Sulphation by the enzyme sulphotransferase facilitates the inactivation of T3 and T4 and occurs rapidly in the fetal liver (Visser *et al.*, 1990). Sulphotransferases are widely expressed before birth and have previously been localised in human fetal tissue such as the kidney, small intestine, testis and the lung (Hume & Coughtrie, 1994; Parker *et al.*, 1994; Hume *et al.*, 1996; Richard *et al.*, 2001; Stanley *et al.*, 2005). The levels of expression are equivalent to or higher than that seen in the adult, indicating that they have a significant role in thyroid hormone metabolism before birth (Stanley *et al.*, 2005).

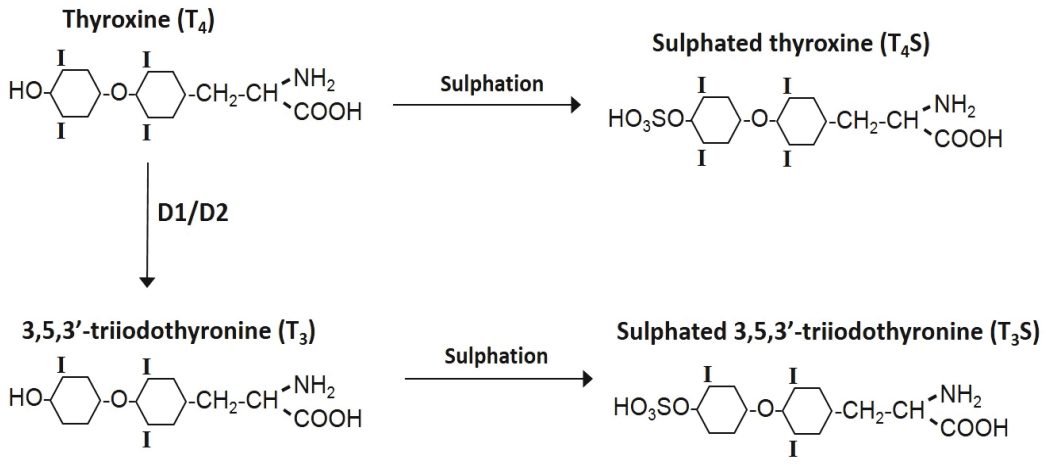

Figure 1.3. The enzymes, sulphotransferases, inactivate T4 and T3 by sulphation of the hydroxyl group present in their molecular structures.

In the sheep fetus, the sulphated forms of T3 (T3S) and T4 (T4S) in circulation peak towards the end of term; 80% of T4 produced by the fetal thyroid is sulphated, suggesting that they are major metabolites during development (Wu *et al.*, 1992; Polk *et al.*, 1994). In comparison, T4S is undetectable in in adult sheep (Wu *et al.*, 1993) Although the sulphated forms of the thyroid hormones are biologically inactive, they are a potential source of active thyroid hormones as desulphation by sulphatase can occur in a variety of tissues, such as the liver and placenta (Kester *et al.*, 2002). The sulphated form of T3 has a longer half-life than the non-sulphated form and is therefore an important source of T3, especially during hypothyroidism. Following thyroidectomy in the sheep fetus, serum concentrations of T4S are decreased, but T3S remain unchanged for at least 2 weeks (Wu *et al.*, 1993).

1.2.4 Thyroid hormone receptors

Triiodothyronine binds to thyroid hormone receptors (TR), which belong to a superfamily of nuclear receptors. There are two receptor genes, TRα and TRβ. Each receptor is also spliced into different isoforms: TRα1-3, of which only TRα1 is able to bind T3 and TRβ1-3 which are all T3 binding (Zhang & Lazar, 2000; Brent, 2012; Chi *et al.*, 2013). The TR isoforms are expressed in a temporal and tissue-specific manner in adults and during development. In adult brain, white adipose tissue and heart atria,

TRα1 is preferentially expressed, whereas TRβ is the dominant form in the liver and heart ventricles (Mullur *et al.*, 2014).

Developmentally, TRα is expressed first in gestation followed by TRβ, in a pattern which is seen across several species including *Xenopus*, chickens, rodents, sheep and humans (Mullur *et al.*, 2014). The different patterns of expression of these receptor isoforms influence thyroid hormone activity. Previous studies have identified that abnormalities in the TR can cause changes in circulating thyroid hormone concentrations. For instance, disruption of TRα2 expression in mice leads to overexpression of the TRα1 subtype and hypothyroidism (Saltó *et al.*, 2001).

The thyroid receptors have the ability to exert genomic and non-genomic actions in the cell. In the genomic action, the receptors act as T3 inducible transcription factors (Cheng *et al.*, 2010; Chi *et al.*, 2013). The TR are ligand-dependent receptors that regulate gene expression by binding to specific thyroid hormone-response elements (TRE; Figure 1.2) present in the regulatory region of target genes (Cao *et al.*, 2005). Efficient binding to DNA occurs with the common partner, the retinoid X receptor (RXR), to form heterodimers and the transcriptional activity of TRs is mediated by various co-repressors and co-activators (Brent, 2012).

Non-genomic actions of thyroid hormones do not involve direct transcriptional regulation by TR. Integrin αv/β3 is a heterodimer plasma membrane protein which acts as a cell surface receptor to mediate the actions of the thyroid hormone, as shown in Figure 1.2 (Bergh *et al.*, 2005). Through the integrin receptor, T3 and T4 stimulate the mitogen-activated protein kinase (MAPK) signalling cascade which initiates cell proliferation and angiogenesis (Cheng *et al.*, 2010). The integrin receptor can also activate phosphatidylinositide 3-kinase (PI3K), which initiates trafficking of intracellular proteins such as TRα from the cytoplasm to the nucleus (Cheng *et al.*, 2010). The activation of MAPK and PI3K suggests that the thyroid hormones have the potential to initiate cross-talk through several cellular signalling pathways. Non-genomic actions of thyroid hormones have only been examined *in vitro* using adult fibroblasts and tumour

cell lines and it is not known if this form of thyroid action is cell-specific or occurs in fetal tissues (Bergh *et al.*, 2005; Lin *et al.*, 2009).

There is limited knowledge on the expression of the thyroid hormone receptors in the fetus. In the liver and brain of fetal sheep, there is a progressive increase in T3 nuclear receptor binding from 80dGA towards term when thyroid hormone receptor binding reaches a plateau over the perinatal period (Polk *et al.*, 1989). In thyroidectomised sheep fetuses at 129dGA, the reduction of thyroid hormones has no effect on receptor binding in either the brain or liver. The same pattern of hepatic expression of TR has been identified in fetal pigs (Duchamp *et al.*, 1994). Compared to the fetal liver, skeletal muscle, however, shows a much higher binding affinity for T3 at 80dGA (term 115dGA), indicating that fetal muscle can potentially respond to thyroid hormones earlier in development (Duchamp *et al.*, 1994). In the fetal rat, TR mRNA is not seen until 14dGA, where term is ~22dGA (Perez-Castillo *et al.*, 1985). In rodent tissues, TR are present before activation of the HPT axis, suggesting that the receptors may be bound and activated by maternal thyroid hormones. There is a progressive increase in receptor mRNA and protein in the heart and liver towards term, whereas expression in the lung and brain is maintained throughout gestation. Thyroid hormone receptor mRNA in all organs examined increases into neonatal life and peaks at postnatal day 6, especially in the neonatal brain (Perez-Castillo *et al.*, 1985). The different expression patterns of TR indicates that there may be organ-specific development of thyroid hormone activity in the fetus (Polk *et al.*, 1989).

1.3 Thyroid hormones and fetal growth

In the fetus, thyroid hormones play a key role in regulating growth and metabolism in a variety of developing organs and physiological systems (Brent, 2000; Brent, 2012). In normal human pregnancy, there are significant associations between cord blood concentrations of T4 and birth weight, head circumference and skin fold thickness (Shields *et al.*, 2011) and in human neonates affected by IUGR, serum concentrations of T3 and T4 are reduced (Kilby *et al.*, 1998). Additionally, deficiency of thyroid hormones *in utero* impairs growth in fetal sheep (Fowden & Silver, 1995). In the sheep fetus,

thyroidectomy has been shown to reduce bodyweight and limb and crown-rump lengths in late gestation compared to intact fetuses (Lanham *et al.*, 2011). The same study also found that the mechanical properties of the bones were also affected, as the trabecular bone of the metatarsals in hypothyroid fetuses were stronger, yet more brittle, compared to sham controls. It was suggested that hypothyroidism delays bone development by impairing bone deposition (Lanham *et al.*, 2011). Similar skeletal abnormalities have been demonstrated in a neonatal mouse model of hypothyroidism (Bassett *et al.*, 2008).

Abnormal growth patterns induced by fetal hypothyroidism may compromise the fetus in its preparation for extrauterine life and thyroid hormones are important not only in the control of overall body growth, but also in tissue-specific development (Forhead & Fowden, 2014). The transporters MCT8 and MCT10, as well as the deiodinases D2 and D3, are expressed in skeletal muscle of both human and rodent fetuses (Visser *et al.*, 2008) and it has previously been established that T3 stimulates muscle growth by increasing the number and diameter of muscle fibres *in utero* (Yu *et al.*, 2000; Lee *et al.*, 2014). Mouse models with genetic deletions of both TRα and TRβ have significantly lower muscle weight associated with decreased fibre number and size (Yu *et al.*, 2000). Thyroidectomy in fetal sheep results in decreased contractile force generated by skeletal muscle (Finkelstein *et al.*, 1991), and the normal development of fast and slow muscle fibre types is impaired by pharmacological hypothyroidism in neonatal rats (Butler-Browne *et al.*, 1984).

Organs such as the heart, kidney and brain are also thyroid hormone sensitive before birth. In the sheep fetus, thyroidectomy results in decreased relative heart and lung mass; this is due to decreased cardiomyocyte number in the fetal heart and hypotrophy associated with smaller air spaces in the fetal lungs (Erenberg *et al.*, 1974; van Tuyl *et al.*, 2004; Chattergoon *et al.*, 2012a). The brain is also significantly reduced in hypothyroid fetal sheep in late gestation, but is relatively spared compared to other organs. Hypothyroid fetal sheep have an upregulation of D2 in the brain indicating that the brain can enhance local T3 production when needed (Polk *et al.*, 1988). In fetal rats born to hypothyroid dams, absolute weights of the kidney and liver are decreased, while

the absolute and relative brain mass is increased (Shibutani *et al.*, 2009). These changes in organ mass are seen to persist in adulthood (Shibutani *et al.*, 2009).

Thyroid hormones are able to influence other endocrine systems involved in fetal development. Hypothyroidism has been shown to change the availability of hormones and growth factors *in utero* including growth hormone and the insulin-like growth factors, also known as the IGFs (Forhead *et al.*, 1998; Johnson *et al.*, 2007; Carey *et al.*, 2008). Thyroidectomy in fetal sheep impairs the normal ontogenic expression of growth hormone receptor and insulin-like growth factor-I (IGF-I) mRNA expression in the liver and skeletal muscle (Forhead *et al.*, 2000; Forhead *et al.*, 2002). Pharmacological hypothyroidism in the neonatal mouse also leads to reductions in circulating and liver mRNA levels of IGF-I compared to controls (Ramos *et al.*, 1998). Additionally, oxygen consumption in hypothyroid sheep fetuses is reduced by 20-45% (Fowden & Silver, 1995), thus indicating fetuses generate less energy by oxidative phosphorylation. The decrease in oxygen consumption is restored to normal levels after administration of T4, indicating a positive correlation between thyroid state and umbilical oxygen uptake.

1.3.1 Thyroid hormones and fetal maturation

Near term, there is also a surge in plasma cortisol concentrations from the fetal adrenal gland, which is responsible for stimulating aspects of fetal maturation, including the prepartum increase in circulating T3 (Hillman *et al.*, 2012). The increase in plasma T3 concentrations near term is due to the influence of rising D1 and D2 activities in peripheral tissues, stimulated by cortisol (Forhead *et al.*, 2006; Chattergoon *et al.*, 2014) and removal of the adrenal gland *in utero* abolishes the prepartum rise in both cortisol and T3 (Forhead *et al.*, 2006). The rise in circulating T3 levels has been shown to be responsible for mediating some of the maturational effects of cortisol near term (Forhead & Fowden, 2014).

The maturational surge in plasma T3 late in gestation coincides with acceleration of alveolar septation, a period of pulmonary remodelling to increase the blood-gas interface (Massaro & Massaro, 2002). This has been demonstrated in fetal mice by administration of glucocorticoids, which causes a rise in circulating T3 and results in early

fetal lung maturation (Ansari *et al.*, 2000). In the hypothyroid mouse neonate, the lungs have altered air spaces with less alveolar septae and reduced surfactant content, indicating that there are impairments in structural and functional maturation (deMello *et al.*, 1994; van Tuyl *et al.*, 2004).

Thyroid hormones are known to be essential in cardiomyocyte maturation as the increase in circulating T3 concentrations towards term promotes a switch from cell proliferation to differentiation (Chattergoon *et al.*, 2012a). In fetal sheep, T3 stimulates up-regulation of cell cycle suppressors and increases the population of differentiated binucleated cells (Chattergoon *et al.*, 2012b). Consequently, thyroidectomy in the fetal sheep leads to a decrease in the proportion of terminally differentiated cardiomyocytes (Segar *et al.*, 2012). In fetal rats and mice, T3 has been shown to be necessary for the upregulation of the cardiac insulin-sensitive glucose transporter type-4 (GLUT4) towards term and for the transition from β- to α-myosin heavy chain expression (Castello *et al.*, 1994; van Tuyl *et al.*, 2004).

Thyroid hormones also have an important role in preparing the fetus for hepatic gluconeogenesis and endogenous glucose production at birth (Forhead & Fowden, 2014). In the liver and kidney of fetal sheep, thyroidectomy suppresses the normal increase in the gluconeogenic enzymes, phosphoenol-pyruvate carboxykinase (PEPCK) and glucose-6-phosphatase (Forhead *et al.*, 2003). Fetal thyroidectomy in sheep has also been shown to abolish the normal rise in hepatic glycogen content, which provides an important source of glucose for metabolism before and after birth (Forhead *et al.*, 2009).

1.3.2 Hypothyroidism in the fetal sheep

No animal model can truly emulate human development *in utero*; however, the sheep has been used extensively in studies of fetal growth and development. The sheep is a precocious species, meaning that its young are well developed in comparison to rodent offspring. Because of this, the sheep fetus has many commonalities with the human fetus. The degree of maturity of the new born lamb suggest that this species may be more dependent on the presence of the thyroid hormones than species which give birth

to less developed young, such as mice (Hopkins & Thorburn, 1972). Studies in fetal sheep have shown that a functional thyroid gland is present from as early as 70dGA which is able to incorporate iodine and produce measurable circulating amounts of the thyroid hormones. This is a similar time frame to thyroid gland development in the human.

The transfer of thyroid hormones from mother to fetus via the placenta varies between human and sheep. The human placenta is permeable to thyroid hormones and a variety of thyroid hormone transporters are expressed throughout development (Loubière *et al.*, 2010). Once the fetus is able to produce its own thyroid hormones (around 12 weeks of gestation), maternal T4 makes only a modest contribution to the circulating pool (Morreale de Escobar *et al.*, 1990). Placental transfer of thyroid hormones becomes particularly important in disorders such as fetal hypothyroidism. Congenital hypothyroidism affects approximately 1 in 3000 human births a year in the UK and can cause severe mental and physical retardation if untreated (LaFranchi, 2011). The most common cause of congenital hypothyroidism is thyroid dysgenesis, where the thyroid gland fails to develop normally (LaFranchi, 2011). The gland may be ectopic and develop away from the normal position, or the gland may be completely absent. Human fetuses with congenital hypothyroidism have reduced cord concentrations of T4 which are 20-50% of normal values (Vulsma *et al.*, 1989), indicating that the fetus can acquire substantial amounts of thyroid hormones when there is a steep gradient in hormone concentrations. Because of placental transfer of thyroid hormones, human neonates with hypothyroidism tend to have little evidence of the condition at birth (Vulsma *et al.*, 1989); however, few studies have examined tissue development in the neonate with congenital hypothyroidism.

The ovine placenta appears to be impermeable to thyroid hormones, at least at 108dGA (Hopkins & Thorburn, 1972), meaning that the transfer of thyroid hormone from mother to fetus is restricted. The ovine fetus is therefore completely dependent on its own thyroid gland for appropriate thyroid hormone secretions during development (Hopkins & Thorburn, 1972).

1.4 Insulin signalling

The hormone insulin is produced by β-cells in the islets of Langerhans in the pancreas. It is an important growth promoting hormone before birth and there is a positive correlation between plasma insulin concentrations *in utero* and growth rates in the sheep fetus in late gestation (115 dGA onwards; Fowden *et al.*, 1989).

The insulin signalling pathway is a key metabolic pathway which involves numerous intracellular proteins, growth factors and transcription factors in a complex, interacting network. The pathway is conserved across a range of species (Rhodes & White, 2002). Downstream targets of the pathway stimulate cell growth and differentiation and also increase the uptake of glucose by stimulating the translocation of GLUT4 from intracellular storage to the cell surface, as illustrated in Figure 1.4 (Saltiel & Kahn, 2001). Serial muscle biopsies in fetal sheep show an increase in insulin signalling proteins when stimulated with a hyperinsulinaemic clamp, thus providing evidence that the insulin pathway is well-developed in the sheep fetus during late gestation (Anderson *et al.*, 2004).

1.4.1 The insulin receptor

The insulin receptor (InsR) belongs to a subfamily of tyrosine kinase receptors. It is a tetrameric protein and is comprised of two α and two β-subunits. The α-subunits are extra-cellular insulin binding sites; the β-units are membrane-spanning with core tyrosine kinase activity, which is essential for insulin action within the cell. When insulin binds to the receptor at an α-subunit, the β-subunit undergoes autophosphorylation and this in turn leads to tyrosine phosphorylation of other protein substrates (Figure 1.4), known as insulin receptor substrates, or IRS (Rhodes & White, 2002).

The IRS proteins play an important role in regulating downstream effects in the insulin signalling cascade and are linked to the PI3K pathway which is responsible for the majority of the metabolic actions of insulin, and the MAPK pathway which regulates gene expression (Taniguchi *et al.*, 2006). Removal of the I*rs2* gene in adult mice induces a diabetic phenotype in which mice have increased insulin resistance and a reduction of

β-cell mass in the pancreas (Withers *et al.*, 1998; Cantley *et al.*, 2007). Deletion of this gene also has an impact on other organs during development, such as the kidney, where *Irs2* knock out causes a reduction in kidney size in fetal mice (Carew *et al.*, 2010).

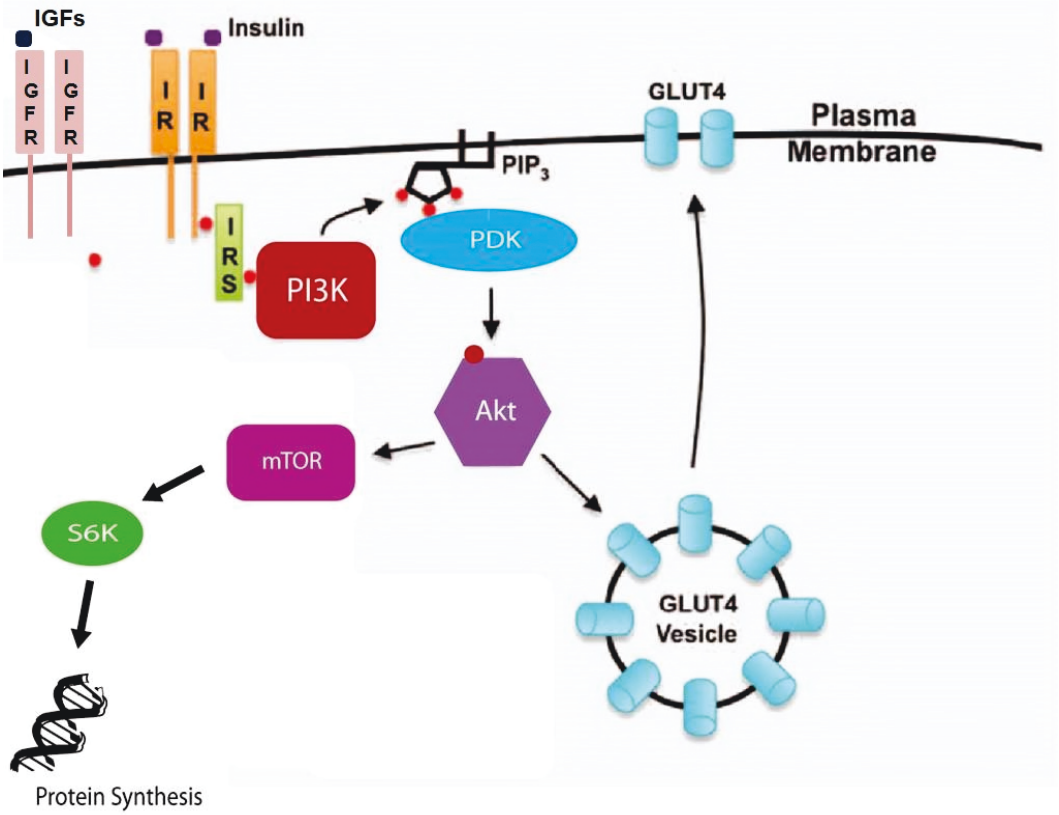

Figure 1.4. A simplified diagram of the insulin signalling pathway. The binding of insulin to its receptor induces autophosphorylation of the receptor β-subunit and insulin receptor substrate (IRS). This leads to the recruitment of PI3K which, in turn, converts PIP2 to PIP3 at the cell membrane. An increase in PIP3 at the membrane activates PDK and Akt to enhance phosphorylation of mTOR and, eventually, S6 kinase. Akt also stimulates the translocation of GLUT4 to the membrane. IGFR: IGF receptor, IR: insulin receptor, PI3K: phosphatidylinositide 3-kinase, PIP3: phosphatidylinositol-3,4,5-trisphosphate, PDK: phosphoinositide-dependent kinase, Akt: protein kinase B, GLUT4: glucose transporter type 4, mTOR: mammalian target of rapamycin, S6K: S6 kinase. Adapted from McCurdy and Klemm (2013).

1.4.2 Downstream proteins

Binding of IRS to the insulin receptor leads to conformational changes that reduce kinase inhibition leading to recruitment of PI3K (Taniguchi *et al.*, 2006). The role of PI3K is to convert phosphatidylinositol-4,5-bisphosphate (PIP2) into phosphatidylinositol-3,4,5-

trisphosphate (PIP3) and to increase the levels of PIP3 at the membrane to stimulate signalling proteins, protein kinase B (Akt) and phosphoinositide-dependent kinase (PDK), as shown in Figure 1.4 (McCurdy & Klemm, 2013). Protein kinase B stimulates the translocation of the glucose transporter, GLUT4, to the plasma membrane. Insulin is able to promote GLUT4 translocation in a dose-dependent manner and translocation is suppressed when the Akt gene is deleted in an adipocyte cell line (Tsuchiya *et al.*, 2014). All eukaryotes express Akt where it exists in 3 different isoforms, Akt1, Akt2 and Akt3, of which only Akt1 and Akt2 are expressed in all tissue types (Brazil *et al.*, 2004). The roles of Akt1 and Akt2 are isoform-specific; isoform-specific knock-out mouse models have revealed that Akt1 regulates cell proliferation and Akt2 is important in glucose and lipid metabolism (Manning & Cantley, 2007).

Activation of PI3K also leads to the phosphorylation of mammalian target of rapamycin (mTOR) which regulates proteins such as S6 kinase (S6K) to promote protein synthesis and growth. The kinase mTOR is the core of two distinct complexes, mTORC1 and mTORC2. Each complex is defined by associated proteins, Raptor in mTORC1 and Rictor and Sin1 in mTORC2 (Liu *et al.*, 2013). It is known that mTORC1 promotes cellular metabolism and is an important regulator of cell growth (Huang & Fingar, 2014), however the role of mTORC2 in the insulin signalling pathway is less well defined.

1.5 Insulin-like growth factors

The insulin-like growth factors, IGF-I and IGF-II, are important in the control of fetal growth, and are ubiquitously expressed in all tissues and circulation in relatively high concentrations before birth (Kawai & Rosen, 2010; Bloomfield *et al.*, 2013). Binding of IGF-I to the cell surface receptor, IGF type 1 receptor (IGF-IR), triggers the activation of intracellular kinases such as PI3K (Figure 1.4) in the same manner as insulin in the same pathway (Burks & White, 2001; Lai *et al.*, 2004).

The expression of IGF-I and IGF-II *in utero* varies with gestational age and nutritional state in a tissue-specific manner (Fowden & Forhead, 2009). In humans and rodent fetuses, tissue expression of IGF-II mRNA is more abundant than IGF-I mRNA in mid

gestation and then decreases towards term (Delhanty & Han, 1993; Fowden, 2003). Serum levels of IGF-II however, are 3-10 fold higher than IGF-I during late gestation in human, sheep and rodents (Fowden, 2003). Abundance of IGF mRNA also differs between fetal sheep tissues, as IGF-I mRNA is highest in abundance in the liver and skeletal muscle and IGF-II mRNA is highly expressed in the lung and kidney (Delhanty & Han, 1993).

Insulin-like growth factor-I is more responsive to stimuli than IGF-II and rises with increasing fetal concentrations of glucose, induced by maternal nutritional state (Fowden & Forhead, 2009). In the fetal sheep, plasma concentrations of IGF-I also rise with increasing oxygen availability and are reduced in hypothyroidism (Mesiano *et al.*, 1987; Iwamoto *et al.*, 1992). Compared to IGF-I, IGF-II gene expression is relatively unresponsive to nutritional stimuli and is posited to be an important regulator of whole body growth before birth. Disruption of IGF-II in mice by gene targeting produces growth restricted offspring (DeChiara *et al.*, 1990). Conversely, the relative weights of the heart, kidney, brain and liver are increased in a transgenic mouse model of IGF-II overexpression (Petrik *et al.*, 1999). Taken together, previous studies suggest that IGF-II acts as a constitutive growth factor for intrauterine growth, while IGF-I regulates fetal growth in relation to the nutrient and oxygen supply.

The activity of the IGFs is regulated by their binding proteins (IGFBP), which can inhibit or potentiate depending on subtype of binding protein and their targets (Duan & Xu, 2005). They function as carrier proteins for IGFs in the circulation and regulate physiological concentrations at the tissue level. In the human and sheep fetus, IGFBP-3 is the most abundant IGFBP in serum, followed by IGFBP-2, suggesting that these are important in IGF modulation during development (Lord *et al.*, 1991; Delhanty & Han, 1993). The expression of the IGFBPs during development has also been shown to be tissue-specific: for example, IGFBP-2 expression declines in the muscle, heart and lung at 75dGA but continues in the kidney and adrenal until post natal life (Delhanty & Han, 1993).

As studies on experimental hypothyroidism *in utero* have shown growth retardation, it can be postulated that growth mechanisms are altered by changes in insulin and/or IGF signalling. These alterations may affect important downstream signalling proteins which are essential for growth and maturation in the fetus. Interactions between thyroid hormones and insulin, and the development of the pancreas, have not been investigated previously before birth.

1.6 Pancreatic islets of Langerhans

The islets of Langerhans of the pancreas comprise of distinct cell types which secrete different hormones. It is estimated that adult humans have approximately 2 million islets, which make up about 2% of the pancreas by weight (Kulkarni, 2004). Insulin is produced by the β-cells in response to increased blood glucose levels, while pancreatic α-cells secrete the hormone glucagon when blood glucose levels are low. Other endocrine cells in the islets include somatostatin-producing δ-cells and pancreatic polypeptide-producing PP cells. Somatostatin is an inhibitory paracrine hormone which suppresses the secretion of insulin and glucagon, while pancreatic polypeptide is secreted in response to food intake and regulates exocrine pancreatic secretion (Wang *et al.*, 2013). The pancreatic β-cell mass and secretion of insulin are essential in maintaining an optimal range of blood glucose levels in adult life and for normal growth and development in the fetus.

1.6.1 Endocrine islet cell development

Embryonic development of the pancreas is a complex process, as pancreatic cells with profoundly different functions arise from the same progenitor cells. Therefore, specific transcription factors are integral to α and β-cell development by regulating the transcription of genes for cell specification and maturation (Conrad *et al.*, 2014). The pancreas originates from the dorsal and ventral region of the distal foregut endoderm at 4 weeks of gestation and 24dGA in the human and sheep, respectively, and at 10dGA in the mouse (Cole *et al.*, 2009; Jennings *et al.*, 2015). Development of the pancreatic bud is due to inhibition of expression of the gene sonic hedgehog, which normally suppresses the key transcription factor pancreatic duodenal homeobox factor, also

known as PDX1 (Pan & Wright, 2011). In the human embryo by 30dGA, there is a marked expression of PDX1 and GATA binding protein 4 (GATA4) in the ventral and dorsal buds, which are necessary for pancreatic growth. Previous studies have shown that mice with a global loss of *Pdx1* lack a pancreas and die at birth (Offield *et al.*, 1996). Later in embryogenesis, the transcription factors, forkhead box O1 (FOXO1), NK2 homeobox-2 (NKX2-2) and NK6 homeobox-1 (NKX6-1), are all expressed and are vital in maintaining future β-cell identity, as shown in Figure 1.5 (van der Meulen & Huising, 2015).

During the embryonic period, the pancreas undergoes extensive expansion of proliferative progenitor cells and the transcription factor neurogenin 3 (NGN3) is required for the commitment of progenitor cells to an endocrine fate (Figure 1.5). Pancreatic expression of NGN3 increases at the end of the embryonic period (~7 weeks) in the human, at the same time as the first appearance of fetal β-cells and ceases roughly 5 weeks before term (Salisbury *et al.*, 2014). This suggests that human pancreatic development is completed by this time and implies that any alterations in β-cell mass later in life is due to the balance of apoptosis and proliferation of existing β-cells, rather than specification of new β-cells from endocrine progenitor cells (Jennings *et al.*, 2015). The transcription factors v-maf avian musculoaponeurotic fibrosarcoma oncogene homologs a and b (MAFA and MAFB), play important roles in β-cell differentiation, as MAFB expression marks the start of insulin transcription, followed shortly by expression of MAFA (van der Meulen & Huising, 2015). Mice lacking *MafA* in the pancreas have altered islet morphology and impaired insulin secretion, indicating that it is an important factor in developing β-cell function (Hang *et al.*, 2014).

A key transcription factor responsible for α-cell differentiation is encoded by ARX, the aristaless-related homeobox gene (Wilcox *et al.*, 2013). In the embryonic mouse pancreas, *Arx* is restricted to α-cells, where it remains throughout life. Additionally, overexpression of *Arx* is capable of forcing β-cells to adopt an α-cell fate (Collombat *et al.*, 2007). Differentiation of progenitor cells into α-cells also requires NKX2-2 (Prado *et al.*, 2004), and later in α-cell maturation the transcription factors, paired box gene 6 (PAX6) and forkhead box A2 (FOXA2; Figure 1.5) are essential for glucagon production

and secretion (Gosmain *et al.*, 2011; Heddad Masson *et al.*, 2014; van der Meulen & Huising, 2015)

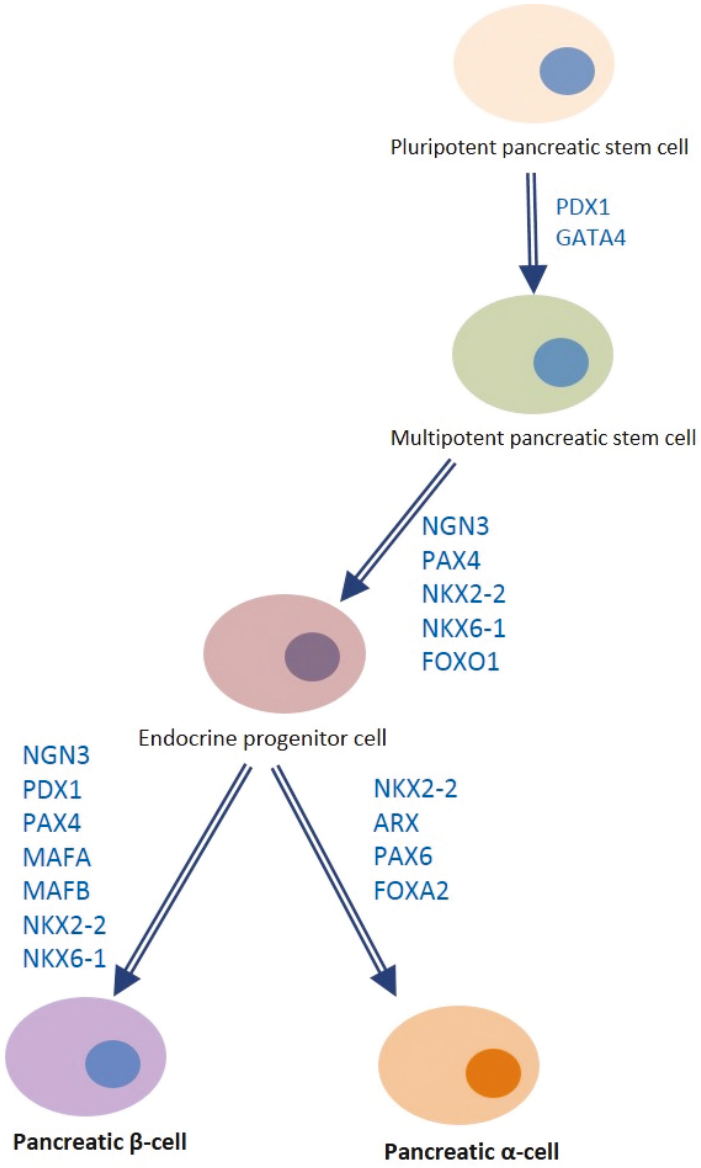

Figure 1.5. Diagram showing embryonic α- and β-cell development in the human pancreas and regulation by transcription factors.

1.6.2 Fetal islet growth and development

In the normal developing human fetus, small clusters of endocrine cells multiply around 25% of gestation (10 weeks) and the islet structure matures in the third trimester (Fowden & Hill, 2001). This is a similar time frame to that found in the ovine fetus, where primitive islets are formed by 33dGA or 23% of gestation (Green *et al.*, 2010). In the rodent however, islets do not form until 78% of gestation (Jensen 2000). For most of human gestation, α-cells are the main cell type and are the first to be identified at 6 weeks of gestation. Detection of pancreatic insulin occurs at around 10 weeks of gestation (Reddy & Elliott, 1988; Fowden & Hill, 2001). In the ovine fetus at 40-45dGA, insulin is the predominant hormone expressed in the endocrine cell population of the pancreas (Reddy *et al.*, 1988).

Fetal human and ovine β-cells continue proliferating throughout gestation and exhibit insulin secretion in parallel with cell number (Fowden & Hill, 2001). In contrast, in rodents, endocrine cells are mitotically quiescent until just before term (Green *et al.*, 2010). In human fetuses, apoptosis of β-cells is rare between 17-32 weeks of gestation, however, during the last 8 weeks of gestation and in the first 8 weeks of postnatal life, there is a wave of apoptosis in pancreatic islets during which new cells are generated by neogenesis. This is known as the period of remodelling (Kassem *et al.*, 2000). The same period of remodelling is also seen in rodents, and takes place at 2-3 weeks of postnatal age around the time of weaning (Hill *et al.*, 2000). The mechanisms controlling islet apoptosis are undefined but in rodents, it is associated with a decrease in circulating IGF-II levels (Hill *et al.*, 2000).

The human fetal β-cell is able to respond to glucose from 16 weeks of gestation and show appropriate responses to fluctuations in blood glucose *in utero* (Otonkoski *et al.*, 1988; Fowden & Hill, 2001). Endocrine β-cells are able to alter their capacity for insulin secretion, in response to insulin demand. This may be achieved by altering secretory function and/or by changing the number or size of β-cells (Hales & Barker, 2001). In humans, the percentage of pancreatic islets is correlated to birth weight and in small-for-gestational age neonates, the percentage of islets is halved to 2% of pancreatic tissue

(van Assche & Aerts, 1979; Fowden & Hill, 2001). This suggests that adverse conditions *in utero* may affect fetal pancreatic development.

1.6.3 Hormonal control of fetal β-cell development and function

Beta cell development has been shown to be controlled and affected by intrauterine availability of growth factors and hormones (Figure 1.6). The fetal pancreas expresses both IGF-I and IGF-II, which have mitogenic actions. In mice, genetic manipulation of IGFs and their receptors leads to changes in pancreatic islet mass (Fowden & Hill, 2001). Transgenic fetal mice with overexpression of IGF-II have increased β-cell hypertrophy (Figure 1.6), increased islet areas and reduced endocrine cell apoptosis (Petrik *et al.*, 1999). Mice deficient for the *igfr1* and *irs2* genes in a double knock out model show a reduction in β-cell mass (Withers *et al.*, 1999). However a subsequent study with a β-cell specific knockout of *igfr1* found that the β-cell mass was unchanged but this was associated with hyperinsulinaemia and glucose intolerance (Kulkarni *et al.*, 2002). This suggests that IGF-IR in β-cells is not necessary for growth but may be more important in the differentiated functions of the β-cell.

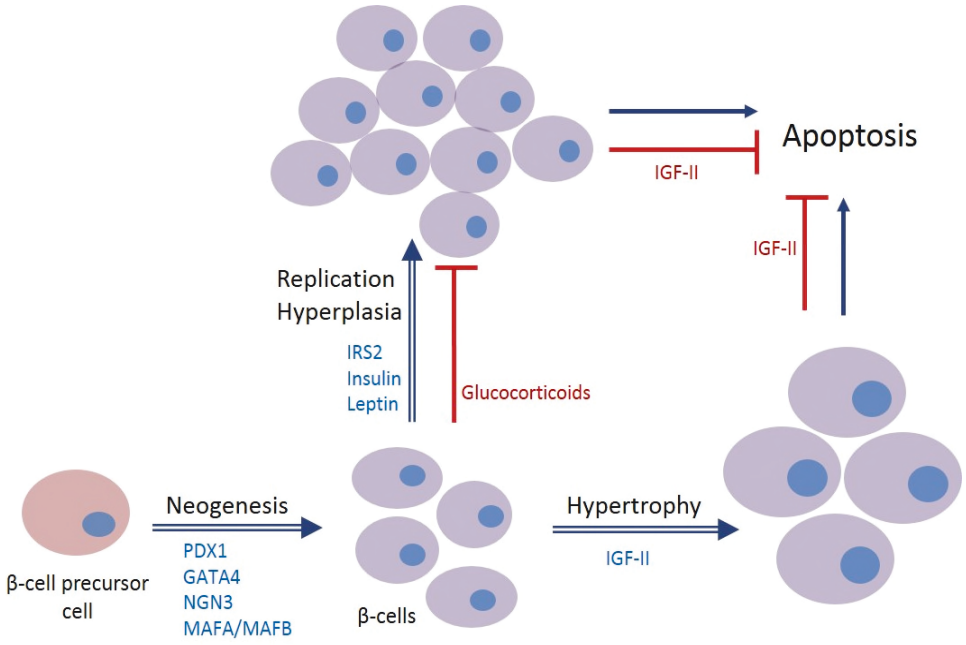

Figure 1.6. Diagram to show the control of fetal β-cell growth. The β-cell mass is maintained by a balance between replication, growth and apoptosis. Transcription factors such as PDX1, GATA4, NGN3 and MAFA initiate neogenesis of β-cells. Hormones such as insulin and leptin induce β-cell replication and hyperplasia, which is inhibited by glucocorticoids. IGF-II has previously been implicated in stimulating β-cell hypertrophy and inhibiting apoptosis.

Disruption of the IRS proteins has been shown to affect the growth and development of the pancreas. Loss of *Irs2* in mice leads to a decrease in β-cell mass compared to wild type controls (Withers *et al.*, 1998). Subsequent immunohistochemical labelling for IRS2 revealed its localisation to the ductal epithelium, the site of islet neogenesis, indicating that IRS2 may play an important role in proliferation (Withers *et al.*, 1998; 1999). Recently, it has been postulated that IRS2 may have more of a maintenance role in the adult pancreas. Analysis of mice with pancreas-specific loss of *Irs2* revealed that the β-cell mass was no different to that of control mice at 2 weeks of age. By 12 weeks of age however, the *Irs2* knockout mice had reduced β-cell mass (Cantley *et al.*, 2007).

Mice deficient for the S6K protein, an endpoint of the insulin pathway, have low circulating insulin and are glucose intolerant; this was found to be due to a reduction in pancreatic endocrine mass and specifically a decrease in β-cell size. This pathology is similar to that seen in chronic type 2 diabetes (Pende *et al.*, 2000).

Glucocorticoids are stress hormones produced by the adrenal gland which are responsible for mobilising glucose into the circulation (Fransson *et al.*, 2013), and appear to have an inhibitory role in β-cell growth. Fetal mice of food restricted mothers have increased plasma cortisol concentrations which are associated with reduced β-cell mass and down-regulation of the genes involved in β-cell function (Valtat *et al.*, 2011). Additionally, an increased β-cell fraction was found during late gestation in fetal mice with glucocorticoid receptor gene knockout (Gesina *et al.*, 2006). At an earlier embryonic stage, the lack of glucocorticoid receptor had no effect on islet formation and β-cell fractions were similar to that in normal mice, suggesting that there is a specific time at which the pancreas becomes glucocorticoid sensitive (Gesina *et al.*, 2006).

Additionally, the hormone leptin, secreted by adipocytes, has previously been found to regulate β-cell proliferation. Leptin receptor protein and mRNA have been located in fetal and adult rat islets, and also in cultured insulinoma cells *in vitro* (Kieffer *et al.*, 1996; Islam *et al.*, 1997; Kulkarni *et al.*, 1997). Addition of leptin to isolated fetal rat islets has been shown to stimulate β-cell proliferation *in vitro* (Islam *et al.*, 2000). In contrast to these findings, a two-fold increase in β-cell mass was observed in neonatal and adult

mice with a pancreas-specific knockout of the leptin receptor (Covey *et al.*, 2006; Morioka *et al.*, 2007). The exact role of leptin in pancreatic β-cell development is yet to be established.

There is limited knowledge on the effects of thyroid hormones on development of pancreatic β-cells. Adult and neonatal mice with a disruption of inactivating D3 have smaller pancreases and a reduced β-cell mass. This suggests that a reduction in active thyroid hormones by D3 near term is required for normal maturation of the pancreas (Medina *et al.*, 2011). There may be specific temporal changes in thyroid hormone activity locally that regulate pancreas development before birth. Neonatal rats which are hypothyroid and growth retarded due to maternal hypothyroidism have been shown to have reduced insulin secretion and impaired glucose tolerance (Karbalaei *et al.*, 2014). When the pancreas was examined, however, there was no difference in the β-cell mass between normal and hypothyroid rats (Karbalaei *et al.*, 2014).

The majority of these previous studies are limited in the use of rodents as an experimental model. It is possible that humans and larger mammals may have a different developmental pattern in the pancreas as they are a precocial species i.e. they are more physiologically mature at birth. Limesand *et al.* (2005) studied an ovine model of IUGR and found that pancreatic islet size and insulin content are lower in growth restricted fetuses compared to controls. However, this study used growth restricted fetuses generated by elevating the environmental temperature of the ewe. Although increasing maternal temperature can reduce the plasma concentrations of cortisol and thyroid hormones in the fetus, it is not sufficient to induce fetal hypothyroidism (Wallace *et al.*, 2005). The effect of hypothyroidism on fetal islet development in a precocious animal model remains unknown.

1.7 Adipose tissue growth and development

Insulin secretion *in utero* is essential for normal growth and development of the fetus, especially in tissues highly sensitive to insulin such as adipose tissue. Adipose tissue is an endocrine organ composed predominantly of adipocytes. The main physiological role

of adipose is to store glucose in the form of triglycerides for future energy expenditure, and in the fetus, adequate adipose tissue growth is required for thermoregulation as a newborn. In addition to energy storage, adipose is important for secretion of a variety of active peptides, known as adipokines, which can act in both a paracrine and endocrine manner (Kershaw & Flier, 2004). Leptin is one such hormone secreted by adipose tissue which has an important role in energy homeostasis by serving as metabolic signal of energy sufficiency to the hypothalamus and other tissues (Ahima & Flier, 2000).

In mammals, adipose tissue is distributed unevenly throughout the body. Subcutaneous adipose is found under the skin, primarily in thighs and in the trunk. Visceral adipose, however, includes the mesenteric, pericardial and perirenal (Sarr *et al.*, 2012). Visceral adipose depots have been shown to correlate with the development of insulin resistance, while subcutaneous does not (Bjorndal *et al.*, 2011). For large precocious mammals, the majority of fat deposition occurs in the final third of gestation; in the fetal sheep, at least 80% of adipose tissue is perirenal, which is located around the kidneys (Symonds *et al.*, 2003). Additionally, perirenal adipose tissue is known to contain both white and brown adipocytes (Symonds *et al.*, 2012). Perirenal adipose tissue (PAT) is therefore a useful tissue to examine how insulin signalling and thyroid hormone regulate growth.

1.7.1 Adipose development *in utero*

Adipose tissue first appears in human fetuses at 16 weeks of gestation (Poissonnet *et al.*, 1983) and in the sheep fetus at around 80dGA (Symonds *et al.*, 2012). In mammals, adipocyte differentiation is controlled by a network of transcription factors (Poissonnet *et al.*, 1983). The gene zinc finger protein-423 (ZFP423; Figure 1.7) has been identified as an essential determinant of pre-adipocyte commitment from mesenchymal precursor cells and is required for normal adipogenesis (Gupta *et al.*, 2010). Downstream of ZFP423, the transcription factors Kruppel-like factors 4, 5 and 6 (KLF4-6), sterol regulatory element-binding transcription factor 1 (SREBP-1) and CCAAT-enhancer-binding proteins β/δ (C/EBPβ/δ) initiate the critical adipogenic transcription factor, peroxisome proliferator-activated receptor γ (PPARγ), as illustrated in Figure 1.7 (Stephens, 2012).

Differentiation of pre-adipocytes into mature adipocytes requires PPARγ, as demonstrated in PPARγ knockout mice, which do not develop fat cells (Rosen *et al.*, 1999). Expression of PPARγ is important for induction of several lipogenic genes, such as adipocyte fatty acid binding protein, lipoprotein lipase, GLUT4 and PEPCK (Leonardini *et al.*, 2009). Pre-adipocytes can differentiate into mature adipocytes throughout life, thus enabling hyperplastic expansion when increased lipid storage is needed. In situations of overnutrition, adipocytes can also become hypertrophic (Coelho *et al.*, 2013).

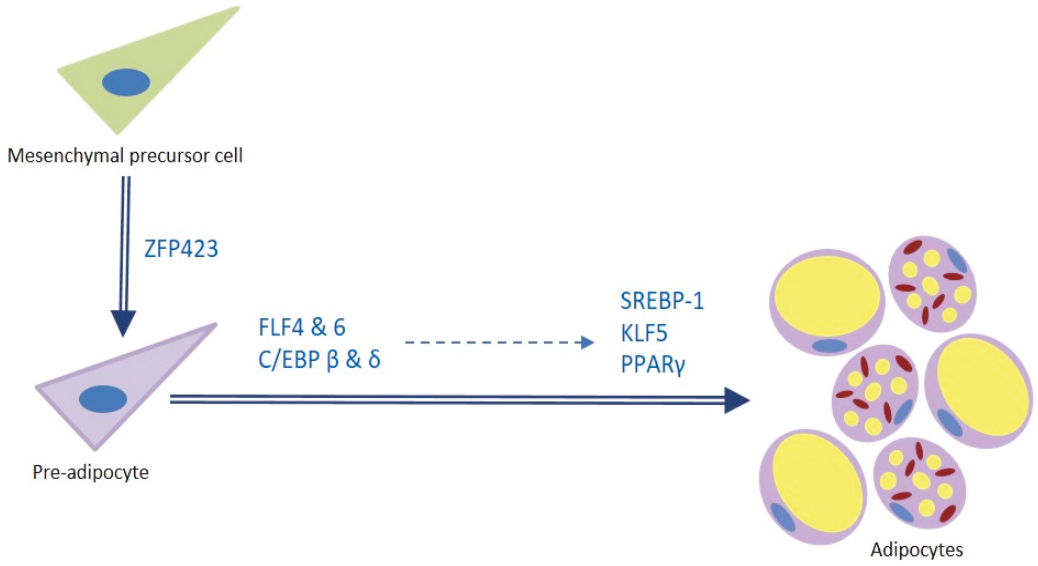

Figure 1.7. Diagram showing adipocyte differentiation and its regulation by transcription factors. The transcription factor ZFP423 determines mesenchymal precursor cells to a pre-adipocyte cell fate. Downstream of ZFP423, transcription factors KLF4, 5 &6, C/EBP β & α and SREBP-1 initiate the critical adipogeneic factor PPARγ. ZFP423: zinc finger protein-423, KLF: Kruppel-like factors, C/EBP: CCAAT-enhancer-binding proteins, SREBP-1: sterol regulatory element-binding transcription factor 1, PPARγ: peroxisome proliferator-activated receptor γ.

There are two different types of adipocytes, white and brown. White adipocytes make up white adipose tissue (WAT) and are leptin immunoreceptive; around 90% of their volume consists of a single large lipid droplet and the nucleus is pushed to the edge of the cell. These white adipocytes are termed unilocular or UL (Cinti, 2012). In brown adipose tissue (BAT), the adipocytes contain several smaller lipid droplets (multilocular,

ML) and are characterised by a large number of mitochondria (Clarke *et al.*, 1997; Symonds *et al.*, 2003). Although both white and brown adipocytes require PPARγ for differentiation and maturation, they arise from different origins (Figure 1.8). It has been shown that brown adipocytes originate from myogenic factor-5 (Myf5) expressing precursor cells, while white adipocytes arise from Myf5-negative mesenchymal precursor cells (Seale *et al.*, 2008; Sarjeant & Stephens, 2012).

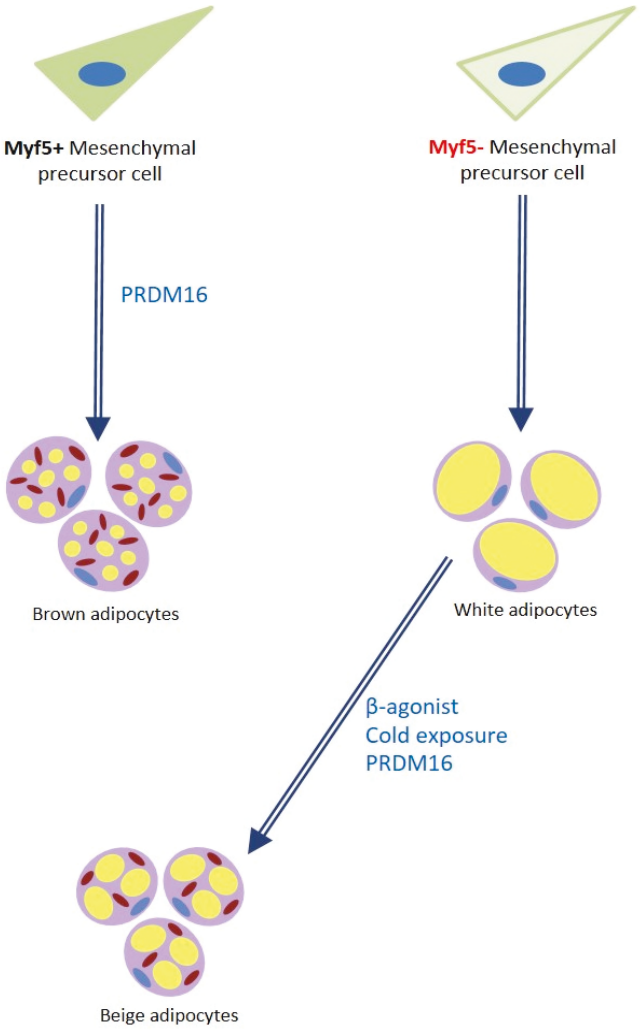

Figure 1.8. Diagram showing brown and white adipocyte differentiation and the transformation of white into brown-like beige cells. Brown adipocytes are thought to derive from Myf5 expressing mesenchymal precursor cells. The transcription factor PRDM16 has been shown to regulate brown adipocyte development and can "brown" white adipocytes to a "beige" state. Cold exposure and β-agonists have also been implicated in "browning". Myf5: myogenic factor 5, PRDM16: positive regulatory domain containing-16.

The transcription factor, positive regulatory domain containing-16 (PRDM16), has been shown to control development of brown adipocytes, and is responsible for the "browning" of some white adipocytes to form beige cells, as shown in Figure 1.8 (Sarjeant & Stephens, 2012; Harms & Seale, 2013). Beige cells can be found within WAT in both human and rodents in adult life, and development of these cells from white adipocytes is stimulated by β3-adrenoreceptors and adaption to cold temperatures (Seale *et al.*, 2008; Harms & Seale, 2013).

1.7.2 Hormonal control of fetal adipose growth

As gestation progresses, total adipose mass in the fetus continues to increase towards term and it comprises of both white and brown adipocytes (Clarke *et al.*, 1997; Symonds *et al.*, 2003). In the sheep fetus during mid-gestation, adipose tissue is largely composed of WAT which is laid down first and when the fetus begins to mature in late gestation, the BAT becomes more dominant (Devaskar & Anthony, 2002). By 30 days of post-natal life, the multilocular BAT has declined, and the fat is mainly composed of unilocular WAT (Symonds *et al.*, 2012).

Insulin is a potent growth factor in fetal adipose tissue. Insulin and IGF-I receptors have been identified in relatively large quantities in brown adipocytes isolated from fetal rats and binding of the hormones to their receptors occurs with high affinity (Teruel *et al.*, 1996). Mice with an adipose-specific deletion of InsR, have decreased body weight and fat mass indicating that insulin is essential in adipose development (Bluher *et al.*, 2002).

The effects of insulin on fetal adiposity can be seen in pregnant women who are hyperglycaemic with gestational diabetes and who give birth to large-for-gestational age babies (Kamana *et al.*, 2015). These babies are macrosomic as hyperglycaemia *in utero* stimulates fetal insulin secretion which, in turn, promotes somatic, especially adipose tissue, growth (Stevens *et al.*, 1990). In a model of IUGR in fetal sheep induced by placental restriction, plasma insulin concentrations are reduced and this is correlated with a decrease in fetal PAT mass (Duffield *et al.*, 2008).

The hormone leptin is synthesised and secreted by white adipocytes (Forhead & Fowden, 2009). It has previously been shown in fetal sheep that adiposity correlates with plasma leptin concentrations (Mühlhäusler *et al.*, 2002), leading to speculation that leptin itself has a role in the maintenance of fat mass before birth. Administration of leptin to sheep fetuses in late gestation had no effect on overall PAT mass, but reduced the proportion of UL adipocytes and increased the proportion of ML cells (Yuen *et al.*, 2003). This suggests that leptin has an important role in regulating the balance of UL and ML adipocyte types.

There are limited reports concerning the effects of thyroid hormones on adipose growth *in utero*. Thyroid hormone receptors, TRα1 and TRβ1, have been identified in cultured brown adipocytes, and during differentiation, the binding capacity of T3 to either TR type is doubled (Hernandez & Obregon, 1996). Transgenic mice with dysfunctional TRα1 have lower body weight than wild-type mice which is associated with decreased WAT mass, suggesting that thyroid hormones play a role in white adipocyte differentiation, possibly through regulation of PPARγ (Ying *et al.*, 2007).

1.7.3 Hormonal control of fetal adipose function

One major function of fetal WAT is the production of leptin and it has previously been reported that this process can be regulated by insulin. Insulin infusion in fetal sheep increases leptin mRNA in WAT, demonstrating that insulin can stimulate production of leptin (Devaskar & Anthony, 2002). This has also been reported *in vitro* in isolated rat adipocytes, where insulin stimulates an 80% increase in the secretion of leptin (Barr *et al.*, 1997). In fetuses of well-fed ewes, plasma insulin concentrations are increased and this is correlated with plasma leptin concentrations (Mühlhäusler *et al.*, 2002). Insulin promotes the synthesis of lipids through lipogenesis by an increase in transcription of the genes encoding acetyl-CoA carboxylase and fatty acid synthase (Kersten, 2001). These lipogenic genes are regulated by SREBP-1, which is stimulated by factors downstream of insulin and PI3K in the insulin signalling pathway (Saltiel & Kahn, 2001). Insulin also promotes the storage of glucose in adipocytes by stimulating the translocation of GLUT4 to cell membranes via the insulin signalling pathway (Saltiel & Kahn, 2001).

In the fetus, BAT is essential for thermoregulation after birth as it expresses the unique uncoupling protein, UCP1, which promotes the rapid generation of heat (Mostyn *et al.*, 2003; Cinti, 2012; Symonds *et al.*, 2012; Pope *et al.*, 2014). Uncoupling proteins are mitochondrial inner membrane proteins which can increase the permeability of the mitochondrial membrane allowing protons to return to the mitochondrial matrix. Heat is generated by uncoupling oxidative phosphorylation from ATP production in the respiratory chain. This process is known as non-shivering thermogenesis (Nedergaard *et al.*, 2001). It has previously been postulated that thyroid hormones stimulate the appearance of BAT and UCP1 in the fetus near term. Polk *et al.* (1987) showed that thyroidectomy in the sheep fetus results in hypothermia in the new born lamb and in a decrease in plasma free fatty acids, which are normally released in association with BAT thermogenesis. Additionally, it has been identified that there is a peak in D2 mRNA expression in fetal PAT close to term, which provides a site for local T3 production and activity (Clarke *et al.*, 1997; Pope *et al.*, 2014). Consequently, transgenic mice with D2 deletion have severe defects in thermogenesis due to a reduction in UCP1 of 50% (Hall *et al.*, 2010). In fetal rat adipocytes in culture, Guerra *et al*. (1996) demonstrated that the presence of T3 in media significantly increased UCP1 mRNA levels and that this was due to increased gene transcription. Consistent with this finding, Rabelo *et al*. (1995) identified, in a brown fat cell line, that T3 stimulates the UCP gene by acting on up-stream TREs positioned on the gene.

The abundance of UCP1 in fetal adipose tissue is also closely related to the elevation in circulating cortisol before birth and a functional adrenal gland is essential for the developmental increase in PAT UCP1 expression (Mostyn *et al.*, 2003). In fetal sheep, UCP1 protein expression in PAT is positively correlated with both plasma T3 and cortisol (Mostyn *et al.*, 2003). Therefore, the extent to which cortisol alone, or in parallel with T3, affects BAT development in late gestation remains to be determined.

1.8 Renal growth and development

The prepartum rise in T3 may also influence the growth and maturation of the fetal kidneys as it has previously been shown in the sheep fetus that hypothyroidism *in utero*

increases relative kidney mass (Chattergoon *et al.*, 2012a). The main role of the adult kidney is to maintain electrolyte and water balance and to excrete waste through nephrons. In the fetus, fluid homeostasis is maintained primarily by the placenta. However, the fetus starts to produce urine early on in gestation which is the main component of amniotic fluid (Guron & Friberg, 2000).

1.8.1 Kidney growth *in utero*

The kidney is derived from three embryonic structures: the pronephros and mesonephros, which appear early in gestation and then regress, and the metanephros, which will differentiate into the kidney (Guron & Friberg, 2000). In humans, development of the kidneys begins early in gestation, at around 4 weeks, with the final number of nephrons formed by 36 weeks (Blackburn, 2003b). In the ovine fetus, the pattern of renal development is similar to that of humans, as nephrogenesis ends at around 130dGA, when the number of nephrons will persist into adulthood (Gimonet *et al.*, 1998; Wintour *et al.*, 2003; Figueroa *et al.*, 2005). Rodents differ from this pattern of development in that nephrogenesis begins at mid-gestation and continues until 10 days after birth (Guron & Friberg, 2000).

Several experimental studies have reported that growth restriction *in utero* results in reduced nephron number (Zimanyi *et al.*, 2000; Mitchell *et al.*, 2004). In twin sheep fetuses, which are an example of natural *in utero* growth restriction, both the relative kidney mass and total nephron number are lower than that seen in single fetuses (Mitchell *et al.*, 2004; MacLaughlin *et al.*, 2010). In a model of IUGR induced in fetal sheep by placental embolism nephron number was unchanged, although relative kidney mass was reduced in late gestation (Mitchell *et al.*, 2004). Intrauterine growth restriction due to twinning reduces nephron endowment, whereas IUGR in late gestation does not, indicating that the timing of growth restriction in gestation contributes to renal development.

1.8.2 Hormonal control of fetal renal growth

Regulation of fetal renal growth may be influenced by several hormonal factors, including insulin. In the fetal mouse kidney, InsR protein and mRNA are present in the whole metanephros from 13dGA (~60% gestation) until birth, when InsR expression declines in newborns (Liu *et al.*, 1997). Additionally, metanephros isolated from fetal mice respond to insulin in culture in a dose-dependent manner and exhibit hyperplasia and hypertrophy (Liu *et al.*, 1997), suggesting that insulin has a potential role in nephrogenesis. Insulin-like growth-factor I has also been implicated as a potent growth stimulus in the developing kidney (Marsh *et al.*, 2001). In the sheep fetus, there is a positive relationship between renal IGF-I mRNA abundance and relative kidney weight (Lok *et al.*, 1996; Marsh *et al.*, 2001; MacLaughlin *et al.*, 2010), and intravenous infusion of IGF-I causes a substantial increase in kidney mass (Lok *et al.*, 1996; Marsh *et al.*, 2001).

Changes in the insulin-IGF signalling pathway have been demonstrated to affect kidney mass. In a transgenic mouse model of renal *Irs2* deletion, neonatal kidneys are reduced in size and remain smaller in aged mice compared to same age controls (Carew *et al.*, 2010). Quantification of the glomeruli number indicated no change in glomeruli density, suggesting that there is an overall reduction in kidney size affecting all of the components of the organ. It may be hypothesized that the insulin pathway may not be required for nephrogenesis specifically, but may be important for overall organ growth (Carew *et al.*, 2010).

Leptin has also been implicated in the control of growth in the developing kidney. Neonatal rats treated with a leptin antagonist have decreased kidney mass but an increased number of glomeruli, however, these appeared to be smaller and more immature compared to those in control animals (Attig *et al.*, 2011). Leptin, therefore, may have a role in nephron branching and glomerular maturation.

The renin-angiotensin system (RAS) is an important regulator of nephrogenesis (Blackburn, 2003b). Angiotensin II is the main effector of the RAS system and in humans and sheep, angiotensin II exerts its effects via two main receptors (Chen *et al.*, 2004),

type 1 and 2 (AT_1R and AT_2R). Changes in the fetal RAS at specific time points during gestation can program changes in the developing kidney. For example, fetal sheep infused with a AT_1R antagonist have reduced kidney weights (Forhead *et al.*, 2011) and human neonates exposed to inhibitors of the RAS cascade during gestation demonstrate renal dysplasia (Cooper *et al.*, 2006).

The activity of the renal RAS increases developmentally towards term alongside plasma cortisol and T3 concentrations and in the sheep fetus, renal activities of D1 increase, and D3 decrease, towards term (Polk *et al.*, 1988; Forhead *et al.*, 2006), suggesting that thyroid hormone exposure and action increase in the fetal kidneys during late gestation. Experimental thyroidectomy in the fetal sheep leads to a decrease in renin mRNA, total renin and AT_1R mRNA in the kidney and these changes are normalised when thyroid hormone replacement is administered (Chen *et al.*, 2005b; 2007). Indeed, it has been identified *in vitro* that the 5' flanking DNA sequence in the promoter of the renin gene contains a TRE (Kobori *et al.*, 2001). Although the effects of fetal hypothyroidism on the renal RAS have been examined, the consequence of thyroid hormone deficiency for the structure of the developing kidney remains unknown.

1.8.3 Hormonal control of fetal renal function

Renal sodium (Na^+) reabsorption requires coordinated expression of apical and basolateral channels in the tubules (Figure 1.9). The epithelial Na^+ channel (ENaC) and the sodium/potassium ATPase (Na^+/K^+ ATPase) in the kidney contribute to the regulation of body salt and water homeostasis and blood pressure (Bhalla & Hallows, 2008). The ENaC is expressed as 3 subunits, α, β and γ, and synthesis of the α subunit is the rate limiting step in assembly of the whole ENaC complex (Bhalla & Hallows, 2008). In the fetal rat, ENaC transcripts are expressed primarily in the apical plasma membrane of the distal tubules and the collecting ducts of the kidney, and increase in abundance in the final 3-4 days of gestation (Watanabe *et al.*, 1999). Several endocrine factors may be responsible for this developmental increase in ENaC towards the end of term.

The Na^+/K^+ ATPase pump consists of a catalytically active α subunit and a glycosylated β subunit (Horowitz *et al.*, 1990). The pump plays a vital role in renal reabsorption by transporting Na^+ out of the cell and K^+ into the cell against their concentration gradients in an ATP dependent manner (Figure 1.9) and establishes a sodium gradient for a variety of secondary active transport systems (Féraille *et al.*, 1999).

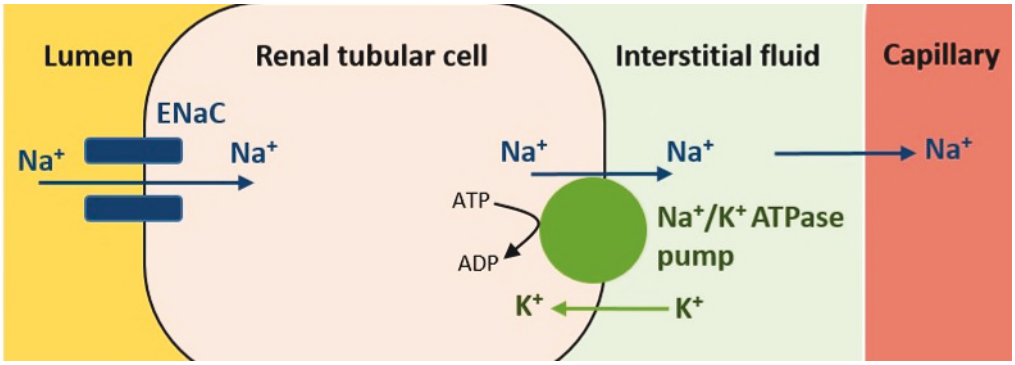

Figure 1.9. Diagram showing sodium reabsorption in a renal tubule cell. Epithelial sodium channels (ENaC) facilitate Na^+ reabsorption across the apical membranes of epithelia in the distal nephron. At the basal membrane the Na^+/K^+ ATPase pump transports Na^+ out of the cell and K^+ into the cell against their concentration gradients in an ATP dependent manner.

Glucocorticoids are known to have an influence on renal ion transporters *in utero*. Glucocorticoid receptor mRNA is expressed from 80dGA in the renal cortex of fetal sheep and continues to increase towards term, when it decreases post-natally (Keller-Wood *et al.*, 2008). Fetuses born to ewes treated with dexamethasone or cortisol have increased renal mRNA expression of ENaC and Na^+/K^+ ATPase compared to controls in late gestation (Moritz *et al.*, 2011). As the thyroid hormones also increase in the circulation towards term in parallel with cortisol, and in response to glucocorticoid treatment, they may also have a role in increasing ENaC expression to prepare the fetus for neonatal life.

Another hormone which may regulate ENaC is insulin. In an epithelial cell line, it has been shown that ENaC expression is upregulated by the serine-threonine kinase, under

stimulation of PI3K through the insulin signalling pathway (Wang *et al.*, 2001). Furthermore, chronic hyperinsulinaemia *in vivo* in rats increases ENaC trafficking to the apical membrane (Song *et al.*, 2006). Previously, angiotensin II has also been shown to regulate ENaC. In adult rats infused with an AT_1R blocker, decreases in ENaC mRNA and protein abundance are observed in the proximal tubules. This decrease was reversed after an infusion of angiotensin II (Beutler *et al.*, 2003). As the thyroid hormones have previously been reported to regulate the fetal renal RAS (Chen *et al.*, 2005b; Chen *et al.*, 2007), it may be possible that hypothyroidism can alter the expression of the ENaC and therefore affect Na^+ and water reabsorption in the developing kidney.

It has been well established that the thyroid hormones regulate the Na^+/K^+ ATPase pump in adult life. Previous experimental studies have shown increased Na^+/K^+ ATPase mRNA abundance in the kidney of hypothyroid rats injected with T3 (McDonough *et al.*, 1988). Further to this, in adult rat kidney cortex, hypothyroidism did not change the mRNA levels of α or β subunits, whereas hyperthyroidism led to an increase in both subunits (Horowitz *et al.*, 1990). It was later identified that a TRE exists in the 5' region of the β subunit (Feng *et al.*, 1993). Interestingly, when the protein levels of each subunit were examined, hypothyroidism caused a decrease in the β, but not α, subunit (Horowitz *et al.*, 1990). This suggests that the thyroid hormones can also act post-transcriptionally to regulate the pump.

Insulin has also been implicated in the regulation of Na^+/K^+ ATPase. In the isolated tubules of rats, insulin incubation increases phosphorylation of the α subunit at a tyrosine residue (Féraille *et al.*, 1999). The insulin receptor stimulates tyrosine phosphorylation after insulin binding, making the insulin receptor a candidate for phosphorylation of the Na^+/K^+ ATPase α subunit. While previous knowledge of the Na^+ channels and transporters focuses on adult physiology, it may be plausible that the same processes occur *in utero.* The maturation of the transporters may be influenced by both insulin and the thyroid hormones, in addition to cortisol. Thus, there is potential for thyroid hormone deficiency to alter the expression patterns of the ENaC and Na^+/K^+ ATPase directly and indirectly through the insulin signalling pathway.

1.9 AIMS

The thyroid hormones are responsible for growth and maturation in many fetal organs, such as the heart, lungs, brain and muscle. There is limited knowledge however, on the role of T3 and T4 in the growth and development of other important metabolic organs, namely the pancreas, adipose tissue and kidney. Furthermore, insulin signalling has been proposed to be an important regulatory pathway in tissue growth and development *in utero*, but their interactions with the thyroid hormones in late gestation are unknown.

The overall aim of the project is to elucidate the effects of hypothyroidism on the growth and development of the sheep fetus in late gestation. The specific objectives are to identify the effects of thyroid hormone deficiency *in utero* on (1) the development of fetal pancreatic islets and (2) insulin signalling pathways in the sheep fetus, in particular in adipose tissue and the kidneys.

The hypothesis is that growth retardation in the hypothyroid sheep fetus is a result of a decreased pancreatic β-cell mass and reduced circulating insulin levels, resulting in a downregulation of cellular markers of the insulin signalling cascade in fetal tissues (Figure 1.10).

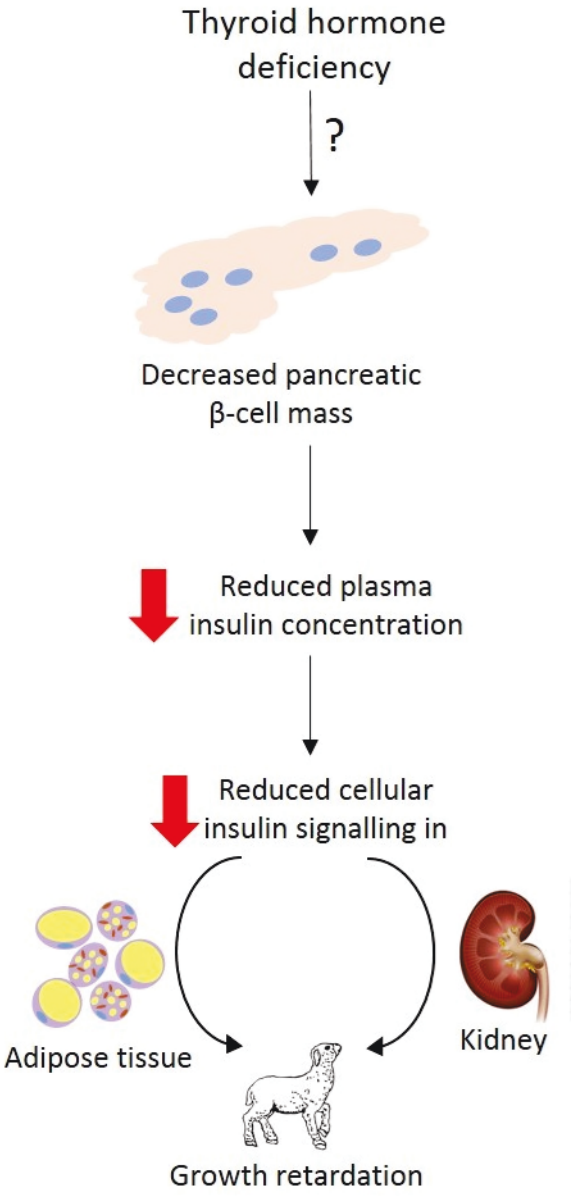

Figure 1.10. It is proposed that thyroid hormone deficiency *in utero* leads to decreased pancreatic β-cell mass, which reduces plasma insulin concentrations resulting in a downregulation of components of the insulin signalling cascade in fetal tissues such as adipose and kidney, thus compromising fetal growth.

2. MATERIALS AND METHODS

2.1 Sheep husbandry

All surgical and experimental procedures were carried out in accordance with UK Home Office legislation and the Animals (Scientific Procedures) Act 1986. Unless where stated otherwise, 38 twin Welsh mountain sheep fetuses were used in this study, 15 were female and 23 were male. The nineteen pregnant ewes were maintained with 200g/day concentrates, hay and water *ad libitum* with access to a salt block. For 18-24 hours before surgery, food was withheld from ewes, with access to water still available.

2.1.1. Surgical procedures

All surgical procedures were carried out under halothane anaesthesia with positive pressure ventilation (1.5% halothane in O_2-N_2O). At 105-110 dGA, where term is 145 ± 2 days, in each ewe, one twin fetus underwent a sham operation in which the thyroid gland was exposed (sham), and the other twin underwent a thyroidectomy (TX), as described by Hopkins and Thorburn (1972). The scheme of work is outlined in Table 2.1. The fetal head was delivered through an incision in the uterus and fetal membranes. The fetal thyroid gland was removed through an incision from the laryngeal cartilage to approximately the 10^{th} tracheal ring. The gland was dissected from surrounding connective tissue using a cautery probe. Prophylactic antibiotics were administered to the fetus and the ewe at surgery, and to the ewe for three days after.

2.1.2 Post mortem procedures

At either 129 or 143dGA, the fetuses were delivered by Caesarean section under general anaesthesia (20mg/kg maternal body weight sodium pentobarbitone I.V.). At delivery, 10ml blood samples were collected by venepuncture of the umbilical artery into EDTA-containing tubes and spun at 1000g for 5 minutes at 4°C. The plasma was stored at -20°C. The fetuses were weighed and biometric assessment was carried out (detailed in Section 3.2). The absence of the thyroid gland was confirmed in the TX fetuses. Various tissues were collected from the fetuses after the administration of a lethal dose of

barbiturate (200 mg/kg body weight sodium pentobarbitone). Tissues were weighed and either fixed in 4% formalin or frozen in liquid nitrogen and stored at -80°C.

Table 2.1. Number and gestational ages of fetuses in each experimental group of the study

Treatment group	Age at surgery (dGA)	Age at collection (dGA)	Number of fetuses (male:female)
Sham	105-110	129	9 (5:4)
	105-110	143	9 (6:3)
TX	105-110	129	10 (6:4)
	105-110	143	10 (6:4)

2.2 Hormone measurements

2.2.1 T3 and T4

Plasma T3 concentrations were measured using a radioimmunoassay (RIA) kit with rabbit monoclonal anti-T3 serum (MP Biomedicals, Loughborough, UK) validated for sheep plasma (Fowden & Silver, 1995). The RIA is a competition based assay in which radioactively labelled and unlabelled T3 antigens compete for binding sites on antibody coated tubes. As the amount of unlabelled antigen increases in the plasma samples, more of it can bind to the antibodies and so displaces the labelled variant. Therefore the level of radioactivity bound is inversely related to the plasma T3 concentration. After incubation, the unbound and bound fractions are separated and the radioactivity of the coated tubes is quantified. The RIA uses the radioactive isotope iodine-125 (^{125}I; 10µCi in total) in phosphate buffer as the tracer solution.

All plasma samples were analysed in duplicate alongside a charcoal-stripped fetal plasma sample (plasma stripped of hormones). Standards and samples (100µl) were added to the coated polypropylene tubes followed by the addition of 1ml tracer solution and mixed well. All the tubes were left to incubate for one hour in a water bath at 37°C. After incubation, all tubes were decanted and emptied of their contents and were washed with distilled water (dH_2O). After blotting dry, the radioactivity was counted for

one minute using a gamma counter (Hewlett Packard, Bracknell, UK). Concentration of T3 was determined by interpolation from the standard curve and the concentration of the stripped plasma was deducted from all the results. All samples were measured in one RIA kit and the intra-assay coefficient variation was 2.86% (n=10). The minimum level of detection was 0.067ng/ml.

Plasma T4 concentrations were measured using a RIA kit with mouse monoclonal anti-T4 serum (MP Biomedicals) validated for sheep plasma (Fowden & Silver, 1995). All plasma samples were analysed in duplicate alongside charcoal-stripped fetal plasma. Standards and samples (25µl) were added to the coated polypropylene tubes followed by the addition of 1ml tracer solution (^{125}I; 9µCi in total) and mixed well. All the tubes were left to incubate at room temperature for one hour. After incubation, the contents of the tubes were decanted and blotted dry. After blotting, the radioactivity was counted for 0.5 minutes using a gamma counter. The concentration of T4 was determined by interpolation from the standard curve and the concentration of the stripped plasma deducted from each reading. All samples were analysed in the same kit and the intra-assay coefficient variation was calculated to be 5.35% (n=10). The minimum level of detection was 7.6ng/ml.

2.2.2 Insulin

Plasma insulin concentrations were determined using an ovine specific enzyme-linked immunosorbent assay (ELISA; Mercodia, Uppsala, Sweden). The ELISA uses a direct sandwich technique in which insulin in the plasma reacts with peroxidase conjugated mouse monoclonal anti-insulin antibodies that coat the wells of a plate. This bound conjugate is detected by a reaction with 3,3'-5,5'-tetramethylbenzidine (TMB), which is light sensitive. The reaction is stopped by the addition of acid, providing a colorimetric endpoint to be read spectrophotometrically. The intensity of the colour change is directly proportional to the concentration of plasma insulin.

Enzyme conjugate solution and buffer solution were diluted in dH_2O to produce working solutions. Duplicates of ovine standards (0-3.0µg/L) and samples (25µl) were transferred into a 96-well plate coated with anti-insulin antibodies. Enzyme conjugate was added

and the plate shaken at 1.6g for 2 hours at room temperature. A series of five washes was carried out using wash buffer avoiding prolonged soaking of the wells. Substrate TMB was added to each well and incubated at room temperature for 15 minutes. To stop the reaction, 0.5M sulphuric acid was added. The optical density was read at an absorbance of 450nm on a plate reader (Biorad, Hemel Hempstead, UK). Plasma insulin concentration was calculated from regression of the standard curve. All samples were measured in one kit and the intra-assay coefficient of variation was 9.3% (n=10). The minimum level of detection was 25ng/L.

2.2.3 Cortisol

Plasma cortisol concentrations were determined using an ELISA kit for human serum (IBL International, Hamburg, Germany). The cortisol ELISA is based on the competition principle. An unknown concentration of cortisol present in the plasma and a fixed amount of enzyme labelled cortisol compete for the binding sites of rabbit polyclonal anti-cortisol antibodies that coat the wells of the plate. The enzyme substrate contains cortisol conjugated with horseradish peroxidase (HRP). After the substrate reaction, the intensity of the developed colour is inversely proportional to the amount of cortisol in the sample. The range of cortisol concentrations in the fetal plasma was at the low end of the standard curve and so the plasma samples were concentrated before the assay. Ethanol (1.5ml) was added to 100µl plasma sample, mixed and left to incubate for 30 minutes at room temperature. Samples were centrifuged for 15 minutes at 850g at 4°C. Supernatant was transferred into Eppendorf tubes and dried down using a Speedvac vacuum concentrator (Thermo Scientific, Loughborough, UK) for 50 minutes. The dried residue was resuspended in 25µl assay buffer from the kit and incubated at 4°C overnight.

Duplicates of standards and samples (20µl) were transferred into the antibody-coated 96-well plate with the addition of enzyme conjugate. The plate was mixed for 10 seconds and incubated at room temperature for 1 hour. The plate was washed three times with wash buffer. TMB substrate was added to each well and gently shaken. A stop solution of 0.5M sulphuric acid was added and after 30 minutes the optical density read at 450nm. Plasma concentrations were calculated by interpolation of the standard curve,

and multiplied by 0.5 to account for the concentration of the original sample. Two control standards of known concentrations were run in duplicate and the final concentrations were in the accepted ranges. All samples were measured in one kit and the intra-assay coefficient of variation was 8.6% (n=5). The minimum level of detection was 2.46ng/ml.

2.2.4 Leptin

Plasma concentrations of leptin, IGF-I and IGF-II were measured by RIA by Dr Dominique Blache at the School of Animal Biology, University of Western Australia.

Plasma concentrations of leptin were determined by RIA using antibodies raised against biologically active recombinant bovine/ovine leptin raised in emu (Greenwood *et al.*, 1963; Blache *et al.*, 2000). Triplicates of standards (bovine/ovine leptin) and duplicates of unknown samples were analysed by the addition of emu polyclonal anti-bovine/ovine leptin (1:500) and normal emu serum (1:500). Following incubation overnight at 4°C, ^{125}I-bovine/ovine leptin (4.5µCi total) was added and samples were incubated for 48 hours at 4°C. For precipitation of the antibody-antigen complex, sheep anti-emu immunoglobulin G (IgG; 1:12) was added to the samples, followed by further incubation for 48 hours at 4°C. Following the addition of 0.01M phosphate buffered saline (PBS) and 3% polyethylene glycol, the samples were spun at 2000g for 30 minutes. This was to improve the stability of the pellet. The supernatant was decanted and pellets left to dry. Radioactivity was counted on a gamma counter and the minimum level of detection was 0.09ng/ml. The intra-assay coefficient of variation was 5.7%.

2.2.5 IGF-I and IGF-II

Plasma concentrations of IGF-I and IGF-II were determined by RIA as described by Forhead *et al*. (2011). To avoid interference by the IGF binding proteins, IGFs were extracted by the acid-ethanol cryoprecipitation method developed by Breier *et al*. (1991). Plasma samples were mixed with acid-ethanol, containing 87.5% ethanol and 12.5% 2M hydrochloric acid to a ratio of 1:4 and incubated for 30 minutes at room temperature. Samples were spun at 3000g for 30 minutes at 4°C to obtain a pellet of

precipitated IGF protein. A second precipitation was obtained by decanting the supernatant and neutralising with 0.855M Tris base at a ratio of 5:2. Samples were stored at -20°C for 1 hour and then immediately centrifuged at 3000g at 4°C for 30 minutes.

Antibodies (rabbit polyclonal anti-human IGF-I, provided by the National Hormone and Peptide Program, National Institute of Diabetes, Torrance, CA, USA, 1:15000; rabbit polyclonal anti-human IGF-II, GroPep, Adelaide, Australia, 1:5000) were added to diluted (1 in 10) samples and left to incubate at 4°C overnight. Tracer solution containing the radioactively labelled IGF (^{125}I, 5.4µCi total) and secondary antibody (donkey polyclonal anti-rabbit IgG in normal rabbit serum, University of Western Australia, 1:20) was added, and samples were incubated overnight at 4°C. A 6% polyethylene glycol buffer was added to the samples and these were centrifuged at 1500g for 30 minutes at 4°C. The supernatant was precipitated and the radioactivity of the precipitate was determined on a gamma counter. The minimum levels of detection were 0.08 ng/ml for IGF-I and 4.0 ng/ml for IGF-II and the intra-assay coefficient of variation was 5.3 and 4.3%, respectively.

2.3 Histology

2.3.1 Wax embedding

Tissues were fixed in 4% formalin for 48 hours and rinsed in water before dehydration through a series of graded industrial methylated spirits (IMS; 75, 90 and 100%). Tissues were cleared in xylene and impregnated with paraffin wax. The samples were transferred to a tissue embedding processor where the specimens were embedded in a fresh paraffin wax block and left to solidify.

2.3.2 Sectioning

Paraffin wax blocks were sectioned on a semi-automated rotary microtome (Leica Biosystems, Milton Keynes, UK). Sections were cut to the desired thickness using HP35 coated microtome blade (Thermo Scientific). Cut sections were gently placed onto dH_2O

at 50°C to float and then manoeuvred onto a poly-l-lysine coated glass slide (Polysine, VWR International, Litterworth, UK). The slide was left to dry on a heat block at 37°C.

2.3.3 Haematoxylin and eosin (H&E) staining

Haematoxylin is a basic dye and binds to acidic components in cells such as nuclear DNA and stains them blue in colour. Eosin is an acidic dye; it binds to basic structures such as cell cytoplasm and membranes, thus staining them pink.

Slides were de-waxed by submerging in xylene for 10 minutes followed by rehydration through decreasing grades of IMS (100, 95, 70 and 50%) and finally dH_2O. Slides were immersed in Mayer's haematoxylin (Sigma, Poole, UK) for 3 minutes, rinsed in dH_2O and differentiated in acid alcohol (containing hydrochloric acid in 70% IMS) to remove background staining. To blue the nuclei, the sections were immersed in Scotts tap water (containing sodium bicarbonate and magnesium sulphate) for 5 to 10 minutes. Slides were rinsed again in dH_2O, before staining in eosin (Sigma) for 1 minute. They were washed briefly, no longer than one minute, in dH_2O and dehydrated through increasing concentrations of IMS (70, 95, 100%) and finally cleared in xylene. Slides were permanently mounted using a mixture of distyrene, a plasticiser, dissolved in toluene-xylene (DPX; Sigma) and coverslips. Sections were scanned using a NanoZoomer digital slide scanner (Hamamatsu Photonics, Welwyn, UK) to create digital images for analysis.

2.4 Immunohistochemistry

Immunohistochemistry is a method which identifies protein distribution in tissues of interest. It provides a visual observation to complement protein assays such as ELISA and molecular biology techniques. Immunolabelling the protein of interest is achieved with antibodies that target the protein in the tissue section. The antibody-antigen interaction is often visualised by the addition of an enzyme which conjugates to the antibody. Binding of the enzyme to a substrate produces a coloured precipitate at the cellular location of the protein.

2.4.1 Blocking

Sections were de-waxed in xylene for 10 minutes followed by rehydration through decreasing percentages of IMS (100, 95, 70, 50%) and finally dH_2O. Endogenous peroxidase in the section was blocked by incubation in 3% hydrogen peroxidase (Sigma) for 15 minutes. Sections were rinsed in running water and washed in PBS.

2.4.2 Antigen retrieval

When required, antigen retrieval was conducted after de-waxing and rehydration to unmask antigens from formaldehyde bonds. In the presence of a high salt buffer, such as citrate, cross-linkages between formalin and protein can be disrupted and broken down by heating to temperatures of around 100°C. Heat retrieval was used with a 10mM citrate buffer for the anti-proliferating cell nuclear antigen (PCNA) antibody. The slides were placed in a pressure cooker and heated in a microwave at pressure for 2 minutes (850W). Sections were left to cool and washed in PBS.

2.4.3 Antibodies

After peroxidase blocking and antigen retrieval (if required), all tissue sections were drawn around with a hydrophobic pen to provide a barrier. To minimise non-specific antibody binding, approximately 150µl of blocking solution (5% horse or goat serum in 2% bovine serum albumin (BSA) in PBS) was added to each section and incubated in a humidified chamber for 1 hour at 4°C. The blocking serum used depended on which species the primary antibody was raised. After rinsing in PBS, the sections were incubated for either 1 hour at 37°C or overnight at 4°C with primary antibody diluted in blocking serum. Blocking solution was used as a negative control. A biotinylated secondary antibody (horse serum and mouse anti-IgG or goat serum and rabbit anti-IgG) was added to create a secondary complex with the primary antibody and left to incubate at room temperature for 1 hour and then washed in PBS.

2.4.4 Detection

Using the Vectastain Elite ABC kit (Vector Labs, Peterborough, UK), the ABC reagent containing avidin solution and biotinylated HRP was added to each slide and incubated for 30 minutes at room temperature, followed by washes in PBS.

The chromogen diaminobenzidene (DAB, SigmaFast DAB tablets, Sigma) is a peroxidase substrate and was prepared by dissolving one DAB tablet and one urea hydrogen peroxide tablet in 5ml of dH_2O to provide a substrate solution containing 0.7mg/ml DAB, 2.0mg/ml hydrogen peroxide and 60mM Tris buffer. Substrate solution was added to each slide for 1 minute to produce a brown colour change to localise the protein of interest. To counterstain, the slides were incubated in pre-heated methyl green (Vector Labs) at 60°C in an oven for 3 minutes. They were washed briefly in dH_2O, for no longer than one minute, and dehydrated through increasing concentrations of IMS (70, 90 and 100%) and finally cleared in xylene. Slides were permanently mounted using DPX and coverslips. Sections were scanned using a NanoZoomer digital slide scanner to create digital images for analysis.

2.5 Western blotting

2.5.1 Tissue homogenisation

To quantify various proteins in fetal tissues using western blotting, each tissue of interest was first homogenised physically and chemically to break down tissue and cells. Homogenisation buffer was prepared on ice and contained final concentrations of 20mM Tris-base, 1mM ethylene glycol tetraacetic acid, 0.01% Triton-X 100, 1mM sodium pyrophosphate, 1mM sodium orthovandate, 10mM β-glycerolphosphate, 50mM sodium fluoride and a cocktail of protease inhibitors (Complete Mini, Roche, Burgess Hill, UK). Frozen tissue was weighed at 100mg and homogenised in lysing matrix tubes (MP Biomedicals) containing 1.4mm ceramic beads with 1ml of cold homogenisation buffer using a handheld rotary homogeniser (SuperFastPrep-1, MP Biomedicals) for 20 seconds at 400g. The samples were centrifuged at 14000g for 10 minutes at 4°C. Supernatant was transferred to fresh tubes and the extracted protein lysate was stored at -80°C.

2.5.2 Protein assay

To determine the concentration of protein lysate, a bicinchoninic acid (BCA) protein assay kit was used (Sigma). The assay relies on the formation of a copper (II) ion (Cu^{2+})-protein complex under alkaline conditions, following the reduction of Cu^{2+} to Cu^{+}. The amount of reduction is proportional to the amount of protein present and can be monitored by a colour change as BCA forms a purple-blue complex with Cu^{1+} in alkaline environments. The BCA working solution was prepared by mixing 50 parts reagent A, containing BCA, sodium carbonate, sodium tartrate and sodium bicarbonate, with 1 part reagent B, containing 4% (w/v) Cu^{2+} sulphate pentahydrate. Five standards were prepared from dilutions of 1mg/ml of BSA protein standard (0, 50, 100, 150, 200µg/ml). Standards and samples (25µl) were run in duplicate on a 96-well plate. To the samples, 200µl BCA working solution was added and the plate was incubated for 30 minutes at room temperature. The plate was read in a spectrophotometer at an absorbance of 490nm and a standard curve produced from which the protein concentrations of the samples could be interpolated.

2.5.3 SDS-PAGE

The quantification of specific proteins was determined using sodium dodecyl sulphate polyacrylamide gel electrophoresis (SDS-PAGE). Sodium dodecyl sulphate is an anionic detergent which is used to denature proteins. Secondary and tertiary structures of proteins are denatured by SDS, which confers its negative charge to the now linear protein. This negative charge is proportionate to the length of the polypeptide. All samples acquire a uniform charge so electrophoretic movement should depend entirely on molecular size and the negatively charged protein samples are run through a polyacrylamide gel towards the anode. The speed with which they travel is inversely related to their size.

Protein lysates of known concentration were diluted to a concentrations of either 3 or 4µg/µl in a final volume of 25µl to give 75 or 100µg of protein per well. NuPage LDS loading buffer (2% lithium dodecyl sulphate, 141mM Tris Base, 10% glycerol, 0.51mM EDTA, 0.22mM Coomassie blue, 0.175mM phenol red; Thermo Scientific) was added to

each sample. To reduce the protein in the lysates, 2% fresh 100mM dithiothreitol (DTT; Sigma) was added to each sample directly before heating at 70°C for 10 minutes. Samples were loaded into a 7.5% pre-cast polyacrylamide gel (Biorad) alongside 5µl molecular marker (Prism Ultra Protein Ladder 10-245 kDa, Abcam, Cambridge, UK). The gel was run at 100V for 10 minutes to stack the proteins and then at 150V for 45 minutes until the samples had run through the length of the gel.

2.5.4 Membrane transfer

After separation, the proteins were transferred to a microporous membrane for immunoblotting. Using the application of an electric current, the proteins were transferred to the membrane in the same pattern that they were separated by SDS-PAGE. Transfer of the proteins to a polyvinylidene fluoride microporous membrane (Immobilon P 0.45µm, Millipore, Sigma) was achieved using the Pierce G2 Fast Blotter (Thermo Scientific). The gel and membrane were stacked between two layers of filter paper soaked in high salt transfer buffer (Pierce 1-Step Transfer buffer, Thermo Scientific). The stack was placed in the blotter and sandwiched between two plates which were subjected to 11V, 1.3A for 7 minutes.

2.5.5 Ponceau S staining and blocking

Ponceau S staining of total protein was used as a loading control as described by Romero-Calvo *et al*. (2010). After transfer, the membrane was washed in dH_2O before staining in Ponceau S (Sigma) for 8 minutes. The membrane was briefly washed in dH_2O and an image of the blot was captured using an imager (ChemiDoc, Biorad**)**. The stain was washed away using dH_2O and the membrane was incubated in an appropriate concentration of blocking buffer, consisting of non-fat dried milk (Marvel, Birmingham, UK) or BSA (Sigma) in Tris-buffered saline with 20% Tween (TBST) for 1 hour at room temperature on a roller.

2.5.6 Incubation with antibodies

After blocking, the membrane was incubated overnight at 4°C with the appropriate primary antibody. The membrane was washed with TBST three times for 3 minutes. An

enhanced chemiluminescence (ECL) donkey anti-rabbit or sheep anti-mouse IgG HRP-linked secondary antibody (GE Healthcare, Amersham, UK) at an appropriate dilution in blocking buffer was incubated with the membrane for 1 hour at room temperature. The secondary antibody used depended on the species from which the primary antibody was raised. The membrane was washed again in TBST. Detection occurred after the application of ECL substrate (Clarity Western ECL Substrate, Biorad) to the membrane for 1 minute, which omitted light upon its reaction with the antibody complex forming a visible band. The membrane was exposed in an imager (ChemiDoc, Biorad) and the length of time of exposure differed between antibodies and tissues analysed. Densitometry on the protein bands was carried out using Image Lab software (Biorad).

All of the samples were analysed across four gels which were run and transferred together, to minimise variation. A single control sample was run on each of the gels and the results of this control sample were used to standardise the values obtained from all of the membranes. After densitometry and normalisation to total protein, the results were standardised to the mean of the sham group at 129dGA. Results are therefore expressed as fold changes in arbitrary units (au).

2.6 Statistical analysis

All values are expressed as mean ± standard error of the mean (SEM) unless otherwise indicated. Statistical comparison between two groups was assessed by Students unpaired t-test. When analysing groups with more than one factor, comparisons were assessed using a two or three-way analysis of variance test (ANOVA), using treatment, age and/or sex as factors, followed by the Tukey *post hoc* test (Sigmastat 3.5, Systat Software, Chicago, USA). Correlations were assessed using linear regression. In all cases, significance was accepted at $P<0.05$. Normality of data was assessed using the Kolmogorov-Smirnov test prior to each statistical comparison (Sigmastat 3.5). If data presented as non-normal, it was transformed into $\log_{10}$ and a normal distribution.

For the ovine studies *in vivo*, to achieve 80% power at the 5% significant level, a sample size of 7 would be required to find a mean difference in plasma insulin concentrations

of 1.31ng/ml, assuming a standard deviation of 0.81ng/ml (Holleran & Ramakrishnan, 2003; Rosner & Rosner, 2010). This sample size determination is based on a t-test and a standard deviation from previous studies examining the effects of dexamethasone treatment on fetal glucogenic capacity (Franko *et al.*, 2007). An additional two fetuses were added to the cohort to account for fetal loss.

3 EFFECTS OF HYPOTHYROIDISM ON FETAL GROWTH AND PANCREATIC ISLET DEVELOPMENT

3.1 Introduction

Thyroid hormones have an important role in fetal growth and maturation *in utero*. Reduced fetal thyroid hormones concentrations have previously been reported in IUGR in human and guinea pig models (Jones *et al.*, 1984; Kilby *et al.*, 1998). Hypothyroidism *in utero* in humans and sheep can induce low birth weight and reduced body lengths (Hopkins & Thorburn, 1972; LaFranchi, 2011). Fowden and Silver (1995) reported that thyroidectomy in the sheep fetus in late gestation led to decreases in body weight and crown-rump length. It has also been shown that thyroid hormones are important not only in the control of overall body growth, but also in tissue-specific development. Developmental abnormalities in the hypothyroid sheep fetus are seen in multiple systems such as the skeletal system, the kidneys, and the heart (Finkelstein *et al.*, 1991; Lanham *et al.*, 2011; Chattergoon *et al.*, 2012a).

The actions of thyroid hormones on fetal growth and development may be direct and/or indirect as thyroid hormones are able to influence other endocrine systems. Thyroidectomy has previously been shown to change the availability of hormones and growth factors *in utero*, such as leptin and the IGFs (Ramos *et al.*, 1998; Iglesias *et al.*, 2001; Ramos *et al.*, 2001; O'Connor *et al.*, 2007). Insulin is a potent growth hormone in the fetus (Taniguchi *et al.*, 2006; Bloomfield *et al.*, 2013), however, the role of the thyroid hormones in the development of the insulin producing β-cells in the pancreatic islets of Langerhans before birth remains unknown.

The aims of the study were therefore to identify the effects of hypothyroidism induced by fetal thyroidectomy on (1) the circulating concentrations of insulin, cortisol, leptin and the IGFs, (2) fetal biometry and (3) the development of α- and β-cell mass in the fetal pancreas. Delivery of fetuses and collection of tissues took place at either 129 or 143dGA, to ascertain the effects of hypothyroidism over the period of the normal surge in plasma T3 close to term. It was hypothesised that thyroid hormone deficiency in the

sheep fetus during late gestation causes growth retardation due to a decrease in circulating insulin concentration as a result of a decreased pancreatic β-cell mass.

3.2 Methods

3.2.1 Animals

All animals, treatments and post mortem procedures are described in Section 2.1. Four treatment groups were analysed: TX at 129dGA (n=9), sham at 129dGA (n=9), TX at 143dGA (n=10) and sham at 143dGA (n=10). After the collection of 10ml blood from the umbilical artery into tubes containing EDTA, samples were centrifuged for 5 minutes at 1000g at 4°C. Plasma from the samples was extracted and aliquots stored at -20°C.

After the administration of a lethal dose of barbiturate (Section 2.1.2), each fetus was weighed, the sex noted and measurements of fetal biometry performed, including measurements of crown-rump length, abdominal circumference, limb lengths and organ weights. Limbs were divided into hind leg and front leg regions. From the organ weights, the percentage mass relative to the body weight of the fetus was calculated (organ mass divided by fetal body weight and expressed as a percentage). The fetal pancreas was collected and immersed in 4% formalin for wax embedding (Section 2.3.1).

3.2.2 Plasma hormone concentrations

Concentrations of T3, T4, insulin, cortisol, IGFs and leptin were measured in the plasma aliquots. Plasma insulin, cortisol, T3 and T4 concentrations were determined by ELISA and RIA using kits validated for ovine serum (Section 2.2). Plasma concentrations of IGF-I, IGF-II and leptin were measured using RIA by Dr Dominique Blache, School of Animal Biology, University of Western Australia as described in Section 2.2.

3.2.3 Pancreas stereology

Exhaustive pancreas sectioning

Wax embedded pancreases were sectioned using a rotary microtome according to the methods described by Bock *et al*. (2003, 2005). To determine stereologically the fetal

pancreatic α- and β-cell mass, each pancreas was exhaustively sectioned using a section thickness of 5µm.

With a random start between 1 and 100, every 100th section was sampled. The random number read from a random number table was 84, and therefore sections 84, 184, 284, 384 etc. were sampled. The first section was counted from when the tissue was first hit by the microtome blade. At least 10 evenly-spaced sections were required from each pancreas. As every section was 5µm thick, it was calculated that there was a distance of 500µm between the sections (Figure 3.1). Cut sections were gently placed into a warm water bath and then manoeuvred onto a poly-l-lysine coated glass slides (Section 2.3.2). The slides were left to dry on a warm heat block.

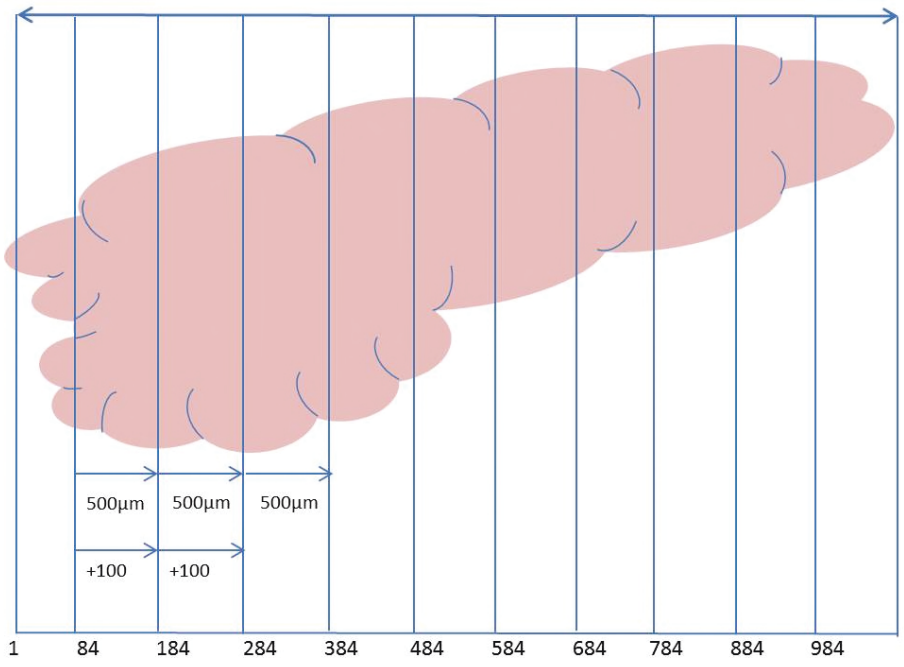

Figure 3.1. A schematic diagram of exhaustive sectioning used in pancreas stereology. The sections were collected from number 84 at intervals of 100 sections which equates to a distance of 500µm apart.

Immunohistochemistry

Immunohistochemistry was used to localise insulin and glucagon containing cells as described in detail in Section 2.4. Preliminary trials showed that an antigen retrieval step was not required for either insulin or glucagon labelling. The blocking solution consisted of 5% horse serum in 2% BSA in PBS.

Following blocking, sections were incubated with either a mouse monoclonal anti-insulin antibody (1:1000 whole serum; Sigma) or a mouse monoclonal anti-glucagon antibody (1: 1000 whole serum; Sigma) for one hour at 37°C. The blocking solution was used on one section as a negative control. The secondary antibody consisted of a mouse anti-IgG antibody in a vehicle solution containing horse serum in PBS (Section 2.4.3). The method of detection is described in Section 2.4.4.

Relative α-cell and β-cell mass

Relative α- and β-cell mass was determined using the Cavalieri principle, a stereological method used to estimate volume (Gundersen & Jensen, 1987; Howard & Reed, 2010). Analysis was conducted using NewCAST stereological software (Visiopharm, Hoersholm, Denmark). Using meander sampling, the immunolabelled pancreas was investigated using systematic uniform random sampling (SURS). Starting at a random position within the region of interest, the software generated fields of view at fixed step lengths in x and y directions. The magnification at analysis was x200.

A point counting grid containing 100 (α-cells) or 36 points (β-cells), of which a sub-set of 8 were circled, was applied over the sections and an α- or β-cell was counted when a point overlaid a brown coloured cell. Simultaneously, the pancreatic tissue (exocrine and endocrine tissue) was counted when one of four yellow-circled points overlaid the tissue (Figure 3.2). Adipose tissue, blood vessels, lymph nodes and connective tissue were counted alongside exocrine and endocrine pancreatic tissue as total tissue by the other sub-set of purple-circled points. Over the whole section, approximately 9% of the tissue was sampled and assessed. The sections were analysed blind to the treatment group.

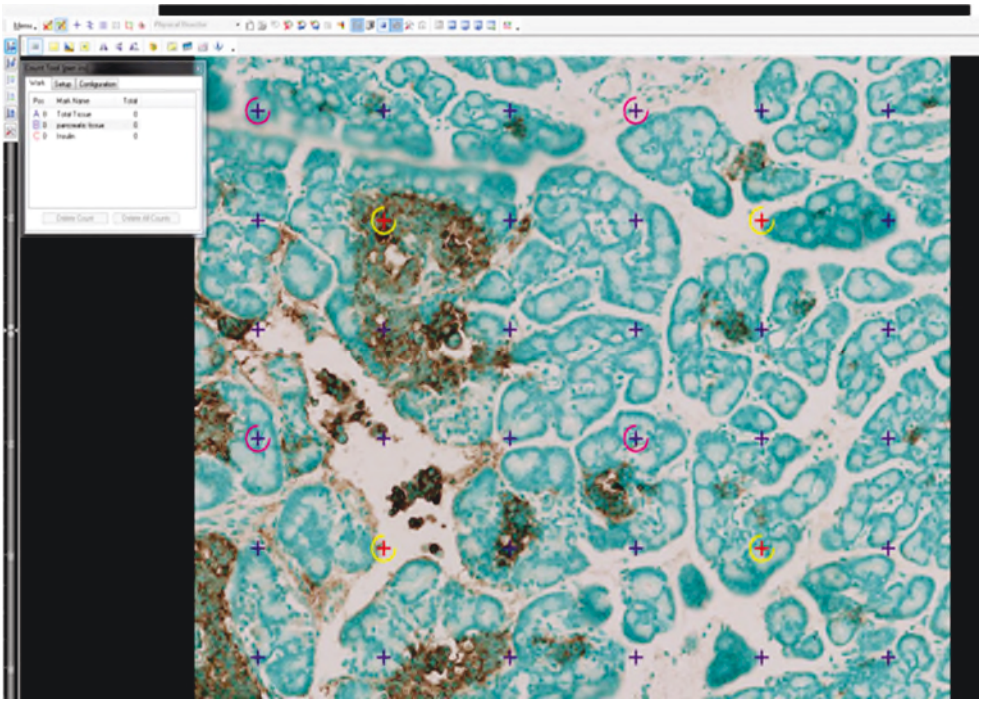

Figure 3.2. Counting grid used in meander sampling of α- and β-cells in pancreas sections. A α- or β-cell is counted when a purple '+' overlays brown (DAB) labelling of insulin or glucagon. Total tissue is counted when the pink circled '+' overlay pancreatic, fat or connective tissue, and pancreatic tissue (exocrine and endocrine) is counted when underneath yellow circled '+'.

The values for the total volume of the pancreas and the α- and β-cells (Vol_{est}) were calculated by the Cavalieri principle (Equation 3.1):

$$Vol_{est} = \frac{t \times {}^{a}/_{p} \times \sum p}{asf}$$

Equation 3.1.

Where t = distance between sections, a/p = area associated with each point, ∑p = sum of counts and asf = fraction of the section sampled. The volume of α- and β-cells was divided by the volume of total tissue to obtain the percentage of the pancreas occupied by each islet cell. The absolute and relative islet cell masses were calculated using the following formula:

$$\text{Relative islet cell mass} = \frac{(\text{Pancreas weight (mg)} \times \%\ \text{islet cells of total tissue})}{\text{Fetal body weight (kg)}}$$

Equation 3.2.

Only a subset of 20 animals (n=5 in each treatment group) was analysed for α-cell mass. From the results obtained, a power analysis test (Holleran & Ramakrishnan, 2003) identified that statistical significance for relative α-cell mass would only be achieved after sampling a total of 240 animals (n=60 in each group).

Stereological statistics

Because of the unbiased nature of the Cavalieri principle, the coefficient of variation (CV) uses a predictive formula that accounts for the systematic nature of sampling. The CV is a function of two independent factors.

1. Noise effect: This is the point counting variance and represents the independent variance of each estimate (Pi). It reports the variance of point counting and indicates how much the overall estimate would change if the counting grid was placed differently on the section.

$$\mathrm{CV_{noise}} = 0.0724 \times \frac{\bar{\mathrm{B}}}{\sqrt{\bar{\mathrm{A}}}} \times \sqrt{\mathrm{n} \times \sum \mathrm{P}}$$

Equation 3.3.

Where $\sum \mathrm{P}$ = sum of points, n = number of sections (sample size), $\frac{\bar{\mathrm{B}}}{\sqrt{\bar{\mathrm{A}}}}$ = the shape coefficient. The shape coefficient takes into account the complexity of the shape of the section and is assigned a number (Gundersen & Jensen, 1987). It can be estimated from a nomograph or, in calculated terms, it is the boundary length (B) divided by the square root of the sampling area (A; Howard & Reed, 2010).

2. Variance of ∑area: For a given direction of sectioning, this variance is a function of the number of sections. It computes the variance under SURS (Gundersen *et al.*,

1999). The more variable a structure is in the direction of sectioning, the more sections are required to accurately measure volume.

$$\mathrm{Var}_{\mathrm{SURS}(\sum \mathrm{area})} = (3\,(\mathrm{A} - \mathrm{CV}_{\mathrm{noise}}) - 4\mathrm{B} + \mathrm{C}) \div 240$$
$$\mathrm{A} = \sum_{\mathrm{i}=1}^{\mathrm{m}} \mathrm{P_i} \times \mathrm{P_i}$$
$$\mathrm{B} = \sum_{\mathrm{i}=1}^{\mathrm{m}-1} \mathrm{P_i} \times \mathrm{P_{i+1}}$$
$$\mathrm{C} = \sum_{\mathrm{i}=1}^{\mathrm{m}-2} \mathrm{P_i} \times \mathrm{P_{i+2}}$$

Equation 3.4.

Where, Pi = number of points per section. Therefore, $\sum_{\mathrm{i}=1}^{\mathrm{m}} \mathrm{P_i}$ = the sum of the point counts from all sections in one animal. Thus, the overall CV is calculated as:

$$\text{Total Variance of } \sum \mathrm{P} = \mathrm{CV}_{\mathrm{noise}} + \mathrm{Var}_{\mathrm{SURS}}$$
$$\mathrm{CV}\ (Vol_{est}) = \frac{\sqrt{\text{Total Variance}}}{\sum \mathrm{P}}$$

Equation 3.5.

Therefore, more sections and more counts result in less variability. Approximately 150-200 points over 8 sections is usually enough to produce a CV of less than 3%. All of the samples had a CV of less than 3%.

3.2.4 Statistical analysis

All values are expressed as mean ± standard error of the mean (SEM) unless otherwise indicated. Initially, statistical significance for comparisons between the groups was assessed using a three-way ANOVA, using treatment, gestational age and sex as factors, followed by the Tukey *post hoc* test. As there was no effect of sex in any results, statistical significance was assessed by two-way ANOVA using treatment and gestational age as factors, followed by the Tukey test. Correlations were assessed using linear regression. For comparison between two groups, a Student's unpaired t-test was used. In all cases, significance was accepted at $P<0.05$.

3.3 Results

3.3.1 Plasma hormone concentrations

T4 and T3

In the TX fetuses, plasma T4 and T3 concentrations decreased to below, or close to, the limit of assay detection (T3, 0.067ng/ml; T4, 7.6ng/ml) at both 129dGA and 143dGA (Figure 3.3A-B). In both cases, these were significantly lower than the sham controls (P<0.05). In the sham fetuses, plasma concentrations of T3 at 143dGA were significantly greater than those at 129dGA (Figure 3.3B), indicative of the normal pre-partum surge.

Insulin

The TX fetuses had significantly higher plasma insulin concentrations than the sham fetuses at both 129dGA (sham 30.1 ± 9.4ng/L vs TX 129.4 ± 31.3ng/L, P<0.05) and at 143dGA (sham 55.7 ± 12.0ng/L vs TX 167.9 ± 19.3ng/L, P<0.05, Figure 3.3C). There was no effect of gestational age on plasma insulin concentrations in either treatment group.

Cortisol

Plasma cortisol concentrations were significantly higher in the fetuses studied at 143dGA (sham 54.9 ± 12.7ng/ml; TX 28.7 ± 3.9ng/ml) compared with the fetuses at 129dGA (sham 12.6 ± 3.1ng/ml; TX 9.8 ± 1.5ng/ml, P<0.05, Figure 3.3D). At 143dGA, the TX fetuses tended to have lower cortisol levels compared to sham controls (P=0.06, Figure 3.3D). When data from the fetuses at 143dGA were analysed alone by Student's t-test, plasma cortisol concentrations in the TX fetuses were significantly lower than those in the sham controls (P<0.01).

Leptin, IGF-I and IGF-II

Plasma concentrations of leptin were significantly greater in the TX fetuses compared to the sham fetuses at both 129dGA (sham 517 ± 32pg/ml vs TX 983 ± 58pg/ml, P<0.05) and 143dGA (sham 669 ± 47pg/ml vs TX 1046 ± 79pg/ml, Figure 3.4A). There was no effect of gestational age on plasma leptin concentrations in either treatment group.

Neither gestational age nor thyroidectomy altered the umbilical plasma concentrations of IGF-I or IGF-II at delivery (Figure 3.4B, C).

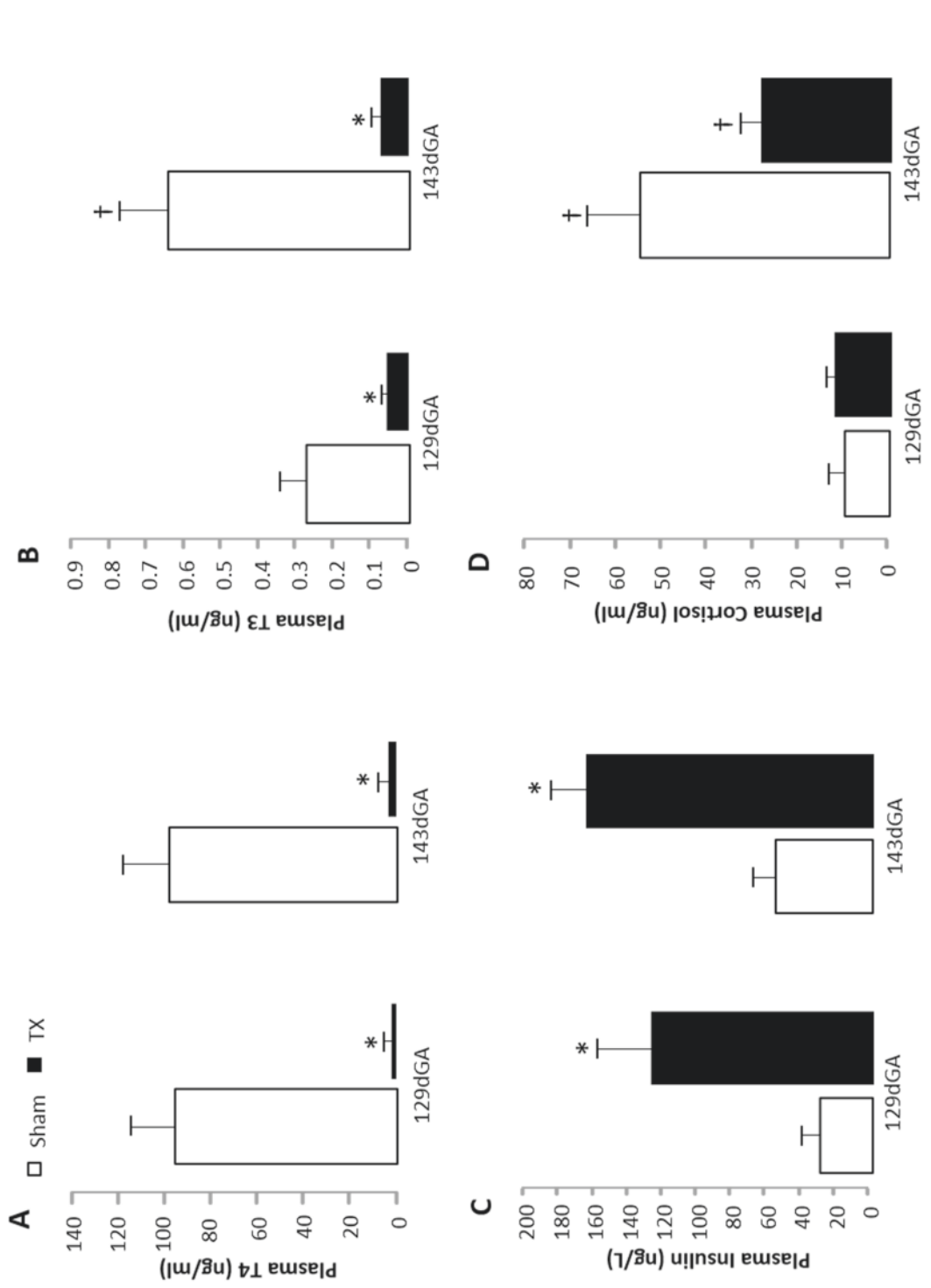

Figure 3.3. Mean ± SEM plasma concentrations of (A) T4, (B) T3, (C) insulin and (D) cortisol in TX and sham fetuses at 129dGA and 143dGA. † Significantly different from fetuses in the same treatment group at 129dGA. * Significantly different from sham fetuses at the same dGA, 2-way ANOVA, $P<0.05$. n = 8-10 fetuses in each group.

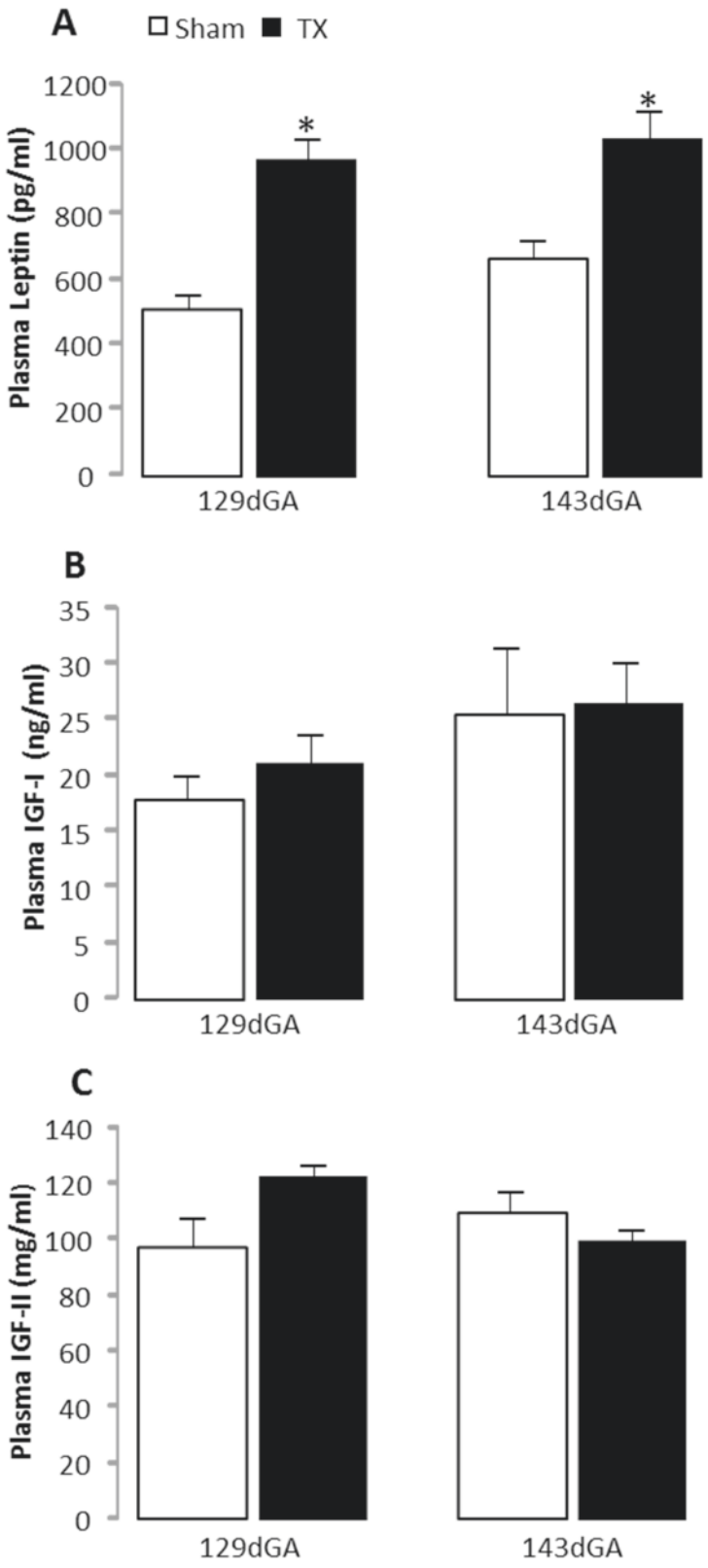

Figure 3.4. Mean ± SEM plasma concentrations of (A) leptin (B) IGF-I and (C) IGF-II in sham and TX fetuses at 129dGA and 143dGA. * Significantly different from sham fetuses at the same dGA, 2-way ANOVA, $P<0.05$. n = 9-10 in each group.

3.3.2 Fetal morphometry and organ weights

Fetal body weight, crown-rump length and abdominal circumference remained unaltered by fetal thyroidectomy at both 129 and 143dGA. In the sham and TX fetuses, there was a significant increase in these parameters at 143dGA compared to the younger fetuses at 129dGA (P<0.05 in all cases; Table 3.1).

In the skeletal system, all of the limb bones that were measured displayed growth retardation in the TX fetuses at 143dGA in comparison to the sham controls (P<0.05 in all cases; Table 3.1). At 129dGA, three of the six bones measured were significantly growth retarded in the TX fetuses compared to controls. The mass (relative to fetal body weight) of the biceps femoris was significantly enlarged in the TX fetuses compared to controls at 143dGA (P<0.05; Table 3.1). The relative mass of the soleus and semitendinosus remained unchanged in the TX fetus at both 129 and 143dGA, and there was no effect of gestational age on these muscle weights in either treatment group.

The lungs, heart, stomach and small intestine were growth retarded in the TX fetuses compared to sham fetuses at both gestational ages studied (P<0.05 in all cases; Table 3.2). The relative mass of the perirenal adipose tissue and the pituitary gland, however, were significantly enlarged in the TX fetuses at both 129 and 143dGA (P<0.001). Additionally, the relative mass of the kidneys was significantly increased in the TX fetus at 143dGA (P<0.01). There were no changes in the relative mass of the pancreas, liver, testes, ovaries or adrenal gland with treatment or gestational age (Table 3.2). No thyroid gland was found in the TX fetuses.

Table 3.1. Mean ± SEM measurements of biometry and components of the musculoskeletal system in sham and TX sheep fetuses at post mortem.

Body measurements	129 dGA		143 dGA	
	Sham (n=9)	TX (n=9)	Sham (n=10)	TX (n=10)
Body Weight (kg)	2.61 ± 0.20	2.49 ± 0.20	3.58 ± 0.23†	3.13 ± 0.13†
Crown Rump Length (cm)	43.6 ± 1.1	42.1 ± 1.0	48.3 ± 1.1†	45.7 ± 0.7†
Abdominal Circumference (cm)	30.8 ± 0.9	29.6 ± 1.2	34.9 ± 0.9†	33.5 ± 0.7†
Hind Limb Femur (cm)	9.8 ± 0.4	8.9 ± 0.3	11.3 ± 0.4†	10.2 ± 0.3†*
Hind Limb Tibia (cm)	12.8 ± 0.5	11.8 ± 0.3	14.8 ± 0.4†	13.7 ± 0.2†*
Hind Limb Metatarsal (cm)	15.1 ± 0.5	13.3 ± 0.4*	17.0 ± 0.5†	15.0 ± 0.3†*
Front Limb Humerus (cm)	8.4 ± 0.2	7.8 ± 0.2	9.6 ± 0.3†	8.5 ± 0.3*
Front Limb Radius (cm)	10.4 ± 0.2	9.4 ± 0.2*	11.7 ± 0.3†	10.7 ± 0.2†*
Front Limb Metacarpal (cm)	12.7 ± 0.4	11.2 ± 0.3*	14.6 ± 0.3†	12.6 ± 0.3†*
Absolute skeletal muscle weight (g)				
Semitendinosus	3.90 ± 0.35	3.77 ± 0.34	5.45 ± 0.42†	5.34 ± 0.28†
Biceps Femoris	11.55 ± 0.84	11.80 ± 0.87	14.80 ± 1.29†	14.63 ± 0.84†
Soleus	1.67 ± 0.13	1.60 ± 0.14	2.29 ± 0.22†	2.08 ± 0.12†
Skeletal muscle weight relative to body weight (%)				
Semitendinosus	0.149 ± 0.008	0.151 ± 0.006	0.151 ± 0.005	0.171 ± 0.007
Biceps Femoris	0.444 ± 0.012	0.476 ± 0.011	0.410 ± 0.017	0.467 ± 0.015*
Soleus	0.064 ± 0.002	0.064 ± 0.002	0.064 ± 0.004	0.066 ± 0.002

† Significantly different from fetuses in the same treatment group at 129dGA. * Significantly different from sham fetuses at the same dGA, 2-way ANOVA, $P<0.05$.

Table 3.2. Mean ± SEM organ weights in sham and TX sheep fetuses at post mortem.

Absolute organ weights (g)	129 dGA		143 dGA	
	Sham (n=9)	TX (n=9)	Sham (n=10)	TX (n=10)
Heart	16.4 ± 1.2	12.2 ± 0.8*	21.9 ± 1.6†	16.4 ± 0.8*†
Lungs	73.1 ± 4.8	58.3 ± 4.6	93.2 ± 9.42†	71.59 ± 5.6*
Liver	72.0 ± 7.7	69.2 ± 7.6	78.7 ± 5.7	90.3 ± 5.4†
Kidneys	15.4 ± 0.8	16.8 ± 1.5	18.7 ± 1.6	19.7 ± 1.3
Pancreas	2.2 ± 0.2	2.3 ± 0.2	2.9 ± 0.2†	2.8 ± 0.2
Empty stomach	20.5 ± 1.9	17.6 ± 1.2	28.9 ± 1.6†	21.5 ± 0.9*
Small intestine	48.6 ± 6.4	34.5 ± 3.5	83.9 ± 6.4†	42.7 ± 3.2*
Perirenal adipose	9.9 ± 0.6	12.7 ± 1.4	10.9 ± 1.1	14.7 ± 1.1*
Brain	42 ± 1.0	41 ± 1.0	49 ± 1.0†	44 ± 2.0
Pituitary (mg)	86 ± 6	123 ± 11.0*	96 ± 9.0	148 ± 11.0*
Adrenals (mg)	304 ± 20	305 ± 40	417 ± 42	372 ± 21
Testes (mg)	834 ± 48 (n=5)	915 ± 116 (n=6)	1175 ± 106 (n=6)	1058 ± 102(n=6)
Ovaries (mg)	52 ± 6 (n=4)	52 ± 10 (n=3)	69 ± 6 (n=4)	80 ± 8 (n=4)
Thyroids (mg)	514 ± 47	NP	606 ± 72	NP
Organ weights relative to body mass (%)				
Heart	0.633 ± 0.03	0.520 ± 0.01*	0.612 ± 0.02	0.527 ± 0.02*
Lungs	2.86 ± 0.18	2.36 ± 0.08*	2.55 ± 0.12	2.29 ± 0.15*
Liver	2.85 ± 0.36	2.73 ± 0.17	2.20 ± 0.07	2.94 ± 0.22
Kidneys	0.603 ± 0.03	0.682 ± 0.04	0.525 ± 0.03	0.628 ± 0.03*
Pancreas	0.086 ± 0.005	0.093 ± 0.005	0.081 ± 0.005	0.089 ± 0.004
Empty stomach	0.81 ± 0.04	0.72 ± 0.02*	0.82 ± 0.02	0.69 ± 0.03*
Small intestine	2.00 ± 0.19	1.35 ± 0.07*	2.34 ± 0.07†	1.36 ± 0.08*
Perirenal adipose	0.39 ± 0.03	0.52 ± 0.05*	0.31 ± 0.03	0.48 ± 0.04*
Brain	1.68 ± 0.12	1.72 ± 0.14	1.44 ± 0.09	1.42 ± 0.05†
Pituitary	0.003 ± 0.001	0.005 ± 0.001*	0.003 ± 0.001	0.005 ± 0.001*
Adrenals	0.012 ± 0.001	0.012 ± 0.001	0.011 ± 0.001	0.011 ± 0.001
Testes	0.031 ± 0.002 (n= 5)	0.036 ± 0.003 (n=6)	0.032 ± 0.001 (n= 6)	0.034 ± 0.003 (n=6)
Ovaries	0.0035 ± 0.0003 (n=4)	0.0025 ± 0.0005 (n=3)	0.0020 ± 0.0001 (n=4)	0.0025 ± 0.0002 (n=4)
Thyroids	0.020 ± 0.001	NP	0.017 ± 0.001	NP

† Significantly different from fetuses in the same treatment group at 129dGA. * Significantly different from sham fetuses at the same dGA, 2-way ANOVA, $P<0.05$. NP = not present.

3.3.3 Pancreatic islet mass

Immunohistochemistry was successful in labelling pancreatic insulin and glucagon-containing cells. Insulin was localised mainly in large islets of the pancreas in sham and TX fetuses at both 129 and 143dGA with some labelling in smaller clusters of cells spread throughout the tissue (Figure 3.5A, C, E, G). Glucagon, however, was more sparse compared to insulin in both sham and TX fetuses and was localised in islets alongside insulin or within exocrine tissue, especially around ducts and blood vessels (Figure 3.5B, D, F, H).

α-cell mass

The percentage volume of α-cells in pancreatic tissue was increased in the hypothyroid fetuses compared to the sham controls at 129dGA only (sham 1.8 ± 0.1% vs TX 3.1 ± 0.4%, $P<0.05$). There was no difference in percentage volume in pancreatic tissue between sham and TX fetuses at 143dGA (sham 1.7 ± 0.3 vs TX 2.3 ± 0.2%). The volume of α-cells in total tissue was no different in TX fetuses compared to controls at 129 and 143dGA (Figure 3.6A). There was no effect of gestational age on either parameter.

When adjusted for pancreas mass, there was no effect of thyroidectomy or gestational age on the absolute α-cell mass at either 129 (sham 37.3 ± 7.0mg vs TX 43.3 ± 7.0mg) or 143dGA (sham 41.4 ± 6.8mg vs TX 44.2 ± 4.1mg, Figure 3.6B). Additionally, when adjusted for fetal body weight, there was no change in the relative α-cell mass at either gestational age (129dGA: sham 12.6 ± 1.9mg/kg vs TX 15.1 ± 2.3mg/kg; 143dGA: sham 11.7 ± 0.9mg/kg vs TX 14.5 ± 1.4mg/kg, Figure 3.6C). Gestational age had no effect on either absolute or relative α-cell mass.

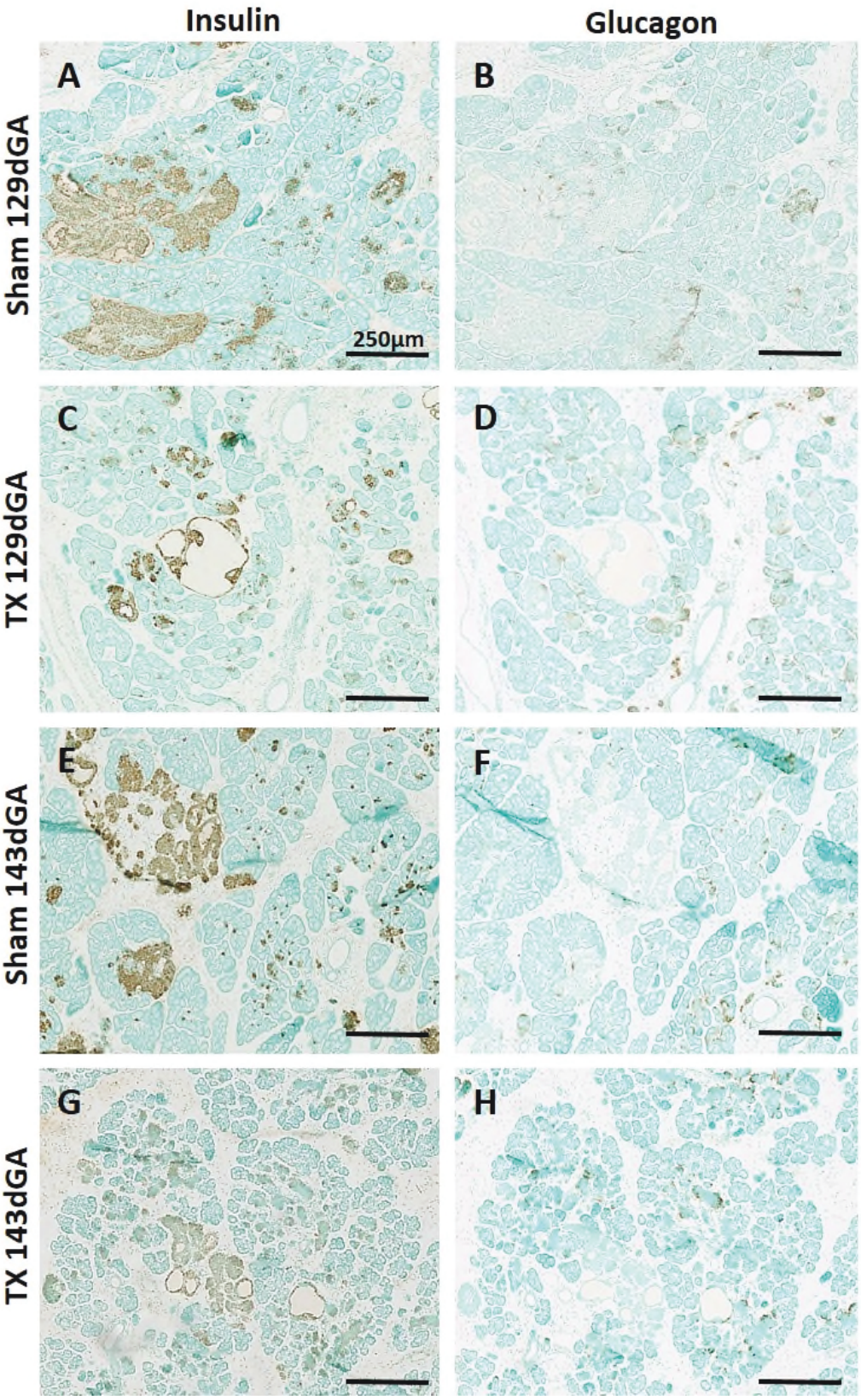

Figure 3.5. Sections of pancreas labelled with insulin and glucagon (brown) in sham and TX fetuses at 129 and 143dGA. Insulin and glucagon in a sham fetus (A, B) and TX fetus (C, D) at 129dGA. Insulin and glucagon in a sham (E, F) and TX fetus (G, H) at 143dGA. Scale bar 250µm.

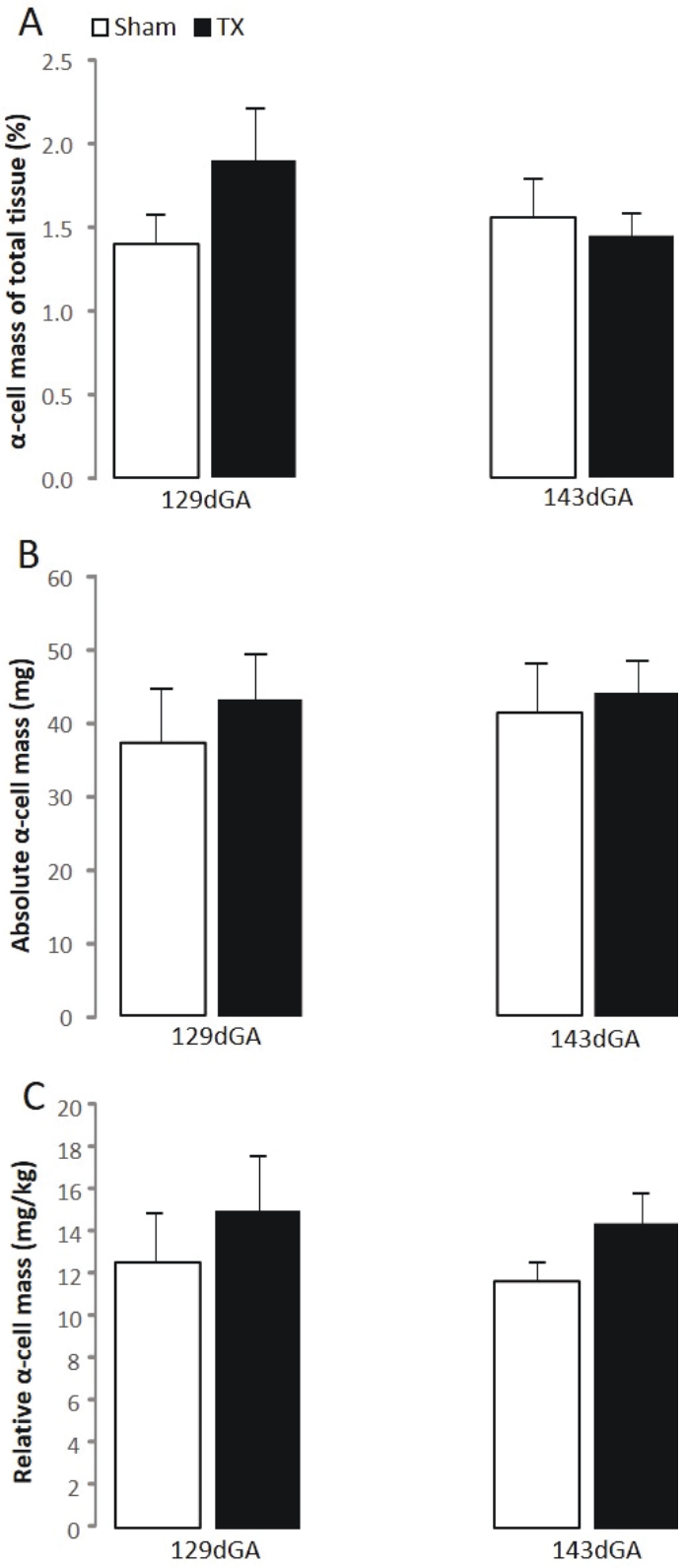

Figure 3.6. Mean ± SEM pancreatic α-cell mass expressed as (A) % of total tissue, (B) absolute α-cell mass and (C) relative α-cell mass per kg of fetus. n = 4-5 fetuses in each group.

β-cell mass

The percentage volume of β-cells on pancreatic tissue was increased in the TX fetuses at both 129 (sham 6.0 ± 0.5% vs TX 10.4 ± 0.8%, *P*<0.05) and 143dGA (sham 6.7 ± 0.8% vs TX 11.0 ± 1.0%, *P*<0.05) compared to controls. The fractional volume of β-cells in total tissue was increased at 129dGA in TX fetuses compared to sham controls (sham 3.6 ± 0.4% vs TX 6.2 ± 0.5%, *P*<0.05, Figure 3.7A). There was no effect of gestational age on β-cell volume in pancreatic or total tissue.

The absolute β-cell mass tended to be greater in the TX fetuses than in the sham controls at both 129 (sham 92.3 ± 24.1mg vs TX 144.6 ± 23.5mg) and 143dGA (sham 143.9 ± 20.9mg vs TX 183.4 ± 26.8mg, *P*=0.08, Figure 3.7B). In the sham fetuses at 143dGA, there was a significant increase in the absolute β-cell mass compared to the younger fetuses at 129dGA (*P*<0.05, Figure 3.7B). This effect of gestational age was not evident in the TX fetuses.

When adjusted for pancreas mass and fetal body weight, it was identified that the relative β-cell mass was significantly increased in the TX fetuses compared to the sham controls at both 129 (sham 35.0 ± 7.6mg/kg vs TX 55.4 ± 5.9mg/kg, *P*<0.05) and 143dGA (sham 39.7 ± 3.7mg/kg vs TX 58.3 ± 6.9mg/kg, *P*<0.05) by 40% and 30% respectively (Figure 3.7C). There was no effect of gestational age on the relative β-cell mass in either treatment group. Plasma insulin concentrations in the sham and TX fetuses were positively correlated with relative β-cell mass (R=0.50, R^2=0.25, n=36, *P*<0.005, Figure 3.8). There was no correlation between relative β-cell mass and plasma concentrations of cortisol or leptin.

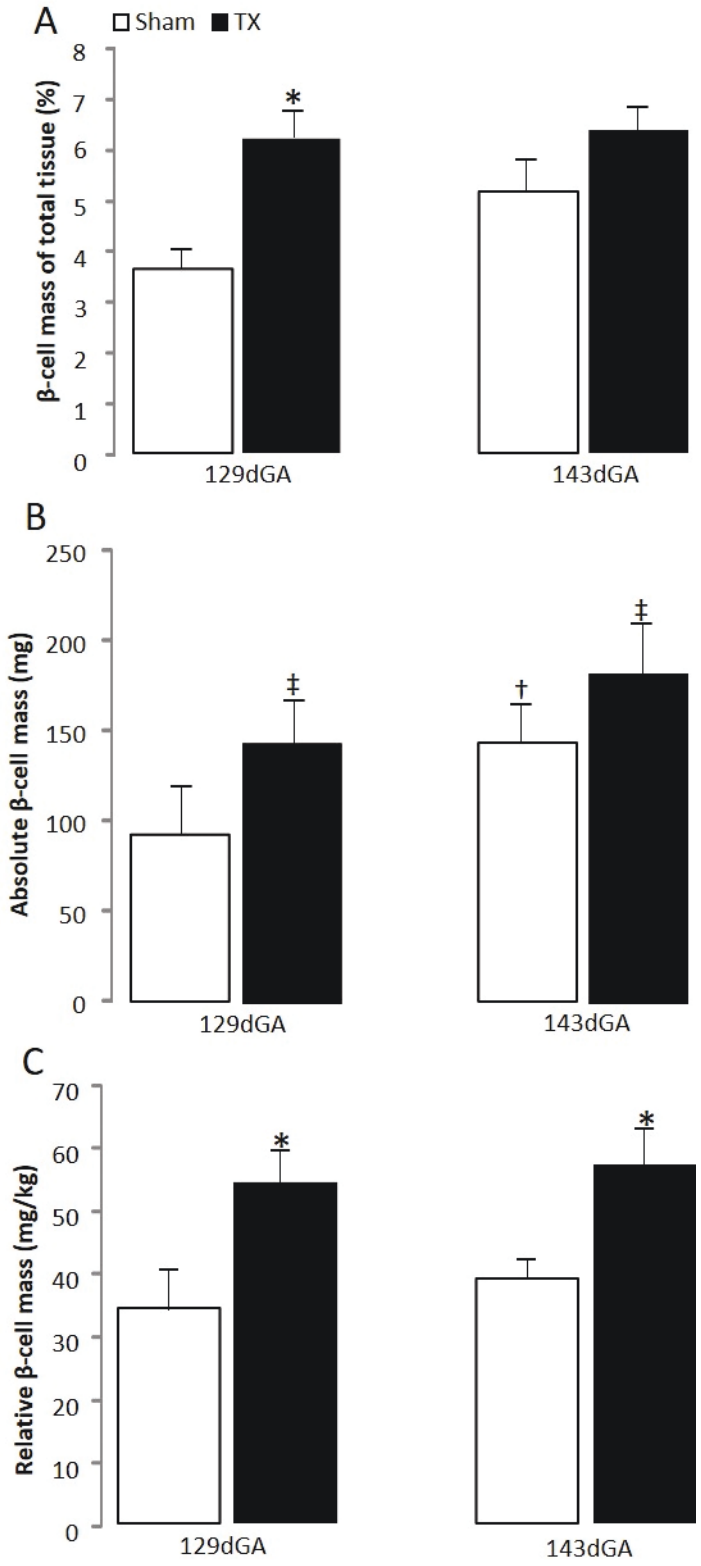

Figure 3.7. Mean ± SEM pancreatic β-cell mass expressed as (A) % of total tissue, (B) absolute β-cell mass and (C) relative β-cell mass per kg of fetus. * Significantly different from sham fetuses at the same dGA, $P<0.05$. ‡ Different from sham fetuses at the same dGA, $P=0.08$. † Significantly different from fetuses in the same treatment group at 129dGA, 2-way ANOVA, $P<0.05$. n = 9-10 fetuses in each group.

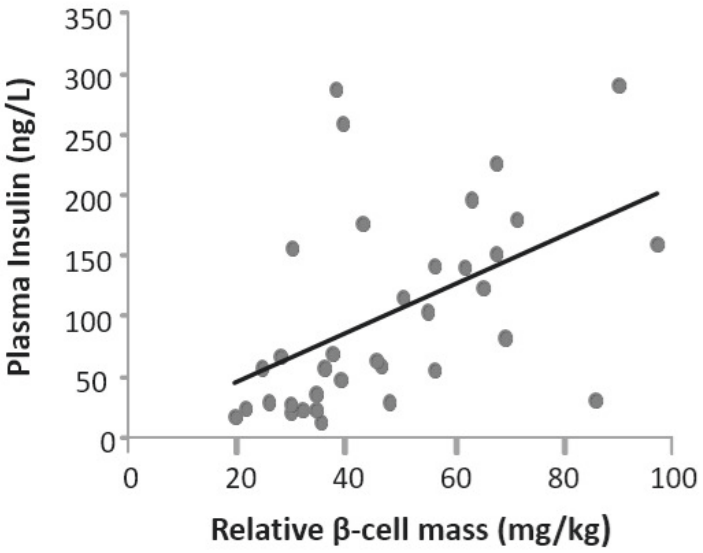

Figure 3.8. The positive correlation between plasma insulin concentrations and relative β-cell mass in all fetuses. n =36, R= 0.50, R^2 = 0.25, *P*<0.005.

3.4 Discussion

This study has shown for the first time, and contrary to the original hypothesis, that thyroid hormone deficiency in the ovine fetus caused a 30-40% increase in pancreatic β-cell mass and a concomitant rise in circulating insulin concentration *in utero*. These changes were also associated with normal bodyweight but impaired skeletal growth and disproportionate organ growth patterns.

3.4.1 Plasma hormones in hypothyroidism

Plasma T3 and T4 concentrations in the TX fetuses were at or below assay detection, and significantly lower than those in the sham controls at both 129 and 143dGA. Towards term, the normal rise in plasma T3 seen in the sham fetuses was abolished in the TX fetuses. This demonstrates that the experimental model is effective and that the fetuses which underwent thyroidectomy were hypothyroid.

Residual thyroid hormone levels in the circulation of the TX fetus may be due to ectopic thyroid tissue or fragments of thyroid regrowth not identified at post-mortem. However, detectable thyroid hormone may have arisen from metabolism of the sulphated forms of the thyroid hormones (Wu *et al.*, 1993; Polk *et al.*, 1994). Significant amounts of the sulphated forms have been characterised in the sheep fetus, in which levels peak in the circulation at around 130dGA. Wu *et al*. (1993) identified in TX sheep fetuses that, while the circulating concentrations of sulphated T4 and rT3 decreased, plasma levels of sulphated T3 were maintained for 2 weeks post thyroidectomy.

Plasma cortisol concentrations in the TX fetus were within the normal range and followed the same developmental pattern as that seen in the sham controls. Towards term, an increase in plasma cortisol concentration was observed in both groups of fetuses. However, cortisol levels tended to be lower in the TX fetuses compared to the sham fetuses at 143dGA. Since the prepartum cortisol surge is the trigger for the onset of parturition in sheep, the tendency for TX fetuses to have a lower cortisol concentration at 143dGA may contribute to the prolonged gestation length reported previously in the hypothyroid fetus (approximately 7 days longer; Hopkins & Thorburn, 1972). The TX fetuses therefore may not have been exposed to as much cortisol as their sham counterparts in the last few days before tissue collection. The delay in the prepartum cortisol surge may contribute to the immaturity in fetal organ systems associated with hypothyroidism near term (Forhead & Fowden, 2014).

Plasma insulin concentrations were significantly higher in the hypothyroid fetus at both 129 and 143dGA. A previous study in the sheep fetus during late gestation did not identify any effect of hypothyroidism on plasma insulin concentrations (Fowden & Silver, 1995). However the study of Fowden and Silver did not use twin fetuses as the control group and the insulin ELISA used was less sensitive and did not use species-specific antibodies. The current study is the first report of higher plasma insulin concentration in the TX sheep fetus and suggests that some of the tissue-specific changes in organ growth may be mediated by changes in insulin signalling. An increase in plasma insulin concentration has been reported previously in the TX neonatal mouse and was associated with a reduction in body weight (Ramos *et al.*, 1998). Determination of

plasma glucagon concentrations was attempted with a glucagon ELISA (Mercodia), however the plasma samples were not collected in the correct preservative and the levels of glucagon measured were highly variable and unreliable.

Thyroidectomy in the sheep fetus increased plasma leptin concentrations at both 129 and 143dGA. This finding has been reported previously in hypothyroid fetal sheep, in association with an increase in adipose leptin mRNA (O'Connor *et al.*, 2007). It can be postulated, therefore, that the increase in plasma leptin may be due to both the greater relative mass and secretory capacity of the perirenal adipose tissue. The increase in plasma insulin may also be responsible for the increase in plasma leptin concentrations. Mühlhäusler *et al*., (2007) showed an increase in adipose leptin gene expression in fetuses of over-nourished ewes and that this correlates to plasma insulin *in utero*. Similarly, adipose leptin mRNA and plasma leptin concentrations increase in fetal sheep directly infused with insulin (Devaskar & Anthony, 2002).

It was surprising that there were no changes in the plasma concentrations of IGF-I or IGF-II in the TX fetuses. In the adult human, plasma IGF-I and IGF-II decrease in hypothyroid patients and the levels of plasma IGF-I positively correlate with plasma T3 (Miell *et al.*, 1993). Hypothyroid neonatal mice and rats have decreased circulating IGF-I concentration compared to controls (Ramos *et al.*, 1998; Johnson *et al.*, 2007; Chang *et al.*, 2014) and thyroidectomy in the neonatal mouse results in abolition of the normal decrease in plasma IGF-II that is seen in the controls with age (Ramos *et al.*, 1998). In fetal sheep and pigs, plasma IGF-I levels are reduced by hypothyroidism, and can be restored after thyroid hormone treatment (Mesiano *et al.*, 1987; Latimer *et al.*, 1993). In the sheep fetus during late gestation, thyroidectomy decreases IGF-I mRNA abundance in skeletal muscle, but increases IGF-II mRNA levels in the liver, which may contribute to stable IGF levels in the circulation overall (Forhead *et al.*, 1998; 2002). Changes in plasma IGF levels may not have been seen in this study due to the timing of thyroidectomy and the collection of blood samples. In addition, circulating and tissue IGF binding proteins were not measured, which may influence tissue levels of these growth factors.

3.4.2 Musculoskeletal system in the hypothyroid fetus

This study aimed to elucidate the effects of thyroidectomy on the biometry and overall body growth of the sheep fetus. Previous studies have shown that thyroidectomy in the sheep fetus alters the growth of organs, and bone and skeletal muscle development (Lanham *et al.*, 2011; Chattergoon *et al.*, 2012a; Forhead & Fowden, 2014). The growth retardation observed in fore-limb and hind-limb bones is consistent with a previous study by Lanham *et al*. (2011), in which hypothyroid fetal sheep had reduced limb lengths in association with decreased plasma levels of the non-collagenous protein osteocalcin, a marker of bone deposition. Mouse fetuses with a genetic TSH receptor knockout also demonstrate reduced limb lengths (Bassett *et al.*, 2008). More recently, it was reported that mice with deficient TRα1 show impaired differentiation of chondrocytes, which leads to delayed ossification of bone (Desjardin *et al.*, 2014). This suggested that T3 plays a critical role in chondrocyte proliferation and maturation to promote skeletal growth.

Interestingly, although the bones of the TX fetus were growth retarded, only the relative mass of the biceps femoris was altered by thyroidectomy and this was enlarged at 143dGA relative to sham controls. This is inconsistent with previous data that showed hypothyroidism in fetal sheep reduces myofibre size (Finkelstein *et al.*, 1991). The enlargement of the biceps skeletal muscle in the older fetuses may be due to changes in local IGF synthesis. In fetal sheep during late gestation, there is an ontogenic decrease in IGF-I mRNA in skeletal muscle towards term, which is abolished in hypothyroid fetuses (Forhead *et al.*, 2002). Additionally, the increase in mass of the biceps skeletal muscle may be due to alterations in GLUT4. Neonatal mice which are hypothyroid have increased protein levels of GLUT4 in skeletal muscle, which may indicate increased insulin signalling and glucose uptake and could therefore contribute to the growth of the muscle (Ramos *et al.*, 2001).

3.4.3 Changes in organ mass in the hypothyroid fetus

As expected, fetal thyroidectomy affected the growth of several organs. The heart and the lungs of the hypothyroid sheep fetus were smaller in comparison to sham controls

at both 129 and 143dGA. These findings confirm those from previous studies (Erenberg *et al.*, 1974; Chattergoon *et al.*, 2012a). In fetal sheep, thyroidectomy suppresses the normal maturational response to adrenaline in late gestation to promote lung liquid reabsorption (Barker *et al.*, 1988; 1990). In the fetal lungs, the prepartum surge in plasma T3 is also known to promote alveolar septation (Massaro & Massaro, 2002). In hypothyroid neonatal mice, the lungs display smaller air spaces and have reduced surfactant content, indicating that there are impairments in structural and biochemical maturation (deMello *et al.*, 1994).

Segar *et al*. (2012) previously identified that thyroidectomy in fetal sheep leads to a decrease in the proportion of terminally differentiated cardiomyocytes, without any change in heart mass. This may be because, in their study, the fetal sheep were only hypothyroid for one week and thyroidectomy took place later in gestation at 129dGA. The decrease in heart mass found in the present study is more consistent with that reported in the studies by Chattergoon *et al*. (2012a), in which the hearts of TX fetal sheep at 136dGA were lower in relative mass compared to controls and also had fewer terminally differentiated cardiomyocytes. This suggests that, in the fetal heart, thyroid hormones need to be maintained within a specific range near term to stimulate cell proliferation and to promote the cardiomyocyte differentiation and maturation.

In the present study, the increase in circulating insulin may account, in part, for the different growth patterns seen in the TX fetus as different adaptions may have occurred in response to the deficit in thyroid hormones. This study has highlighted that hypothyroid fetal sheep have an asymmetric pattern of growth and development. The effects of thyroid hormone deficiency on organ mass can either be growth promoting or growth retarding. Deficiency in thyroid hormones *in utero* affected overall body growth and individual organs, and the findings demonstrate that thyroid hormones can exert their effects in a tissue-specific manner. It can be proposed that the tissues from the TX fetuses which are enlarged may demonstrate upregulation in key growth factors or proteins involved in the insulin signalling pathway.

The absolute and relative mass of the pituitary gland was increased in the hypothyroid fetuses at both 129 and 143dGA. This is likely to be due to an increase in the number of pituitary thyrotrophs producing excess TSH, due to the lack of feedback from circulating concentrations of T4 and T3. However, the endocrine cells and secretions of the pituitary gland from thyroid hormone deficient fetuses should be examined to determine this. It has been previously shown that the plasma concentrations of growth hormone, produced by the anterior pituitary, is reduced in hypothyroid sheep fetuses (Richards et al., 1993), although the mechanisms surrounding this suppression are unknown. The pituitary gland also secretes adrenocorticotropic hormone (ACTH) to increase production and release of cortisol from the adrenal gland (Bornstein *et al.*, 2008). As the plasma concentration of cortisol in the TX fetuses tended to be decreased (at 143dGA), it can be postulated that the secretion and action of ACTH may be suppressed. This has previously been reported after thyroidectomy in adult rats (Johnson *et al.*, 2012).

The perirenal adipose tissue of the hypothyroid fetus was enlarged in the TX fetuses compared to sham controls at both 129 and 143dGA. O'Connor *et al*. (2007) has previously reported that TX sheep fetuses have increased adipose mass at 144dGA compared to sham controls. The mechanisms of adipose overgrowth in hypothyroidism *in utero* are largely unknown and will be examined in more detail in Chapter 5.

The kidneys, when relative to fetal body weight, were also larger in the TX fetuses compared to sham controls at 143dGA. Overgrowth of the kidney has been seen previously in hypothyroid fetal sheep (Chattergoon *et al.*, 2012a) but the mechanisms underlying these changes remain unknown. The circulating concentrations of thyroid hormones are known to be reduced in IUGR in mammals (Jones *et al.*, 1984; Kilby *et al.*, 1998) and previous studies in rats of IUGR induced by maternal protein restricted diet have shown decreased kidney mass and nephron number in offspring at birth (Zimanyi *et al.*, 2000). Similarly, a fetal sheep model of natural IUGR from twinning also shows a decrease in nephron number (Mitchell *et al.*, 2004). In the present study, the increase in renal mass that was only seen in the older fetuses could be associated with changes in renal RAS activity which normally increase from 130-136dGA towards term (Chen *et al.*, 2005a). Thyroidectomy in fetal sheep leads to alterations in renin mRNA, total renin

and AT_1R mRNA in the kidney (Forhead & Fowden, 2002; Chen *et al.*, 2005b; 2007). It is possible that the kidney may only be sensitive to the deficiency in thyroid hormones at the later stages of gestation. To ascertain how the kidney has enlarged in the TX fetus, renal structure was determined stereologically and will be discussed in Chapter 6.

3.4.4 Hypothyroidism increased fetal pancreatic β-cell mass

This study has shown for the first time that the hypothyroid sheep fetus has an increased relative pancreatic β-cell mass compared to sham controls at both 129 and 143dGA, without any change in the absolute or relative mass of the pancreas. However, a difference in overall pancreatic mass was unlikely to be seen as β-cells only make up approximately 7% of the total pancreas mass. This is the first report of increased pancreatic β-cell mass in the hypothyroid sheep fetus associated with an increase in circulating insulin concentration. There was no change in the relative α-cell mass in the hypothyroid sheep fetuses at either gestational age, indicating that this is a β-cell specific phenotype.

There is limited knowledge on the direct effects of fetal hypothyroidism on pancreatic β-cell development. Neonatal mice with disruption of pancreatic D3 have smaller pancreases and reduced β-cell mass compared to controls (Medina *et al.*, 2011; 2014), indicating that inactivation of local thyroid hormones by D3 during pancreas development is required for attainment of normal β-cell mass. In contrast to these findings, neonatal rats which are hypothyroid due to maternal hypothyroidism show no alterations in β-cell mass compared to controls (Karbalaei *et al.*, 2014). Furthermore, mouse models of TR deletion do not show any morphological changes in the neonatal pancreas (Mastracci & Evans-Molina, 2014). However, *in vitro* studies using islets cultured from neonatal rodents have shown that TRα1 and TRβ1 are important for normal islet development and proliferation (Aguayo-Mazzucato *et al.*, 2013).

It remains unclear whether the growth in pancreatic β-cell mass in the TX sheep fetus is due to the lack of the thyroid hormones and/or the increased circulating concentrations of insulin and leptin. Fetal rat islets have been shown to express leptin receptors and leptin is able to stimulate islet cell proliferation *in vitro* (Islam *et al.*, 2000). In contrast

to these findings, a two-fold increase in β-cell mass is observed in adult rat islets with a pancreas-specific knockout of the leptin receptor (Morioka *et al.*, 2007). Therefore, previous studies suggest leptin may have a role in β-cell growth; however, effects of leptin on the development of the pancreas in fetal sheep are unknown.

It is possible that the increase in circulating insulin concentration in the TX fetus was due to the increase in relative pancreatic β-cell mass. Indeed for all fetuses, the relative β-cell mass was positively correlated with the plasma insulin concentration. Insulin may act in a positive feedback loop, in which insulin stimulates pancreas growth and further insulin production and secretion. Increased β-cell mass has been reported previously in neonatal mice with upregulation of pancreatic mTOR, which was observed into adulthood (Rachdi *et al.*, 2008). This demonstrates that altering a component of the insulin signalling pathway can have effects on pancreatic growth. Changes in plasma insulin may also be due to alterations in pancreatic β-cell function.

3.5 Conclusions

Thyroidectomy in the ovine fetus in late gestation causes an asymmetric pattern of growth and development with some tissues enlarged while others are growth retarded. The tissue-specific changes in growth may be the result of increased circulating insulin concentrations and altered insulin signalling. The increase in plasma insulin concentration in the TX fetuses was associated with an increase in pancreatic β-cell mass. These findings are in contrast to the initial hypothesis that hypothyroidism in the sheep fetus leads to growth retardation due to a decrease in pancreatic β-cell mass and therefore decreased circulating insulin concentration. It remains unclear which factors and mechanisms are responsible for driving the growth of the pancreas in the hypothyroid fetus.

4 ENDOCRINE CONTROL OF FETAL PANCREATIC β-CELL PROLIFERATION *IN VITRO*

4.1 Introduction

In the fetus, the period during late gestation is critical for pancreatic β-cell proliferation and changes in plasma nutrients and hormones *in utero* can influence the development of the pancreas (Holemans *et al.*, 2003; Fernández *et al.*, 2007). In the study reported here, hypothyroidism in the sheep fetus during late gestation has been shown to enhance pancreatic β-cell mass and increase circulating insulin concentration (Chapter 3). These effects may be a direct consequence of thyroid hormone deficiency and/or due to other endocrine systems affected by hypothyroidism *in utero*.

Thyroid hormones have been implicated in the control of β-cell proliferation before birth (Bouwens & Rooman, 2005; Medina *et al.*, 2011). *In vitro* studies using β-cell derived cell lines have shown that both TRα1 and TRβ1 are present in pancreatic β-cells (Verga Falzacappa *et al.*, 2007; Furuya *et al.*, 2010). The data suggest that the increase in β-cell mass seen in the TX sheep fetus may be due to an increase in cell proliferation and that the thyroid hormones may have an inhibitory effect on β-cell proliferation and neogenesis in the late stages of gestation. Local thyroid hormone concentrations in the developing pancreas are determined, in part, by the relative activites of D2 (conversion of T3 from T4) and D3 (inactivation of T3 and T4). In the human pancreas, D2 expression is at its highest at 8 weeks of gestation and then progressively decreases towards term (Medina *et al.*, 2011). Expression of D3 co-localises with β-cells and its mRNA is observed from 11 weeks onwards (Medina *et al.*, 2011). The relative expression of D2 and D3 in the pancreas may protect β-cells from the anti-mitotic actions of thyroid hormones and enable proliferation.

The increase in β-cell mass in the TX fetus may be responsible for the increased production and secretion of insulin, which in turn, may act on pancreatic islets as a growth factor. Otani *et al*. (2004) created a transgenic mouse model in which the animals lacked insulin receptors specifically on pancreatic β-cells. The adult mice had lower β-

cell mass and reduced pancreatic insulin content. A similar phenotype has been described in 12 week old mice with deletion of *Irs2* in the pancreas which shows a decrease in β-cell mass (Cantley *et al.*, 2007). These studies, however, did not demonstrate any change in pancreatic β-cell mass in the mutant neonates at 2 weeks of age. This suggests that the insulin receptor and IRS2 are not essential for development of the pancreas, but participate in the control of β-cell mass expansion later in life (Kido *et al.*, 2002; Otani *et al.*, 2004; Cantley *et al.*, 2007) .

Leptin may also contribute to the endocrine control of β-cell mass during hypothyroidism *in utero* as plasma concentrations of leptin were increased in the TX sheep fetus. Leptin receptor protein and mRNA are present in cultured insulinoma cells *in vitro* and in fetal and adult rat islets *in vivo* (Kieffer *et al.*, 1996; Islam *et al.*, 1997; Kulkarni *et al.*, 1997). However, despite the presence of leptin receptors, there is contrasting evidence concerning the role of leptin in β-cell growth. One investigation using isolated islets from fetal rats found that leptin was able to stimulate β-cell proliferation *in vitro* (Islam *et al.*, 2000). In contrast to these findings, a two-fold increase in β-cell mass was observed in neonatal and adult mice with a pancreas-specific knockout of the leptin receptor (Covey *et al.*, 2006; Morioka *et al.*, 2007). The effect of leptin on pancreatic development in fetal sheep remains to be established.

The aim of this study was to investigate the effects of T3, insulin and leptin on β-cell proliferation and glucose-stimulated insulin secretion using islets isolated from normal fetal sheep. From the results obtained in Chapter 3, it is hypothesised that β-cell proliferation will be inhibited by thyroid hormone and stimulated by insulin and leptin.

4.2 Methods

4.2.1 Animals

All of the proliferation studies were carried out in collaboration with Dr. Sean Limesand at the Department of Animal Sciences, University of Arizona, Tucson, Arizona, USA. To determine the endocrine control of the rate of β-cell proliferation, islets were isolated from untreated sheep fetuses aged between 133 and 142dGA and subjected to

proliferation assays *in vitro*. Islets were allocated to each treatment by equally distributing islets from different aged fetuses.

Five Columbia-Rambouillet crossbred ewes carrying twin fetuses were purchased from Nebeker Ranch (Lancaster, USA) and managed in compliance with the Institutional Animal Care and Use Committee at the University of Arizona, which approved the study and is accredited by the American Association for Accreditation of Laboratory Animal Care. Ewes were fed Standard-Bread Alfalfa Pellets (Sacate Pellet Mills, Laveen Green, USA) and provided with water *ad libitum*. The gestational age, body weight and sex of each fetus are displayed in Table 4.1. The body weights were all within the normal range for the breed and comparable to those of the sham control group in the previous study (Chapter 3).

Table 4.1. Gestational age, body weight and sex of twin fetuses used in proliferation studies.

Sheep	Gestational age (days)	Weight (kg)		Sex	
		Twin A	Twin B	Twin A	Twin B
1	133	2.83	2.52	Male	Female
2	136	3.31	3.43	Male	Female
3	139	3.29	2.90	Male	Male
4	142	3.07	3.39	Female	Female
5	136	4.00	4.47	Male	Male

4.2.2 Surgical procedures

Ewes and fetuses were euthanized by maternal I.V. administration of pentobarbital sodium (86mg/kg) and phenytoin sodium (11mg/kg; Euthasol, Virbac Animal Health, Fort Worth, USA). After hysterectomy, each fetus was removed, blotted dry and weighed. An incision was made down the length of the abdomen of the fetus. The common bile duct was clamped at the proximal duodenum and the pancreas was injected via the common bile duct with 20ml cold collagenase solution containing Krebs Ringer Buffer (KRB; 118mM sodium chloride, 4.8mM potassium chloride, 1.2mM magnesium sulphate, 1.2mM potassium phosphate, 2.5mM sodium bicarbonate,

2.5mM calcium chloride), 0.425mg/ml collagenase V (Sigma) and 0.2% DNAse1 (Roche). The perfused pancreas became distended and visible. The pancreas was dissected free and divided from the common bile duct to the left of the portal vein. It was placed into a tube containing 40ml cold collagenase solution.

4.2.3 Islet Isolation

Islets were isolated from the fetal pancreas as described previously (Limesand *et al.*, 2006; Rozance *et al.*, 2006). The pancreas was minced with scissors and the tube containing the pancreas in collagenase solution was heated in a water bath at 37°C to digest for approximately 15-20 minutes, with vigorous shaking every 5 minutes. The tissue was cooled on ice to stop the collagenase activity and washed with approximately 40ml cold quench buffer containing KRB and 5% BSA for 7 minutes on ice. The tissue was filtered through a mesh filter (26 gauge) and the remaining solution was separated into two 50ml tubes and washed again in cold quench buffer and incubated on ice for a further 7 minutes. After a pellet had formed at the bottom of each tube, the supernatant was removed and the pellets were resuspended in quench buffer and combined back into one tube. To this tube, 40ml of quench buffer was added and the solution was divided into four tubes equally. To each tube, 10ml of Histopaque (Sigma) was added. Histopaque contains a solution of polysucrose and sodium diatrizoate, adjusted by quench buffer to a density of 1.083g/ml to facilitate the recovery of islets. The tubes were centrifuged for 20 minutes at 1600g at room temperature so that pancreatic acinar cells collected at the bottom of the tube and the islets were suspended in the interphase above the Histopaque. The interphase was removed from each tube, combined and washed with 40ml quench buffer, and briefly centrifuged at 1600g. The pellet of islets was resuspended in 10ml quench buffer and added to a 100mm Petri dish (Fisher Scientific, Pittsburgh, USA). The islets were identified visually from acinar cells using a dissecting microscope and were transferred using a pipette into a 100mm Petri dish containing RPMI 1640 media (Sigma) with 10% fetal bovine serum (500U; EquaFetal, Atlas Biologicals, Fort Collins, USA), penicillin-streptomycin (50µg and 100µg, Sigma) and 2.8mM glucose (D-glucose, Fisher Scientific). The islets were subjected to 95% O_2/5% CO_2 gas for 5 minutes in a humidity chamber before incubation at 37°C for 24 hours before treatment began.

4.2.4 EdU proliferation assay

To determine cell proliferation, the Click-iT EdU Imaging kit (Invitogen, Grand Island, USA) was used to immunolabel and image isolated islets undergoing proliferation. The most accurate method for assessing cell proliferation is by directly measuring DNA synthesis. 5-ethynyl-2'-deoxyuride (EdU) is a nucleoside analogue of thymidine. It is incorporated into DNA during active DNA synthesis in the S-phase of the cell cycle when the DNA content doubles. The detection method is based on a copper-catalyzed covalent reaction between the EdU which contains an alkyne and the fluorescent dye which contains an azide.

Cell culture

Islets were picked randomly and placed into 100mm Petri dishes containing RPMI 1640 media with 10% fetal bovine serum, penicillin-streptomycin and 2.8mM glucose supplemented with four different concentrations of each hormone treatment: 0, 0.1, 1.0 and 10ng/ml. A positive control treatment of 10ng/ml IGF-I was also used, as IGF-I has previously been shown to stimulate β-cell proliferation *in vitro* (Hogg *et al.*, 1993; Withers *et al.*, 1999; Fernández *et al.*, 2007). At least 50 islets were handpicked for each treatment dish. The hormones used in each treatment group were as follows:

10ng/ml IGF-I (Sigma) 50µg IGF-I was resuspended in 1ml dH_2O to make a stock solution of 50µg/ml.

T3 (Sigma) T3 is insoluble in water, therefore 1mg T3 was dissolved in 1ml of 1M sodium hydroxide and then added to 49ml RPMI media to make a 20µg/ml stock solution.

Insulin (Humulin R U-100, Lilly, Indianapolis, USA) Humulin R U-100 is synthetic insulin synthesised by recombinant DNA technology using *Escherichia coli* bacteria. The solution contained 100IU/ml, and there was 6nM insulin per IU. The molecular weight of Humulin R is 5808g; therefore, a solution of 10ng/ml contained 2.86µl Humulin R U-100.

Leptin (Abcam) Active sheep full length leptin protein was made into a 200µg/ml stock by the addition of 0.5ml dH_2O.

After 24 hours incubation, the islets were moved to smaller 35mm dishes (Cell Treat, Shirley, USA) and the media was replaced with fresh media containing the appropriate dose of hormone treatment. The media was spiked with EdU at a final concentration of 10µM. Again the islets were subjected to 95% O_2/5% CO_2 gas for 5 minutes in a humidity chamber before incubation at 37°C for 24 hours.

Fixation, embedding and sectioning

After a total incubation period of 48 hours, the islets and media were transferred into an Eppendorf tube and centrifuged until the islets had formed a pellet. The islets were fixed in 4% paraformaldehyde. After fixation, the islets were resuspended and stored in PBS. Embedding of islets was aided visually by the use of blue beads in order for the islets to be visualised when sectioning. Approximately 100µl Affi-Gel 100-200 mesh beads (Biorad) were washed twice in PBS. The islets were transferred in PBS to a 0.2µl Eppendorf tube and approximately 10µl bead solution was added to the islets. After mixing, the solution was spun for 10-20 seconds until a pellet of islets and beads had formed at the bottom. The PBS was removed and 50µl warm Histogel (Thermo Scientific) was added; the contents were mixed and spun for 1 minute at 1400g. The Histogel was left to solidify at 4°C and was dislodged from the tube and placed in a cryomould (Tissue Tek, Torrance, USA) containing optimum cutting temperature compound (Tissue Tek). The block containing islets was frozen and stored at -80°C. The blocks were sectioned on a cryostat kept at a constant temperature of -20°C. Sections were cut at a thickness of 10µm at 100µm intervals and mounted onto glass microscope slides.

Immunocytochemistry

Using the EdU Click-iT kit, the slides were labelled for EdU positive cells. The slides were heated for 30 minutes at 37°C, followed by a wash in dH_2O. The cells were permeabilised in PBS with 0.1% Triton X-100 (Sigma) for 15 minutes followed by two washes in PBS. The cells were incubated with the Click-iT reaction cocktail mix (containing reaction

buffer (Tris buffered saline), 100mM copper sulphate, Alexa Fluor azide and a reducing agent) for 30 minutes at room temperature in the dark. The cocktail was removed and the slides washed with rinse buffer containing 3% BSA in PBS.

The slides were incubated with a blocking agent (0.5% BSA in Tris-sodium chloride-Tween buffer) for 1 hour at room temperature in the dark. Insulin was identified in the sections by incubation overnight at 4°C in the dark with a guinea pig polyclonal anti-porcine insulin antibody (Dako, Carpinteria, USA) diluted to 1:500 in 1% BSA. Following washes in PBS, immunocomplexes were detected by incubation for 1 hour at room temperature with a polyclonal donkey anti-guinea pig IgG with Alexa Fluor 594 conjugate (Jackson Immunoresearch, West Grove, USA) diluted to 3µg/ml in 1% BSA. The slides were incubated in 1mg/ml 4',6-diamidino-2-phenylindole (DAPI, Vector Labs) as a nuclear counterstain for 3 minutes at room temperature in the dark. The slides were rinsed in dH_2O and mounted with 50% glycerol in 10mM Tris-hydrochloric acid and coverslips (pH 8.0).

Morphometric analysis

Fluorescent images were visualised on a fluorescence microscope system (Leica DM5500) and captured with a camera (Persuit 4 Megapixel CCD Camera, Diagnostic Instruments, Sterling Heights, USA). Analysis was performed using ImageJ (US National Institutes of Health, http://imagej.nih.gov/ij/). Approximately 2500-3000 insulin-positive cells were counted over at least 6 sections for each treatment. Every EdU positive cell also positive for insulin was counted to a minimum of 200 per treatment group. The proportion of EdU/insulin positive cells was calculated relative to the total number of insulin positive cells.

4.2.5 Glucose stimulated insulin secretion assay

Glucose stimulation

Preliminary studies were carried out to assess the functionality of isolated islets. A static glucose stimulated insulin secretion (GSIS) assay was performed on islets incubated in the different treatment groups as described by Rozance *et al* (2006). The GSIS was

carried out with Amy Kelly in the Department of Animal Sciences at the University of Arizona.

Around 30 islets were picked randomly and placed into 35mm Petri dishes containing RPMI 1640 media with 10% fetal bovine serum, penicillin-streptomycin and 2.8mM glucose supplemented with 10ng/ml hormone. The islets were subjected to 95% O_2/5% CO_2 gas for 5 minutes in a humidity chamber before incubation at 37°C. After 24 hours, 5-10 islets were transferred into 1.5ml tubes and there were 5 replicates per condition. Islets were incubated in KRB-BSA at 37°C for 1 hour to equilibrate, followed by stimulation with 1.1mM glucose for 1 hour. Supernatant was removed before stimulating with 11mM glucose for 1 hour. A sample of incubation media was taken after 5 minutes to account for mechanical release of insulin and test islet incubations on ice with 11mM glucose were carried out to control for cellular breakdown.

An assessment of insulin secretion was attempted in cells cultured with insulin, but it became difficult to ascertain the extent to which the insulin detected in the media was the result of production by the β-cells or the exogenous insulin added to the media. Furthermore, it has previously been reported that insulin potentiates GSIS in humans and neonatal mice *in vitro* (Kulkarni *et al.*, 1999; Bouche *et al.*, 2010). For this reason, the data were omitted and only the effects of leptin and T3 on GSIS were assessed.

Insulin concentration

After one hour, the islets were pelleted by centrifugation at 800g and the supernatent was removed for analysis of insulin concentration. Total cellular insulin was extracted from the fetal islets by acid-ethanol extraction with insulin content buffer containing 11.6M hydrochloric acid, 100% ethanol and dH_2O at 20°C for 24 hours. Insulin concentration was analysed by ELISA validated for ovine insulin (ALPCO, Salem, USA) using dilutions of the incubation media (insulin released) and the acid-ethanol extract (insulin content). The minimum detection level of the ELISA kit was 0.14ng/ml. Total insulin content of the islets was determined by the addition of the amount insulin

released and the islet insulin content. Islet insulin secretion was quantified as the fraction of total insulin content that was released into the incubation media.

4.2.6 Statistical analysis

All values are expressed as mean ± SEM unless otherwise indicated. The results obtained in the proliferation assays were compared by one-way ANOVA followed by the *post-hoc* Tukey test. The GSIS assay data was assessed using a two-way ANOVA using treatment and glucose concentration as factors, followed by the Tukey test, or by a Student's t-test. Significance was accepted at $P<0.05$.

4.3 Results

4.3.1 β-cell proliferation

T3

Visually, immunocytochemistry identified that islets cultured in the higher concentrations of T3 showed a decrease in number of EdU/insulin positive cells (Figure 4.1).

In islets cultured in 1.0ng/ml and 10ng/ml T3, EdU positive cells appeared to aggregate in the centre of the islets, where there was a distinct absence of insulin positive cells. The proliferation rate of β-cells in media without T3 (0ng/ml) was 6.8 ± 0.5%. With the addition of T3, the rates of β-cell proliferation decreased compared to the 0ng/ml control at all T3 doses in a dose-dependent manner (Figure 4.2A, 0.1ng/ml: 4.6 ± 0.4%; 1.0ng/ml: 3.3 ± 0.3%; 10ng/ml: 2.5 ± 0.2%; $P<0.05$). The IGF-I positive control stimulated proliferation to a rate of 8.2 ± 0.9%.

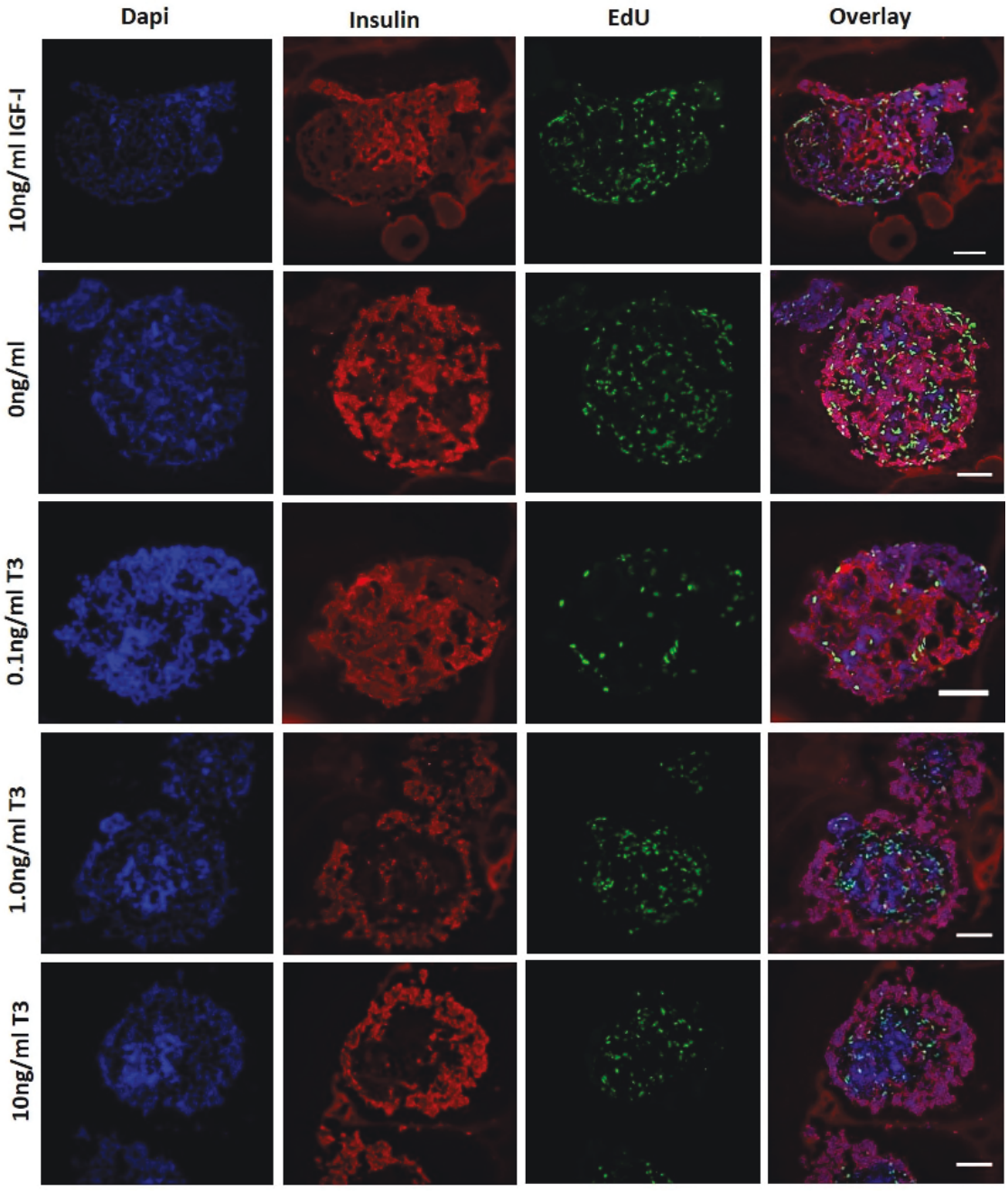

Figure 4.1. Immunofluorescence of fixed ovine fetal islets shows insulin labelling (red) and EdU positive cells (green) with Dapi nuclei staining (blue). Islets were cultured in 10ng/ml IGF-I (positive control) or 0, 0.1, 1.0 and 10ng/ml T3. Approximately 15-20 islets imaged for each treatment. Scale bar 25µm, one islet per image.

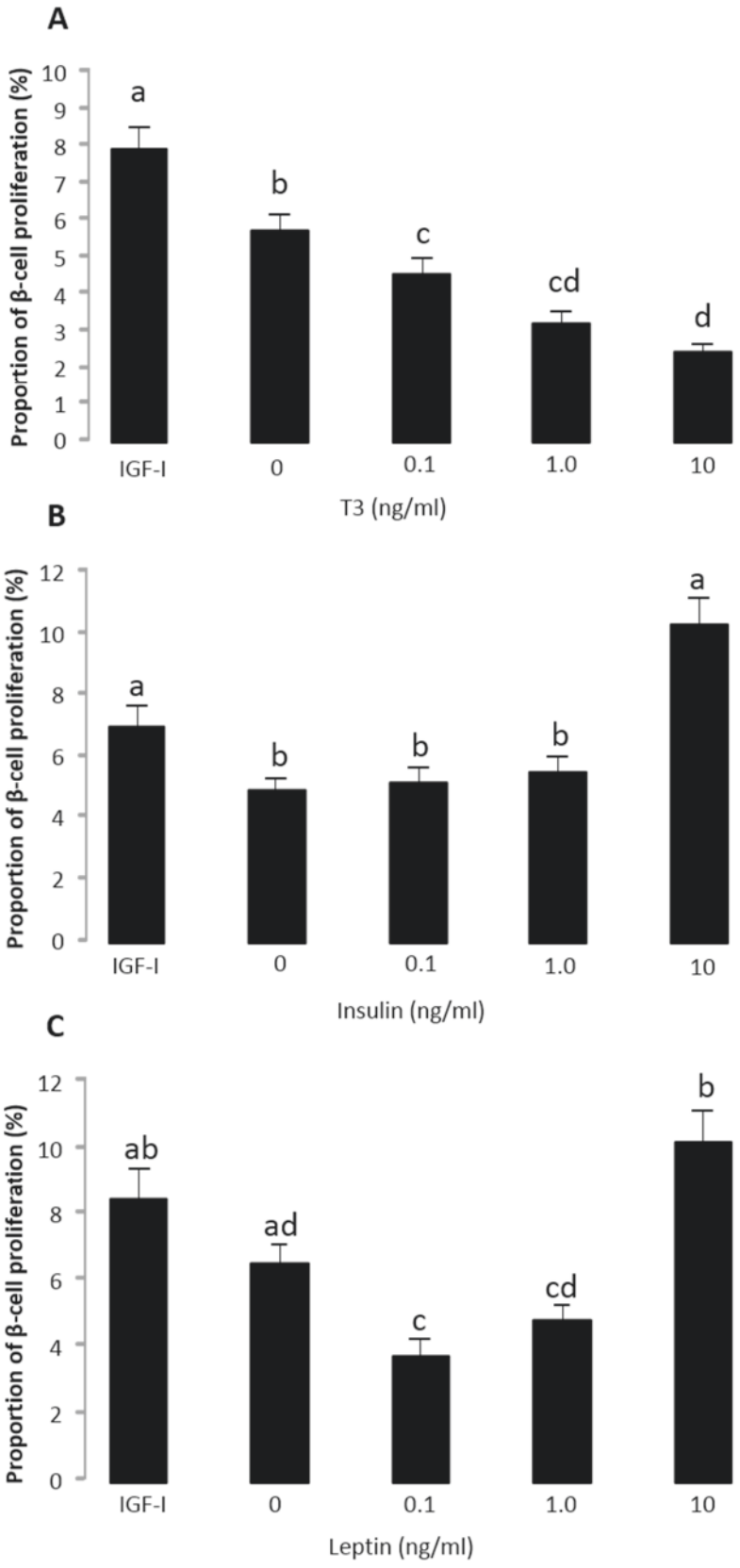

Figure 4.2. Mean ± SEM proliferation rates of β-cells after 24 hours incubation in 0, 0.1, 1.0 and 10ng/ml of (A) T3, (B) insulin and (C) leptin, compared to 10ng/ml IGF-I as a positive control. Differing letters signify significance between treatment groups, 1-way ANOVA, $P<0.05$, 200 cells in each treatment group.

Insulin

Immunofluoresent labelling of β-cells cultured in increasing insulin concentrations revealed no obvious change in the number of EdU/insulin positive cells, with the exception of the highest concentration, 10ng/ml, which induced an increase in the number of Edu/insulin positive cells (Figure 4.3).

The islets cultured in media without insulin had a proliferation rate of 4.5 ± 0.4% (Figure 4.2B). Insulin treatment at 0.1 and 1ng/ml had no significant effect on the number of EdU/insulin-positive cells in fetal islets (0.1ng/ml: 5.2 ± 0.5%; 1.0ng/ml: 5.6 ± 0.5%, Figure 4.2B). At the higher dose of 10ng/ml insulin, however, the rate of β-cell proliferation was increased significantly compared to the basal condition and lower doses of insulin (10ng/ml: 10.4 ± 0.9%, $P<0.05$; Figure 4.2B) and tended to be higher than that induced by IGF-I at 10ng/ml (7.1 ± 0.7%; $P=0.07$, Figure 4.2B).

Leptin

Immunocytochemistry revealed a decrease in the number of EdU/insulin positive cells at the lowest concentration of leptin (0.1ng/ml, Figure 4.4). However, at the highest dose of 10ng/ml, leptin stimulated proliferation as the appearance of EdU positive β-cells was more prominent.

The islets cultured in media without leptin had a proliferation rate of 6.6 ± 0.5%. The rate of proliferation was significantly lower in cells cultured in 0.1ng/ml leptin (3.8 ± 0.8%; $P<0.05$, Figure 4.2C). At 10ng/ml leptin, the proportion of β-cells proliferating was significantly higher than the other doses of leptin ($P<0.05$ in all cases) and equivalent to the level of the IGF-I control group (10ng/ml: 10.3 ± 0.9%; IGF-I: 8.5 ± 0.8%; Figure 4.2C).

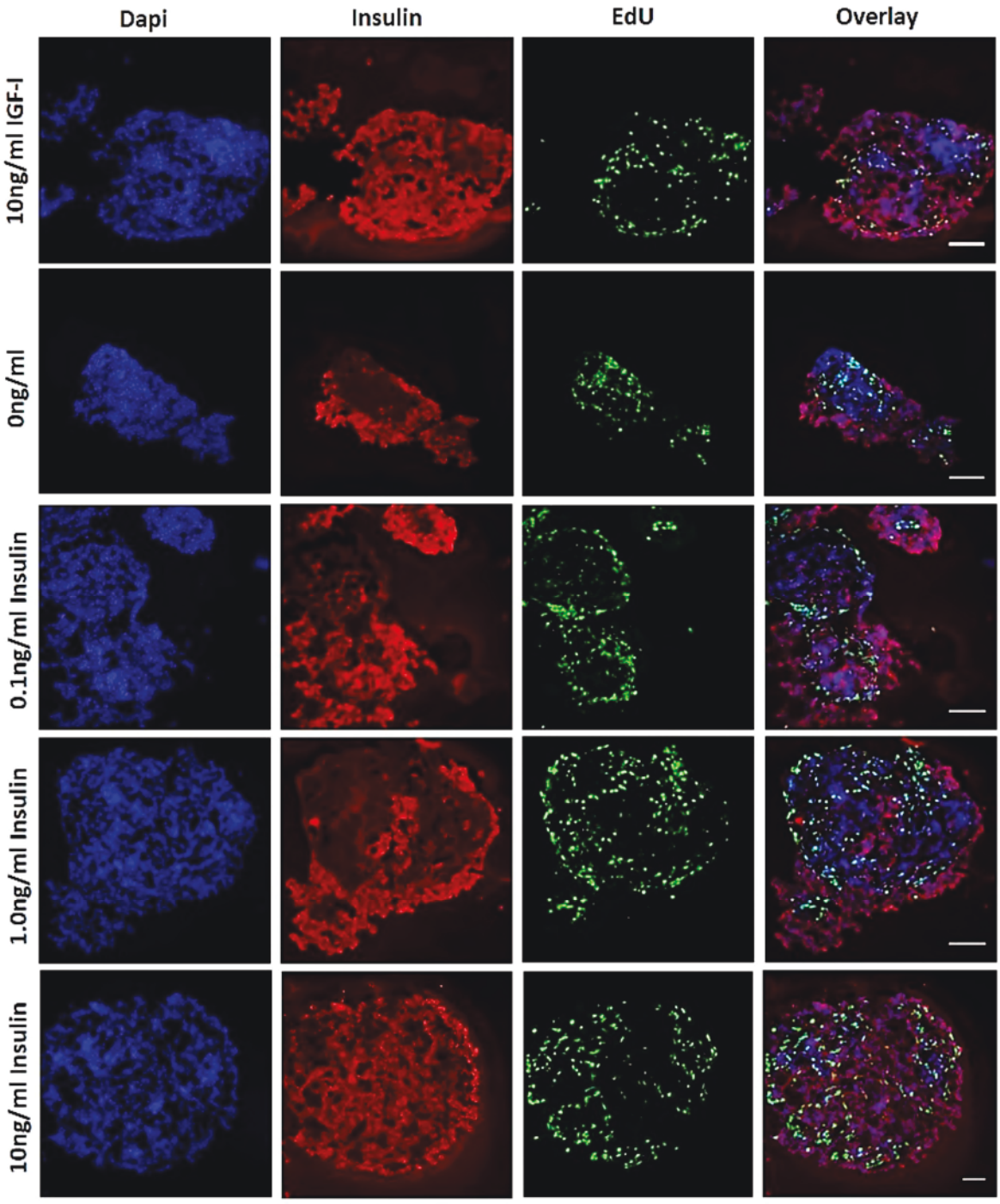

Figure 4.3. Immunofluorescence of fixed ovine fetal islets shows insulin labelled (red) and EdU positive cells (green) with Dapi nuclei staining (blue). Islets were cultured in 10ng/ml IGF-I (positive control) or 0, 0.1, 1.0 and 10ng/ml insulin. Approximately 15-20 islets imaged for each treatment. Scale bar 25µm, one islet per image.

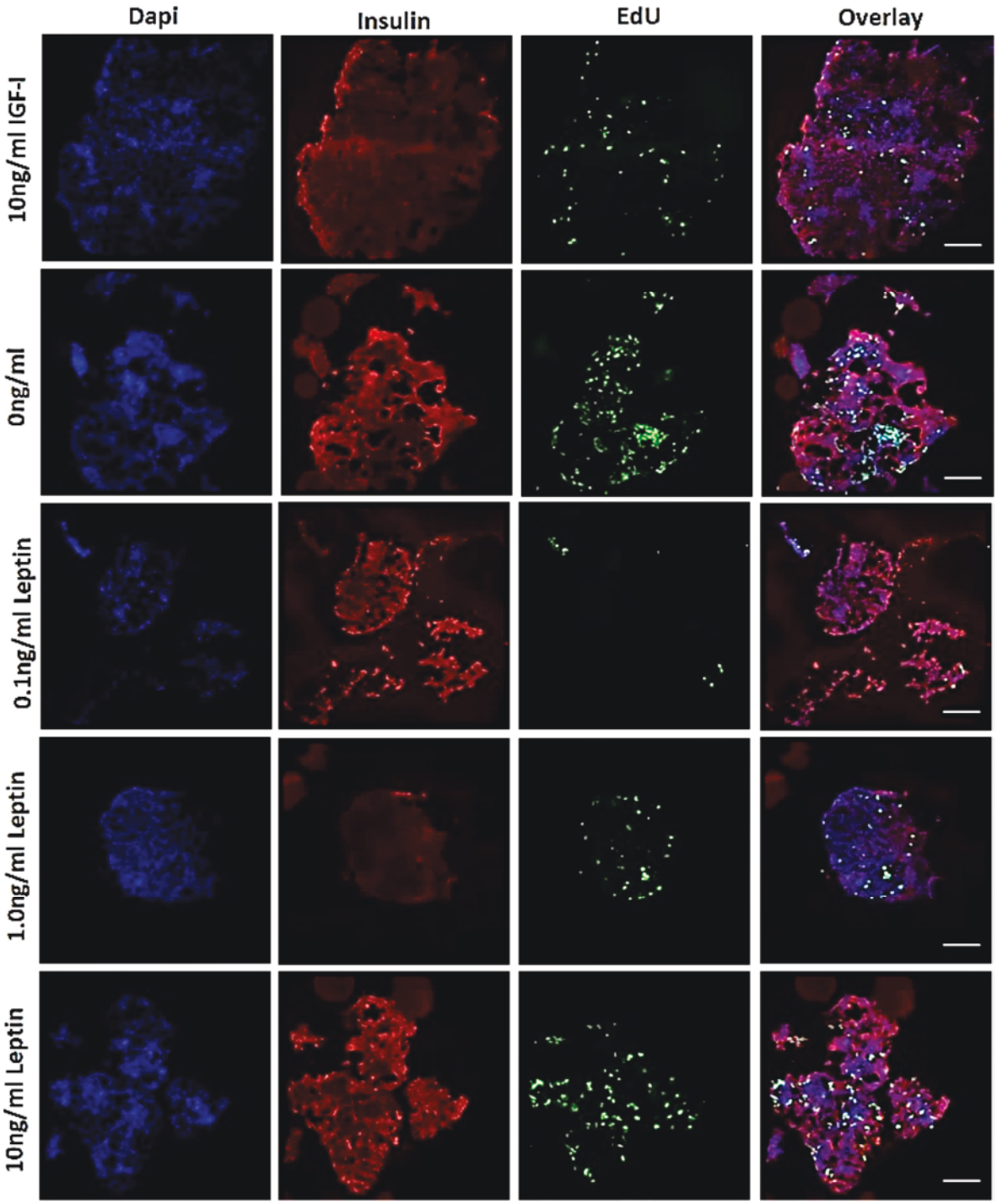

Figure 4.4. Immunofluorescence of fixed ovine fetal islets shows insulin labelling (red) and EdU positive cells (green) with Dapi nuclei staining (blue). Islets were cultured in 10ng/ml IGF-I (positive control) or 0, 0.1, 1.0 and 10ng/ml leptin. Approximately 15-20 islets were imaged for each treatment. Scale bar 25µm, one islet per image.

4.3.2 GSIS

Insulin secretion stimulated by 1.1mM and 11mM glucose in the β-cells cultured in normal media without hormone, once normalised to total insulin content, was 5.7 ± 1.3pg/ml/ng and 7.8 ± 4.6pg/ml/ng, respectively (Figure 4.5). Using a two-way ANOVA to compare the data between hormone treatment and concentration of glucose added, the islets cultured in 10ng/ml T3 tended to increase insulin secretion when stimulated by both 1.1mM and 11mM glucose compared to the control group (1.1mM glucose: 12.8 ± 2.3pg/ml/ng; 11mM glucose: 14.8 ± 2.3pg/ml/ng, P=0.08, Figure 4.5). When the data for the responses to 1.1 and 11mM glucose were combined, there was a significant increase in GSIS in islets treated with T3 compared to those without hormone when assessed by a Student's t-test (P<0.05, Figure 4.5).

There was no significant change in the insulin secretion in the islets incubated in 10ng/ml leptin when stimulated by either 1.1mM (6.6 ± 1.5pg/ml/ng) or 11mM glucose (7.7 ± 6.2pg/ml/ng) compared to the control group without hormone (Figure 4.5).

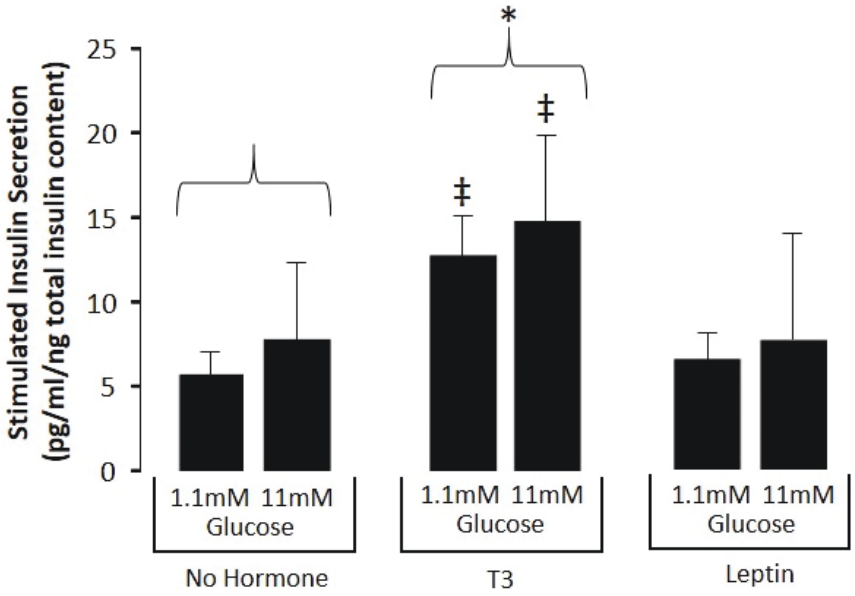

Figure 4.5. Mean ± SEM insulin secretion in response to 1.1 and 11mM glucose in islets cultured in normal media without hormone (control) or with 10ng/ml T3 or 10ng/ml leptin. All of the islets were from the same fetus. ‡ Different from the islets treated with no hormone, 2-way ANOVA, P=0.08. * Significantly different combined response from the islets treated with no hormone, Student's t-test, P<0.05. n= 3-4 in each group.

4.4 Discussion

4.4.1 Thyroid hormone inhibited fetal β-cell proliferation

This study aimed to elucidate the role of T3 in β-cell proliferation in the sheep fetus during late gestation. Using EdU uptake as a measure of proliferation, it was identified that T3 inhibits β-cell proliferation in pancreatic islets taken from normal sheep fetuses and studied *in vitro*. This is a novel finding and contrasts with previous reports in which T3 has a stimulatory effect on β-cell proliferation. In other cell culture models utilising β-cells isolated from adult rats, T3 was shown to increase the viability of the cells *in vitro* and to reduce cell apoptosis (Verga Falzacappa *et al.*, 2010). In a 5-bromo-2-deoxyuridine (BrdU) incorporation assay, the study demonstrated that β-cells cultured with T3 had an increase in BrdU uptake indicating a higher rate of proliferation. Another study using a rat pancreatic β-cell line also showed that incubation with T3 increased cell proliferation (Furuya *et al.*, 2010). In isolated islets from adult rats and in an insulinoma cell line, Verga Falzacappa *et al*. (2007; 2009) have previously found T3 to act as a mitogen and, via TRβ1, to activate Akt to influence cellular processes such as proliferation. However, the previous studies have used isolated rat islets and rodent cell lines, which used adult, rather than fetal, derived cells.

This study is the first to show an inhibitory dose-dependent effect of T3 on fetal pancreatic β-cell proliferation *in vitro*. The concentrations used in this study ranged from the physiological to the supraphysiological in order to mimic circulating and tissue concentrations that are seen in the normal and hyperthyroid fetus. It should be noted that the pancreas has the ability to regulate local T3 production. Human fetal pancreas has been shown to express mRNA for D2 from as early as 8 weeks and D3 mRNA from 11 weeks of gestation (Medina *et al.*, 2011), both of which are important in the regulation of active intracellular T3. An absence in the localisation of sulphotransferase or sulphatase enzymes has been reported in the human fetal pancreas (Miki *et al.*, 2002), suggesting that the pancreas *in utero* may be unable to utilise sulphoconjugated T3 locally. The data from this study complement that from Chapter 3 in which the TX fetuses have an increased pancreatic β-cell mass. Taken together, the results from the studies

in vivo and *in vitro* suggest that T3 has an inhibitory effect on β-cell proliferation in fetal sheep.

Preliminary data from the GSIS assay suggest that T3 increases insulin secretion from isolated fetal ovine islets. Although there was a tendency for greater insulin secretion in response to glucose from islets cultured in T3, these data were not significant. This is most likely due to the low number of replicates (n=3-4) that were used in the investigation. It is plausible that in the fetus, thyroid hormone acts to inhibit β-cell proliferation to switch from cell division to differentiation and thus promote maturation of the β-cells to increase insulin production and secretion. It has previously been shown in fetal mice with a genetic knockout for D3 that reduced β-cell mass is associated with decreases in insulin content and the expression of glucose sensing genes (Medina *et al.*, 2011), indicating that low T3 exposure is required for normal islet development and maturation. The data in this study are consistent with studies on the role of T3 in cardiomyocyte maturation in the sheep fetus by Chattergoon *et al*. (2012a; 2014). Maturation of fetal ovine cardiomyocytes is characterised by a transition from mononucleated to binucleated cells and suppression of mitosis near term. Cardiomyoctyes from TX sheep fetuses show a lower rate of proliferation and a reduced percentage of binucleated cells compared to controls (Chattergoon *et al.*, 2012a). The same principle may be applied to the proliferation of the β-cells in the fetal pancreas, in which T3 inhibits proliferation and stimulates maturation. In the TX fetus, the inhibitory effects of the thyroid hormones are absent and therefore proliferation of β-cells continues. The maturity of the β-cells in the TX fetus in terms of their capacity for insulin secretion and cellular morphology remains unknown, compared to that of the sham controls. A recent study using human embryonic stem cell-derived pancreatic progenitor cells grafted into mice found that chronic thyroid hormone deficiency results in impaired insulin secretion, indicating that the β-cells were not functionally mature (Bruin *et al.*, 2016).

The transcription factor MAFA is implicated in the maturation of pancreatic β-cells. Genes involved in insulin production and secretion are found to be regulated by *Mafa* and pancreatic MAFA protein levels in the mouse neonate increase with age (Aguayo-

Mazzucato *et al.*, 2011). Expression levels of *Mafa* in pancreatic islets from rodent fetuses increase coincident with T3 towards term and it is possible that T3 may regulate *Mafa* expression in β-cells. In newborn rats, an injection of T3 causes an increase in β-cell proliferation and the number of islet cells (Aguayo-Mazzucato *et al.*, 2013). The islets from T3-treated animals show increased islet gene expression of MAFA mRNA and protein levels. It has been identified that the thyroid receptor may interact directly with two putative TREs in the *Mafa* gene (Aguayo-Mazzucato *et al.*, 2013). Using a maturation marker such as MAFA, future studies could analyse the maturity and functionality of the β-cells isolated from sham and TX sheep fetuses.

4.4.2 Insulin stimulated fetal β-cell proliferation at high concentrations

Insulin has long been known to be a potent growth factor *in utero* (Hill & Milner, 1985) and in the sheep fetus, growth rates and plasma insulin concentrations are positively correlated (Fowden *et al.*, 1989). Inhibition of components of the insulin signalling pathway have previously been shown to reduce β-cell growth. Genetic knockout of pancreatic *Irs2* and *Igf1r* results in decreased β-cell mass in adult mice (Withers *et al.*, 1998; Cantley *et al.*, 2007). Furthermore, neonatal rats born to mildly diabetic mothers are hyperinsulinaemic and show greater rates of pancreatic β-cell proliferation compared to rats born to normal dams (Reusens-Billen *et al.*, 1984). It is therefore unsurprising in the present study that the highest concentration of insulin increased the rate of β-cell proliferation. The result however, is in contrast to one study in which deletion the insulin gene in mice led to an increased number of β-cells in the fetus which was associated with an increase in islet cell DNA synthesis (Duvillie *et al.*, 2002).

Alterations in Akt, mTOR and pS6K have previously been shown to have detrimental effects on the development of pancreatic β-cell mass. Genetic overexpression of pancreatic Akt in mice leads to increased β-cell mass, which is associated with hypertrophy as well as hyperplasia (Bernal-Mizrachi *et al.*, 2001; Tuttle *et al.*, 2001). In addition, neonatal mice with a conditional deletion of tuberous sclerosis complex 2 that causes upregulation of mTOR and pS6K, show an increased β-cell mass which persists into adulthood (Rachdi *et al.*, 2008). As Akt, mTOR and pS6K are all integral factors

within the insulin signalling pathway, it can be speculated that excess plasma insulin present in the TX sheep fetus drives proliferation through Akt/PI3K in β-cells.

The results in this study complement those in Chapter 3, as increased circulating insulin concentrations in the TX fetuses were associated with greater β-cell mass compared to sham controls. Although the plasma concentrations of insulin in the TX fetus were between 0ng/ml and 1.0ng/ml, local pancreatic insulin concentrations are likely to be higher due to islet insulin secretion and the paracrine actions of the insulin on the β-cells. These findings provide further evidence that the enhanced pancreatic β-cell mass in the TX fetus is likely to be due to the combined effects of increased insulin and loss of thyroid hormone.

4.4.3. Leptin stimulated fetal β-cell proliferation in a bimodal manner

This is the first report of a bimodal response in β-cell proliferation to leptin in fetal sheep islets *in vitro*. Previous reports are conflicting about the role of leptin in β-cell proliferation, as it has been shown to be both inhibitory and stimulatory, depending on the experimental model used. Leptin has previously been found to stimulate β-cell proliferation in isolated fetal rat islets *in vitro* (Islam *et al.*, 2000); however, an increase in β-cell mass is observed in neonatal mice with a genetic knockout for the leptin receptor (Morioka *et al.*, 2007). The contrasting data from previous investigations of the role of leptin in β-cell proliferation may be due to the differing concentrations of leptin used. Islam *et al*. (1997; 2000) reported stimulation of proliferation in rat fetal islets in response to leptin *in vitro*, but used concentrations that were significantly higher (80 – 1600ng/ml) than the normal physiological range. Investigations by Morioka *et al*. (2007) used a rat model with a leptin receptor deletion where the islets were totally insensitive to leptin. The current study has used concentrations of leptin which are within the physiological range and therefore, the bimodal response observed may be more reflective of the normal response to leptin *in vivo*.

The preliminary data suggest that leptin has no effect on fetal β-cell GSIS. Previous investigations have shown that leptin treatment suppresses insulin secretion in adult rat islets (Kieffer *et al.*, 1996) and transgenic neonatal mice which are leptin receptor

deficient are hyperinsulinaemic (Covey *et al.*, 2006). Further investigations are required to examine the control of GSIS in β-cells exposed to varying concentrations of leptin.

4.5 Conclusions

Thyroid hormone inhibits pancreatic β-cell proliferation *in vitro* in islets isolated from the sheep fetus. These findings complement data from the previous study *in vivo* in which pancreatic β-cell mass is increased in the hypothyroid sheep fetus. The increments in circulating leptin and insulin that accompany the enhanced β-cell mass in the TX fetuses may also contribute towards an increase in β-cell proliferation.

Preliminary data suggest that thyroid hormone may stimulate glucose-stimulated insulin secretion. Therefore, T3 may promote maturation of β-cells near term, by triggering cells to exit the cell cycle and to start expressing maturational signals such as MAFA. However, the results were inconclusive and further investigations into β-cell maturation would be required to confirm this. Furthermore, it is still unclear whether the increase in β-cell mass observed in the TX fetus is due to an increase in neogenesis or to enhanced division of existing cells. To identify neogenesis, the expression of progenitor markers such as PDX1 and Ngn3 could be investigated in islets taken from TX and sham fetuses.

5 EFFECTS OF HYPOTHYROIDISM ON FETAL PERIRENAL ADIPOSE TISSUE DEVELOPMENT

5.1 Introduction

Adipose tissue first appears in the sheep fetus around mid-gestation (~80dGA; Symonds *et al.*, 2012). As gestation progresses, total adipose mass increases and it comprises of both white and brown adipocytes (Clarke *et al.*, 1997; Symonds *et al.*, 2003). In the fetus, WAT is comprised of unilocular (UL) adipocytes, which secrete leptin, and its main function is energy storage as a large single lipid droplet in each cell. Brown adipose tissue contains adipocytes with many mitochondria and numerous smaller lipid droplets, and is termed multilocular (ML). It is essential for thermoregulation after birth as it contains the unique uncoupling protein, UCP1, which can generate rapid amounts of heat from uncoupling oxidative phosphorylation from ATP production in the respiratory chain. This is known as non-shivering thermogenesis (Nedergaard *et al.*, 2001).

In late gestation, the proportion of BAT is greater compared to that of the WAT in the sheep fetus (Devaskar & Anthony, 2002). The appearance of BAT may be regulated by the thyroid hormones, as the rise in BAT mass coincides with the prepartum surge in plasma T3 concentrations (Rabelo *et al.*, 1995; Clarke *et al.*, 1997). Thyroidectomy in the sheep fetus has previously been shown to decrease rectal temperatures in neonates (Polk *et al.*, 1987), indicating a deficiency in either BAT mass and/or function at birth induced by hypothyroidism. In contrast, hypothyroidism in the sheep fetus results in overgrowth of perirenal adipose tissue in association with increased circulating levels of insulin and leptin (Chapter 3).

Insulin is a potent growth factor for adipose tissue *in utero* (Saltiel & Kahn, 2001; Kamana *et al.*, 2015). Insulin receptors have been identified in isolated adipocytes from fetal rats (Teruel *et al.*, 1996) and insulin is able to influence fetal adiposity. Mice with an adipose-specific deletion of InsR have decreased fat pad mass (Bluher *et al.*, 2002) and fetal sheep with IUGR have decreased plasma insulin concentrations which are correlated

with decreased PAT mass (Duffield *et al.*, 2008). Maternal hyperglycaemia leads to hyperinsulinaemia and hyperglycaemia in the sheep fetus (Stephens *et al.*, 2001), and the high circulating insulin levels *in utero* is posited to contribute to somatic overgrowth, especially adipose tissue, of the fetus.

Thyroidectomised sheep fetuses have increased plasma leptin concentrations (Chapter 3) and adipose leptin mRNA abundance is associated with increased PAT mass in late gestation (O'Connor *et al.*, 2007). It has also been shown that birth weight and adiposity correlate to the plasma leptin concentrations and mRNA abundance in fetal ovine adipose tissue (Mühlhäusler *et al.*, 2003). In fetuses of ewes over-nourished in late gestation, leptin gene expression in adipose tissue is increased and adipose leptin mRNA levels are positively correlated with plasma insulin concentrations (Mühlhäusler *et al.*, 2007). Furthermore, greater adipose tissue leptin mRNA levels are observed in fetal sheep which have been intravenously infused with insulin (Devaskar & Anthony, 2002).

Growth of adipose tissue requires the differentiation of adipocytes and this is known to be regulated primarily by PPARγ through activation of adipose specific genes (Vidal-Puig *et al.*, 1997). Expression of PPARγ is high in early differentiation of pre-adipocytes to adipocytes, and ectopic expression of PPARγ in non-adipogenic murine fibroblasts causes the cells to undergo adipogenesis (Tontonoz *et al.*, 1994; Wu *et al.*, 1999). In fetal sheep, it has been shown that adipose mRNA levels of PPARγ are directly correlated to the relative PAT mass (Duffield *et al.*, 2009). The effects of thyroid hormone deficiency *in utero*, however, on the development of adipose tissue, and the role of insulin signalling in this process, are unknown.

The aims of the study were to examine the effects of hypothyroidism *in utero* on (1) the relative proportions of UL and ML adipocytes, (2) the expression of proliferative and adipogenic markers and (3) the insulin signalling pathway in perirenal adipose tissue. These aims together will aid in the understanding of the mechanisms behind the overgrowth of fetal adipose tissue observed during thyroid hormone deficiency.

It is hypothesized that the greater perirenal adipose tissue mass seen in the hypothyroid sheep fetus is due to overgrowth of UL adipocytes. This is caused by increased levels of plasma insulin and adipose PPARγ, and leads to higher circulating leptin concentrations. In contrast, hypothyroidism *in utero* suppresses the development of ML adipocytes which is responsible for impaired thermogenesis at birth.

5.2 Methods

5.2.1 Animals

All animals, treatments and post mortem procedures are described in Section 2.1. Four treatment groups were analysed: TX at 129dGA (n=9), sham at 129dGA (n=9), TX at 143dGa (n=10) and sham at 143dGA (n=10). The perirenal adipose tissue collected from each fetus was weighed and samples were either immersed in 4% formalin for paraffin wax embedding or frozen immediately in liquid nitrogen before storage at -80°C.

5.2.2 Histology

All histology processing steps are described in detail in Section 2.3. Sections of wax embedded adipose tissue were cut to a thickness of 7µm and left to dry overnight before H&E staining, as described in section 2.3.3. Stained sections were scanned using a NanoZoomer digital slide scanner (Hamamatsu Photonics) to create digital images for analysis. All stereological measurements were performed and analysed blind to the treatment group.

5.2.3 Percentage volume of adipocyte type

The percentage volumes of ML and UL adipocyte types were determined using NewCAST stereological software (Visiopharm). A point counting grid containing 25 points was applied over the adipose sections. Using meander sampling, adipocyte type was classified using SURS (Figure 5.1).

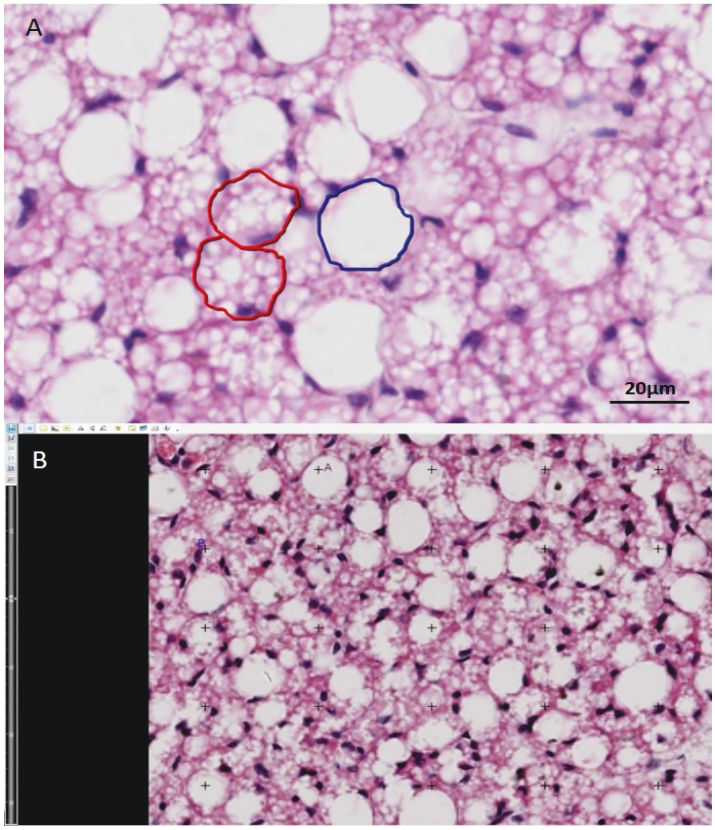

Figure 5.1. H&E stained adipose section from fetal sheep. (A) Red circles indicate multilocular adipocytes and blue circle shows a typical unilocular adipocyte. (B) Counting grid used in meander sampling adipocytes. A multilocular or unilocular was counted when underneath a black '+'.

The final magnification at analysis was x400. A total of 40 counting frames were used per slide to provide at least 200 points per animal. An UL cell was defined as an adipocyte containing a single lipid droplet with a diameter larger than 60µm, after shrinkage. The fractional volume ($Vol_{fraction}$) was calculated using the equation:

$$Vol_{fraction} = P \div T \qquad \textbf{Equation 5.1.}$$

Where P is the number of points falling on either UL or ML cells, and T is the total number of sampling points counted in the adipose tissue.

5.2.4 Relative adipose mass

The mass of each adipocyte component was calculated by multiplying the percentage volume by the total PAT mass at post mortem. The relative mass of each cell type was calculated by dividing the adipose mass by the fetal bodyweight (Equation 5.2):

$$Relative\ adipose\ mass\ (UL\ or\ ML) = \frac{(PAT\ mass\ (g) \times Vol_{fraction})}{Fetal\ Bodyweight\ (kg)}$$

Equation 5.2.

5.2.5 Measurement of UL cell size

Unilocular adipocyte size was determined by measuring cell perimeter using a function of the stereology software NDP.view (Hamamatsu Photonics, Figure 5.2).

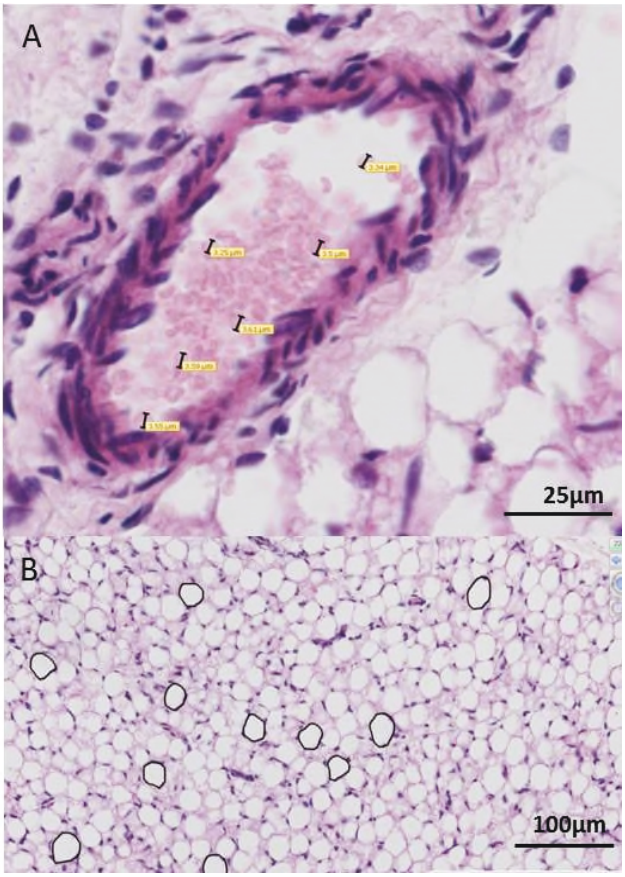

Figure 5.2. Methodology used to measure UL cell size. (A) Adjustment for shrinkage by measurement of red blood cell diameter. (B) Determination of UL cell perimeter.

Between 60 and 80 of the largest UL cells in the sections were measured and the average cell perimeter was calculated for each treatment group. To account for tissue shrinkage, the diameter of red blood cells was also determined. It is known that the average diameter of a red blood cell in fetal sheep is 6µm (Karvonen, 1954) and this was used to calculate the percentage shrinkage in the tissue which was then applied to adjust the cell measurements (Equations 5.3 and 5.4). The amount of tissue shrinkage ranged from 40-50% and there was no difference in the shrinkage between the TX and sham groups.

$$Shrinkage\ factor = 6\mu m\ \div RBC\ diameter$$ **Equation 5.3.**

$$Corrected\ Parameter = \frac{Original\ measurement}{Shrinkage\ factor}$$ **Equation 5.4.**

5.2.6 Western blotting

Quantification of protein in fetal adipose tissue was determined using western blotting. Adipose tissue from each fetus was homogenised (100mg) and its protein concentration determined by a BCA protein assay (described in Section 2.5). The Western blotting procedure is described in detail in Section 2.6.

Components of the insulin signalling pathway as well as PPARγ and proliferating cell nuclear antigen (PCNA) were analysed. In the nuclei of mitotic cells, PCNA is expressed in high levels during the last 5% of the G1-phase and the first 35% of the S-phase of the cell cycle (Bravo *et al.*, 1984; Mathews *et al.*, 1984). The protein, PCNA, is essential for progression through the cell cycle and levels of PCNA indicate the extent of cell proliferation in the tissue. The specific conditions for each antibody used are shown in Table 5.1. The amount of protein loaded was 100µg, with the exception of the measurements of Akt1, Akt2 and pAkt where 75µg protein was used. All samples were heated to 70°C for 10 minutes with the exception of those for p-S6K quantification which were heated to 99°C for 10 minutes.

After detection with ECL, the protein visualised in each sample was normalised to the total protein content measured by Ponceau S. All of the samples were analysed across four gels which were run and transferred together, to minimise variation. A single control sample was run on each of the gels and the results of this control sample were used to standardise the values obtained from all of the membranes. After densitometry and normalisation to total protein, the results were standardised to the mean of the sham group at 129dGA. Results are therefore expressed as fold changes in arbitrary units (au).

Table 5.1. Antibodies used in Western blotting of adipose protein

Primary antibody	Concentration	Blocking agent	Secondary antibody
Rabbit polyclonal anti-InsRβ (Santa Cruz Biotechnologies, Heidelberg, Germany)	10µg/ml	2% Non-fat milk	Anti-rabbit 1:1750 (GE Healthcare)
Rabbit polyclonal anti-IGF-1Rβ (Santa Cruz Biotechnologies)	10µg/ml	2% Non-fat milk	Anti-rabbit 1:1500 (GE Healthcare)
Rabbit polyclonal anti-leptin receptor (LRL, Biorbyt, Cambridge, UK)	1µg/ml	2.5% Non-fat milk	Anti-rabbit 1:2000 (GE Healthcare)
Rabbit polyclonal anti-p-Akt (Ser473, Cell Signaling Technology, Hitchin, UK)	1:800	2.5% BSA	Anti-rabbit 1:2500 (GE Healthcare)
Mouse monoclonal anti-Akt1 (Cell Signaling Technology)	1:1000	2.5% Non-fat milk	Anti-mouse 1:2500 (GE Healthcare)
Rabbit monoclonal anti-Akt2 (Cell Signaling Technology Technology)	1:1000	2.5% Non-fat milk	Anti-rabbit 1:2500 (GE Healthcare)
Rabbit polyclonal anti-pmTOR (Ser 2448, Cell Signaling Technology)	1:800	2% BSA	Anti-rabbit 1:2000 (GE Healthcare)
Rabbit polyclonal anti-pS6K (Thr 389, Cell Signaling Technology)	1:1000	No blocking	Anti-rabbit 1:1500 (GE Healthcare)
Rabbit polyclonal anti-GLUT4 (Abcam)	2.5µg/ml	2% Non-fat milk	Anti-rabbit 1:2000 (GE Healthcare)
Mouse monoclonal anti-PCNA (Dako, Cambridge UK)	2.0µg/ml	No blocking	Anti-mouse 1:1500 (GE Healthcare)
Rabbit polyclonal anti-PPARγ (Biorbyt)	4.0 µg/ml	2.5% Non-fat milk	Anti-rabbit 1:2000 (GE Healthcare)

InsRβ = insulin receptor subunit β, IGF-1Rβ = IGF-I receptor subunit β, LRL = leptin long form receptor, Akt = protein kinase B, pAkt = phosphorylated protein kinase B, pmTOR = phosphorylated mTOR, pS6K = phosphorylated S6 kinase

5.2.7 qRT-PCR

In order to further investigate the mechanism of increased adipose protein content of GLUT4 and PPARγ in the TX fetuses, the mRNA levels of these genes were determined by quantitative reverse transcription polymerase chain reaction (qRT-PCR). Following the reverse transcription of RNA into cDNA, the amplification reaction is monitored in real-time for quantitative analysis. The detection is based on a fluorescent signal and the higher the starting copy number of the nucleic acid target, the sooner a significant increase in fluorescence is seen (Bustin & Mueller, 2005). Quantification is based on threshold cycle values (C_T) and the C_T is the point at which the PCR cycle reaches a fixed fluorescent threshold.

TaqMan probes have gene-specific sequences which are labelled with a fluorescent reporter dye at the 5' end and a quencher dye at the 3' end. When the probe is intact, the quencher dye suppresses the fluorescence of the reporter dye. If the target sequence is present, the probe anneals downstream of one of the primers and is subsequently cleaved by the activity of *Taq* DNA polymerase. This cleavage separates the reporter dye from the quencher dye, and thus increases the reporter signal. Reporter dye is cleaved from the probe with every cycle resulting in an increase in fluorescence which is proportional to the amount of amplicon.

Primer design

Pilot studies with fetal adipose tissue identified the reference genes, β-actin, cyclophilin A and glyceraldehyde 3-phosphate dehydrogenase (GAPDH) to be unsuitable in this study, as C_T values significantly changed with either treatment or gestational age (Figure 5.3). The genes, TATA-box binding protein (TBP) and ribosomal protein L13a (RPL13a), showed no change with treatment or age and were therefore used as reference genes. Ovine-specific TaqMan primers and probes were designed for the reference genes, TBP and RPL13a and for the gene of interest, PPARγ (Thermo Scientific). Probes which spanned the exon-exon boundary were specifically designed to minimise amplification of genomic DNA during PCR. Primers and probes for bovine GLUT4 were purchased ready-made (Thermo Scientific), again, with a reporter sequence that spanned the exon-exon boundary.

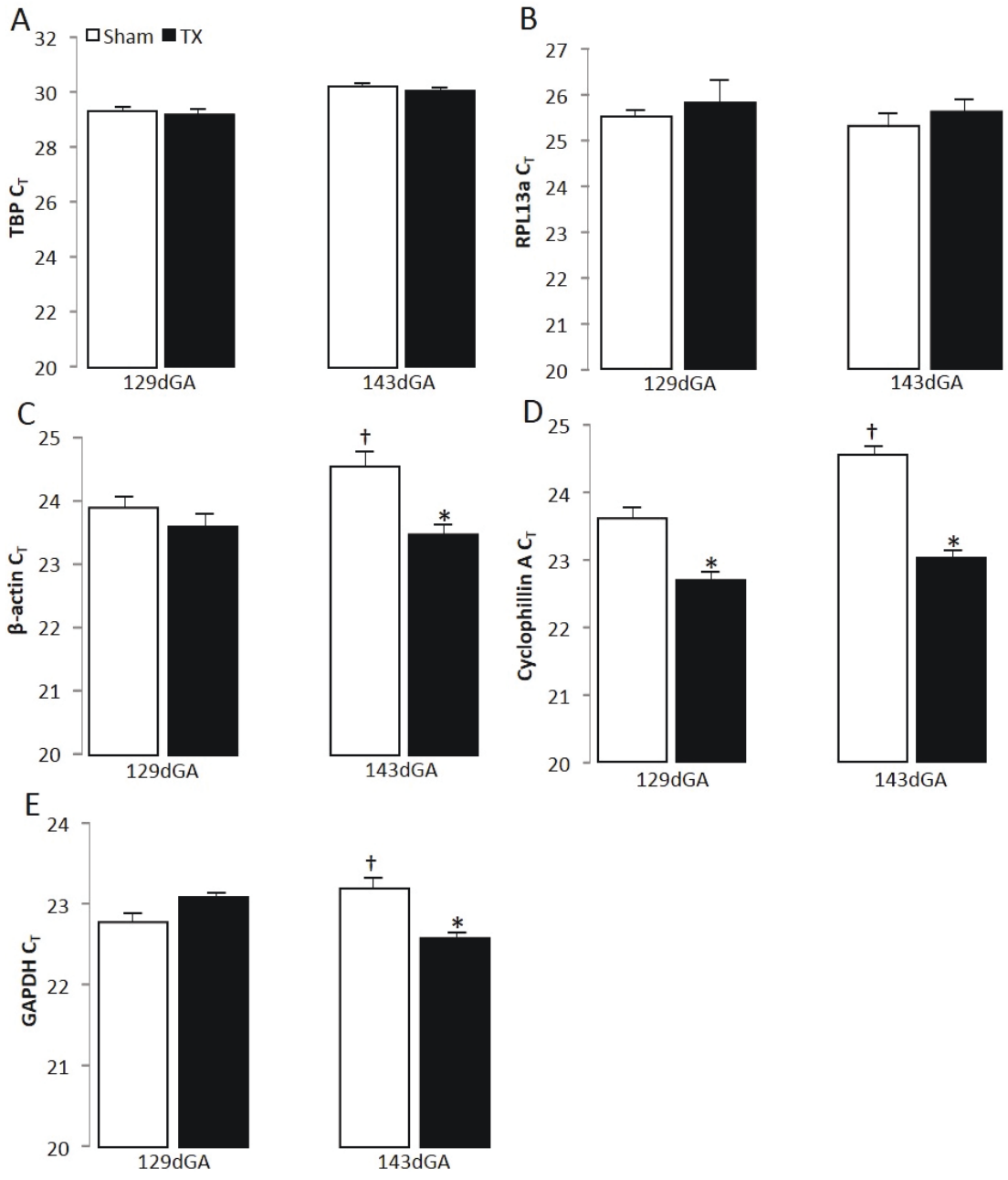

Figure 5.3. Mean ± SEM C_T number of (A) TBP, (B) RPL13a, (C) β-actin, (D) cyclophilin A and (E) GPADH in perirenal adipose tissue from sham and TX fetuses at 129 and 143dGA. * Significantly different from sham fetuses at the same dGA. † Significantly different from fetuses in the same treatment group at 129dGA, 2-way ANOVA, $P<0.05$. n = 4-6 in each group.

All the information for the qRT-PCR primers and probes is detailed in Table 5.2. All probes were attached to a fluorescein (FAM) dye and were used at a concentration of 5µM.

Table 5.2. Gene primers and probes for qRT-PCR in adipose tissue

Gene	Forward Primer	Reverse Primer	Probe reporter sequence	Probe dye
Ovine TBP	CTGGACTTCAAGATTCA GAACATGGT	GGGTTAGCACAAGGCCTT CTA	CACATCACAGCTC CCC	FAM
Ovine RPL13a	CCGGAAAAAGAAGCAG CTCATG	GACCTCTGTGAATTTGCCA ATTTTCT	CAGGCCGAAAAG AACA	FAM
Bovine GLUT4	Taqman(R) Gene Expression Assays. ID: Bt03215316_m1; Part number: 4331182 (Thermo Scientific)		TATGTGGCGGATG CTATGGGTCCCT	FAM
Ovine PPARγ	CGATTCCAGAATGCCTT GCT	GAGATCTCTGCTAACAGCT TTTCCT	CCAAACCTGATGG CATTAT	FAM

TBP = TATA-box binding protein, RPL13a = ribosomal protein L13a, GLUT4 = glucose transporter 4, PPARγ = peroxisome proliferator-activated receptor γ, FAM = fluorescein dye.

RNA extraction

Extraction of adipose tissue RNA was carried out using the RNeasy Mini Kit (Qiagen, Manchester, UK). Frozen adipose tissue was weighed at 30mg and homogenised in lysing matrix tubes containing 600µl RLT lysis buffer using the SuperFastPrep-1 homogeniser (MP Biomedicals) for 10 seconds at 400g. The RLT lysis buffer contained 2M DTT and a high concentration of the protein denaturant guanidine isothiocycanate, which aids in the binding of RNA to a silica membrane.

The samples were centrifuged at 17000g for 3 minutes at 4°C. Supernatant was transferred to fresh tubes and an equal volume of 70% ethanol was added and mixed. The samples were transferred to a RNeasy Mini spin column and centrifuged for 30

seconds at 8000g, after which the supernatant was discarded and the RNA was bound to the silica membrane. Genomic DNA was removed by the addition of the enzyme DNAse I (2.73U/µl; Roche); 10µl DNAse I and 70µl DNAse buffer (Roche) were added to the silica membrane in the spin column. The column was left to incubate at room temperature for 15 minutes.

Following incubation, 700µl Qiagen wash buffer was added, containing ethanol and guanidine salt. The wash buffer removes proteins, fatty acids, carbohydrates and other molecules that are not bound to the silica membrane. The column was centrifuged at 9000g for 30 seconds and the flow-through discarded. The column was washed twice with 500µl Qiagen RPE wash buffer containing ethanol, and centrifuged at 14000g for 1 minute between each wash. The column was spun empty to remove any further traces of ethanol. To elute the RNA, 50µl RNAse free water was added to the column which was centrifuged for 1 minute at 9000g.

Determination of RNA concentration

The concentration of extracted RNA was determined using a NanoDrop spectrophotometer (Thermo Scientific). The NanoDrop was calibrated with RNAse free water before measurement of RNA. Surface tension holds 2µl of sample between two optical fibres; a light is emitted and the spectrometer analyses the light passed through the sample. Nucleotides such as RNA absorb light at 260nm and the 260/280nm ratio is a measurement of RNA purity. A ratio of 2.0 is considered to be good quality RNA with low DNA contamination. All samples had a 260/280nm ratio between 1.8 and 2.0.

Generation of cDNA

Complementary DNA is double stranded DNA synthesised from the extracted RNA and this was achieved using the high capacity cDNA reverse transcription kit (Applied Biosystems, Loughborough, UK). The kit uses random primers to initiate cDNA synthesis and the enzyme reverse transcriptase to synthesise the cDNA. A reverse transcription master mix was made by combining buffer, deoxynucleotide solution, random primers, reverse transcriptase and water. To a 0.2µl PCR tube, 10µl master mix was added with 10µl 40ng/µl RNA sample. The samples were heated to 25°C for 10 minutes, 37°C for 2

hours, 85°C for 5 minutes, followed by cooling at 4°C. One sample from each treatment group was treated without the addition of reverse transcriptase as a negative control.

qRT-PCR reaction

Samples were analysed for mRNA abundance using the CFX Connect Real Time PCR detection system and data were acquired and processed with CFX Manager Software (BioRad). Each sample was measured in triplicate and the C_T value of the target gene was normalised to the geometric mean of TBP and RPL13a. For each plate, a negative control without cDNA was included to ensure that no amplicon contamination had occurred in the reaction. In addition, cDNA from one sample was measured on each plate across all assays as a quality control. To confirm the absence of genomic DNA, the reverse transcriptase negative controls were also included. For all qRT-PCR reactions (optimisation and experimental) the plates were incubated for 40 cycles at: 50°C for 2 minutes, 95°C for 10 minutes (polymerase activation), 95°C for 15 seconds (denaturation) and 57°C for 1 minute (annealing).

In a reaction tube, 10µl TaqMan gene expression master mix with uracil-N-glycosylase (Applied Biosystems) was added to 1µl primer/probe mix. In a white 96 well plate (BioRad), 11µl master mix solution was added to each well followed by 9µl diluted cDNA (1:10). The plate was sealed with an optical adhesive film (Applied Biosystems).

Standard curves

With test adipose cDNA, PCR reactions using reference and target genes were run to obtain standard curves to determine the reaction efficiency. If the standard curves for each gene are parallel, it indicates that the reactions have equal efficiency (Bustin *et al.*, 2009).

The cDNA was serially diluted seven times to a final dilution of 1 in 320. From the measurements, the log of the dilution was plotted against the mean C_T. The reaction efficiency was determined from the slope using Equation 5.5 (Bustin *et al.*, 2009). The slopes for each gene were parallel and the linear relationships, denoted by R^2, were all over 0.98 (Figure 5.4).

$$Efficiency = 10^{(-1 \div slope)}$$ **Equation 5.5.**

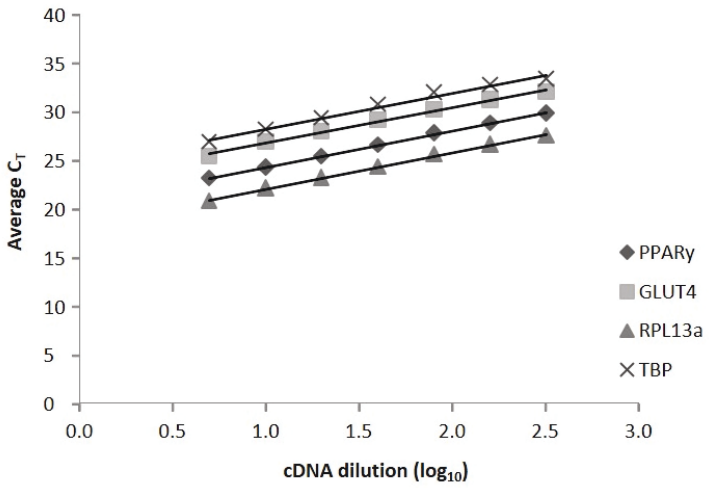

Figure 5.4. Standard curves of average C_T for genes of interest and reference genes in fetal adipose tissue. TBP = TATA-box binding protein, RPL13a = ribosomal protein L13a, GLUT4 = glucose transporter 4, PPARγ = peroxisome proliferator-activated

Quantification of gene expression

As the standard curves for all assays were parallel, the geometric mean of the two reference genes (Rf) was used to analyse the C_T number of the genes of interest (GOI) using the comparative $\Delta\Delta C_T$ method, which is summarised in Equation 5.6 (Vandesompele *et al.*, 2002; Garcia-Crespo *et al.*, 2005; Schmittgen & Livak, 2008). The results were expressed as mean fold changes compared to sham fetuses at 129dGA.

$$\Delta C_T 1 = C_T(TX, GOI) - C_T(TX, Rf)$$
$$\Delta C_T 2 = C_T(Sham, GOI) - C_T(Sham, Rf)$$
$$\Delta\Delta C_T = \Delta C_T 1 - \Delta C_T 2$$
$$Normalised\ target\ gene\ expression\ level = 2^{-\Delta\Delta CT}$$ **Equation 5.6.**

5.2.8 Statistical analysis

All values are expressed as mean ± SEM unless otherwise indicated. The CV was calculated for each stereological parameter using Equation 5.7, where S is the standard deviation and $\overline{x}$ is the mean of the samples. All of the measurements had a CV of 15% or less.

$$\%CV = (S \times 100) \div \overline{x}$$

Equation 5.7.

Statistical significance for comparisons between all parameters was assessed using a three-way ANOVA using sex, treatment and gestational age as factors, followed by the Tukey *post hoc* test. Once it was established that sex had no effect, parameters were assessed using a two-way ANOVA with treatment and gestational age as factors, followed by the *post hoc* Tukey test. For assessment of differences between the data from two groups, a Student's t-test was implemented. For correlation analysis, a linear regression was used. In all cases, significance was accepted at $P<0.05$.

5.3 Results

5.3.1 Adipose tissue composition

From the H&E stained sections, it was clear that the structure of the adipose tissue in the TX fetuses differed in the relative composition of UL and ML adipocytes, compared to that of the sham controls at both 129 and 143dGA (Figure 5.5). The TX fetuses appeared to have more UL and fewer ML adipocytes compared to the sham controls at both 129 and 143dGA.

In the sham fetuses, there was a significantly greater proportion of ML relative to UL adipocytes at both 129dGA (ML 69 ± 3% vs UL 31± 3%) and 143dGA (ML 68 ± 3% vs UL 32 ± 3%, Student's t-test, $P<0.001$, Figure 5.6). In contrast, the proportions of ML and UL adipocytes in the TX fetuses were similar at both 129dGA (ML 46 ± 4% vs UL 53 ± 4%) and 143dGA (ML 49 ± 4% vs UL 51 ± 4%).

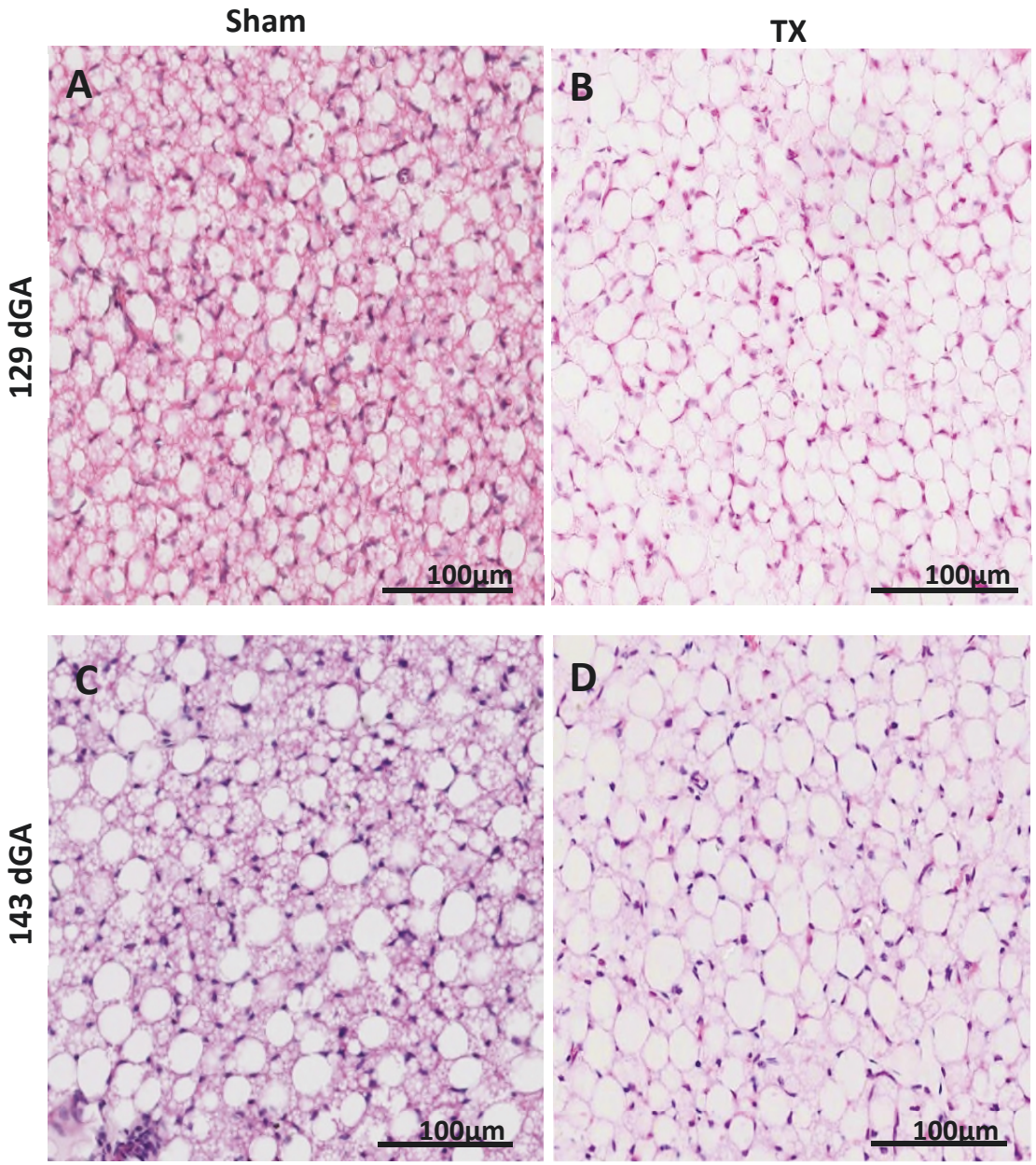

Figure 5.5. H&E stained sections of perirenal adipose tissue in (A) sham 129dGA, (B) TX 129dGA, (C) sham 143dGA and (D) TX 143dGA.

A significant increase in the percentage of UL adipocytes, and a significant reduction in ML adipocytes, were observed in the TX fetuses compared to the sham controls ($P<0.05$, Figure 5.6). There was no effect of gestational age on the adipocyte proportions in either treatment group.

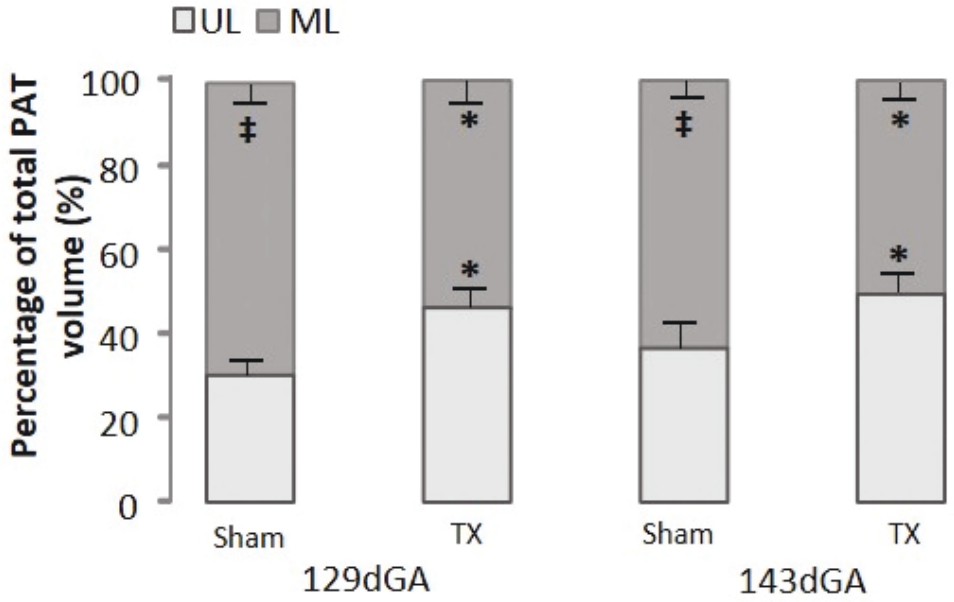

Figure 5.6. Mean ± SEM ML and UL adipose cell proportion expressed as % of total perirenal adipose tissue (PAT) volume, in sham and TX fetuses at 129 and 143dGA. * Significantly different from sham fetuses at the same dGA, 2-way ANOVA, *P*<0.05. ‡ Significantly different from the UL cell type in same treatment group, Student's t-test, *P*<0.001, n = 9-10 in each group.

When the percentages of ML and UL adipocytes were expressed as absolute and relative adipocyte mass, significant increases in UL cell mass were observed in the TX fetuses compared to sham fetuses at both 129 and 143dGA (*P*<0.05, Figure 5.7). The relative mass of the UL cells in the TX fetuses was double that seen in the sham fetuses at both 129dGA (sham 1.2 ± 0.2g/kg vs. TX 2.4 ± 0.3g/kg) and 143dGA (sham 1.1 ± 0.2g/kg vs. TX 2.3 ± 0.3g/kg, *P*<0.05, Figure 5.7B). There was no effect of hypothyroidism on the absolute or relative ML adipocyte mass (Figure 5.7). Gestational age had no effect on the absolute or relative adipocyte mass in either treatment group (Figure 5.7).

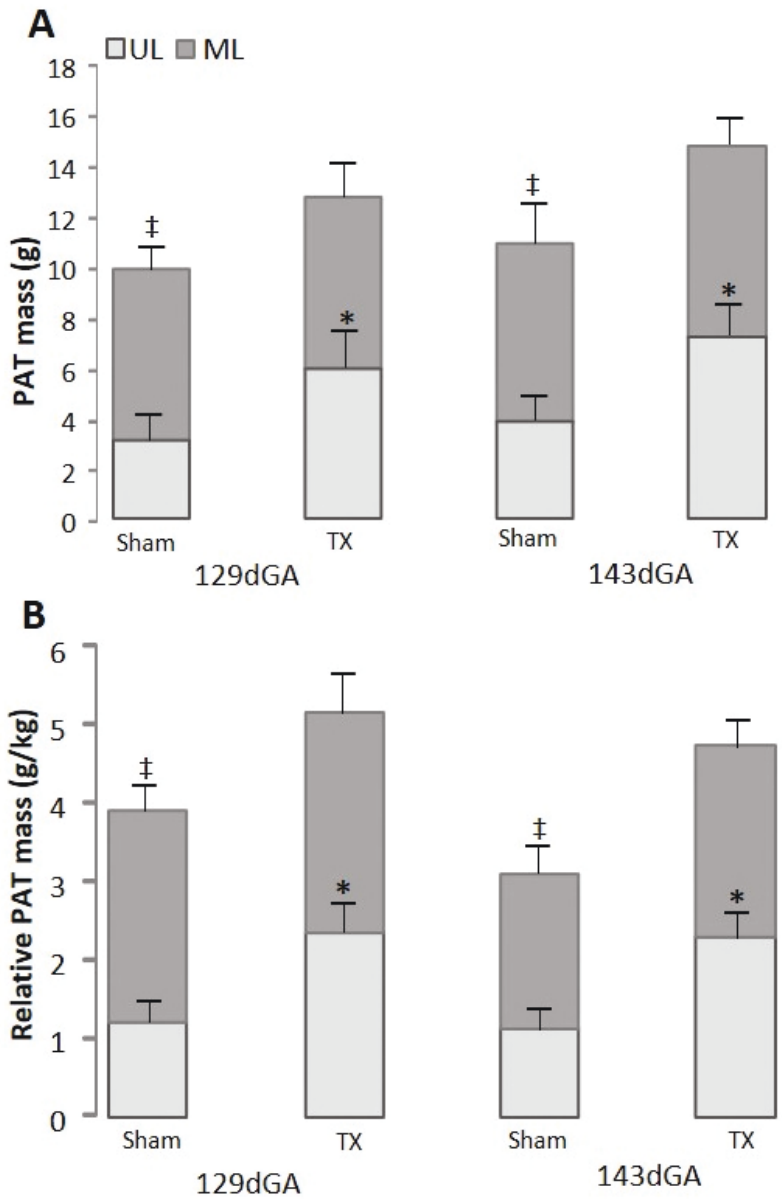

Figure 5.7. Mean ± SEM UL and ML adipocyte mass expressed as (A) absolute PAT mass and (B) relative PAT mass in sham and TX fetuses at 129 and 143dGA. * Significantly different from sham fetuses at the same dGA, 2-way ANOVA, *P*<0.05. ‡ Significantly different from the UL cell type in same treatment group, Student's t-Test, *P*<0.001. n = 9-10 in each group.

When all data were combined, significant positive correlations were observed between the relative UL mass and plasma concentrations of both insulin (R=0.49, R^2 = 0.24, n=37, *P*<0.005, Figure 5.8A) and leptin (R= 0.68, R^2 = 0.46 n=38, *P*<0.001, Figure 5.8B).

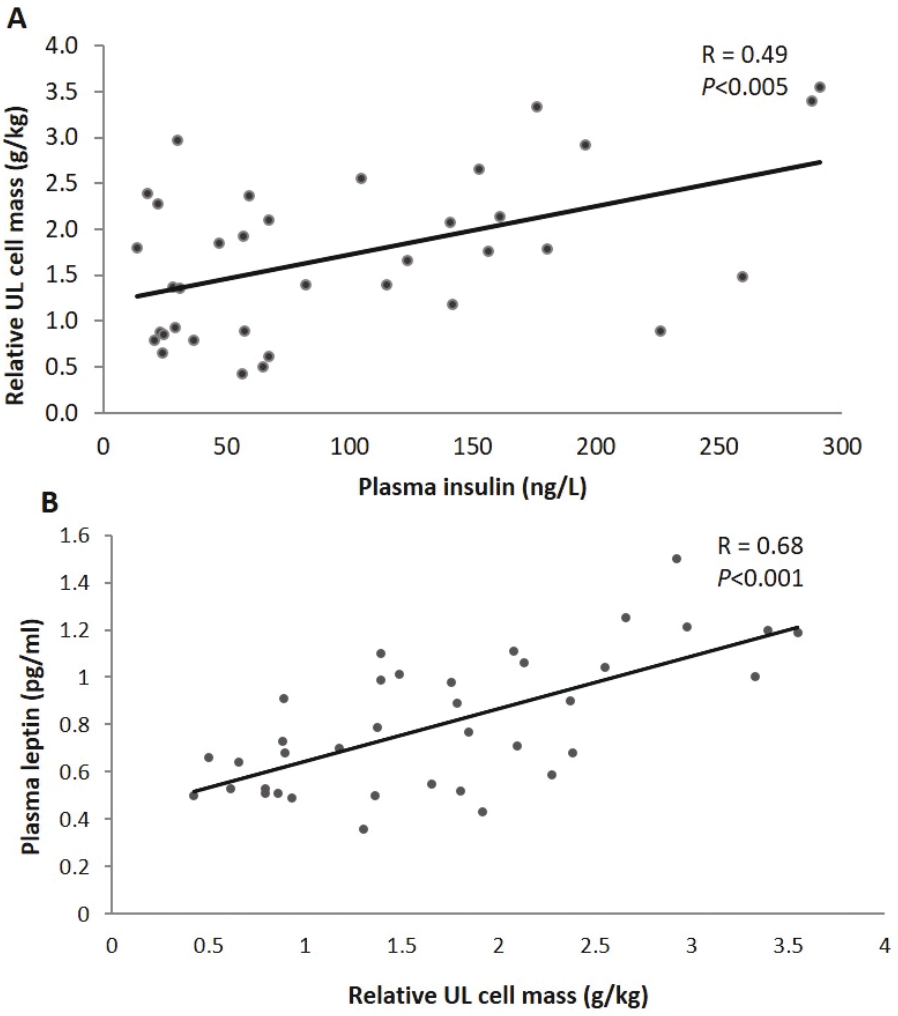

Figure 5.8. Correlation between relative UL cell mass and (A) plasma insulin concentrations, n=37 and (B) plasma leptin concentrations in sham and TX fetuses at 129 and 143dGA, n=38.

5.3.2 Unilocular adipocyte size

There was no difference in the average perimeter of the largest UL adipocytes between the sham and TX fetuses at both 129 and 143dGA (Figure 5.9). In both treatment groups, average UL cell size increased significantly with age between 129dGA and 143dGA ($P<0.05$, Figure 5.9).

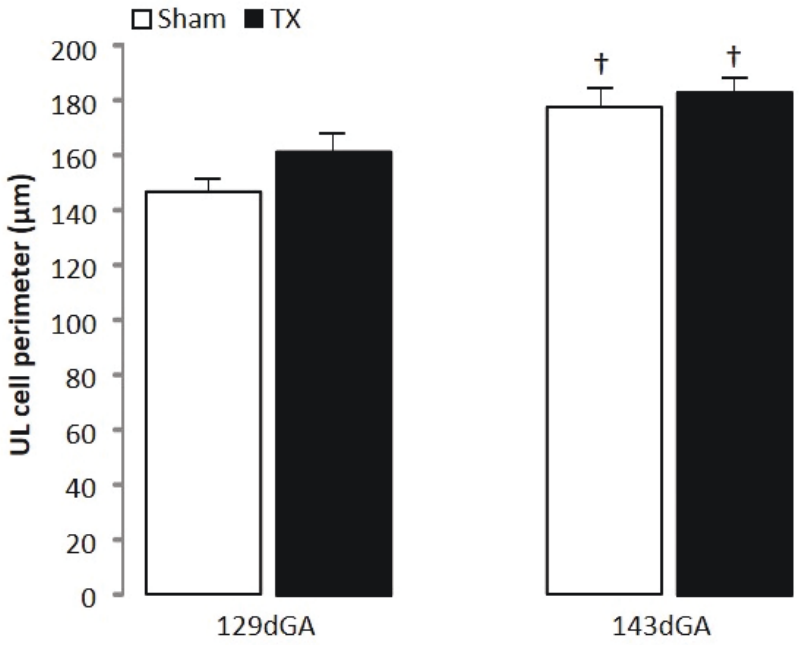

Figure 5.9. Mean ± SEM UL adipocyte perimeter, after correction for shrinkage, in PAT from sham and TX fetuses at 129 and 143dGA. † Significantly different from fetuses in the same treatment group at 129dGA. 2-way ANOVA, *P*<0.05. n = 9-10 in each group.

5.3.3 Proliferative and adipogenic markers

PCNA

In PAT from hypothyroid fetuses PCNA protein content was significantly greater than that in sham controls at both 129 and 143dGA (*P*<0.05, Figure 5.10), with no effect of gestational age in either treatment group.

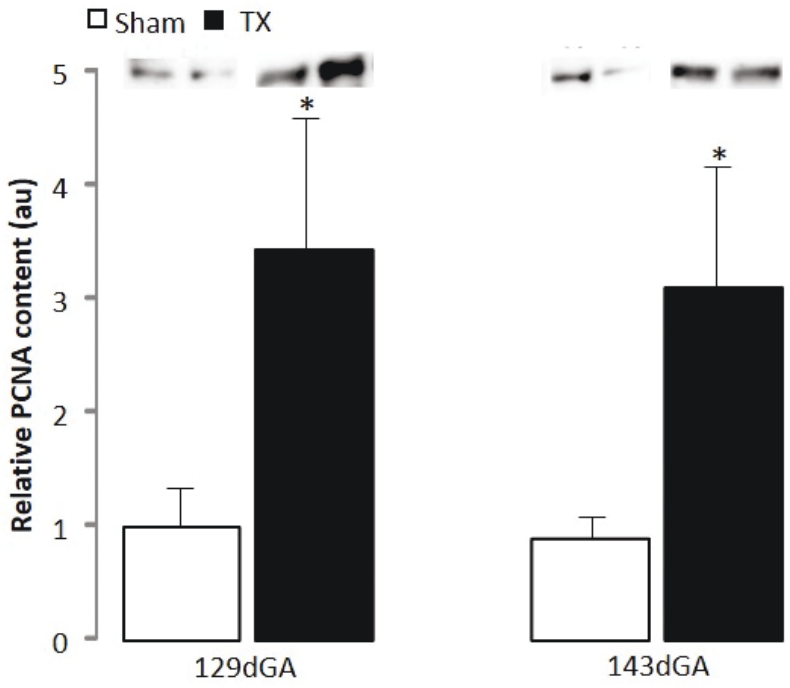

Figure 5.10. Mean ± SEM relative protein expression of PCNA in PAT from sham and TX fetuses at 129 and 143dGA. Representative blot images from two fetuses in each treatment group are shown. * Significantly different from sham fetuses at the same dGA, 2-way ANOVA, *P*<0.05. n = 8-10 in each group.

PPARγ

The adipose protein levels of PPARγ were significantly increased in the hypothyroid fetuses at both 129 and 143dGA, compared to the sham fetuses (*P*<0.05, Figure 5.11A). There was no effect of gestational age on PPARγ protein expression in either treatment group.

The mRNA abundance of PPARγ was increased by approximately 33% in the TX fetuses at both 129 and 143dGA, compared to sham controls (*P*<0.05, Figure 5.11B). In both the sham and TX fetuses there was a near significant effect of gestational age in PPARγ mRNA between 129 to 143dGA (*P*=0.06, Figure 5.11B).

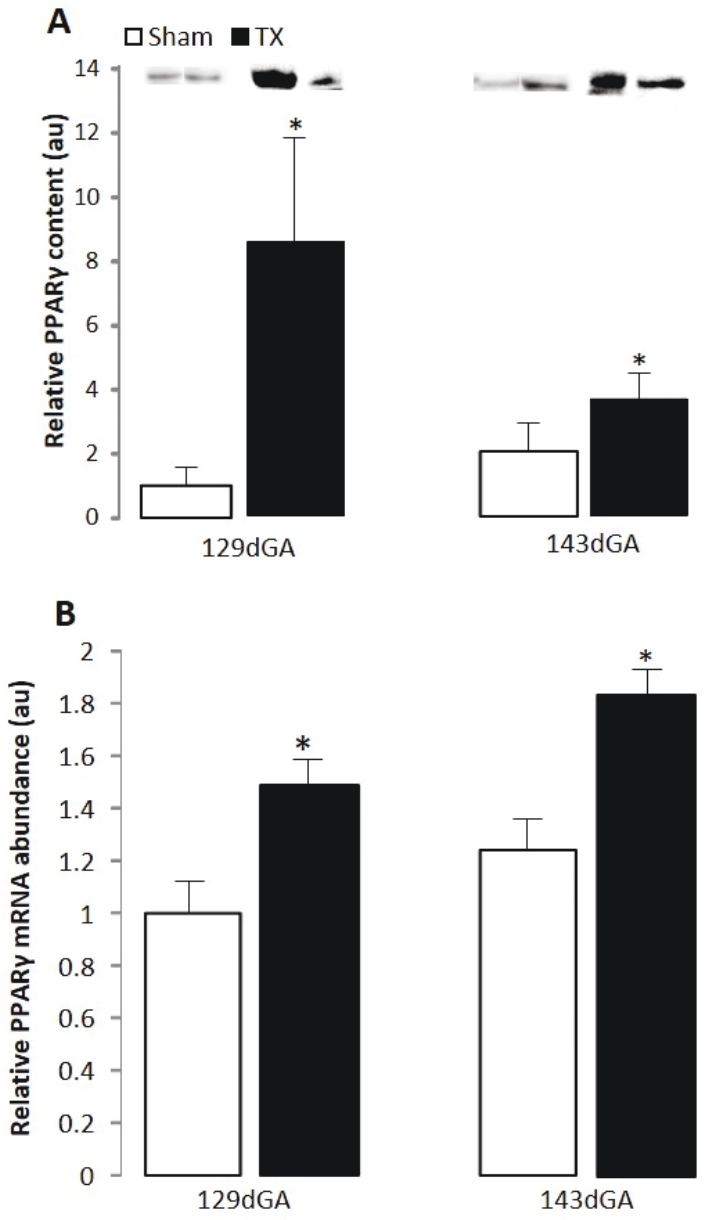

Figure 5.11. Mean ± SEM relative (A) protein expression and (B) mRNA abundance of PPARγ in PAT from sham and TX fetuses at 129 and 143dGA. * Significantly different from sham fetuses at the same dGA, 2-way ANOVA, *P*<0.05. n = 8-10 in each group

5.3.4 Insulin signalling proteins

Receptors

The amount of InsRβ protein was significantly lower in the TX fetuses compared to sham controls at 129dGA (P<0.05, Figure 5.12A). At 143dGA, there was no significant difference in adipose InsRβ levels between the sham and TX fetuses. A significant reduction in InsRβ protein was seen between 129 and 143dGA in the sham, but not TX, fetuses (P<0.05, Figure 5.12A).

Adipose IGF-1Rβ protein content was also significantly decreased in the TX fetuses compared to sham controls at 129dGA (P<0.05, Figure 5.12B). By 143dGA, however, the amount of IGF-1Rβ in the TX fetuses increased above that seen at 129dGA (P<0.05) and to the same level seen in the sham controls (Figure 5.12B). There was no change in IGF-1Rβ content in the sham fetuses with gestational age.

The amount of long form leptin receptor in adipose tissue was unaffected by gestational age or thyroidectomy (Figure 5.12C).

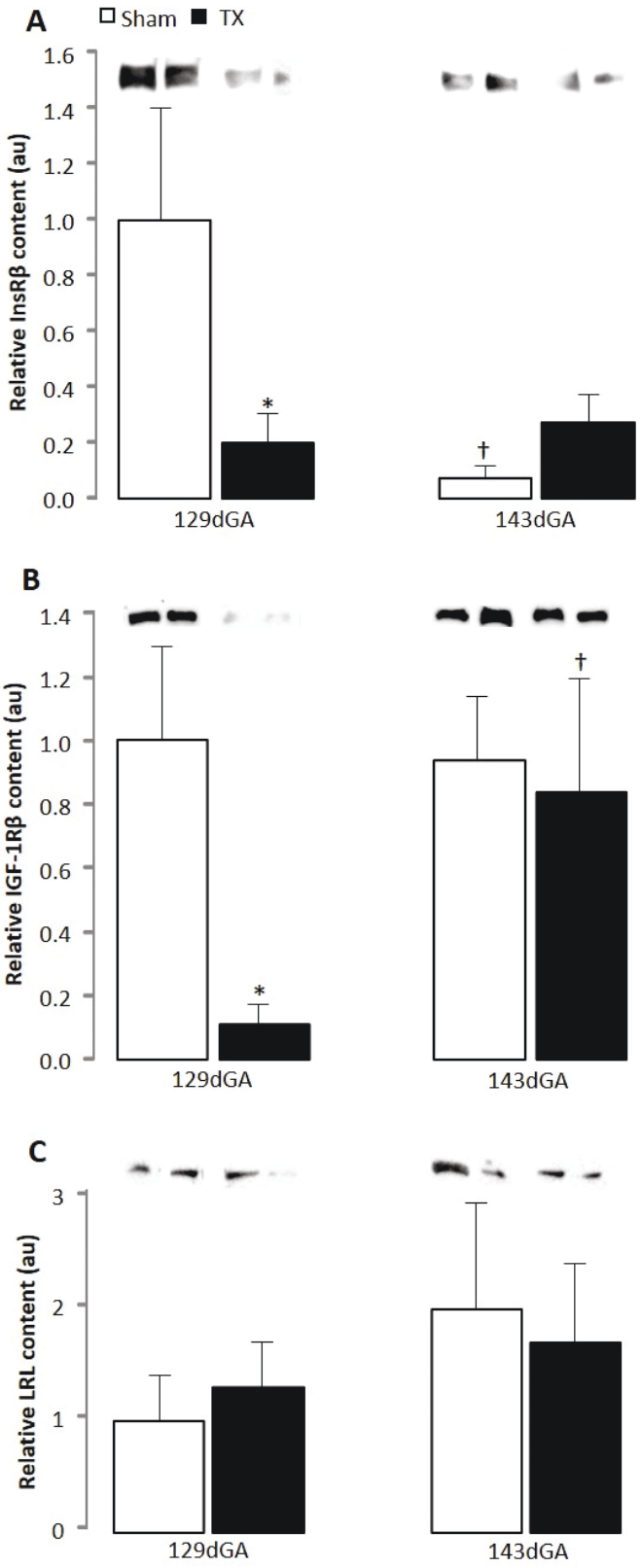

Figure 5.12. Mean ± SEM relative protein expression of (A) InsRβ, (B) IGF-IRβ and (C) LRL in PAT from sham and TX fetuses at 129 and 143dGA. * Significantly different from sham fetuses at the same dGA , † Significantly different from fetuses in the same treatment group at 129dGA, 2-way ANOVA, $P<0.05$. n = 9-10 in each group.

Akt

Adipose protein levels of Akt1 were significantly increased, while Akt2 levels were significantly decreased in TX fetuses compared to sham controls at both 129 and 143dGA (P<0.05, Figure 5.13A, B). In both treatment groups, there was no effect of gestational age on adipose protein content of either Akt1 or Akt2.

The amount of pAkt was significantly decreased in the TX fetuses at 129dGA when compared to sham controls (P<0.05, Figure 5.13C). In the hypothyroid fetuses, there was a significant effect of gestational age, with the amount of pAkt increased between 129 and 143dGA (P<0.05, Figure 5.13C). At 143dGA, therefore, there was no difference in the protein expression of pAkt between the TX and sham fetuses (Figure 5.13C).

Downstream targets

Protein expression levels of pmTOR tended to be lower in the TX fetuses at 129 and 143dGA compared to sham controls (2-way ANOVA, P=0.08, Figure 5.14A). When a Student's t-test was used to compare the data from TX and sham fetuses, there was a significant decrease in pmTOR at 143dGA in response to hypothyroidism (P<0.05, Figure 5.14A). There was no effect of gestational age on pmTOR protein content in either treatment group.

The adipose levels of pS6K were significantly increased in the TX fetuses at both 129 and 143dGA compared to the sham fetuses (P<0.05, Figure 5.14B). In the TX, but not sham fetuses, a significant decrease in pS6K was observed between 129 and 143dGA (P<0.05, Figure 5.14B).

In the hypothyroid fetuses, the protein expression of GLUT4 in PAT was significantly increased by 60 and 80%, at 129 and 143dGA, respectively, compared to sham controls (P<0.05, Figure 5.14C). There was no effect of gestational age on adipose GLUT4 levels in either treatment group.

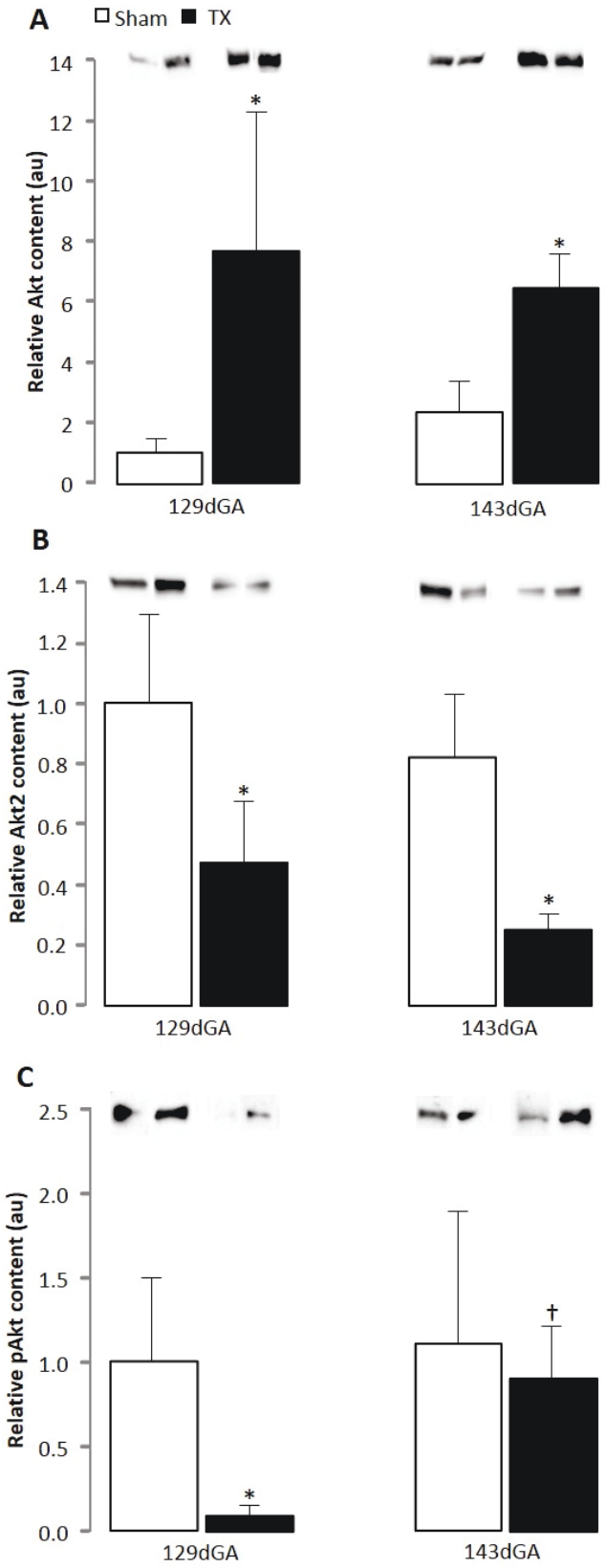

Figure 5.13. Mean ± SEM relative protein expression of (A) Akt1 (B) Akt2 and (C) pAkt in PAT from sham and TX fetuses at 129 and 143dGA. * Significantly different from sham fetuses at the same dGA, † significantly different from fetuses in the same treatment group at 129dGA, 2-way ANOVA, $P<0.05$. n = 9-10 in each group.

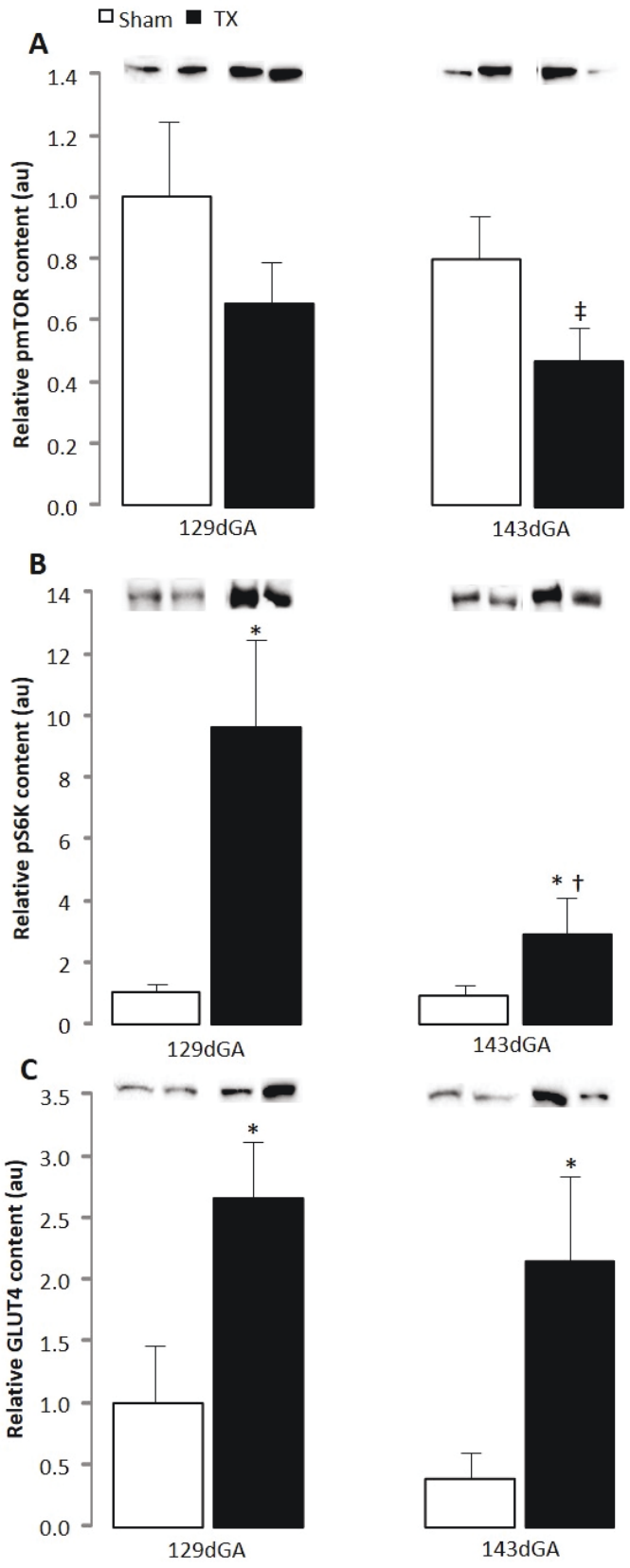

Figure 5.14. Mean ± SEM relative protein expression of (A) pmTOR (B) pS6K and (C) GLUT4 in PAT from sham and TX fetuses at 129 and 143dGA. * Significantly different from sham fetuses at the same dGA, † significantly different from fetuses in the same treatment group at 129dGA, 2-way ANOVA, $P<0.05$. ‡ Significantly different from sham fetuses at 143dGA, Student's t-test $P<0.05$. n = 8-10 in each group.

At 129dGA, adipose GLUT4 mRNA abundance was significantly increased by approximately 25% in the TX fetuses, compared to sham controls (P<0.05, Figure 5.15). A developmental increment in GLUT4 mRNA level was observed between 129 and 143dGA in the sham but not the TX fetuses (P<0.05, Figure 5.15). Adipose GLUT4 mRNA abundance was similar in the TX and sham fetuses at 143dGA (Figure 5.15).

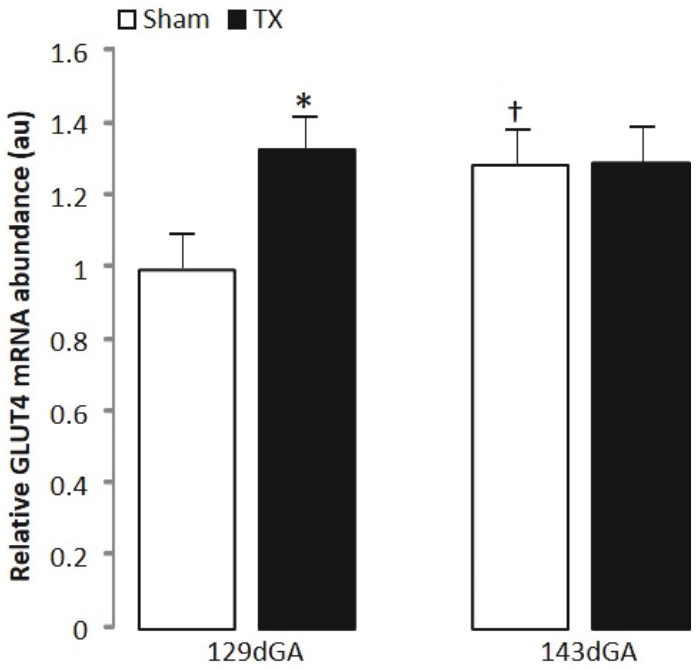

Figure 5.15. Mean ± SEM relative mRNA abundance of GLUT4 in PAT from sham and TX fetuses at 129 and 143dGA. * Significantly different from sham fetuses at the same dGA, † significantly different from fetuses in the same treatment group at 129dGA, 2-way ANOVA, P<0.05, n = 8-10 in each group.

5.4 Discussion

5.4.1 Hypothyroidism induced unilocular cell hyperplasia

Development of adipose tissue *in utero* is vital for fat storage, energy provision and metabolism, and thermoregulation in the offspring over the perinatal period. This study has shown that thyroid hormone deficiency in the sheep fetus during late gestation leads to enlargement of relative PAT mass, which was due to a specific increase in UL

adipocyte mass. The relative mass of the ML adipocytes, however, was not altered in the TX fetus. As there was no effect of gestational age on the adipocyte composition in either treatment group, it is indicated that this phenotype was established prior to 129dGA and maintained to term.

To determine if the increase in UL adipocyte mass in response to hypothyroidism was due to hypertrophy and/or hyperplasia, UL adipocyte size was measured by perimeter. If the growth in PAT was due to adipocyte hypertrophy, the average cell perimeter would be expected to be larger in the hypothyroid fetuses. As there was no apparent difference in the UL adipocyte size between the TX and sham fetuses, it can be postulated that the overgrowth of the adipose tissue in the TX fetus was due to adipocyte hyperplasia. This was confirmed by the increase in the protein level of the mitotic marker, PCNA, in the TX fetus at both 129 and 143dGA. In both treatment groups, the average UL cell size increased with gestational age. This is to be expected as lipid deposition occurs in fetal adipose tissue in preparation for energy availability after birth.

Hypothyroidism in the sheep fetus during late gestation may influence PAT mass by changes in lipid metabolism. In human adults, hypothyroidism has previously been shown to reduce catecholamine-stimulated lipolysis (Wahrenberg *et al.*, 1986). Adult rats with a transgenic deletion of TRα1 have a higher fat mass and decreased expression of lipolytic enzymes in the liver compared to wild type controls (Liu *et al.*, 2003). Additionally, it has been reported in adult rats that hypothyroidism reduces expression of β-adrenergic receptors in WAT (Germack *et al.*, 2000). Reduced sensitivity to catecholamine in the TX fetus may result in an inability to utilise fat storage for energy expenditure. Future studies could examine lipid metabolic pathways and β-adrenergic receptor expression in PAT and other tissues in the TX sheep fetus.

Although the relative proportion of ML adipocytes in PAT was decreased by hypothyroidism *in utero*, the overall absolute and relative ML mass was unchanged. However, the functionality of BAT as a thermoregulatory organ in the TX fetus remains unknown. Polk *et al.* (1987) showed that thyroidectomy in the sheep fetus results in hypothermia, impaired thermogenesis and a decrease in circulating free fatty acids in

the newborn lamb. Thermogenesis at birth is regulated, in part, by the expression of UCP1 in BAT, and the UCP1 gene is known to contain a TRE (Rabelo *et al.*, 1995). Adipose UCP1 mRNA levels rise towards term, coincident with the abundance of D2 in fetal PAT, indicating a local site for T3 production and activation of UCP1 (Clarke *et al.*, 1997; Pope *et al.*, 2014). Therefore, adipose UCP1 may be downregulated in the TX fetuses due to the prevention of the prepartum rise in thyroid hormones. The expression of UCP1 and thermogenic capacity of BAT remains to be investigated in the TX sheep fetus.

5.4.2 Hypothyroidism increased expression of adipogenic marker PPARγ

The pro-adipogenic transcription factor, PPARγ, is critical for the differentiation of adipocytes (Stephens, 2012). Mice with genetic deletion of PPARγ fail to develop adipocytes, indicating its importance in adipose growth (Rosen *et al.*, 1999). Thyroidectomy in the sheep fetus led to an increase in adipose PPARγ mRNA and protein at both 129 and 143dGA compared to controls. This is the first report of increased adipose PPARγ in the hypothyroid sheep fetus, indicating that thyroid hormones may regulate UL adipogenesis via PPARγ action before birth.

It has previously been reported that adipose PPARγ mRNA levels are higher in the lamb one month after birth compared to the fetus (Mühlhäusler *et al.*, 2007) and, therefore the hypothyroid fetus may show precocious expression of PPARγ in PAT and an early transition in adipose function from thermogenesis to lipid storage, which would normally take place sometime after birth. The exact regulation of PPARγ by T3 is unknown. It has been identified that TRα1 competes with PPARγ for binding to the peroxisome proliferator response element on target genes (PPRE; Ying *et al.*, 2007). Binding of T3 to TRα1 results in the recruitment of a co-repressor to the PPRE and prevents the binding of PPARγ to RXR (Ying *et al.*, 2007), thus repressing PPARγ transcription of other regulatory genes. This example of crosstalk between TR and PPARγ indicates that further knowledge is required to understand the regulation of adipogenesis by thyroid hormones before and after birth.

5.4.3 Plasma insulin concentrations correlated with UL adipocyte mass

When all data were considered, there was a significant positive correlation between circulating insulin concentrations and relative UL adipocyte mass, suggesting that the rise in the population of UL adipocytes present in the TX fetus may be a direct result of increased insulin action.

Insulin is known to promote growth of adipose tissue before birth (Teruel *et al.*, 1996; Kamana *et al.*, 2015). Human offspring born to obese mothers have increased total fat mass and a greater percentage adiposity which are associated with higher umbilical cord concentrations of insulin, compared to offspring of lean mothers (Catalano *et al.*, 2009b). In adult humans, it has previously been reported that the circulating insulin concentrations correlate with the number of adipocytes in subcutaneous adipose tissue (Arner *et al.*, 2010). Furthermore, in obese adult rats, adipocyte proliferative capacity correlates with increased plasma insulin concentrations (Johnson *et al.*, 1978).

Increased circulating insulin concentrations in the TX fetus may have contributed to UL adipose growth through increased glucose uptake. Fetal thyroid hormone deficiency increased the mRNA abundance of adipose GLUT4 at 129dGA and the protein expression at both 129 and 143dGA. Elevated levels of adipose GLUT4 in the TX fetus may promote glucose uptake which is stored as lipid, through the process of lipogenesis, thus contributing to the increased unilocular adipocyte mass. Indeed, in adult mice with an overexpression of adipose GLUT4, adipocyte number was increased two-fold, with no change seen in adipocyte cell size (Shepherd *et al.*, 1993). It is not known, however, whether the increased adipose levels of GLUT4 seen in the TX fetus are representative of cytoplasmic and/or membrane bound GLUT4. The trafficking of GLUT4 needs to be assessed to ascertain whether there is simply an increase in the number of transporters and whether this is translated to functional glucose uptake. Additionally, GLUT4 protein was increased without any change in mRNA abundance in the TX fetus at 143dGA, suggesting that there may be changes in post-transcriptional processes. This is the first report of increased GLUT4 protein and mRNA in the adipose tissue of the thyroid deficient sheep fetus and is consistent with previous studies in the neonatal rat, where thyroidectomy induced adipose GLUT4 protein and mRNA (Castello *et al.*, 1994).

Insulin may stimulate an increase in fetal UL adipose mass by a variety of mechanisms, including increased expression of PPARγ. In adult life, insulin is known to promote lipogenesis by an increase in the genes encoding acetyl-CoA carboxylase and fatty acid synthase (Kersten, 2001). The transcription factor, SREBP-1, increases lipogenic gene transcription and is stimulated by the insulin signalling pathway (Saltiel & Kahn, 2001). In a rodent model of type 1 diabetes, adipose PPARγ mRNA abundance is decreased by 80% compared to controls, and this is restored to normal levels after treatment with insulin (Vidal-Puig *et al.*, 1996). Additionally, in human adults, insulin infusion via euglycaemic-hyperinsulinaemic clamp increased PPARγ mRNA in biopsied adipose tissue (Rieusset *et al.*, 1999). It has also been demonstrated that PPARγ activation can influence various components of the insulin signalling pathway to increase glucose uptake and enhance lipid metabolism in skeletal muscle. In adult human subjects, treatment with a PPARγ agonist increases PI3K and Akt activity in skeletal muscle (Meyer *et al.*, 2002). Adipose PPARγ may also indirectly regulate GLUT4 expression. Expression of PPARγ induces C/EBP α, which then acts in a positive feedback loop to maintain normal levels of PPARγ (Wu *et al.*, 1999). It has been demonstrated that induction of C/EBPα by PPARγ is necessary for insulin-induced glucose transport in adipose cells (Wu *et al.*, 1999) and, therefore, in the TX fetus the rise in PPARγ may also contribute to the increase in GLUT4 protein expression in PAT to promote further growth of UL adipose tissue.

5.4.4 Hypothyroidism altered insulin signalling in fetal adipose tissue

Insulin and IGF-I receptor expression

Thyroid hormone deficiency in the sheep fetus during late gestation altered normal insulin signalling in PAT. Protein expression of both the insulin and IGF-I receptors was decreased in the TX fetus at 129dGA compared to controls, indicating that hypothyroidism altered adipose insulin sensitivity in the younger fetuses. This may be a consequence of hyperinsulinaemia in the TX fetus which causes downregulation of the insulin receptor by a homeostatic negative feedback mechanism in adipocytes. In the sham fetuses, there was suppression of PAT InsRβ protein content with age towards term. This may be due to other hormonal influences during late gestation, such as

cortisol, possibly to reduce insulin signalling and limit adipose proliferation near term to promote thermogenic function.

Downstream targets in insulin signalling

Previous studies have reported that Akt is essential in adipocyte development. Neonatal mice which are deficient in both Akt1 and Akt2 are severely growth impaired with sparse fat pads and no visible lipid droplets (Peng *et al.*, 2003). In addition, it has previously been established that Akt1 has a wide tissue distribution in adults and is important for cell proliferation, whereas Akt2 is highly expressed in adipose tissue and skeletal muscle and contributes to the regulation of insulin-mediated glucose uptake (Hers *et al.*, 2011). In this study, the adipose protein expression of Akt1 was increased, and Akt2 decreased, in the TX fetuses compared to sham controls at both 129 and 143dGA. The rise in Akt1 may contribute to the mechanism whereby insulin promotes UL adipocyte proliferation. The coincident decrease in Akt2, however, suggests that there may be a defect in insulin signalling that could result in impaired insulin-mediated glucose uptake, although adipose GLUT4 expression was elevated in the TX fetus. Alternatively, the reduction in Akt2 seen in the TX fetuses may result from negative feedback to limit adipocyte glucose uptake. Interestingly, Akt2 has also been shown to control cell cycle exit. Studies using small interfering RNA in mouse and human fibroblasts *in vitro* identified that Akt2 had no role with respect to cell cycle entry or cell proliferation, but was required for cell cycle exit by targeting cell cycle inhibitors (Heron-Milhavet *et al.*, 2006). These findings support the data in this study in which adipose Akt2 was decreased in the TX sheep fetus. As a consequence, fewer cells exit the cell cycle and continue to proliferate and contribute to the increased UL adipocyte mass.

The activated phosphorylated form of total Akt, pAkt, was decreased in the hypothyroid fetus at 129dGA, and was restored to normal levels by 143dGA. The Akt phosphorylation site analysed in this study was Ser473, which is the dominant site of phosphorylation by mTORC2 (Copp *et al.*, 2009). This suggests that there may be suppression of adipose mTORC2 levels in response to hypothyroidism *in utero* (Figure 5.16). Once activated, Akt phosphorylates mTOR at Ser2448, which predominately activates mTORC1 (Copp *et al.*, 2009). The mTORC1 complex regulates cell growth and translation, in part, by

phosphorylation of the downstream target, S6K (Hara *et al.*, 2002). A recent study has identified a negative feedback mechanism regulating the downstream targets of the insulin pathway. In an epithelial tissue cell line, mTORC2 is negatively regulated by S6K through the phosphorylation of Sin1, a component of the mTORC2 complex (Liu *et al.*, 2013). It is possible that the increased pS6K in the adipocytes of the TX fetus inhibits mTORC2 (Figure 5.16).

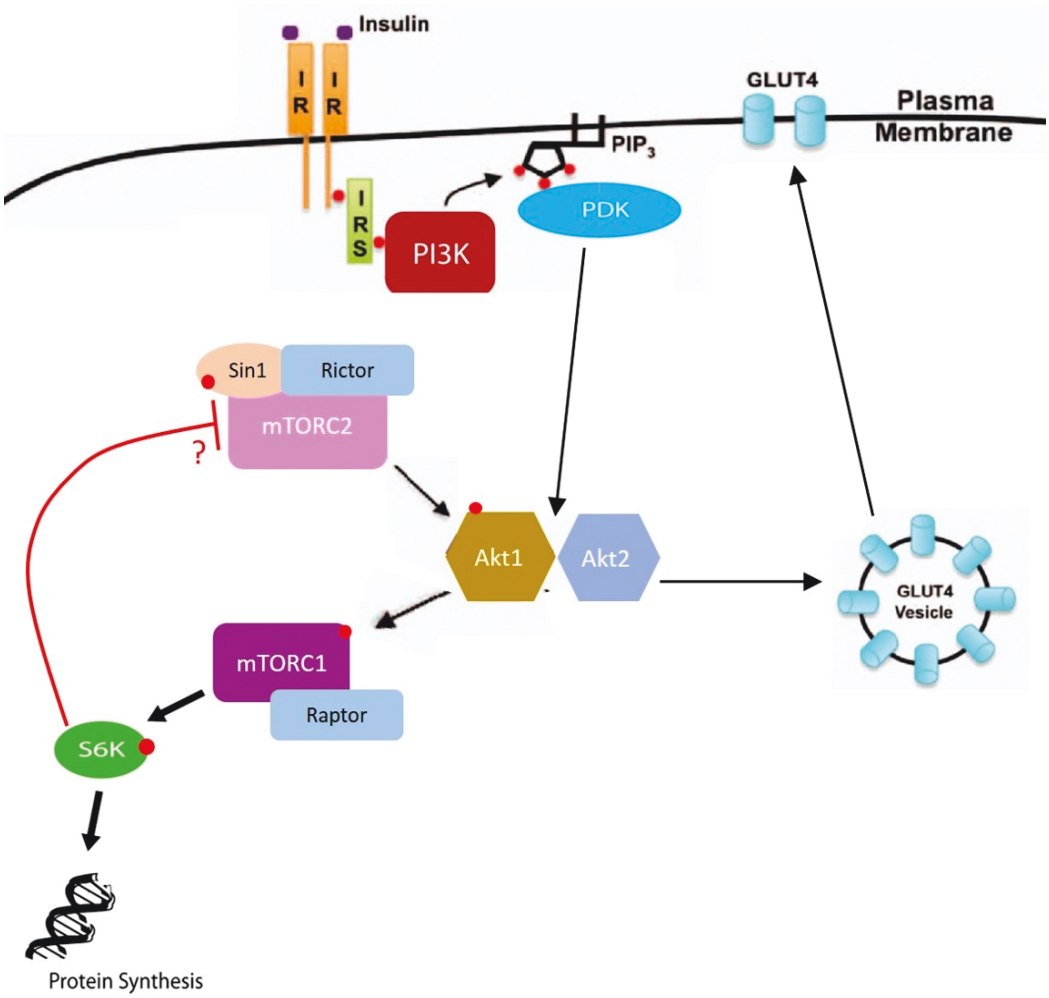

Figure 5.16. A diagram of the insulin signalling pathway including the two Akt isoforms and mTOR complexes. During hypothyroidism *in utero*, stimulation of mTORC1 by elevated Akt1 may be responsible for the rise in pS6K. However, the inhibitory actions of S6K on mTORC2 may account for the overall lack of effect of hypothyroidism on pmTOR. Red dots signify phosphorylation sites.

The protein level of the activated pmTOR (Ser2448) tended to decrease in the TX fetus but this represents the combined level of both mTOR complexes. Indeed, the lack of change in adipose pmTOR in the TX fetus may be a consequence of increased mTORC1 and decreased mTORC2 levels. Further characterisation of the distinct roles of mTORC1 and mTORC2, and their response to hypothyroidism *in utero*, is required to fully understand their contribution to adipocyte growth before and after birth.

Although there are no reports of a TRE present in the enhancer regions of insulin signalling genes, thyroid hormone has previously been shown to stimulate Akt1 expression via TRα1 non-transcriptionally, in a ligand dependent manner in human endothelial cells *in vitro* (Hiroi *et al.*, 2006). Additionally, in a human insulinoma cell line, thyroid hormone induces Akt phosphorylation non-genomically by interaction with TRβ (Verga Falzacappa *et al.*, 2007). In adipose tissue, the primary outcomes of the insulin signalling pathway are cell proliferation by activation of S6K and glucose uptake by GLUT4 translocation. As both adipose pS6K and GLUT4 were upregulated in the TX fetus, it can be postulated that UL adipocyte proliferation originated from hyperinsulinaemia secondary to increased β-cell mass, rather than a direct consequence of the deficiency in thyroid hormones.

5.4.5 Plasma leptin concentrations correlate with UL cell mass

In the present study, the increase in plasma leptin in the TX fetus was likely to be due to the larger proportion of UL adipocytes as these cells are characteristic of WAT which secretes and synthesises leptin. Indeed, a positive correlation was observed between plasma leptin concentration and UL cell mass in all fetuses. This correlation has been reported previously in the fetuses of well-fed ewes (Mühlhäusler *et al.*, 2002). Thyroid hormone deficiency in the sheep fetus has also previously been shown to increase adipose leptin mRNA levels (O'Connor *et al.*, 2007). The increase in circulating leptin concentrations seen in the TX fetus, therefore, may be due to the greater UL adipose mass and/or secretory capacity of the adipocytes; these changes may be secondary to hypothyroidism and/or hyperinsulinaemia *in utero*. Adult rat adipocytes *in vitro* produce and secrete leptin in response to insulin (Barr *et al.*, 1997). In addition, adipose

leptin mRNA abundance is increased in sheep fetuses infused with insulin (Devaskar & Anthony, 2002).

In the TX sheep fetus, it is possible insulin and leptin interact in a positive feedback mechanism that enhances both fat mass and pancreatic β-cell mass (Figure 5.17). Elevated insulin concentrations in the TX fetus may be responsible for UL adipocyte proliferation and increased leptin secretion. The high circulating leptin concentrations may, in turn, contribute to the proliferation of pancreatic β-cells which produce more insulin.

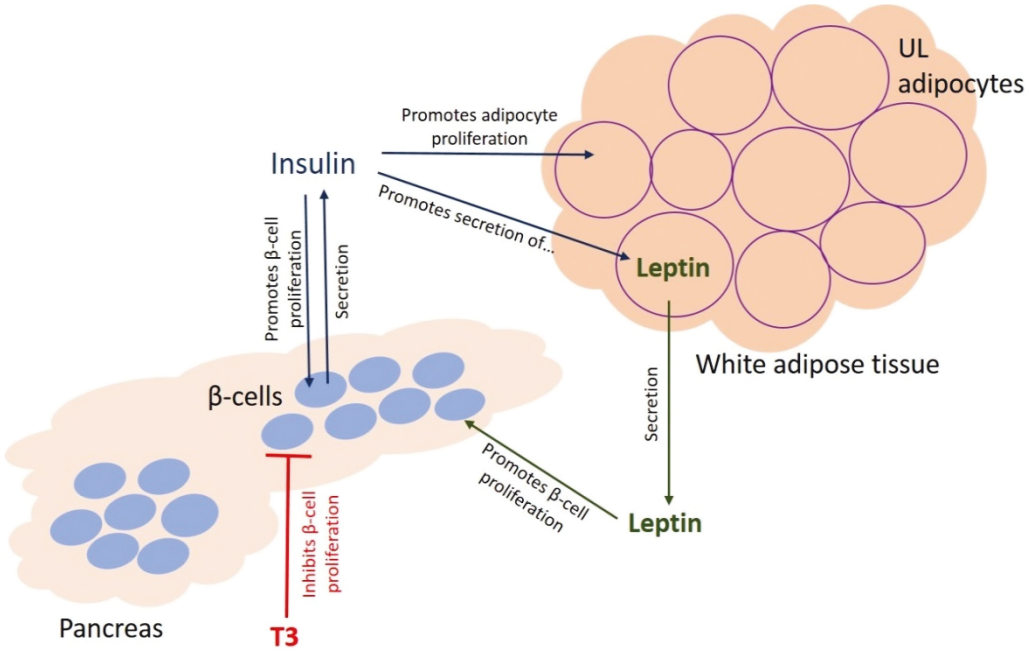

Figure 5.17. Proposed feedback model responsible for increased UL adipocyte mass and pancreatic β-cell mass associated with increased plasma concentrations of insulin and leptin in the TX sheep fetus.

5.5 Conclusions

Hypothyroidism in the sheep fetus during late gestation was associated with increased PAT mass which appeared to be due to UL adipocyte hyperplasia. The greater deposition of WAT in the TX fetus may be secondary to increased mRNA and protein expression of

pS6K, GLUT4 and PPARγ. Expansion of the UL cell type was likely to be a consequence of the concomitant increases in plasma concentrations of insulin and leptin. There was no change in the ML adipocyte mass in response to hypothyroidism *in utero*, however, further studies on adipocyte function are required to determine adipose thermogenic capacity in the TX fetus.

Thyroid hormone deficiency was associated with altered insulin signalling in the PAT of fetuses in late gestation. Expression of the insulin and IGF type 1 receptors decreased, which is characteristic of PAT insulin resistance and could have consequences for neonatal and adult metabolism. Furthermore, alterations in downstream factors, such as the Akt1 and 2 and mTOR, may have short and long-term effects on normal glucose and lipid metabolism. Further work is needed to characterise the role of signalling protein isoforms, and the consequences of hypothyroidism for adipose metabolic function before and after birth.

6 EFFECTS OF HYPOTHYROIDISM ON FETAL KIDNEY DEVELOPMENT

6.1 Introduction

In precocious mammals, like the sheep and human, development of the kidneys begins early in gestation with nephrogenesis completed just before birth. This means that the final number of nephrons generated will persist into adulthood and no further nephrons can be generated after birth (Gimonet *et al.*, 1998; Wintour *et al.*, 2003; Figueroa *et al.*, 2005). Nephrogenesis is, in part, regulated by the fetal renin-angiotensin system, which in turn, is sensitive to changes in thyroid hormones (Kobori *et al.*, 2001; Chen *et al.*, 2007). Since nephron number is determined before birth, any alterations in thyroid hormones *in utero* have the potential to have a significant impact on renal function in neonatal and adult life.

The adult kidney is essential in blood filtration and fluid homeostasis, while before birth, these functions are mediated by the placenta. In fetal sheep and rats, there is an increase in the expression of the sodium transporters, ENaC and Na^+/K^+ ATPase pump towards term, with abundance at its highest shortly before birth (Watanabe *et al.*, 1999; Keller-Wood *et al.*, 2008). The maturational changes in renal transporters in preparation for neonatal life are known to be influenced by changes in circulating glucocorticoid and insulin concentrations (Wang *et al.*, 2001; Song *et al.*, 2006; Keller-Wood *et al.*, 2008). The role of thyroid hormones, however, in the control of renal development is unknown.

It has been demonstrated that hypothyroidism in the sheep fetus leads to an increase in relative kidney mass during late gestation (Chapter 3; Chattergoon *et al.*, 2012a). The high plasma insulin concentration observed in the thyroid hormone deficient fetus (Chapter 3) may contribute to changes in kidney growth. In neonatal mice, kidney size was reduced by deletion of the *irs2* gene (Carew *et al.*, 2010), suggesting that the insulin signalling pathway has an important role in kidney development.

The aims of the study were (1) to identify structural changes in the fetal kidney which may account for the greater relative kidney weight induced by hypothyroidism, (2) to

elucidate if renal overgrowth is associated with any changes in the insulin signalling pathway in the fetal kidney, and (3) to investigate whether tubular ion channel protein expression is affected by hypothyroidism *in utero*.

It was hypothesised that enhanced renal growth in the hypothyroid sheep fetus is due to greater number of glomeruli and tubules in the kidney cortex which is secondary to insulin signalling in the fetal kidney. Furthermore, the expression of the transporter proteins in the fetal kidney will be downregulated by thyroid hormone deficiency *in utero* and prevention of the prepartum surge in T3 concentration.

6.2 Methods

6.2.1 Animals

All animals, treatments and post mortem procedures are described fully in Section 2.1. As reported in Chapter 3, an increase in kidney mass was only seen in the TX fetuses compared to the sham controls at 143dGA and therefore only these fetuses were used in the study (sham n=10, TX n=10). One kidney portion was collected from each fetus and immersed in 4% formalin for paraffin wax embedding, as described in Section 2.3. The second kidney was frozen at -80°C until required for analysis.

6.2.2 Histology

The sectioning, staining and stereological measurements of the glomerulus were undertaken by Mona Hasim, an undergraduate student at Oxford Brookes University, as part of her final-year project while under my supervision.

All histology processing steps are described in detail in Section 2.3. Serial sections of wax embedded kidney were cut to a thickness of 5µm and left to dry overnight before H&E staining. Stained sections were scanned using a NanoZoomer digital slide scanner (Hamamatsu Photonics) to create digital images for analysis. All stereological measurements were performed blind to the treatment group.

6.2.3 Glomerulus size

Using the stereology software NDP.view (Hamamatsu Photonics), the diameters of the largest glomeruli in the outer renal cortex were determined using a ruler function (Figure 6.1). Large glomeruli were defined to have a diameter of at least 45µm at the widest axis, before shrinkage, to ensure as far as possible that glomeruli measured were in transverse mid-line section. At least 25 glomeruli were analysed per animal. To adjust measurements for tissue shrinkage in processing, the diameters of red blood cells in the sections were measured and used to calculate shrinkage (6µm; Karvonen, 1954; Equations 5.3 and 5.4, Chapter 5). The percentage of tissue shrinkage ranged from 45 to 60% and there was no significant difference in shrinkage between treatment groups. The CV for glomerular diameter within each fetus was calculated using Equation 5.7 (Chapter 5) and all fetuses had a CV of less than 12%.

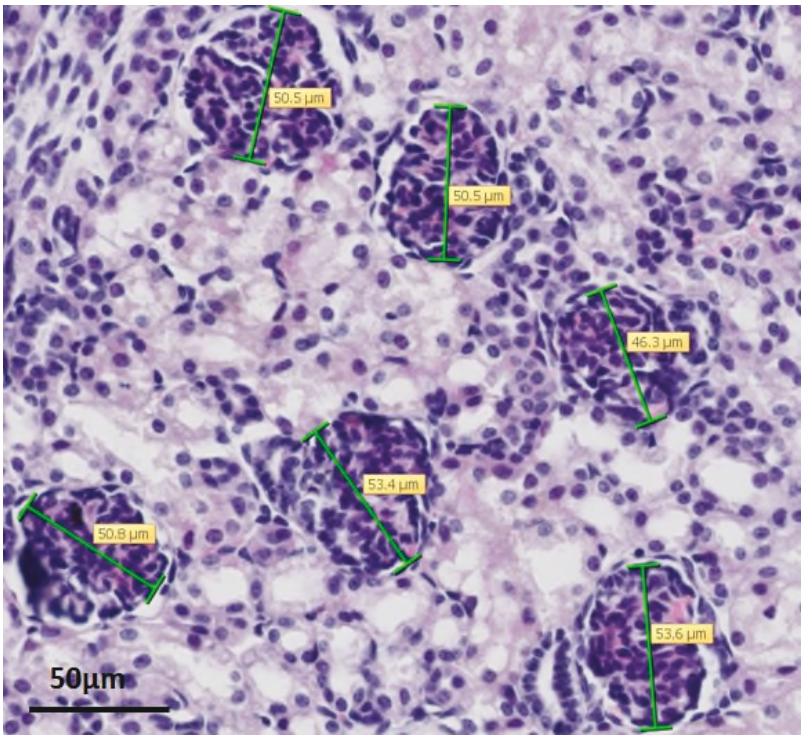

Figure 6.1. Analysis of glomerular diameter in kidney from sham and TX sheep fetuses at 143dGA.

6.2.4 Fractional glomerular and tubular volume

The fractional volumes of glomeruli and tubules were determined using NewCAST stereological software (Visiopharm). Only the renal cortex was used as the region of interest and a point counting grid containing 64 points was applied over the sections. Using meander sampling, kidney tissue was investigated using SURS (Figure 6.2).

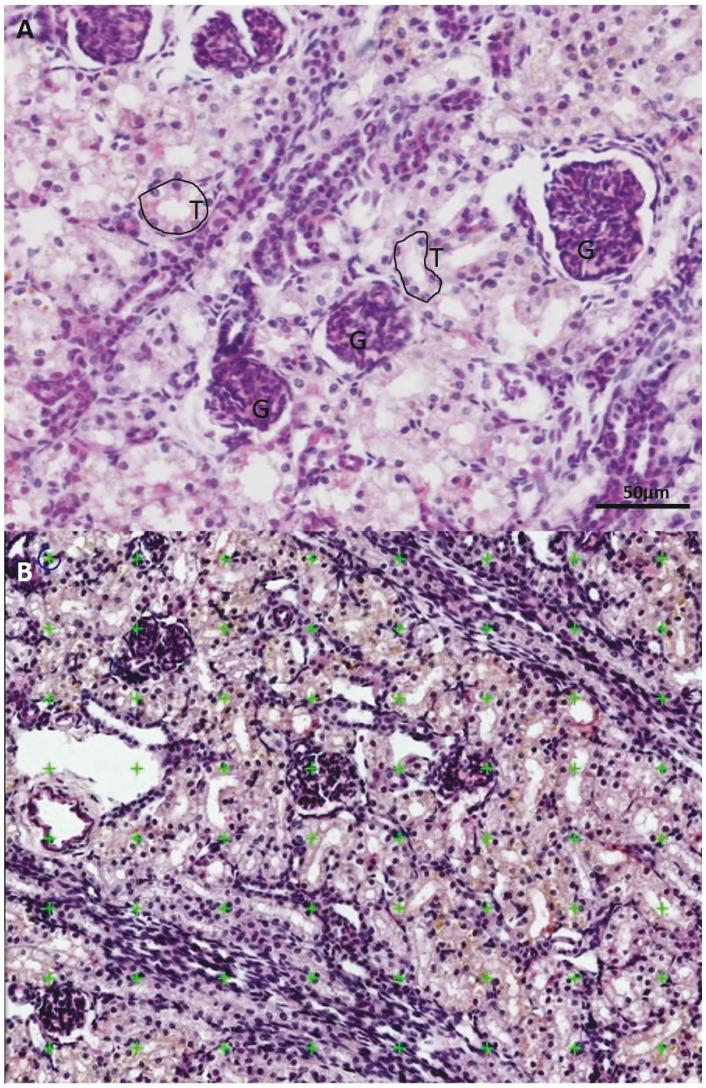

Figure 6.2. H&E stained kidney section from fetal sheep. (A) 'G' indicate glomeruli and circled structures labelled 'T' indicate tubules. (B) Counting grid used in meander sampling of glomeruli and tubules. A structure would be counted when underneath a green '+'.

The final magnification at analysis was x400. Between 40 and 50 counting frames per slide were used to provide at least 200 counts per animal for each variable. The fractional volumes of glomeruli and tubules ($Vol_{fraction}$) were calculated using equation 6.1:

$$Vol_{fraction} = P \div T$$

Equation 6.1.

Where P is the number of points falling on either glomeruli or tubules, and T is the total number of sampling points.

6.2.5 Glomerular density and volume

The physical dissector method was used to measure the density of glomeruli in the renal cortex. The physical dissector is a stereological technique used to count particles in a virtual 3D volume generated by two sections separated by a known distance. Only transects which are partially or completely inside a counting frame are counted in pairs of serial sections (the reference and the 'look-up' sections). The only particles that are counted are the ones which appear on the reference section but not on the lookup section (Kaplan *et al.*, 2012). These are known as the dissector particles, Q-. The number of particles in a unit volume (numerical density) was calculated by dividing the counted number of particles by the dissector volume (Gundersen & Jensen, 1987; Howard & Reed, 2010; Kaplan *et al.*, 2012).

The stereological software NewCAST (Figure 6.3, Hamamatsu Photonics) was used to implement the dissector. The distance between the pair of slides should be less than one third of the average height of the particle examined (Howard & Reed, 2010). Using the mean diameter of the glomerulus in the ovine fetal kidney as approximately 150µm, the 1st and 5th sections were used, separated by a distance of 20µm between the pair. Between 55 and 60 counting frames were assessed and the area of the counting frame was 0.13mm^2.

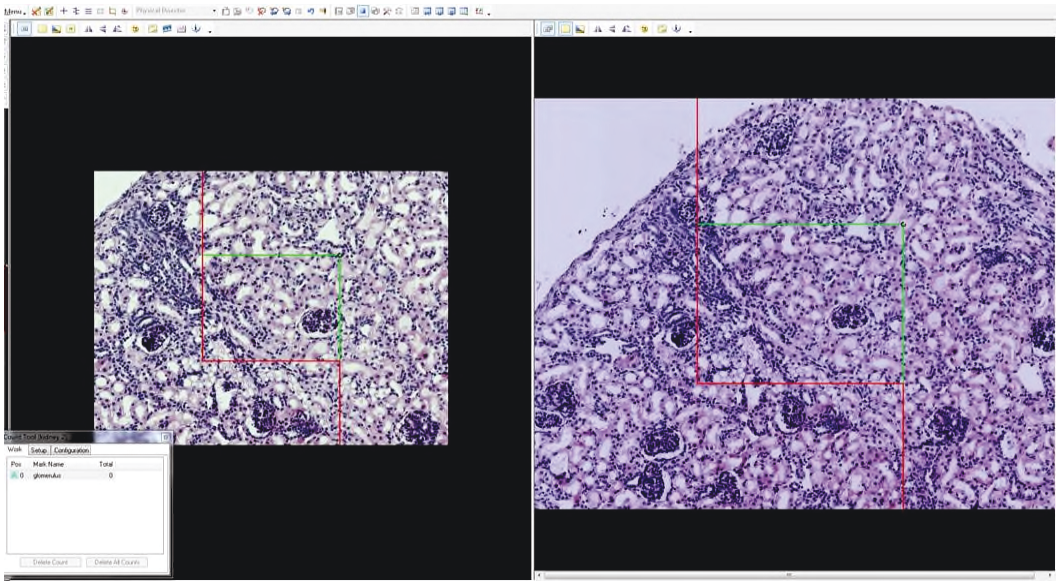

Figure 6.3. The physical dissector used to measure glomeruli density in kidney cortex from a sheep fetus at 143dGA. Section pairs 20µm apart were analysed for glomerular structures in the counting frame in the reference (left) and look-up (right) sections.

The number of dissector frames was measured by counting the corner points of the counting frame. Glomerular density (Num_{den}) was calculated using Equation 6.2:

$$Num_{den} = \left(\frac{\sum Q-}{([\sum P \times a] \times h)}\right) \div 2 \qquad \textbf{Equation 6.2.}$$

Where $\sum Q$- is the total sum of the glomeruli points, $\sum P$ is the total number of corner points, and a and h are the frame area and dissector height, respectively. The whole equation was divided by two to account for the counting taking place in two directions. The mean glomerular volume was calculated by dividing the fractional glomerular volume (Section 6.2.3) by the numerical density. The CV for the mean glomerular volume for each individual animal was under 9%.

6.2.6 Glomerular proliferation

In order to identify cells undergoing proliferation, sections were immunolabelled using a mouse monoclonal anti-PCNA antibody at a concentration of 4.1µg/ml (Dako) and visualised using the Vectastain Elite ABC kit (anti-mouse secondary antibody; Vector Laboratories, Section 2.4). Counterstaining of cells was carried out using the nuclear

stain methyl green (Vector Laboratories, Section 2.4). Slides were scanned into digital images using a NanoZoomer (Hamamatsu Photonics). In glomeruli judged to be sectioned approximately mid-line, the expression of PCNA was scored using the following criteria: 0 = absent PCNA labelling, 1 = 1-10 PCNA-positive cells, 2 = 11-20 PCNA-positive cells, 3 = 21 or more PCNA-positive cells. The scoring reflected the number of positively labelled cells and not the intensity of the labelling (Figure 6.4). Between 40 and 50 glomeruli from the outer cortex were sampled for each animal. The glomerulus diameter was also measured.

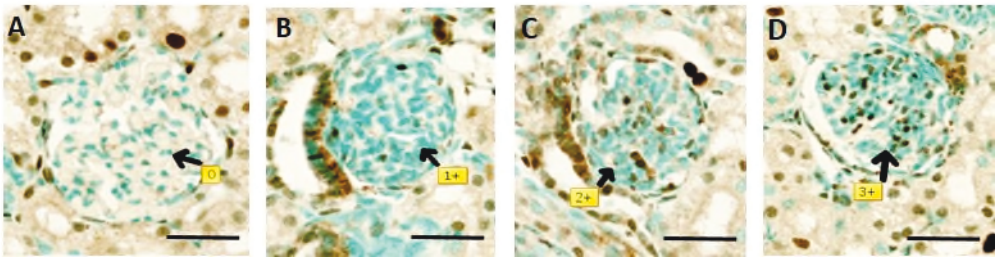

Figure 6.4. Scoring of PCNA immunolabelling in the kidney glomerulus of a sheep fetus at 143dGA. (A) Absence of PCNA labelling and scored 0, (B) scored 1 for 1-10 labelled cells, (C) scored 2 for the presence of 11-20 labelled cells and (D) scored 3, due to the presence of more than 20 positively labelled cells. Scale bar: 25µm.

6.2.7 Tubule length density

Tubule length density is a measure of renal tubule length in a reference volume. In order to analyse the length density of proximal and distal tubules in the renal cortex, a counting frame was used within the NewCAST stereological software (Figure 6.5). The stereological method assumes that the length of the structure is larger than the width (Howard & Reed, 2010). Only fully cross-sectioned tubules with a visible lumen were counted by meander sampling and tubules were only counted if they were within the 0.017mm^2 counting frame.

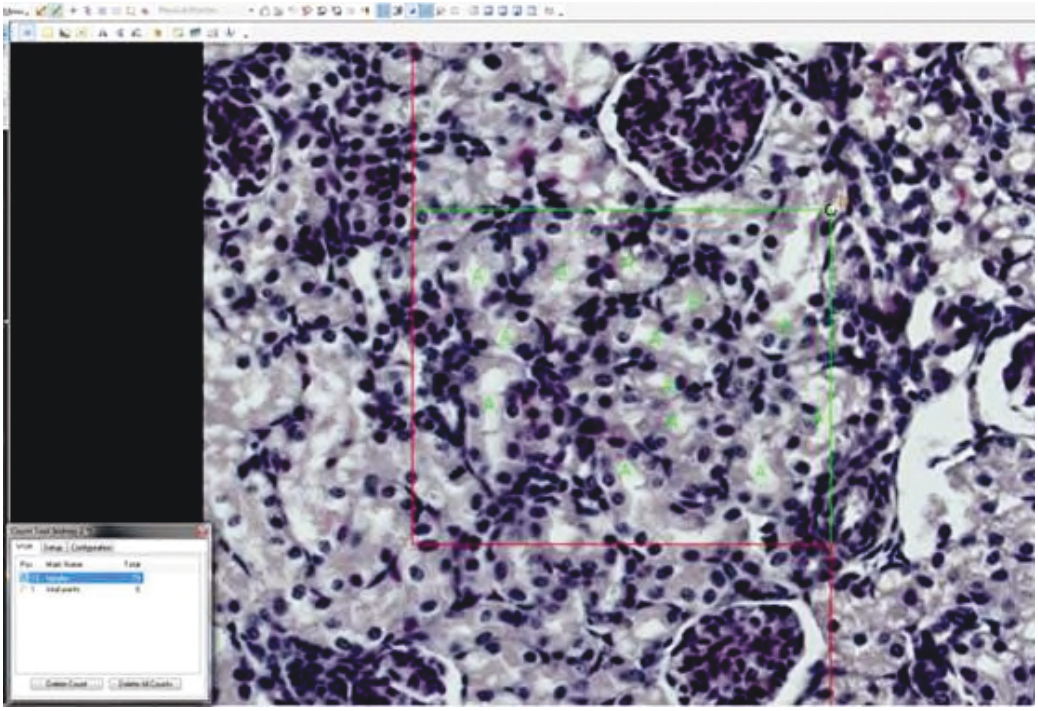

Figure 6.5. The counting frame used to analyse tubule length density in the kidney cortex of a sheep fetus at 143dGA. A tubule should be counted if it lies within the frame. It will be excluded if it touches a red line, but included if it touches a green line. The green 'A' indicates a counted tubule.

Tubule length density ($Length_{den}$) was calculated using Equation 6.3:

$$Length_{den} = 2 \times \frac{\sum Q}{a \cdot \sum P} \qquad \textbf{Equation 6.3.}$$

Where $\sum Q$ is the total number of tubules counted, a is the area of the counting frame and $\sum P$ is the total number of counting frames per section (Noorafshan, 2014). At least 200 tubules were counted over 30 fields of view per section at a final magnification of x400. The CV for tubule length density was 7% or less for each fetus.

6.2.8 Tubule surface area density

Tubule surface area density is the measure of tubule surface (internal and external) per length of tubule in a reference volume. Surface area density of proximal and distal tubules in the renal cortex was determined using the NewCAST stereological software

and a set of isotropic linear test line probes. Lines of a fixed length were superimposed onto each section in a random orientation and intersections were counted where the line probe crossed a tubule surface (Figure 6.6). End-points associated with each line were also counted to determine a reference volume.

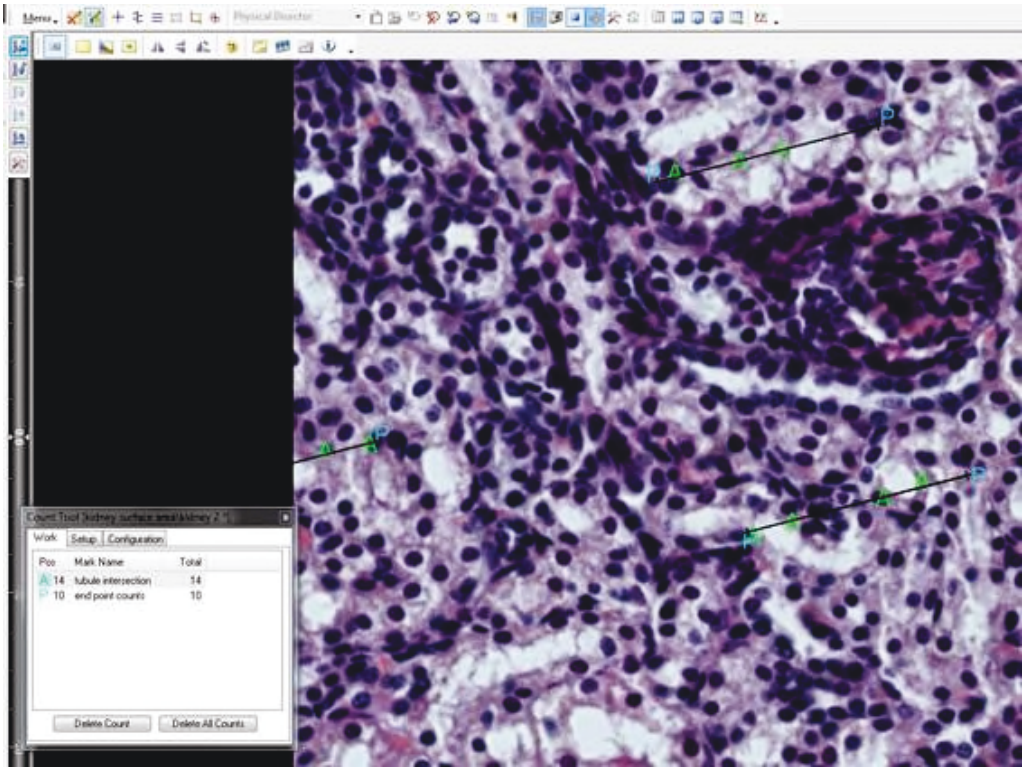

Figure 6.6. Isotropic linear test lines used to determine tubule surface area density in kidney cortex from a sheep fetus at 143dGA. The green 'A' indicate where a tubule has crossed the isotropic line and the blue 'P' are the end-points of the line counted to determine reference volume.

Surface area density (*Sv*) was calculated as:

$$Sv = 2 \times I_l$$

Equation 6.4.

Where I_l is the number of intersection points per test line in a reference space; this was determined by Equation 6.5:

$$I_l = \frac{\sum Q}{I_p \times \sum P_l}$$ **Equation 6.5.**

Where $\sum Q$ is the sum of the tubule intersections, I_p is the length of the test line and $\sum P_l$ is the total number of line end-points (Noorafshan, 2014). At least 200 intersections were counted per kidney in over 30 fields of view at a final magnification of x400. The CV for tubule surface area density was calculated using Equation 5.7 (chapter 5) and was 7% or less for each fetus.

6.2.9 Western blotting

The kidney was divided into the cortex and the medulla for quantification of proteins by western blotting. Cortical and medullary tissue from the kidney of each fetus (100mg) was homogenised in lysis buffer and the protein concentration was determined using a BCA protein assay (Section 2.5). The western blotting procedure is described in detail in Section 2.6.

Components of the insulin signalling pathway, as well as protein content of PCNA and the ion transporters, ENaCα and Na^+/K^+ ATPase α and β subunits were assessed. The specific conditions for each antibody used are shown in Table 6.1. The amount of protein loaded was 75µg with the exception of the gel used for IGF-1Rβ quantification, in which 100µg protein was used. All samples were heated to 70°C for 10 minutes with the exception of those used for p-S6K quantification, which were heated to 99°C for 10 minutes. After detection, the protein visualised in each sample was normalised to the total protein content assessed by Ponceau S staining. The samples of cortex and medulla from all animals were loaded across four gels which were separated and transferred together to minimise variation. A control sample was loaded on each of the gels and the results of the control were used to normalise the values across all membranes. After densitometry and normalisation to total protein content, the results were standardised to the mean value of the sham group. Results are therefore expressed as fold changes in arbitrary units.

Table 6.1 Antibodies used in Western blotting of kidney protein

Primary antibody	Concentration	Blocking agent	Secondary antibody
Rabbit polyclonal anti-InsRβ (Santa Cruz Biotechnologies)	10µg/ml	2% Non-fat milk	Anti-rabbit 1:1750 (GE Healthcare)
Rabbit polyclonal anti-IGF-1Rβ (Santa Cruz Biotechnologies)	10µg/ml	2% Non-fat milk	Anti-rabbit 1:1500 (GE Healthcare)
Rabbit polyclonal anti-pAkt (Ser 473 , Cell Signaling Technology)	1:1000	2.5% BSA	Anti-rabbit 1:2500 (GE Healthcare)
Rabbit polyclonal anti-leptin receptor (LRL, Biorbyt)	1µg/ml	2.5% Non-fat milk	Anti-rabbit 1:2500 (GE Healthcare)
Mouse monoclonal anti-Akt1 (Cell Signaling Technology)	1:1000	2.5% Non-fat milk	Anti-mouse 1:3000 (GE Healthcare)
Rabbit monoclonal anti-Akt2 (Cell Signaling Technology)	1:1000	2.5% Non-fat milk	Anti-rabbit 1:3000 (GE Healthcare)
Rabbit polyclonal anti-pmTOR (Ser 2448 , Cell Signaling Technology)	1:1000	2% BSA	Anti-rabbit 1:2500 (GE Healthcare)
Rabbit polyclonal anti-pS6K (Thr 389 , Cell Signaling Technology)	1:1000	No blocking	Anti-rabbit 1:1500 (GE Healthcare)
Rabbit polyclonal anti-GLUT4 (Abcam)	2.5µg/ml	2% Non-fat milk	Anti-rabbit 1:2500 (GE Healthcare)
Mouse monoclonal anti-PCNA (Dako)	0.41µg/ml	No blocking	Anti-mouse 1:2500 (GE Healthcare)
Rabbit polyclonal anti-epithelial sodium channel α (ENaCα; Abcam)	1:1000	5% Non-fat milk	Anti-rabbit 1:5000 (GE Healthcare)
Mouse monoclonal anti-sodium/potassium ATPase α1 (Na^+/K^+ ATPase α1; Thermo Scientific)	Medulla: 2.5µg/ml Cortex: 0.5µg/ml	5% Non-fat milk	Anti-mouse 1:3000 (GE Healthcare)
Mouse monoclonal anti-sodium/potassium ATPase β (Na^+/K^+ ATPase β; Thermo Scientific)	Medulla: 0.5µg/ml Cortex: 0.1µg/ml	5% Non-fat milk	Anti-mouse 1:5000 (GE Healthcare)

InsRβ = insulin receptor subunit β, IGF-1Rβ = IGF-I receptor subunit β, LRL = leptin long form receptor, Akt = protein kinase B, pAkt = phosphorylated protein kinase B, pmTOR = phosphorylated mTOR, pS6K = phosphorylated S6 kinase.

6.2.10 Kidney wet and dry weights

In a separate cohort of fetal sheep, hypothyroidism was induced as described previously (Section 2.1) and tissues were collected at 129 and 143dGA (n=6 in each sham and TX group). One kidney from each fetus was weighed as wet after dissection and was dehydrated in a freeze-dryer for 48 hours and weighed again to determine kidney water content. Wet and dry kidney weights were expressed relative to the fetal body weight and the water content was calculated as a percentage.

6.2.11 Statistical analysis

All values are expressed as mean ± SEM unless otherwise indicated. Statistical differences were assessed using a two-way ANOVA with treatment and fetal sex as factors. If it was established that sex had no effect, parameters were assessed using a Student's t-test. Wet and dry kidney weights were assessed by three-way ANOVA with treatment, age and fetal sex as factors. Similarly, if it was established that fetal sex had no effect, a two-way ANOVA was used to assess these parameters. Distribution of glomerular PCNA scoring between the sham and TX fetuses was also assessed by two-way ANOVA, using PCNA score and treatment as factors. Linear regression was used to examine relationships between variables. To determine significant differences between the correlations of glomerular PCNA counts, a Fisher's z-transformation test was performed. In all cases, significance was accepted at $P<0.05$.

6.3 Results

6.3.1 Glomerulus size and fractional glomerular volume and density

The average glomerulus diameter in the TX fetuses (148.1 ± 6.0μm) was not significantly different from that seen in the sham fetuses (151.1 ± 4.9μm).

There was no significant difference in the percentage glomerular volume between the sham (5.5 ± 0.2%) and TX (5.4 ± 0.3%) fetuses. Additionally, there were no significant differences in glomerular density (Figure 6.7A) or mean glomerular volume between the sham and TX fetuses (Figure 6.7B).

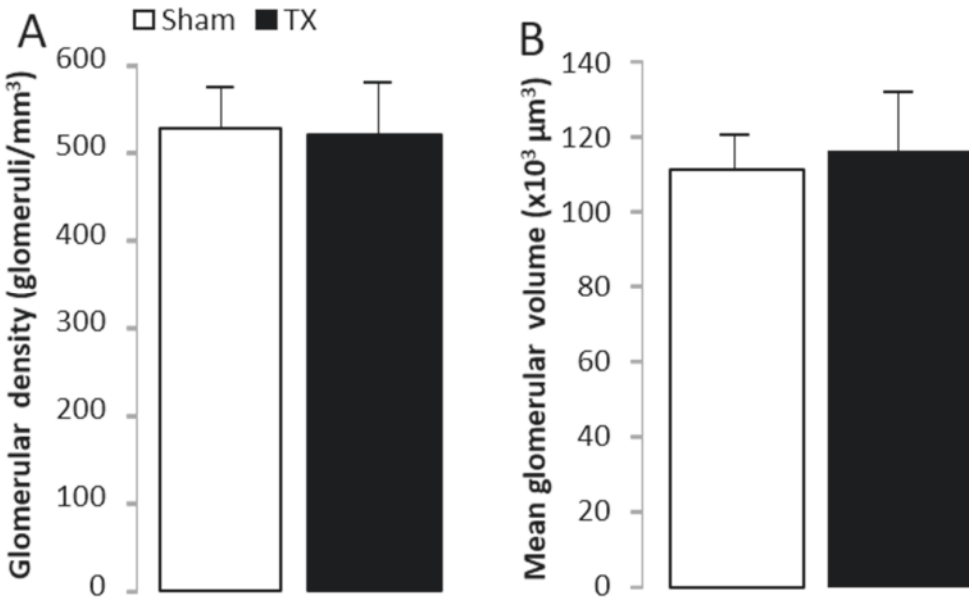

Figure 6.7. Mean ± SEM (A) glomerular density and (B) glomerular volume in the renal cortex of sham and TX fetuses at 143dGA. n = 10 fetuses in each group.

6.3.2 Glomerular proliferation

There was no significant difference in the distribution of glomerular PCNA scoring between the sham and TX fetuses (Figure 6.8).

There was a positive correlation between glomerulus diameter and PCNA score in the sham fetuses (R=0.58, R^2=0.34, n=10, *P*<0.001) and that was not seen in the TX fetuses (R=0.25, R^2=0.06, n=9). The correlations between sham and TX fetuses were not significantly different to each other (Fisher's z-transformation test, *P*=0.56, Figure 6.9).

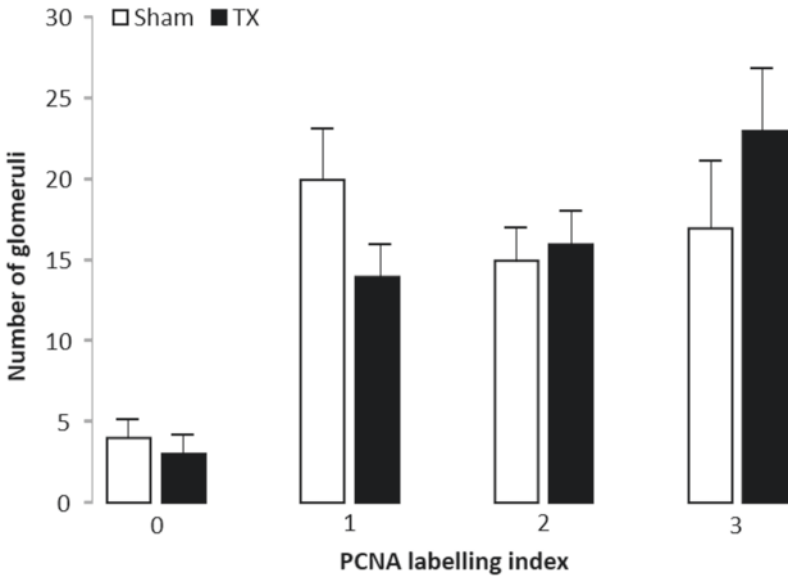

Figure 6.8. Mean ± SEM glomeruli per PCNA score in sham and TX fetuses at 143dGA. n = 10 fetuses in each group.

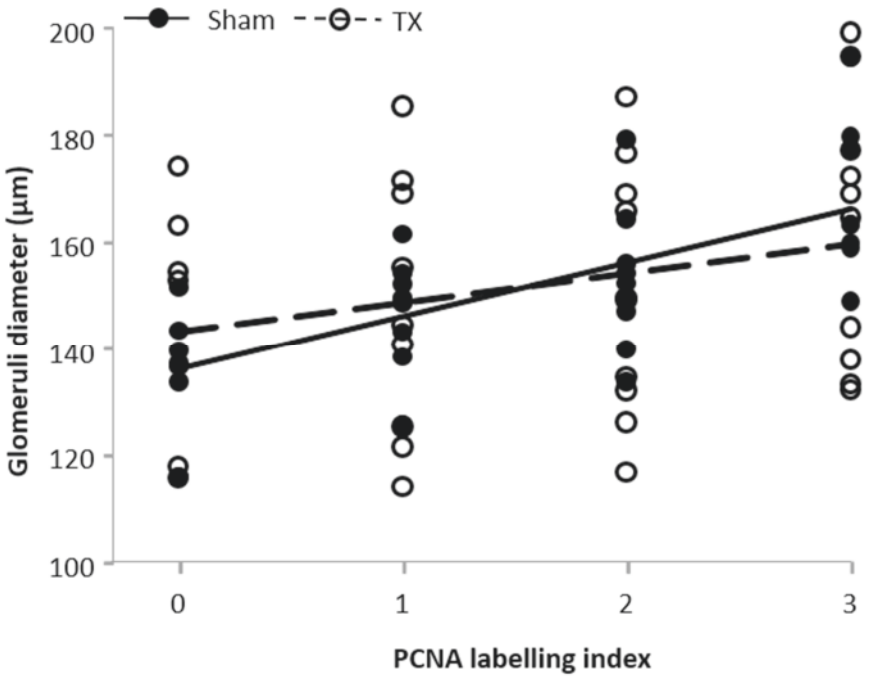

Figure 6.9. Correlations between glomerulus diameter and scored PCNA-positive cells in kidney cortex from sham and TX fetuses at 143dGA. Sham: n=10, R= 0.58, R^2=0.34, p<0.001; TX: n=9, R=0.24, R^2=0.06.

6.3.3 Tubule length density and surface area density

There was no effect of thyroid hormone deficiency on the tubule length density in the kidney cortex (sham 215 ± 21cm/mm^3 vs TX 212 ± 15cm/mm^3, Figure 6.10A).

Thyroidectomy had no effect on tubule surface area density in the kidney cortex; tubule surface area density in the TX fetuses (1.7 ± 0.1cm^2/mm^3) was similar to that observed in the sham fetuses (sham 1.6 ± 0.2cm^2/mm^3, Figure 6.10B).

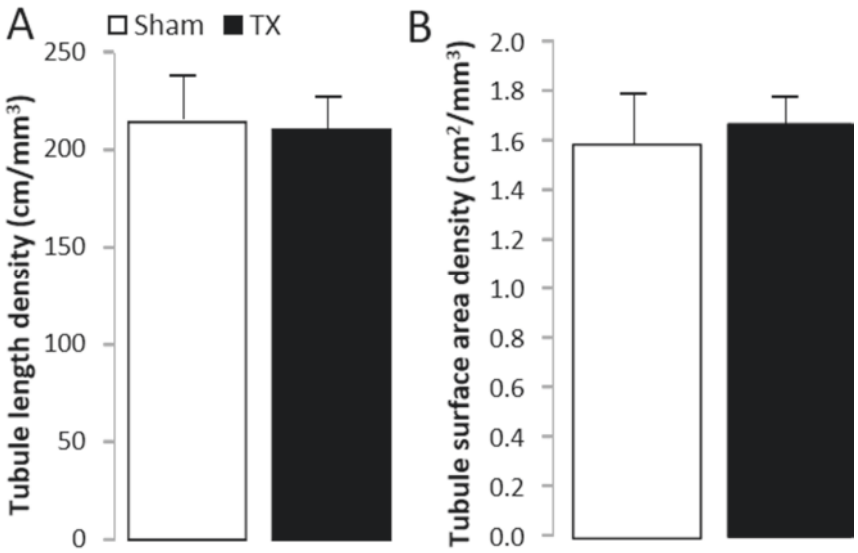

Figure 6.10. Mean ± SEM (A) tubule length density and (B) tubule surface area density in kidney cortex from sham and TX fetuses at 143dGA. n=10 fetuses in each group.

6.3.4 Insulin signalling proteins

Receptors

There were no significant differences in the relative protein contents of the insulin, IGF type 1 and leptin long-form receptors in the renal cortex or medulla in the TX fetuses compared to sham controls (Figure 6.11). In addition, there was no effect of sex on the relative levels of any of the receptor proteins measured.

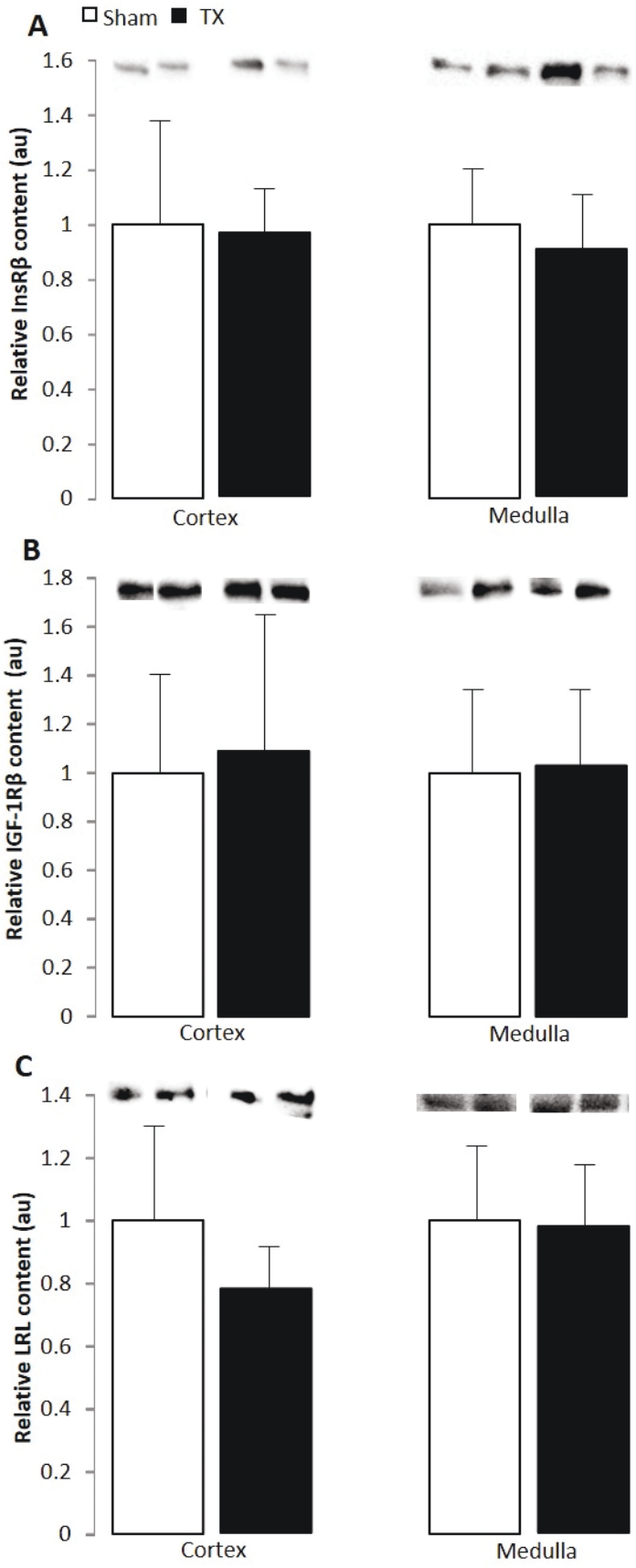

Figure 6.11. Mean ± SEM relative protein expression of (A) IRβ, (B) IGF-1Rβ and (C) LRL in the kidney cortex and medulla from sham and TX fetuses at 143dGA. n=9-10 in each group.

Akt

In the cortex, there was an effect of fetal sex on Akt1 content (P<0.05); greater Akt1 expression was observed in the female fetuses compared to the male fetuses, regardless of treatment group (P<0.05; Figure 6.12A). There was no significant effect of thyroidectomy or fetal sex on the relative protein expression of Akt1 in the renal medulla (Figure 6.12B).

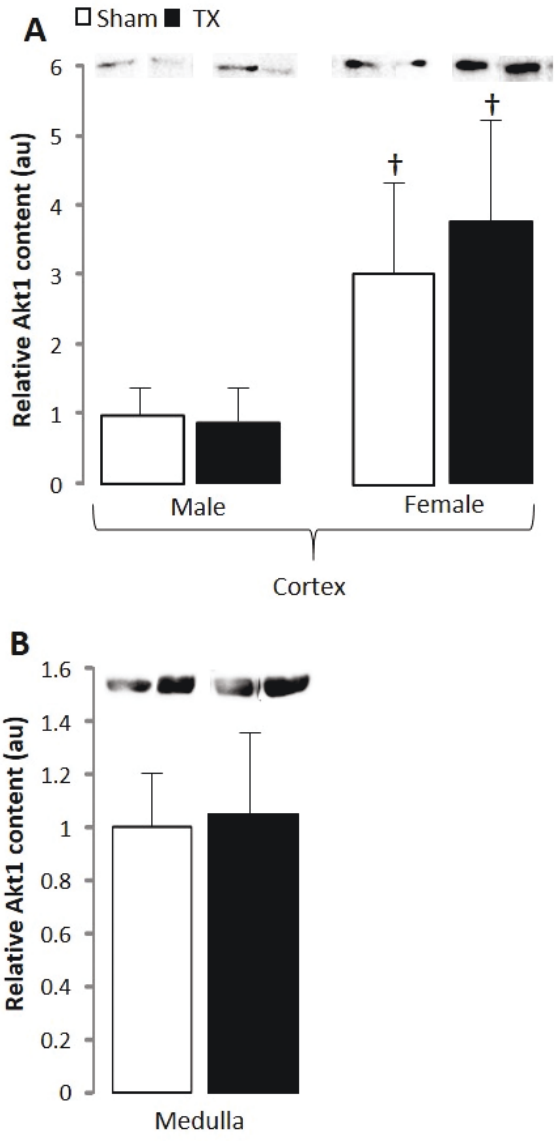

Figure 6.12. Mean ± SEM relative protein expression of (A) Akt1 in male and female fetuses in the kidney cortex from sham and TX fetuses at 143dGA, normalised to sham male fetuses and (B) Akt1 in the kidney medulla. † Significantly different from male fetuses in the same treatment group, 2-way ANOVA, P<0.05. n=9-10 in each group, balanced by sex (n=4-6 in each group).

There was no significant change in the relative levels of either Akt2 or pAkt in the medulla or cortex in the TX fetuses compared to the sham fetuses (Figure 6.13). There was no significant effect of fetal sex on either Akt2 or pAkt expression.

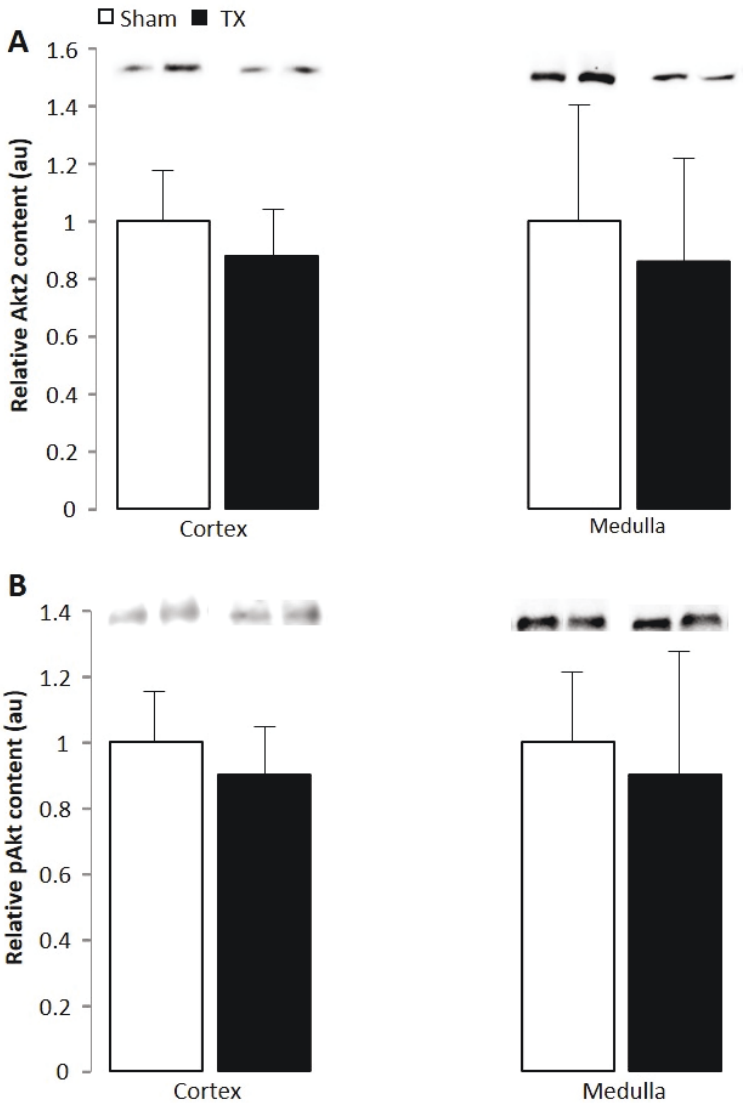

Figure 6.13. Mean ± SEM relative protein expression of (A) Akt2 and (B) pAkt in kidney cortex and medulla from sham and TX fetuses at 143dGA. n=9-10 in each group.

Downstream targets

Protein expression levels of pmTOR and pS6K in the renal cortex and medulla were unchanged in the TX fetuses compared to sham controls (Figure 6.14A, B).

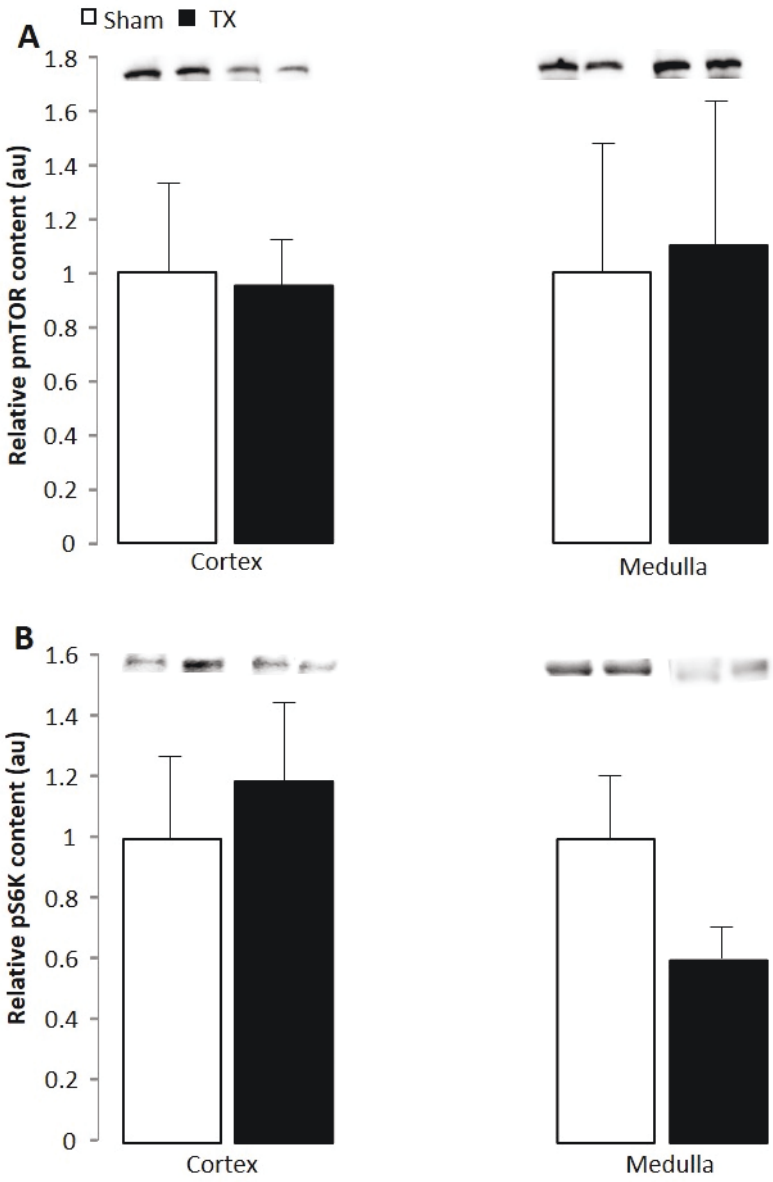

Figure 6.14. Mean ± SEM relative protein expression of (A) p-mTOR and (B) pS6K in kidney cortex and medulla from sham and TX fetuses at 143dGA. n=9-10 in each group.

In the renal cortex, there was a significant interaction between the effects of treatment and fetal sex on GLUT4 protein content (P<0.05). Although hypothyroidism had no effect on GLUT4 expression in the male fetuses, a decrease in GLUT4 protein was observed in the female TX fetuses compared to female sham controls (P<0.05; Figure 6.15A). In addition, cortical GLUT4 content was higher in the sham female fetuses compared to the sham male fetuses (P<0.05, Figure 6.15A). There was no effect of fetal

hypothyroidism on the relative expression of GLUT4 in the renal medulla; however, significantly lower GLUT4 content was seen in the female fetuses compared to the male, regardless of treatment (P<0.05; Figure 6.15B).

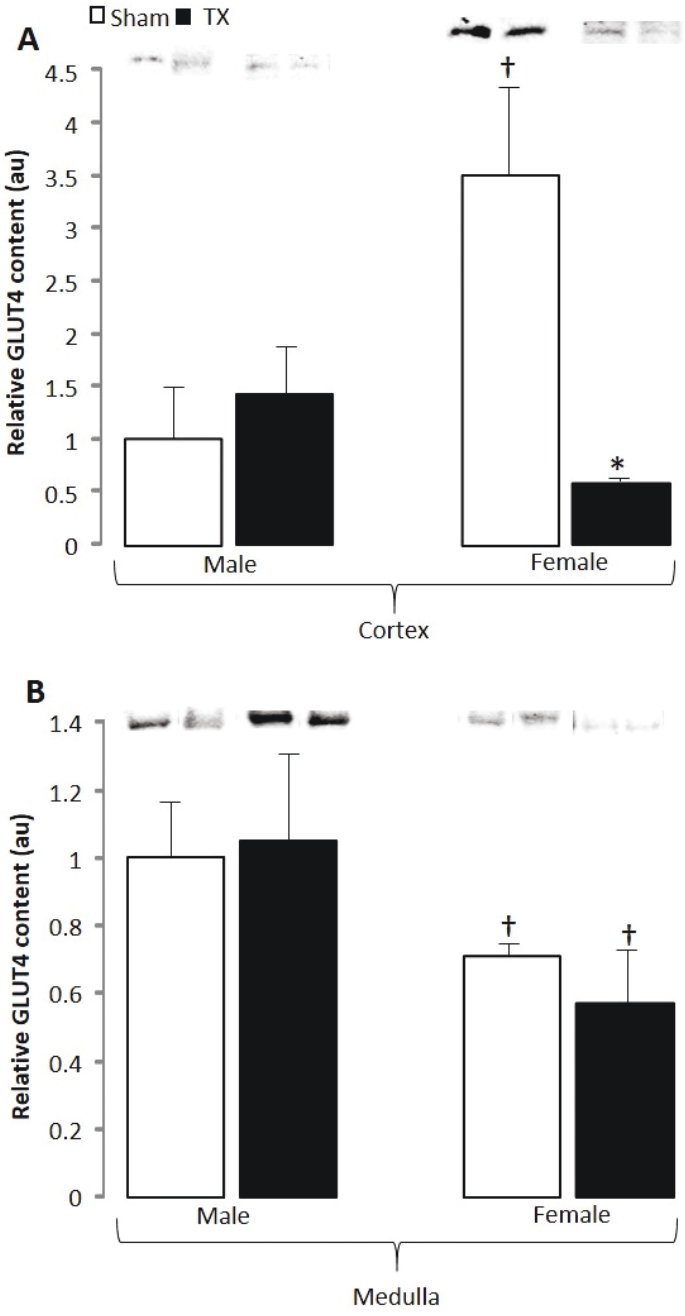

Figure 6.15. Mean ± SEM relative protein expression of GLUT4 in the (A) kidney cortex and (B) kidney medulla from male and female sham and TX fetuses at 143dGA. † Significantly different from male fetuses in the same treatment group, *significantly different from sham fetuses of the same sex, 2-way ANOVA, p<0.05. n=9-10 in each group, balanced by sex (n=4-6 in each group).

6.3.5 Cell proliferation

There were no significant changes in the protein expression of PCNA in either the renal cortex or medulla in TX fetuses compared to sham controls (Figure 6.16). Relative PCNA content in the kidney was not affected by fetal sex.

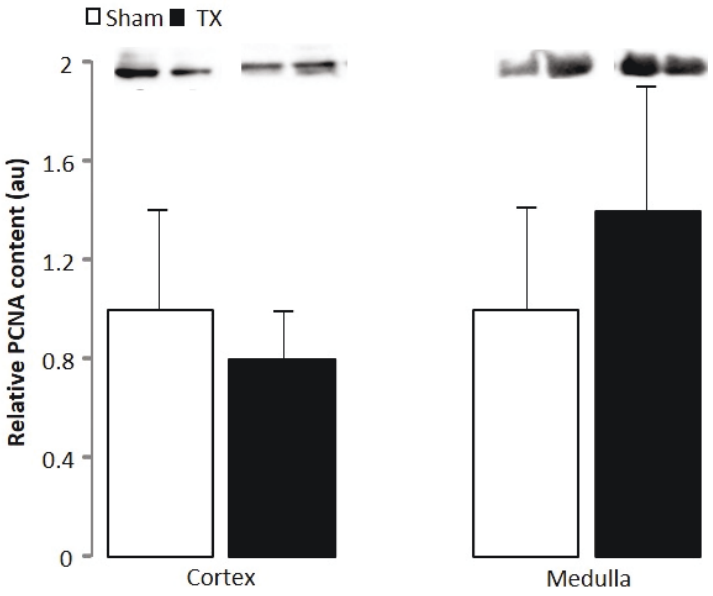

Figure 6.16. Mean ± SEM relative protein expression of PCNA in the kidney cortex and medulla from sham and TX fetuses at 143dGA. n=9-10 in each group.

6.3.6 Sodium channels and transporters

There were no significant changes in the renal protein expression of the ENaCα, Na^+/K^+ ATPase α1 and Na^+/K^+ ATPase β in the TX fetuses compared to sham controls (Figure 6.17). There was no effect of sex on any of the transporter proteins measured.

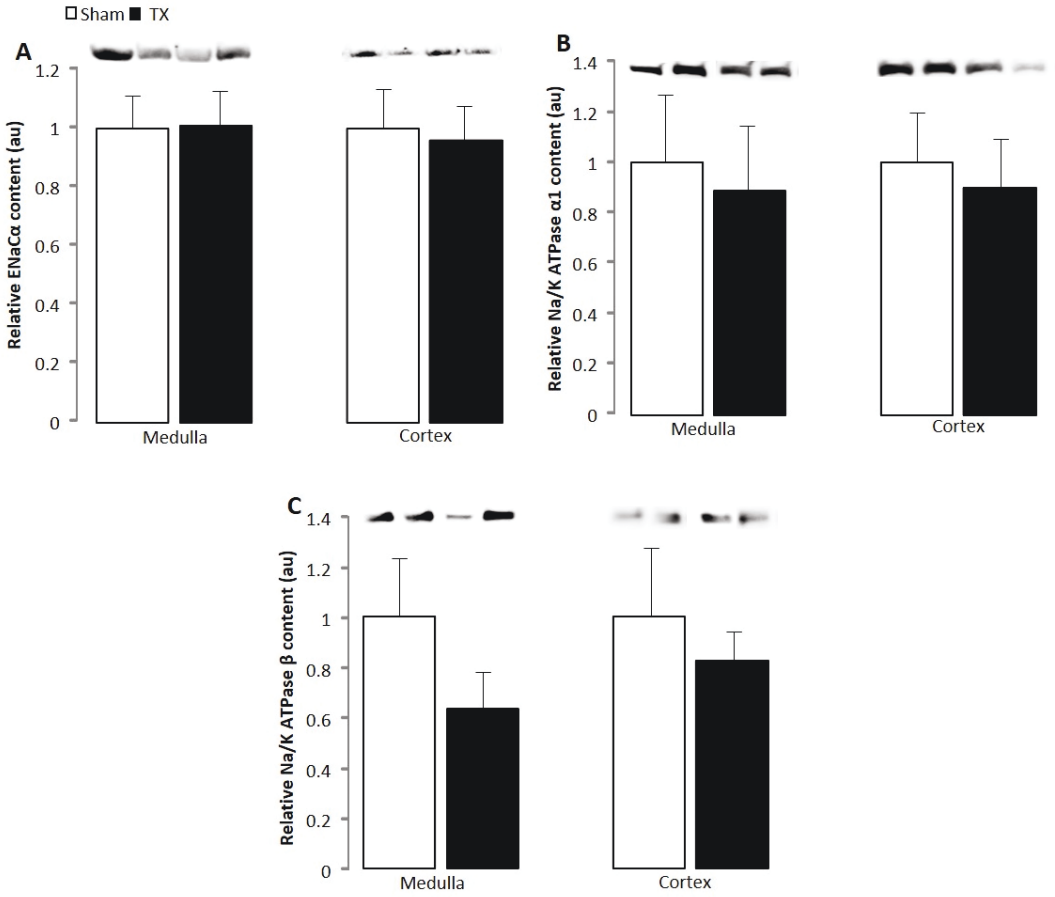

Figure 6.17. Mean ± SEM protein expression of (A) ENaCα (B) Na^+/K^+ ATPase α1 and (c) Na^+/K^+ ATPase β in the kidney cortex and medulla from sham and TX fetuses at 143dGA. n=9-10 in each group.

6.3.7 Kidney wet and dry weights

There was no significant difference in the absolute kidney wet weight in the TX fetuses compared to sham controls at 129 (sham 6.5 ± 0.5g vs TX 6.4 ± 0.6g) or 143dGA (sham 7.0 ± 0.6 vs TX 8.1 ± 0.5g; Figure 6.18A). There was no effect of gestational age on absolute kidney wet weight in either treatment group. There was no significant change in the absolute dry weight of kidneys from TX fetuses compared to sham controls at either age group, however, there was a significant increase in absolute dry weight in the older fetuses compared to those at 129dGA, in both treatment groups (P<0.05, Figure 6.18B).

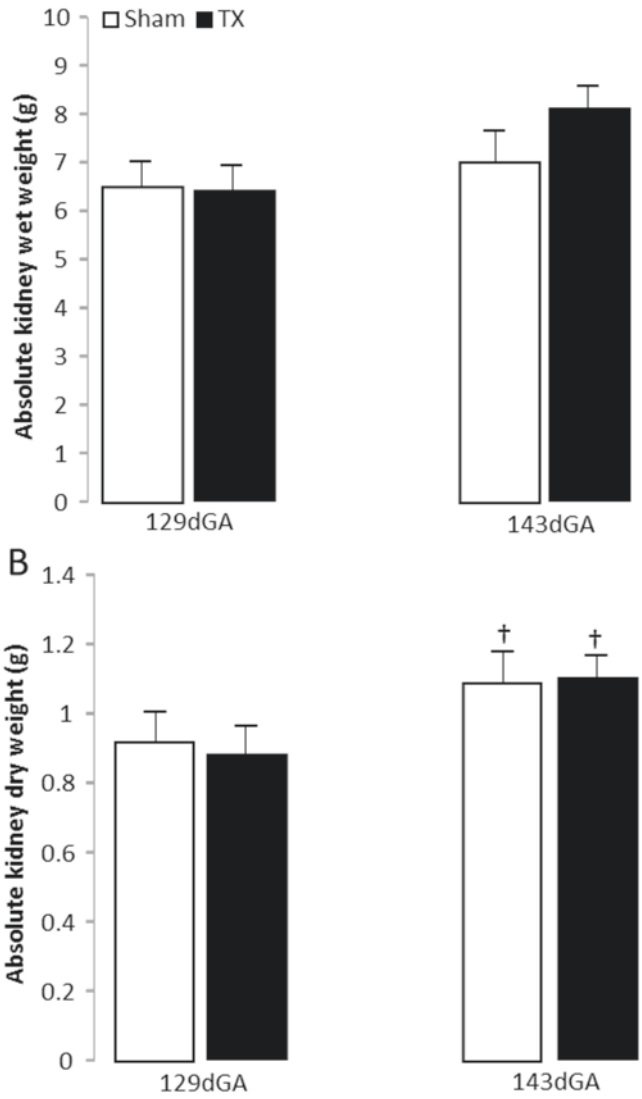

Figure 6.18 Mean ± SEM (A) absolute kidney wet weight and (B) absolute kidney dry weight from sham and TX fetuses at 129 and 143dGA. † Significantly different from fetuses in the same treatment group at 129dGA, $P<0.05$, 2-way ANOVA. n = 6 fetuses in each group.

Relative kidney wet weights were significantly greater in the TX fetuses compared to the sham controls at 143dGA only ($P<0.05$, Figure 6.19A), which is consistent with previous data in this study (Chapter 3). In the sham, but not TX, fetuses, there was a significant decrease in relative wet weight between 129 and 143dGA ($P<0.05$, Figure 6.19A). Relative dry weight tended to decrease at 143dGA compared to 129dGA (Student's t-test, $P=0.06$, Figure 6.19B). There was no significant difference in relative kidney dry weights between the TX and sham fetuses at either 129 or 143dGA (Figure 6.19B).

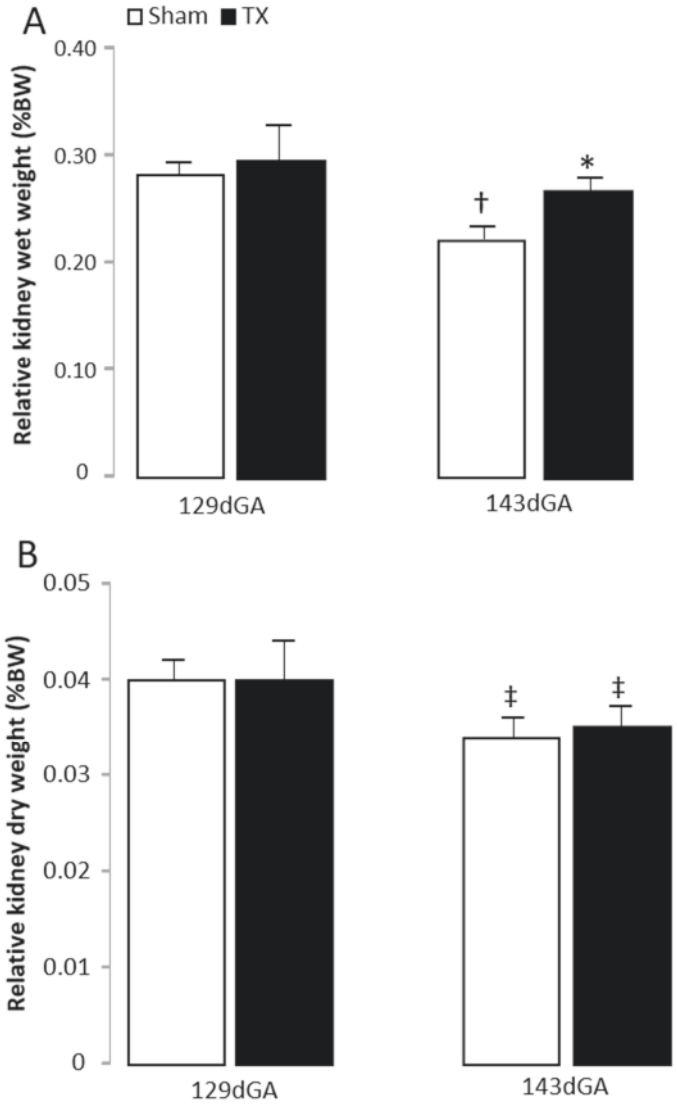

Figure 6.19 Mean ± SEM (A) kidney wet weight and (B) kidney dry weight, relative to fetal body weight, from sham and TX fetuses at 129 and 143dGA. * Significantly different from sham fetuses at the same dGA, † significantly different from fetuses in the same treatment group at 129dGA, $P<0.05$, 2-way ANOVA. ‡ Different from fetuses in the same treatment group at 129dGA, $P=0.06$, Student's t-test. n = 6 fetuses in each group.

There was no effect of thyroidectomy on the kidney water content at 129dGA (Figure 6.20). At 143dGA, the kidneys from the TX fetuses had a significantly higher water content of 86.5 ± 0.2% compared to 84.4 ± 0.2% in the sham fetuses ($P<0.05$, Figure 6.20). In the sham, but not TX, fetuses, kidney water content was significantly lower at 143dGA compared to 129dGA ($P<0.05$, Figure 6.20).

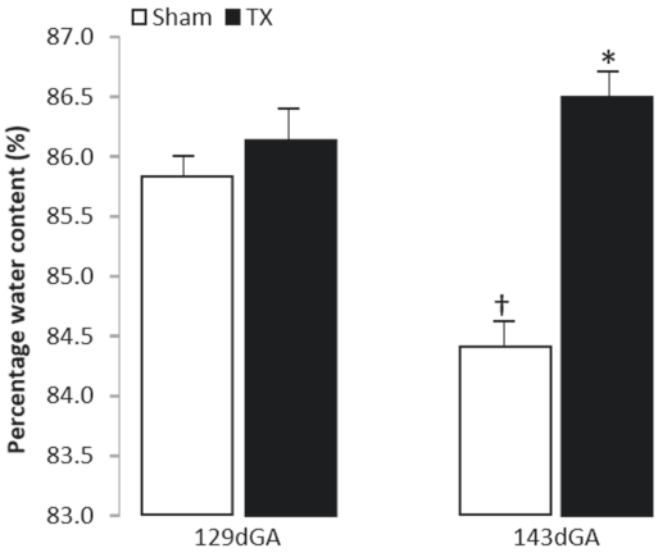

Figure 6.20 Mean ± SEM kidney water content, expressed as a percentage of wet kidney weight in sham and TX fetuses at 129 and 143dGA. * Significantly different from sham fetuses at the same dGA, † significantly different from fetuses in the same treatment group at 129dGA, *P*<0.05, 2-way ANOVA. n=6 in each group.

6.4 Discussion

6.4.1 Fetal hypothyroidism had no effect on renal glomerular or tubular growth

At 143dGA, the relative mass of the kidney was increased in TX fetuses compared to sham controls (Chapter 3) and contrary to the original hypothesis, this did not appear to be associated with alterations in glomerular and tubule density or size. There were no differences in glomerular diameter, volume or number of PCNA-positive cells between the sham and TX fetuses. Analysis of tubule length and surface area densities demonstrated that the overgrowth of the kidney in the TX fetuses was not associated with any apparent structural changes in the tubules. Overall, the stereological data suggest that there did not appear to be structural changes in the renal cortex that accounted for the increase in relative kidney mass in response to fetal hypothyroidism. It should be noted, however, that all stereological analyses used only the cortex of the kidney and the medulla was not examined. This was because the tubular and vascular structures in the medulla are more difficult to distinguish from one another.

Furthermore, the study did not distinguish between the proximal and distal tubules in the renal cortex and these were analysed together. The study was somewhat restricted by the sample collection and preparation. Whole kidney stereology could not be performed as the entire kidney was not wax embedded; therefore all stereological measurements were expressed relative to the reference volume studied.

It may be possible that there was no change in renal development during hypothyroidism *in utero* as local T3 synthesis in the kidney may have been maintained by the actions of sulphatase and/or deiodinase enzymes. Currently there are no reports on the localisation of sulphatases in the fetal kidney and this requires further investigation. Previous studies in fetal sheep have shown that developmental changes in renal structure coincide with changes in renal RAS activity, and that the RAS in the fetal kidney is known to be sensitive to thyroid hormones *in utero* (Chen *et al.*, 2005a). Thyroidectomy in fetal sheep has been demonstrated to reduce renal levels of renin mRNA and protein, ACE and AT_1R and AT_2R mRNA (Forhead & Fowden, 2002; Chen *et al.*, 2005b; 2007). Additionally, hypothyroid sheep fetuses show lower renal protein expression of the β1-adrenergic receptor, which regulates the renin gene response to β-adrenergic stimulation (Liu *et al.*, 2005). It was surprising, therefore, that measurements of glomerular and tubular structure were unaffected by fetal thyroidectomy. Alternatively, it is possible that changes in plasma insulin and leptin seen in the TX fetus may have normalised aspects of renal development.

Insulin has previously been shown to be important in fetal kidney growth. Fetal mice express insulin receptor mRNA and protein from 60% gestation onwards, and insulin causes hyperplasia in a dose-dependent manner in metanephroi isolated from fetal mice (Liu *et al.*, 1997). However, there was no evidence of changes in components of the insulin-IGF signalling pathway in the kidneys of TX compared to sham fetuses which suggests that the fetal kidney is relatively unresponsive to the increased plasma insulin concentration observed during hypothyroidism *in utero*.

There was no change in the protein content of the leptin receptor in the cortex or medulla in the TX fetuses. In neonatal rats, leptin appears to be required for normal

glomeruli development as leptin antagonism leads to the development of small and immature glomeruli (Attig *et al.*, 2011). Further studies are necessary to determine the specific effects of the endocrine environment on the development of the kidney in the TX fetus.

6.4.2 Insulin signalling components exhibited sexual dimorphism in the fetal sheep

Interestingly, there was an effect of fetal sex on the protein expression of various components of the insulin signalling pathway in the fetal ovine kidney. Renal cortical Akt1 levels were two-fold higher in the female, compared to male fetuses, regardless of treatment. There has been no previous report of a sex difference in Akt1 in the fetal kidney. However, greater Akt1 in cardiomyocytes has been reported in female compared to male adult mice; in these cells, oestrogen receptors mediate anti-apoptotic protection through activation of PI3K and Akt1 (Wang *et al.*, 2009). Sexual dimorphism in oestrogen receptors has been reported in the kidneys of adult rats (Sharma & Thakur, 2004). Oestrogen receptors are present in the kidneys of fetal mice, human and pigs (Brandenberger *et al.*, 1997; Lemmen *et al.*, 2002; Knapczyk *et al.*, 2008), although there is no difference in serum oestrogen levels in males and females *in utero* in humans and sheep (Hickey *et al.*, 2014; Reddy *et al.*, 2014).

The renal levels of GLUT4 protein were also affected by fetal sex. In the renal cortex, higher levels of GLUT4 were observed in the female sham fetuses compared to the male sham fetuses. In contrast, in the medulla, the female fetuses of both treatment groups had lower GLUT4 protein expression compared to the male fetuses. Furthermore, renal cortical GLUT4 protein was decreased by hypothyroidism in the female, but not male, fetuses. The reduction in cortical GLUT4 observed in the female TX fetuses was surprising, as previously it has been demonstrated in dogs and humans that insulin infusion increases renal glucose uptake (Cersosimo *et al.*, 1994; Meyer *et al.*, 1998). However, it is also known glucose uptake and utilisation occurs predominately in the medulla (Gerich *et al.*, 2001), where there was no change in GLUT4 expression in the TX fetuses, suggesting that renal glucose uptake is unaffected in hypothyroid fetuses. The significance of differences in the renal components of the insulin signalling pathway between male and female sheep fetuses remains to be established.

6.4.3 Fetal hypothyroidism increased kidney water content

Near term, the kidney of the hypothyroid sheep fetuses was composed of a higher water content compared to sham controls, and this may contribute to the greater renal mass. The increase in water content could be due to changes in fluid retention in the organ, which may be a result of altered blood volume and vascular structure and/or nephron filtration and reabsorption rates. Hypothyroidism in adult humans induces an increase in sodium reabsorption in the distal tubule and a decrease in water excretion (Allon *et al.*, 1990). Additionally, in adult rabbits with congenital hypothyroidism, osmotic water permeability in the renal tubules is increased, which means that they retain more water compared to controls (Mulder *et al.*, 2003).

It has previously been shown that capillary density is elevated in both the cortex and medulla of hypothyroid adult rats (Rodríguez-Gómez *et al.*, 2013). To study the vascular structure of the fetal kidney, it would need to be perfused at dissection to ensure that the blood vessels remain distended under perfusion pressure; capillary density could then be measured by use of endothelial markers. Protein content of angiogenic growth factors, such as vascular endothelial growth factor A, angiopoietin 1 and their receptors, could also be determined in the fetal kidney (Dunford *et al.*, 2014). Three dimensional representations of blood vessels could also be obtained to quantify volume and surface area using vascular corrosion casting, as described by Dunford *et al*., (2014). Additionally, renal function should be examined *in vivo* in the TX fetuses by measuring arterial blood pressure, renal blood flow, and glomerular filtration and urine flow rates. Furthermore, the extent to which the effects of hypothyroidism on water content are specific to the kidney or occur in other fetal tissues more globally remains to be established. Interestingly, other tissues from the same cohort of TX fetal sheep also demonstrate a higher water content, such as the biceps femoris and the liver (unpublished data), suggesting that that this may not be an organ specific phenotype.

6.4.4 Fetal hypothyroidism had no effect on sodium transporter protein expression

Western blotting analysis identified similar protein expression of the subunits of ENaC and Na^+/K^+ ATPase in the TX and sham fetuses. However, this method of protein analysis provides limited knowledge on the activity of the sodium channels and transporters. Furthermore, it has previously been reported in fetal sheep that mRNA abundance of these sodium transporters increases towards term, with no change seen in the protein expression (Keller-Wood *et al.*, 2008). To investigate transporter and channel activities *in vivo*, the responses to natriuretic agents could be analysed, such as sodium excretion and transepithelial currents.

While it is well known that glucocorticoids and insulin can regulate ENaC mRNA expression in the fetal ovine kidney towards term (Keller-Wood *et al.*, 2008), it remains unclear whether thyroid hormones also have a role in the maturation of renal ENaC expression. It was surprising, however, that there was no alteration in the protein levels of the Na^+/K^+ ATPase subunits, as it is known that the pump is regulated by thyroid hormones in adult tissues. Previous studies have shown increased mRNA abundance of Na^+/K^+ ATPase in the kidneys of hypothyroid rats injected with T3 (McDonough *et al.*, 1988) and a TRE has been identified in the 5' region of the β subunit (Feng *et al.*, 1993). In contrast, however, other reports have shown that hypothyroidism in rats has no effect on renal mRNA levels of either Na^+/K^+ ATPase subunit (Horowitz *et al.*, 1990).

It was also surprising that the protein expression of the sodium transporters in the fetal kidney did not respond to the hyperinsulinaemia seen in the TX fetus. Adult rats chronically infused with insulin showed a greater response in sodium excretion when treated with natriuretic agents although there was no change in ENaC protein expression in either the whole kidney or renal cortex (Song *et al.*, 2006). In renal tubules isolated from adult rats, insulin incubation causes increased phosphorylation of the Na^+/K^+ ATPase α subunit (Féraille *et al.*, 1999). It may be that while there was no change in the protein content of sodium transporters present in the TX fetuses, the amount of trafficking to the apical and basolateral membranes may be altered and in future this may be detected by electron microscopy. It has previously been reported that chronic insulin infusion in adult rats leads to increased apical membrane localisation of ENaC,

and this is also demonstrated after acute insulin treatment in the mouse (Tiwari *et al.*, 2007). It may be possible that while the development of glomerular and tubular structure in the fetal kidney is relatively unresponsive to the increased circulating insulin concentrations seen in the TX fetus, there may be changes in the expression of apical sodium transporters, enhancing their reabsorptive function to contribute to the increased kidney water content. It is possible that hypothyroidism decreases sodium transporter protein that would normally increase towards term, but hyperinsulinaemia leads to an upregulation in transporter expression, so there is no net effect.

6.5 Conclusions

It has been shown that relative fetal kidney mass was increased in the hypothyroid sheep fetus during late gestation. However, this was not associated with altered glomerular or tubular growth or with any changes in the insulin signalling pathway. It may be possible that there was no change in renal development during hypothyroidism *in utero* due to local T3 synthesis by the actions of sulphatase and/or deiodinase enzymes. Alternatively, it is possible that changes in plasma insulin seen in the TX fetus may have normalised aspects of renal development

Enlargement of the kidney in the TX fetus may be due, in part, to increased water content. Further research is necessary to examine the effects of thyroid hormones on renal function and the vascular structure of the kidney. The protein expression of the ion transporters was also unaffected by fetal hypothyroidism, however more experimental work is needed to identify the role thyroid hormones in regulating renal sodium transporters in late gestation. The extent to which the effects of fetal hypothyroidism on water content are specific to the kidney or occur more globally remains to be established.

7 GENERAL DISCUSSION

In many mammalian species, including humans and sheep, the fetal thyroid gland is functional from mid-gestation. Thyroid hormones influence growth, metabolism and development *in utero*, especially close to term when T3 levels rise in the fetal circulation (Forhead & Fowden, 2014). The aim of the thesis was to examine the effects of hypothyroidism on the growth and development of the sheep fetus during late gestation. Specifically, the research in this study sought to determine the consequences of fetal thyroid hormone deficiency on pancreatic islet development and the extent to which the effects of hypothyroidism on fetal growth may be mediated by changes in insulin signalling pathways.

The data of the thesis contradict that of the initial hypothesis, in which it was speculated that growth retardation in the hypothyroid sheep fetus was due to low circulating insulin concentrations, secondary to a reduction in pancreatic β-cell mass. Thyroidectomy in the sheep fetus resulted in hyperinsulinaemia and increased β-cell mass, which in turn, upregulated the insulin signalling pathway in PAT to contribute to an overgrowth of unilocular adipocytes. Enlargement of the fetal kidney in response to hypothyroidism *in utero*, however, was not associated with changes in insulin signalling, or glomerular or tubular structure, and may have resulted from greater tissue water content (Figure 7.1).

7.1 Role of thyroid hormones in the control of body and organ growth

Thyroidectomy in fetal sheep resulted in an asymmetric pattern of growth, demonstrating that the thyroid hormones exert their effects in a tissue-specific manner. Organs such as the lungs and heart were reduced in mass relative to body weight, whereas organs such as the adipose tissue and kidneys were enlarged. Overall, there was no change in the body weight of the TX fetuses, which may be because the alterations in organ mass balanced to a comparable mass seen in the sham fetuses. Additionally, there was no change in crown-rump length in TX fetuses compared to sham controls, although fore and hind-leg limbs were growth retarded, indicating that there

may be differences in the effects of hypothyroidism *in utero* on regions of the developing skeleton.

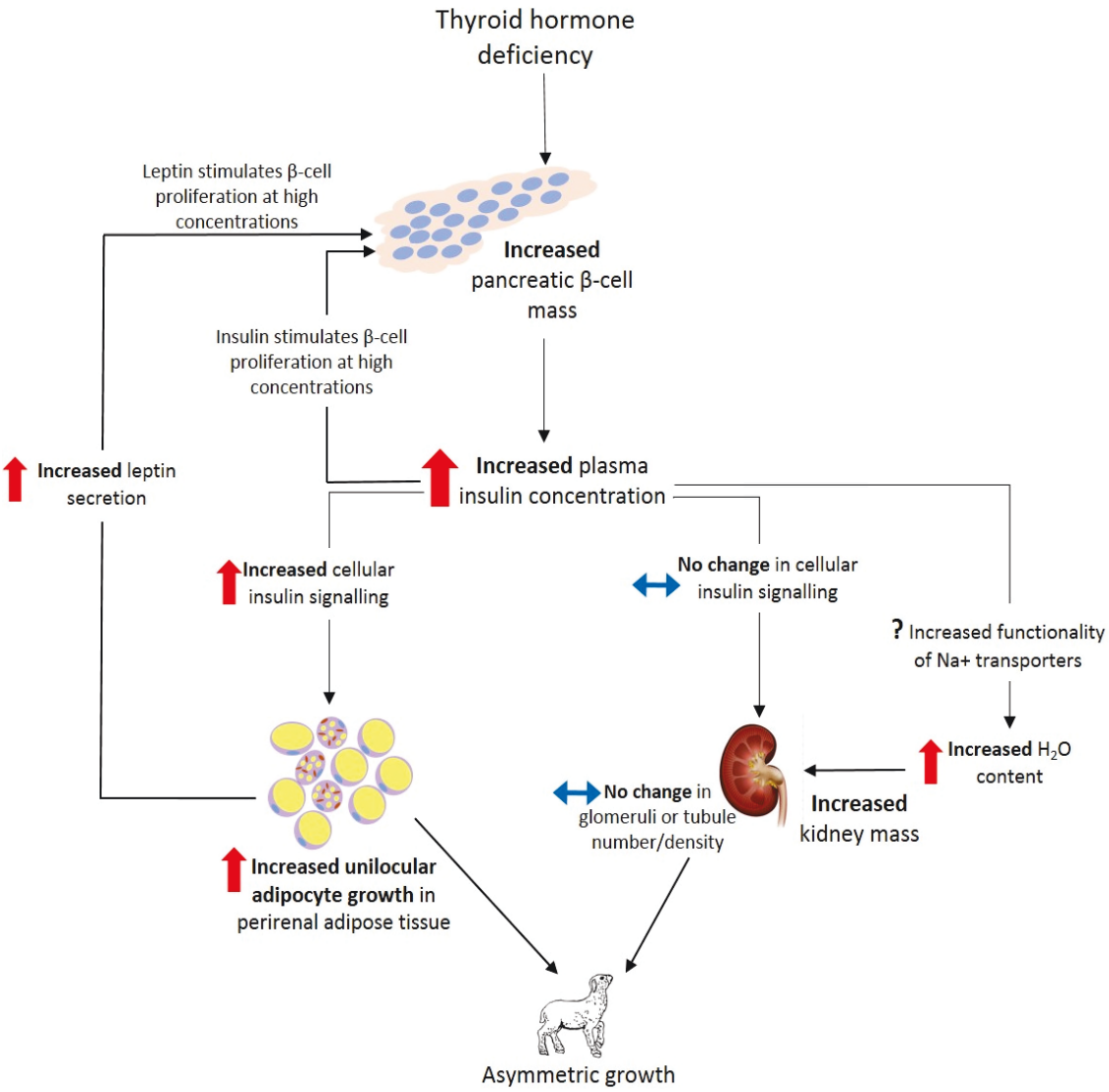

Figure 7.1. Thyroid hormone deficiency *in utero* resulted in an enhanced pancreatic β-cell mass, which increased plasma insulin concentration, which in turn, further stimulated β-cell proliferation. In perirenal adipose tissue, increased cellular insulin signalling promoted unilocular adipocyte growth, leading to a greater plasma concentration of leptin, which could further contribute to pancreatic β-cell mass. There was no change in the expression levels of the markers of the insulin signalling pathway in fetal kidneys, with no alterations in kidney structure. Fetal kidneys had a greater water content which may be a consequence of increased sodium transporter functionality.

The tissue-specific effects of thyroid hormone deficiency suggest that there may be differences in thyroid hormone sensitivity between fetal organs. This may be, in part, due to variation in expression of transporters, receptors and metabolic enzymes between tissues, which determine the local tissue-specific concentrations of thyroid hormones. These factors controlling thyroid hormone metabolism alter in response to thyroid hormone deficiency before birth. For example, in hypothyroid fetal sheep D2 is upregulated in the brain, to maintain the local concentration of T3, which is important for normal brain growth and development (Polk *et al.*, 1988). The asymmetric pattern of growth in the hypothyroid fetuses may also be due to sensitivities to other growth factors such as insulin and the insulin-IGF signalling pathway.

7.2 Role of thyroid hormones in development of fetal tissues

This study reported for the first time that hypothyroidism in the ovine fetus caused a 30-40% increase in pancreatic β-cell mass associated with a rise in plasma insulin concentration *in utero*. It also identified that thyroid hormones inhibited pancreatic β-cell proliferation in a dose-dependent manner in isolated fetal ovine islets studied *in vitro*. While β-cell mass was enhanced in the TX fetus, the maturity and functionality of individual β-cells, in terms of their sensitivity to glucose and capacity for insulin secretion, remains unknown. It is possible that the prepartum surge in T3 in the ovine fetus normally promotes a switch in pancreatic β-cell development from proliferation and growth to maturation, in a manner similar to that seen in fetal cardiomyocytes near term (Chattergoon *et al.*, 2012a; 2014). Therefore, in the sheep fetus, removal of the thyroid gland and prevention of the normal rise in T3 near term may maintain proliferation of pancreatic β-cells and basal insulin secretion, and yet delay the maturation of glucose-stimulated insulin secretion. Indeed, the findings from preliminary experiments suggested that T3 promotes glucose-stimulated insulin secretion in isolated fetal ovine pancreatic islets *in vitro*. In fetal sheep, isolated cardiomyocytes exposed to T3 have an increased expression of the cell cycle inhibitor p21 and a decrease in the cell cycle promotor, cyclin D1, suggesting that T3 initiates cell cycle exiting (Chattergoon *et al.*, 2012b). Hypothyroidism in the neonatal mouse has been shown to downregulate expression of cell cycle inhibitors in developing testis (Holsberger *et al.*, 2003), and the same mechanism may occur in pancreatic β-cells.

It is unknown whether the changes in β-cell mass seen in response to hypothyroidism are due to neogenesis of β-cell progenitor cells or due to replication of mature cells. Pancreatic islets isolated from thyroid deficient fetal sheep should be used in the future to assess the expression patterns of transcription factors involved in neogenesis and maturation (Pdx1, Ngn3, MafA). It will also be necessary to determine the rate of β-cell proliferation in the islets of hypothyroid and sham fetuses, by either PCNA protein determination or proliferation assays *in vitro*. Additionally, future studies may determine the effects of thyroid hormone deficiency on the expression of signalling molecules that regulate β-cell sensitivity to glucose, such as GLUT2 and glucokinase, in pancreatic islets from fetal sheep. To identify the molecular mechanisms by which thyroid hormone deficiency affects pancreatic β-cell development and maturation, genetic knockouts of TRα and TRβ could be generated in β-cells of mouse models. The effects of receptor deletions on fetal and postnatal growth could be examined individually and/or as a double knock-out to assess specific receptor function. In addition, glucose homeostasis and insulin secretion could be examined *in vivo* in postnatal animals using glucose tolerance tests and the morphology and secretory function of the developing pancreas may be examined in wild-type and mutant mice in fetal, neonatal and adult life. Fetal islet structure and function could be further examined in sheep fetuses infused with varying concentrations of T3.

In a novel finding, thyroidectomy in the sheep fetus resulted in an increase in the relative UL adipocyte mass with no change in the ML adipocyte mass. The role of the thyroid hormones in UL adipose development before birth is still relatively unknown. Perirenal adipose tissue from TX fetuses could be assessed for markers of adipogenic pathways, such as C/EBPα and β and SREBP-1, and of lipogenesis, such as the carbohydrate responsive element-binding protein, to determine how thyroid hormone deficiency *in utero* has specifically affected UL adipocyte proliferation. Hypothyroidism in human adults has previously been shown to reduce catecholamine-stimulated lipolysis (Wahrenberg *et al.*, 1986); therefore, β-adrenergic receptor expression should be assessed alongside lipolytic enzymes such as adipose hormone-sensitive lipase to ascertain if these processes are downregulated in adipose tissue from TX sheep fetuses.

It is possible that thyroid hormones act to limit UL adipose growth in the sheep fetus towards term, perhaps by interaction with PPARγ, and promote the maturation of ML adipocytes for thermogenic function. Although there was no change in the ML adipose mass, the functionality of the ML adipocytes in the TX fetus remains unknown. It would therefore be necessary to determine UCP1 expression in the BAT of hypothyroid fetuses. Assessment of β3-adrenergic receptor content will also highlight if there is a dysfunction in normal thermoregulatory control of BAT in the thyroid deficient fetus. In these studies, it would be necessary to isolate UL and ML adipocytes from PAT in order to quantify UCP1 and β3-adrenergic receptors in the ML adipocytes specifically. Indeed, the elevated levels of adipose proteins measured in PAT taken from TX sheep fetuses in the present study, may have been a consequence of the greater proportion of UL, relative to ML, adipocytes.

The increase in kidney mass observed in the TX sheep fetus did not appear to be associated with a greater number or growth of glomeruli or cortical tubules. Further to this, there was no difference in the dry kidney weights between sham and TX fetuses. The percentage of water content in the kidney of the TX fetus was increased compared to sham controls, suggesting that thyroid hormones influence renal water content which may be composed of blood volume and/or tubular filtrate. Fetal urine is a major component of amniotic fluid, which suggests that the thyroid hormones may have a role in renal water excretion and amniotic fluid production which could be investigated further. It is possible that other tissues in the TX fetus may vary their water content; therefore, it would be interesting to measure the dry weights of other organs in the hypothyroid fetus to establish if this effect is specific to the kidney or a more global consequence of thyroid hormone deficiency before birth. It is possible that the higher water content in the TX fetuses may be due to increased function of renal sodium transporters. Although no changes in ENaC or Na^+/K^+ ATPase were observed in response to hypothyroidism *in utero*, the amount of transporter trafficked to and expressed in apical plasma membrane of renal tubules should be determined in the TX fetuses. Upregulation of ENaC at the cellular apical membrane may lead to greater retention of sodium, which in turn would cause increased uptake of water. It will also be necessary to investigate renal function *in vivo* by measuring arterial blood pressure, renal blood

flow, glomerular filtration rates and urine production rates to determine if hypothyroidism affects haemodynamic and fluid homeostasis. In addition, assessment of renal vascular structure may establish if changes in blood volume account for the greater fluid content and mass of the fetal kidney during thyroid hormone deficiency.

The future studies required in this research, highlight a limitation in the use of the sheep model. The whole of the whole pancreas was used for stereological studies, providing no additional tissue for maturational or mechanistic analysis. More thyroid deficient fetal sheep would be needed to fully investigate the role of the thyroid hormones on the pancreas, adipose and kidney. However, sheep are not as readily available as rodent models, such as mice. The experimental design has also limited some of the research in this project. The vessel structure of the kidney could not be assessed as the kidney was not pressure perfused at collection. Additionally, the results obtained in this thesis only provide a snapshot of the physiology of the TX fetuses, as tissue collection occurred after fetal euthanasia.

7.3 Interactions between thyroid hormones and insulin signalling *in utero*

The effects of hypothyroidism in the sheep fetus may have been mediated by interactions with the insulin signalling pathway. It was speculated that growth retardation in the thyroid hormone deficient fetus was due to downregulation of insulin signalling. Although insulin signalling in the smaller tissues was not investigated in this project, the hypothesis could still be valid as the enlarged adipose tissue of the TX fetus was associated with, in part, an upregulation of several insulin signalling proteins. The insulin signalling pathway could be assessed in the growth retarded organs, such as the heart and lungs, to determine if this has been altered by hypothyroidism *in utero*.

The overgrowth of UL adipocytes seen in the TX fetuses may be due to the concomitant increase in plasma concentrations of insulin as insulin promotes local adipose expression of PPARγ and GLUT4. The greater adipose levels of pS6K suggested that UL adipocyte proliferation may have been due to an upregulation of the insulin signalling pathway. The enhanced UL adipocyte mass in the TX fetus was likely to be responsible for the

increased circulating concentrations of leptin and, in turn, leptin may have promoted proliferation of pancreatic β-cells and further insulin secretion. It is, therefore, difficult to separate the effects of higher insulin and leptin concentrations from the effects of hypothyroidism on insulin signalling and other molecules. To determine the specific roles of thyroid hormones on tissue development and insulin signalling pathways, tissue-specific genetic deletions of TRα and TRβ could be utilised. These molecular models create a hypothyroid environment in specific organs without alterations in circulating insulin concentrations, and as such, the effects of thyroid hormone deficiency alone on the development of fetal tissues can be investigated.

7.4 Short-term consequences of hypothyroidism *in utero*

Hypothyroidism *in utero* has consequences for maturation of the neonate. Little is known about the physiology of human neonates born with congenital hypothyroidism as they are treated with T4 soon after birth (LaFranchi, 2011). Furthermore, human neonates with congenital hypothyroidism may have a less severe phenotype to that seen in the TX ovine fetus due to the significant placental transfer of maternal thyroid hormones. The impact of thyroid hormone deficiency before birth on the functioning of organ systems in the neonate has, therefore, not been fully investigated.

Hypothyroid neonates may be unable to maintain stable blood glucose levels. Previous studies have demonstrated that thyroidectomy in the sheep fetus results in decreased hepatic glycogen content and decreased hepatic activity of gluconeogenic enzymes in late gestation (Forhead *et al.*, 2003; 2009). Additionally, the hypothyroid fetus has a higher circulating concentration of insulin, which could further exacerbate neonatal hypoglycaemia. The increased β-cell mass in the hypothyroid fetus may show dynamic changes that lead to pancreatic dysfunction. In sheep fetuses of obese ewes overnourished throughout gestation, pancreatic β-cell proliferation and islet mass were increased at mid-gestation and yet reduced near term, to below that seen in control fetuses, in association with an increased rate of β-cell apoptosis (Zhang et al., 2011). This type of β-cell exhaustion has a similar pathology to that seen in type 2 diabetes (Pende *et al.*, 2000). Further studies should examine pancreatic islet development and insulin secretion in neonates and young animals exposed to hypothyroidism before birth. The

hypothyroid fetus may have impaired tissue sensitivity to insulin at birth, which may, in turn, promote further hyperinsulinaemia in neonatal life. The high insulin and leptin concentrations in the TX fetus are similar to that seen in offspring born of mothers with diabetes and/or obesity (Catalano *et al.*, 2009b; Kamana *et al.*, 2015). The offspring have increased adiposity which increases independently of body weight and is positively correlated with insulin resistance at birth (Catalano *et al.*, 2003; 2009b). A decrease in InsR protein was observed in adipose tissue of the TX fetuses and the higher circulating insulin may have affected insulin receptor sensitivity in other peripheral tissues.

Increased water content in the kidney of the TX fetus may alter haemodynamics *in utero* and early in postnatal life. Previous studies examining the effects of thyroidectomy on blood pressure in fetal sheep have reported conflicting results. Walker and Schuijers (1989) reported that thyroidectomy in fetal sheep at 80dGA results in significantly lower arterial blood pressure in TX fetuses studied at 120dGA. In contrast, no change in arterial pressure was observed in sheep fetuses thyroidectomised at 100dGA and studied at term (Ayromlooi *et al.*, 1983). The data from the previous studies may be variable due to the timing of thyroidectomy and measurement of arterial blood pressure. It has also been shown that hypothyroidism in the sheep fetus causes alterations in plasma noradrenaline concentrations depending on the timing of thyroidectomy (Walker & Schuijers, 1989; Fowden *et al.*, 2001) and highlights the need for further characterisation of the functioning of the sympathetic nervous system and catecholamine receptor expression and tissue sensitivity in the TX sheep fetus. Thyroid hormone deficiency *in utero* may also have a consequence for thermogenesis after birth, such that neonates may fail to maintain body temperature due to abnormal ML adipocyte function and decreased responses to catecholamine stimulation.

7.5 Long-term consequences of hypothyroidism *in utero*

Extensive studies have shown that hormonal and environmental insults early in development have long-term programming effects on hormonal and metabolic homeostasis in later life (Barker, 2007; Lisboa *et al.*, 2015). The adult offspring of rats hypothyroid during pregnancy show reduced glucose tolerance and lower glucose-stimulated insulin secretion from isolated pancreatic islets (Farahani *et al.*, 2010;

Karbalaei *et al.*, 2014). Although these offspring are euthyroid in adult life, the pancreatic islets are less sensitive to glucose with decreased insulin output per islet (Karbalaei *et al.*, 2014). The β-cell mass of these offspring was not determined at birth or in adult life, and there may be dynamic changes in islet morphology and function over the perinatal period and into adulthood.

Offspring born to diabetic mothers, which are hyperinsulinaemic *in utero*, show a positive correlation between percentage body fat as a neonate and as a child (Catalano *et al.*, 2009a). Adolescents born to mothers with gestational diabetes are also hyperinsulinaemic at birth and have increased body weight, greater waist circumference and increased fat storage (Crume *et al.*, 2011; Kamana *et al.*, 2015). Moreover, these offspring are more susceptible to the onset of metabolic diseases, such as high blood pressure, abnormal cholesterol levels and obesity, all of which are risk factors for diseases such as type 2 diabetes and coronary heart disease (Kamana *et al.*, 2015). The increased adipose tissue mass of the hypothyroid fetus may have an intergenerational effect. A recent study of maternal obesity in mice highlighted that hyperinsulinaemia, increased insulin resistance and enlarged islet mass persisted in both F1 and F2 progeny, even after the diet was corrected in the offspring (Graus-Nunes *et al.*, 2015). This suggests that the developmental programming of pancreatic structure and function can persist, although the mechanisms responsible are unknown.

It has been previously been established that changes in cardiovascular development in the prenatal environment can programme adult blood pressure (Barker *et al.*, 1989; Langley & Jackson, 1994; Manning & Vehaskari, 2001; Vehaskari *et al.*, 2001). In humans, offspring of mothers who were hypothyroid during the last 10 weeks of gestation have elevated systolic blood pressure when measured at 20 years of age (Rytter *et al.*, 2016). The hypothyroid sheep fetus had increased renal water content and in the fetal rat, it has previously been shown that increased sodium and fluid retention in the kidney suppresses plasma renin activity and that reduced renin activity prenatally programmes hypertension (Vehaskari *et al.*, 2001; Manning *et al.*, 2002).

Human neonates are screened for thyroid status shortly after birth and in the case of hypothyroidism, synthetic T4 is prescribed as life-long treatment. Although this treatment has been shown to normalise circulating thyroid hormone levels, and prevent cognitive impairment (Arnold *et al.*, 1990), it is unknown whether other physiological changes that have occurred *in utero* have long term consequences. This requires longitudinal studies in experimental animal models to determine if altered fetal growth and development in response to changes in thyroid hormones *in utero* will affect health in the life course of an individual.

8 REFERENCES

Aguayo-Mazzucato C, Koh A, El Khattabi I, Li WC, Toschi E, Jermendy A, Juhl K, Mao K, Weir G, Sharma A & Bonner-Weir S. (2011). Mafa expression enhances glucose-responsive insulin secretion in neonatal rat beta cells. *Diabetologia* **54,** 583-593.

Aguayo-Mazzucato C, Zavacki A, Marinelarena A, Hollister-Lock J, El Khattabi I, Marsili A, Weir G, Sharma A, Larsen P & Bonner-Weir S. (2013). Thyroid hormone promotes postnatal rat pancreatic β-cell development and glucose-responsive insulin secretion through MAFA. *Diabetes* **62,** 1569-1580.

Ahima RS & Flier JS. (2000). Leptin. *Annual Review of Physiology* **62,** 413-437.

Allon M, Harrow A, Pasque C & Rodriguez M. (1990). Renal sodium and water handling in hypothyroid patients: The role of renal insufficiency. *Journal of the American Society of Nephrology* **1,** 205-210.

Anderson M, Thamotharan M, Kao D, Devaskar S, Qiao L, Friedman J & Hay WJ. (2004). Effects of acute hyperinsulinemia on insulin signal transduction and glucose transporters in ovine fetal skeletal muscle. *American Journal of Physiology* **288,** R473–R481.

Ansari MA, de Mello DE & Devaskar UP. (2000). Effect of prenatal glucocorticoid on fetal lung ultrastructural maturation in hyt/hyt mice with primary hypothyroidism. *Biology of the Neonate* **77,** 29-36.

Arner E, Westermark PO, Spalding KL, Britton T, Rydén M, Frisén J, Bernard S & Arner P. (2010). Adipocyte Turnover: Relevance to Human Adipose Tissue Morphology. *Diabetes* **59,** 105-109.

Arnold MB, Bapat V, Baumgartner Y, Bennett A, Biggs ST, Bode HH, Brink S, Brown J, Brown R, Carey D, Carpenter T, Crawford C, Crawford FD, Crigler JE, Danon M, Frederick D, Genel M, Gruppuso P, Haddow JE, Holmes J, Larsen PR, MacCracken J, Man E, Mitchell ML, Orson JM, Page LA, Ratzan S, Reiter E, Russell W, Sadeghi-Nejad A, Senior B, Tamborlane W, Waisbren S & Klein RZ. (1990). Elementary school performance of children with congenital hypothyroidism. *Journal of Pediatrics* **116,** 27-32.

Attig L, Larcher T, Gertler A, Abdennebi-Najar L & Djiane J. (2011). Postnatal leptin is necessary for maturation of numerous organs in newborn rats. *Organogenesis* **7,** 88-94.

Ayromlooi J, Berg PD, Valderrama E & Tobias MD. (1983). Midtrimester thyroidectomy in the ovine fetus. *Pediatric Pharmacology* **3,** 15-28.

Barker DJ, Osmond C, Golding J, Kuh D & Wadsworth ME. (1989). Growth in utero, blood pressure in childhood and adult life, and mortality from cardiovascular disease. *British Medical Journal* **298,** 564-567.

Barker DJP. (2007). The origins of the developmental origins theory. *Journal of Internal Medicine* **261,** 412-417.

Barker PM, Brown MJ, Ramsden CA, Strang LB & Walters DV. (1988). The effect of thyroidectomy in the fetal sheep on lung liquid reabsorption induced by adrenaline or cyclic AMP. *Journal of Physiology* **407,** 373-383.

Barker PM, Strang LB & Walters DV. (1990). The role of thyroid hormones in maturation of the adrenaline-sensitive lung liquid reabsorptive mechanism in fetal sheep. *Journal of Physiology* **424,** 473-485.

Barr VA, Malide D, Zarnowski MJ, Taylor SI & Cushman SW. (1997). Insulin stimulates both leptin secretion and production by rat white adipose tissue. *Endocrinology* **138,** 4463-4472.

Bassett J, Williams A, Murphy E, Boyde A, Howell P, Swinhoe R, Archanco M, Flamant F, Samarut J, Costagliola S, Vassart G, Weiss R, Refetoff S & Williams G. (2008). A lack of thyroid hormones rather than excess thyrotropin causes abnormal skeletal development in hypothyroidism. *Molecular Endocrinology* **22,** 501-512.

Bergh J, Lin H-Y, Lansing L, Mohamed S, Davis F, Mousa S & Davis P. (2005). Integrin alphaVbeta3 contains a cell surface receptor site for thyroid hormone that is linked to activation of mitogen-activated protein kinase and induction of angiogenesis. *Endocrinology* **146,** 2864-2871.

Bernal-Mizrachi E, Wen W, Stahlhut S, Welling CM & Permutt MA. (2001). Islet beta cell expression of constitutively active Akt1/PKB alpha induces striking hypertrophy, hyperplasia, and hyperinsulinemia. *Journal of Clinical Investigation* **108,** 1631-1638.

Beutler KT, Masilamani S, Turban S, Nielsen J, Brooks HL, Ageloff S, Fenton RA, Packer RK & Knepper MA. (2003). Long-term regulation of ENaC expression in kidney by angiotensin II. *Hypertension* **41,** 1143-1150.

Bhalla V & Hallows KR. (2008). Mechanisms of ENaC regulation and clinical implications. *Journal of the American Society of Nephrology* **19,** 1845-1854.

Bjorndal B, Burri L, Staalesen V, Skorve J & Berge RK. (2011). Different adipose depots: their role in the development of metabolic syndrome and mitochondrial response to hypolipidemic agents. *Journal of Obesity* **2011,** 490650.

Blache D, Tellam RL, Chagas LM, Blackberry MA, Vercoe PE & Martin GB. (2000). Level of nutrition affects leptin concentrations in plasma and cerebrospinal fluid in sheep. *Journal of Endocrinology* **165,** 625–637.

Blackburn ST. (2003a). Adaptations in metabolic processes in the pregnant woman, fetus and neonate. In *Maternal, Fetal and Neonatal Physiology: A Clinical Perspective*, 2nd edn, pp. 370-411. Elsevier Science, USA.

Blackburn ST. (2003b). Adaptations in metabolic processes in the pregnant woman, fetus and neonate. In *Maternal, Fetal and Neonatal Physiology: A Clinical Perspective*, 2nd edn, pp. 677-705. Elsevier Science, USA.

Bloomfield F, Spiroski A-M & Harding J. (2013). Fetal growth factors and fetal nutrition. *Seminars in Fetal & Neonatal Medicine* **18,** 118-123.

Bluher M, Michael MD, Peroni OD, Ueki K, Carter N, Kahn BB & Kahn CR. (2002). Adipose tissue selective insulin receptor knockout protects against obesity and obesity-related glucose intolerance. *Developmental Cell* **3,** 25-38.

Bock T, Pakkenberg B & Buschard K. (2003). Increased islet volume but unchanged islet number in ob/ob mice. *Diabetes* **52,** 1716-1722.

Bock T, Pakkenberg B & Buschard K. (2005). Genetic background determines the size and structure of the endocrine pancreas. *Diabetes* **54,** 133-137.

Bornstein SR, Engeland WC, Ehrhart-Bornstein M & Herman JP. (2008). Dissociation of ACTH and glucocorticoids. *Trends in Endocrinol and Metabolism* **19,** 175-180.

Bouche C, Lopez X, Fleischman A, Cypess AM, O' Shea S, Stefanovski D, Bergman RN, Rogatsky E, Stein DT, Kahn CR, Kulkarni RN & Goldfine AB. (2010). Insulin enhances glucose-stimulated insulin secretion in healthy humans. *PNAS* **107,** 4770–4775.

Bouwens L & Rooman I. (2005). Regulation of pancreatic beta-cell mass. *Physiological Reviews* **85,** 1255-1270.

Brandenberger AW, Tee MK, Lee JY, Chao V & Jaffe RB. (1997). Tissue distribution of estrogen receptors alpha (ER-α) and beta (ER-β) mRNA in the midgestational human fetus. *Journal of Clinical Endocrinology & Metabolism* **82,** 3509-3512.

Bravo R, Fey SJ, Bellatin J, Larsen PM, Arevalo J & Celis JE. (1984). Identification of a nuclear and of a cytoplasmic polypeptide whose relative proportions are sensitive to changes in the rate of cell proliferation. *Experimental Cell Research* **136,** 311-319.

Brazil DP, Yang ZZ & Hemmings BA. (2004). Advances in protein kinase B signalling: AKTion on multiple fronts. *Trends in Biochemical Sciences* **29,** 233-242.

Breier BH, Gallaher BW & Gluckman PD. (1991). Radioimmunoassay for insulin-like growth factor-I: solutions to some potential problems and pitfalls. *Journal of Endocrinology* **128,** 347-357.

Brent G. (2000). Tissue-specific actions of thyroid hormone: insights from animal models. *Reviews in Endocrine & Metabolic Disorders* **1,** 27-33.

Brent G. (2012). Mechanisms of thyroid hormone action. *Journal of Clinical Investigation* **122,** 3035-3043.

Bruin JE, Saber N, O'Dwyer S, Fox JK, Mojibian M, Arora P, Rezania A & Kieffer TJ. (2016). Hypothyroidism impairs human stem cell-derived pancreatic progenitor cell maturation in mice. *Diabetes* **db151439**.

Burks DJ & White MF. (2001). IRS proteins and beta-cell function. *Diabetes* **50,** S140-S145.

Bustin SA, Benes V, Garson JA, Hellemans J, Huggett J, Kubista M, Mueller R, Nolan T, Pfaffl MW, Shipley GL, Vandesompele J & Wittwer CT. (2009). The MIQE guidelines: minimum information for publication of quantitative real-time PCR experiments. *Clinical Chemistry* **55,** 611-622.

Bustin SA & Mueller R. (2005). Real-time reverse transcription PCR (qRT-PCR) and its potential use in clinical diagnosis. *Clinical Science* **109,** 365-379.

Butler-Browne GS, Herlicoviez D & Whalen RG. (1984). Effects of hypothyroidism on myosin isozyme transitions in developing rat muscle. *FEBS Letters* **166,** 71-75.

Cantley J, Choudhury AI, Asare-Anane H, Selman C, Lingard S, Heffron H, Herrera P, Persaud SJ & Withers DJ. (2007). Pancreatic deletion of insulin receptor substrate 2 reduces beta and alpha cell mass and impairs glucose homeostasis in mice. *Diabetologia* **50,** 1248-1256.

Cao X, Kambe F, Moeller L, Refetoff S & Seo H. (2005). Thyroid hormone induces rapid activation of Akt/protein kinase B-mammalian target of rapamycin-p70S6K cascade through phosphatidylinositol 3-kinase in human fibroblasts. *Molecular Endocrinology* **19,** 102-112.

Carew R, Sadagurski M, Goldschmeding R, Martin F, White M & Brazil D. (2010). Deletion of Irs2 causes reduced kidney size in mice: role for inhibition of GSK3beta? *BMC Developmental Biology* **10,** 73-80.

Carey L, Valego N, Chen K & Rose J. (2008). Thyroid hormone regulates renocortical COX-2 and PGE2 expression in the late gestation fetal sheep. *Reproductive Sciences* **15,** 598-603.

Castello A, Rodriguez-Manzaneque JC, Camps M, Perez-Castillo A, Testar X, Palacin M, Santos A & Zorzano A. (1994). Perinatal hypothyroidism impairs the normal transition of GLUT4 and GLUT1 glucose transporters from fetal to neonatal levels in heart and brown adipose tissue. Evidence for tissue-specific regulation of GLUT4 expression by thyroid hormone. *Journal of Biological Chemistry* **269,** 5905-5912.

Catalano PM, Farrell K, Thomas A, Huston-Presley L, Mencin P, Hauguel de Mouzon S & Amini SB. (2009a). Perinatal risk factors for childhood obesity and metabolic dysregulation. *American Journal of Clinical Nutrition* **90,** 1303-1313.

Catalano PM, Presley L, Minium J & Hauguel-de Mouzon S. (2009b). Fetuses of obese mothers develop insulin resistance in utero. *Diabetes Care* **32,** 1076-1080.

Catalano PM, Thomas A, Huston-Presley L & Amini SB. (2003). Increased fetal adiposity: a very sensitive marker of abnormal in utero development. *American Journal of Obstetrics and Gynaecology* **189,** 1698-1704.

Cersosimo E, Judd RL & Miles JM. (1994). Insulin regulation of renal glucose metabolism in conscious dogs. *Journal of Clinical Investigation* **93,** 2584-2589.

Chang Y-J, Hwu C-M, Yeh C-C, Wang PS & Wang S-W. (2014). Effects of subacute hypothyroidism on metabolism and growth-related molecules. *Molecules* **19,** 11178-11195.

Chattergoon N, Giraud G, Louey S, Stork P, Fowden A & Thornburg K. (2012a). Thyroid hormone drives fetal cardiomyocyte maturation. *FASEB Journal* **26,** 397-408.

Chattergoon N, Louey S, Stork P, Giraud G & Thornburg K. (2014). Unexpected maturation of PI3K and MAPK-ERK signaling in fetal ovine cardiomyocytes. *American Journal of Physiology* **307,** H1216–H1225.

Chattergoon N, Louey S, Stork P, Giraud GD & Thornburg KL. (2012b). Mid-gestation ovine cardiomyocytes are vulnerable to mitotic suppression by thyroid hormone. *Reproductive Sciences* **19,** 642-649.

Chen K, Carey L, Valego N & Rose J. (2007). Thyroid hormone replacement normalizes renal renin and angiotensin receptor expression in thyroidectomized fetal sheep. *American Journal of Physiology* **293,** R701-R706.

Chen K, Carey LC, Liu J, Valego NK, Tatter SB & Rose JC. (2005a). The effect of hypothalamo-pituitary disconnection on the renin-angiotensin system in the late-gestation fetal sheep. *American Journal of Physiology* **288,** R1279-R1287.

Chen K, Carey LC, Valego NK, Liu J & Rose JC. (2005b). Thyroid hormone modulates renin and ANG II receptor expression in fetal sheep. *American Journal of Physiology* **289,** R1006 – R1014.

Chen Y, Lasaitiene D & Friberg P. (2004). The renin–angiotensin system in kidney development. *Acta Physiologica Scandinavica* **181,** 529-535.

Cheng S-Y, Leonard J & Davis P. (2010). Molecular aspects of thyroid hormone actions. *Endocrine Reviews* **31,** 139-170.

Chi H, Chen C-Y, Tsai M-M, Tsai C-Y & Lin K-H. (2013). Molecular functions of thyroid hormones and their clinical significance in liver-related diseases. *BioMed Research International* **2013,** doi:10.1155/2013/601361.

Cinti S. (2012). The adipose organ at a glance. *Disease Models & Mechanisms* **5,** 588-594.

Clarke L, Bryant MJ & Lomax MA. (1997). Maternal manipulation of brown adipose tissue and liver development in the ovine fetus during late gestation. *British Journal of Nutrition* **77,** 871-883.

Coelho M, Oliveira T & Fernandes R. (2013). Biochemistry of adipose tissue: An endocrine organ. *Archives of Medical Science* **9,** 191-200.

Cole L, Anderson M, Antin PB & Limesand SW. (2009). One process for pancreatic beta-cell coalescence into islets involves an epithelial-mesenchymal transition. *Journal of Enodcrinology* **203,** 19-31.

Collombat P, Hecksher-Sorensen J, Krull J, Berger J, Riedel D, Herrera PL, Serup P & Mansouri A. (2007). Embryonic endocrine pancreas and mature beta cells acquire alpha and PP cell phenotypes upon Arx misexpression. *Journal of Clinical Investigation* **117,** 961-970.

Conrad E, Stein R & Hunter CS. (2014). Revealing transcription factors during human pancreatic beta cell development. *Trends in Endocrinology and Metabolism* **25,** 407-414.

Cooper WO, Hernandez-diaz S, Abogast PHPG, Dudley JA, Dyer S, Gideon PS, Hall K & Ray WA. (2006). Major congenital malformations after first-trimester exposure to ACE inhibitors. *New England Journal of Medicine* **354,** 2443-2451.

Copp J, Manning G & Hunter T. (2009). TORC-specific phosphorylation of mammalian target of rapamycin (mTOR): phospho-Ser2481 is a marker for intact mTOR signaling complex 2. *Cancer Research* **69,** 1821-1827.

Covey SD, Wideman RD, McDonald C, Unniappan S, Asadi A, Speck M, Webber T, Chua SC & Kieffer TJ. (2006). The pancreatic β cell is a key site for mediating the effects of leptin on glucose homeostasis. *Cell Metabolism* **4,** 291-302.

Crume TL, Ogden L, West NA, Vehik KS, Scherzinger A, Daniels S, McDuffie R, Bischoff K, Hamman RF, Norris JM & Dabelea D. (2011). Association of exposure to diabetes in utero with adiposity and fat distribution in a multiethnic population of youth: the Exploring Perinatal Outcomes among Children (EPOCH) Study. *Diabetologia* **54,** 87-92.

DeChiara TM, Efstratiadis A & Robertson EJ. (1990). A growth-deficiency phenotype in heterozygous mice carrying an insulin-like growth factor II gene disrupted by targeting. *Nature* **345,** 78-80.

Delhanty PJD & Han VKM. (1993). The expression of the insulin-like growth factor (IGF)-binding protein-2 and IGF-II genes in the tissues of the developing ovine fetus. *Endocrinology* **132,** 41-51.

deMello D, Heyman S, Govindarajan R, Sosenko IRS & Devaskar UP. (1994). Delayed ultrastructural lung maturation in the fetal and newborn hypothyroid (Hyt/Hyt) mouse. *Pediatric Research* **36,** 380-386.

Desjardin C, Charles C, Benoist-Lasselin C, Riviere R, Gilles M, Chassande O, Morgenthaler C, Laloé D, Lecardonnel J, Flamant F, Legeai-Mallet L & Schibler L. (2014). Chondrocytes play a major role in the stimulation of bone growth by thyroid hormone. *Endocrinology* **155,** 3123–3135.

Devaskar SU & Anthony R. (2002). Ontogeny and insulin regulation of fetal ovine white adipose tissue leptin expression. *American Journal of Physiology* **282,** R431-R438.

Duan C & Xu Q. (2005). Roles of insulin-like growth factor (IGF) binding proteins in regulating IGF actions. *General and Comparative Endocrinology* **142,** 44-52.

Duchamp C, Burton KA, Herpin P & Dauncey MJ. (1994). Perinatal ontogeny of porcine nuclear thyroid hormone receptors and its modulation by thyroid status. *American Journal of Physiology* **267,** E687-693.

Duffield JA, Vuocolo T, Tellam R, McFarlane JR, Kauter KG, Muhlhausler BS & McMillen IC. (2009). Intrauterine growth restriction and the sex specific programming of leptin and peroxisome proliferator-activated receptor gamma mRNA expression in visceral fat in the lamb. *Pediatric Research* **66,** 59-65.

Duffield JA, Vuocolo T, Tellam R, Yuen BA, Muhlhausler BS & McMillen IC. (2008). Placental restriction of fetal growth decreases IGF1 and leptin mRNA expression in the perirenal adipose tissue of late gestation fetal sheep. *American Journal of Physiology* **294**.

Dunford LJ, Sinclair KD, Kwong WY, Sturrock C, Clifford BL, Giles TC & Gardner DS. (2014). Maternal protein-energy malnutrition during early pregnancy in sheep impacts the fetal ornithine cycle to reduce fetal kidney microvascular development. *FASEB Journal* **28,** 4880-4892.

Duvillie B, Currie C, Chrones T, Bucchini D, Jami J, Joshi RL & Hill DJ. (2002). Increased islet cell proliferation, decreased apoptosis, and greater vascularization leading to beta-cell hyperplasia in mutant mice lacking insulin. *Endocrinology* **143,** 1530-1537.

Erenberg A, Omori K, Menkes JH, O W & Fisher DA. (1974). Growth and development of the thyroidectomized ovine fetus. *Paediatric Research* **8,** 783-789.

Farahani H, Ghasemi A, Roghani M & Zahediasl S. (2010). The effect of maternal hypothyroidism on the carbohydrate metabolism and insulin secretion of isolated islets in adult male offspring of rats. *Hormone and Metabolic Research* **42,** 792-797.

Feng J, Orlowski J & Lingrel JB. (1993). Identification of a functional thyroid hormone response element in the upstream flanking region of the human Na,K-ATPase β1 gene. *Nucleic Acids Research* **21,** 2619-2626.

Fernández E, Martín M, Fajardo S, Escrivá F & Álvarez C. (2007). Increased IRS-2 content and activation of IGF-I pathway contribute to enhance β-cell mass in fetuses from undernourished pregnant rats. *American Journal of Physiology* **292,** 187-195.

Figueroa J, Rose J, Massmann G, Zhang J & Acuña G. (2005). Alterations in fetal kidney development and elevations in arterial blood pressure in young adult sheep after clinical doses of antenatal glucocorticoids. *Pediatric Research* **58,** 510-515.

Finkelstein DI, Andrianakis P, Luff AR & Walker D. (1991). Effects of thyroidectomy on development of skeletal muscle in fetal sheep. *American Journal of Physiology* **261,** R1300-R1306.

Fisher D & Polk D. (1989). Development of the thyroid. *Baillière's Clinical Endocrinology and Metabolism* **3,** 627-657.

Forhead A, Cutts S, Matthews P & Fowden A. (2009). Role of thyroid hormones in the developmental control of tissue glycogen in fetal sheep near term. *Experimental Physiology* **94,** 1079-1087.

Forhead A & Fowden A. (2009). The hungry fetus? Role of leptin as a nutritional signal before birth. *Journal of Physiology* **587,** 1145-1152.

Forhead A & Fowden A. (2014). Thyroid hormones in fetal growth and prepartum maturation. *Journal of Endocrinology* **221,** 87-103.

Forhead A, Jellyman J, Gillham K, Ward J, Blache D & Fowden A. (2011). Renal growth retardation following angiotensin II type 1 (AT_1) receptor antagonism is associated with increased AT_2 receptor protein in fetal sheep. *Journal of Endocrinology* **208,** 137-145.

Forhead A, Li J, Gilmour R, Dauncey M & Fowden A. (2002). Thyroid hormones and the mRNA of the GH receptor and IGFs in skeletal muscle of fetal sheep. *American Journal of Physiology* **282,** E80-E86.

Forhead A, Li J, Gilmour R & Fowden A. (1998). Control of hepatic insulin-like growth factor II gene expression by thyroid hormones in fetal sheep near term. *American Journal of Physiology* **275,** E149-E156.

Forhead A, Poore K, Mapstone J & Fowden A. (2003). Developmental regulation of hepatic and renal gluconeogenic enzymes by thyroid hormones in fetal sheep during late gestation. *Journal of Physiology* **548,** 941-947.

Forhead AJ, Curtis K, Kaptein E, Visser TJ & Fowden AL. (2006). Developmental control of iodothyronine deiodinases by cortisol in the ovine fetus and placenta near term. *Endocrinology* **147,** 5988-5994.

Forhead AJ & Fowden AL. (2002). Effects of thyroid hormones on pulmonary and renal angiotensin-converting enzyme concentrations in fetal sheep near term. *Journal of Endocrinology* **173,** 143-150.

Forhead AJ, Li J, Saunders JC, Dauncey MJ, Gilmour RS & Fowden AL. (2000). Control of ovine hepatic growth hormone receptor and insulin-like growth factor I by thyroid hormones in utero. *American Journal of Physiology* **278,** E1166-1174.

Fowden A & Hill D. (2001). Intra-uterine programming of the endocrine pancreas. *British Medical Bulletin* **60,** 123-142.

Fowden A, Mapstone J & Forhead A. (2001). Regulation of glucogenesis by thyroid hormones in fetal sheep during late gestation. *Journal of Endocrinology* **170,** 461-469.

Fowden AL. (2003). The insulin-like growth factors and feto-placental growth. *Placenta* **24,** 803-812.

Fowden AL & Forhead AJ. (2009). Hormones as epigenetic signals in developmental programming. *Experimental Physiology* **94,** 607-625.

Fowden AL, Hughes P & Comline RS. (1989). The effects of insulin on the growth rate of the sheep fetus during late gestation. *Quarterly Journal of Experimental Physiology* **74,** 703-714.

Fowden AL & Silver M. (1995). The effects of thyroid hormones on oxygen and glucose metabolism in the sheep fetus during late gestation. *Journal of Physiology* **482,** 203-213.

Franko KL, Giussani DA, Forhead AJ & Fowden AL. (2007). Effects of dexamethasone on the glucogenic capacity of fetal, pregnant, and non-pregnant adult sheep. *Journal of Endocrinology* **192,** 67-73.

Fransson L, Franzén S, Rosengren V, Wolbert P, Sjöholm Å & Ortsäter H. (2013). β-Cell adaptation in a mouse model of glucocorticoid-induced metabolic syndrome. *Journal of Endocrinology* **219,** 231-241.

Furuya F, Shimura H, Yamashita S, Endo T & Kobayashi T. (2010). Liganded thyroid hormone receptor-α enhances proliferation of pancreatic β-cells. *Journal of Biological Chemistry* **285,** 24477–24486.

Féraille E, Carranza ML, Gonin S, Béguin P, Pedemonte C, Rousselot M, Caverzasio J, Geering K, Martin P-Y & Favre H. (1999). Insulin-induced stimulation of Na^+,K^+-ATPase activity in kidney proximal tubule cells depends on phosphorylation of the α-Subunit at Tyr-10. *Molecular Biology of the Cell* **10,** 2847-2859.

Garcia-Crespo D, Juste RA & Hurtado A. (2005). Selection of ovine housekeeping genes for normalisation by real-time RT-PCR; analysis of PrP gene expression and genetic susceptibility to scrapie. *BMC Veterinary Research* **1,** 1-8.

Gereben B, Zavacki A, Ribich S, Kim B, Huang S, Simonides W, Zeöld A & Bianco A. (2008). Cellular and molecular basis of deiodinase-regulated thyroid hormone signaling. *Endocrine Reviews* **29,** 898-938.

Gerich JE, Meyer C, H.J W & Stumvoll M. (2001). Renal gluconeogenesis: Its importance in human glucose homeostasis. *Diabetes Care* **24,** 382–391.

Germack R, Starzec A & Perret GY. (2000). Regulation of beta 1- and beta 3-adrenergic agonist-stimulated lipolytic response in hyperthyroid and hypothyroid rat white adipocytes. *British Journal of Pharmacology* **129,** 448-456.

Gesina E, Blondeau B, Milet A, Le Nin I, Duchene B, Czernichow P, Scharfmann R, Tronche F & Breant B. (2006). Glucocorticoid signalling affects pancreatic development through both direct and indirect effects. *Diabetologia* **49,** 2939-2947.

Gimonet V, Bussieres L, Medjebeur AA, Gasser B, Lelongt B & Laborde K. (1998). Nephrogenesis and angiotensin II receptor subtypes gene expression in the fetal lamb. *American Journal of Physiology* **274,** F1062-F1069.

Gosmain Y, Cheyssac C, Heddad Masson M, Dibner C & Philippe J. (2011). Glucagon gene expression in the endocrine pancreas: the role of the transcription factor Pax6 in alpha-cell differentiation, glucagon biosynthesis and secretion. *Diabetes, Obesity and Metabolism* **13 Suppl 1,** 31-38.

Graus-Nunes F, Dalla Corte Frantz E, Lannes WR, da Silva Menezes MC, Mandarim-de-Lacerda CA & Souza-Mello V. (2015). Pregestational maternal obesity impairs endocrine pancreas in male F1 and F2 progeny. *Nutrition* **31,** 380-387.

Green A, Rozance P & Limesand S. (2010). Consequences of a compromised intrauterine environment on islet function. *Journal of Endocrinology* **205,** 211-224.

Greenwood FC, Hunter WM & Glover JS. (1963). The preparation of 131I-labelled human growth hormone of high specific radioactivity. *The Biochemical Journal* **89,** 114-123.

Guerra C, Roncero C, Porras A, Fernández M & Benito M. (1996). Triiodothyronine induces the transcription of the uncoupling protein gene and stabilizes its mRNA in fetal rat brown adipocyte primary cultures. *Journal of Biological Chemistry* **271,** 2076-2081.

Gundersen H, Jensen E & Kieu K. (1999). The efficiency of systematic sampling in stereology—reconsidered. *Journal of Microscopy* **193,** 199-211.

Gundersen HJ & Jensen EB. (1987). The efficiency of systematic sampling in stereology and its prediction. *Journal of Microscopy* **147,** 229-263.

Gupta RK, Arany Z, Seale P, Mepani RJ, Ye L, Conroe HM, Roby YA, Kulaga H, Reed RR & Spiegelman BM. (2010). Transcriptional control of preadipocyte determination by Zfp423. *Nature* **464,** 619-623.

Guron G & Friberg P. (2000). An intact renin-angiotensin system is a prerequisite for normal renal development. *Journal of Hypertension* **18,** 123-137.

Hales CN & Barker DJ. (2001). The thrifty phenotype hypothesis. *British Medical Bulletin* **60,** 5-20.

Hall JA, Ribich S, Christoffolete MA, Simovic G, Correa-Medina M, Patti ME & Bianco AC. (2010). Absence of thyroid hormone activation during development underlies a permanent defect in adaptive thermogenesis. *Endocrinology* **151,** 4573-4582.

Hang Y, Yamamoto T, Benninger RK, Brissova M, Guo M, Bush W, Piston DW, Powers AC, Magnuson M, Thurmond DC & Stein R. (2014). The MafA transcription factor becomes essential to islet beta-cells soon after birth. *Diabetes* **63,** 1994-2005.

Hara K, Maruki Y, Long X, Yoshino K, Oshiro N, Hidayat S, Tokunaga C, Avruch J & Yonezawa K. (2002). Raptor, a binding partner of target of rapamycin (TOR), mediates TOR action. *Cell* **110,** 177-189.

Harms M & Seale P. (2013). Brown and beige fat: development, function and therapeutic potential. *Nature Medicine* **19,** 1252-1263.

Heddad Masson M, Poisson C, Guerardel A, Mamin A, Philippe J & Gosmain Y. (2014). Foxa1 and Foxa2 regulate alpha-cell differentiation, glucagon biosynthesis, and secretion. *Endocrinology* **155,** 3781-3792.

Hernandez A & Obregon MJ. (1996). Presence and mRNA expression of T3 receptors in differentiating rat brown adipocytes. *Molecular Cell Endocrinology* **121,** 37-46.

Heron-Milhavet L, Franckhauser C, Rana V, Berthenet C, Fisher D, Hemmings BA, Fernandez A & Lamb NJ. (2006). Only Akt1 is required for proliferation, while Akt2 promotes cell cycle exit through p21 binding. *Molecular and Cellular Biology* **26,** 8267-8280.

Hers I, Vincent EE & Tavare JM. (2011). Akt signalling in health and disease. *Cellular Signalling* **23,** 1515-1527.

Hickey M, Hart R & Keelan JA. (2014). The relationship between umbilical cord estrogens and perinatal characteristics. *Cancer Epidemiology, Biomarkers and Prevention* **23,** 946-952.

Hill DJ & Milner RD. (1985). Insulin as a growth factor. *Pediatric Research* **19,** 879-886.

Hill DJ, Strutt B, Arany E, Zaina S, Coukell S & Graham CF. (2000). Increased and persistent circulating insulin-like growth factor II in neonatal transgenic mice suppresses developmental apoptosis in the pancreatic islets. *Endocrinology* **141,** 1151-1157.

Hillman N, Kallapur S & Jobe A. (2012). Physiology of transition from intrauterine to extrauterine life. *Clinics in Perinatology* **39,** 769-783.

Hiroi Y, Kim HH, Ying H, Furuya F, Huang Z, Simoncini T, Noma K, Ueki K, Nguyen NH, Scanlan TS, Moskowitz MA, Cheng SY & Liao JK. (2006). Rapid nongenomic actions of thyroid hormone. *PNAS* **103,** 14104-14109.

Hogg J, Han V, Clemmons D & Hill DJ. (1993). Interactions of nutrients, insulin-like growth factors (IGFs) and IGF-binding proteins in the regulation of DNA synthesis by isolated fetal rat islets of Langerhans. *Journal of Endocrinology* **138,** 401-412.

Holemans K, Aerts L & Van Assche F. (2003). Lifetime consequences of abnormal fetal pancreatic development. *Journal of Physiology* **547,** 11-20.

Holleran S & Ramakrishnan R. (2003). Power Analysis. In *http://wwwbiomathinfo/*, 3 edn. Division of Biomathematics/Biostatistics, Columbia University Medical Centre.

Holsberger DR, Jirawatnotai S, Kiyokawa H & Cooke PS. (2003). Thyroid hormone regulates the cell cycle inhibitor p27Kip1 in postnatal murine Sertoli cells. *Endocrinology* **144,** 3732-3738.

Hopkins PS & Thorburn GD. (1972). The effects of foetal thyroidectomy on the development of the ovine foetus. *Journal of Endocrinology* **54,** 55-66.

Horowitz B, Hensleyg CB, Quintero M, Azuman KK, Putnam D & Alicia A. McDonough AA. (1990). Differential regulation of Na,K-ATPase alpha1, alpha2 and beta subunit mRNA and protein levels by thyroid hormone. *Journal of Biological Chemistry* **24,** 1430-14314.

Howard CV & Reed MG. (2010). *Unbiased Stereology*. QTP Publications, Liverpool, UK.

Huang K & Fingar DC. (2014). Growing knowledge of the mTOR signaling network. *Seminars in Cell and Developmental Biology* **36,** 79-90.

Hume R, Barker EV & Coughtrie MW. (1996). Differential expression and immunohistochemical localisation of the phenol and hydroxysteroid sulphotransferase enzyme families in the developing lung. *Histochemistry and Cell Biololgy* **105,** 147-152.

Hume R & Coughtrie MW. (1994). Phenolsulphotransferase: localization in kidney during human embryonic and fetal development. *Histochemical Journal* **26,** 850-855.

Iglesias P, Bayon C, Mendez J, Gonzalez Gancedo P, Grande C & Diez JJ. (2001). Serum insulin-like growth factor type 1, insulin-like growth factor-binding protein-1, and insulin-like growth factor-binding protein-3 concentrations in patients with thyroid dysfunction. *Thyroid* **11,** 1043-1048.

Islam M, Morton N, Hansson A & Emilsson V. (1997). Rat insulinoma-derived pancreatic β-cells express a functional leptin receptor that mediates a proliferative response. *Biochemical and Biophysical Research Communications* **238,** 851-855.

Islam M, Sjöholm A & Emilsson V. (2000). Fetal pancreatic islets express functional leptin receptors and leptin stimulates proliferation of fetal islet cells. *International Journal of Obesity* **24,** 1246-1253.

Iwamoto HS, Murray MA & Chernausek SD. (1992). Effects of acute hypoxemia on insulin-like growth factors and their binding proteins in fetal sheep. *American Journal of Physiology* **263,** E1151-1156.

Jennings RE, Berry AA, Strutt JP, Gerrard DT & Hanley NA. (2015). Human pancreas development. *Development* **142,** 3126-3137.

Johnson EO, Calogero AE, Konstandi M, Kamilaris TC, La Vignera S & Chrousos GP. (2012). Effects of short- and long-duration hypothyroidism on hypothalamic-pituitary-adrenal axis function in rats: in vitro and in situ studies. *Endocrine* **42,** 684-693.

Johnson K, Marden C, Ward-Bailey P, Gagnon L, Bronson R & Donahue L. (2007). Congenital hypothyroidism, dwarfism, and hearing impairment caused by a missense mutation in the mouse dual oxidase 2 gene, Duox2. *Molecular Endocrinology* **21,** 1593-1602.

Johnson PR, Stern JS, Greenwood MR & Hirsch J. (1978). Adipose tissue hyperplasia and hyperinsulinemia on Zucker obese female rats: a developmental study. *Metabolism* **27,** 1941-1954.

Jones CT, Lafeber HN & Roebuck MM. (1984). Studies on the growth of the fetal guinea pig. Changes in plasma hormone concentration during normal and abnormal growth. *Journal of Developmental Physiology* **6,** 461-472.

Kamana KC, Shakya S & Zhang H. (2015). Gestational diabetes mellitus and macrosomia: a literature review. *Annals of Nutrition and Metabolism* **66,** 14-20.

Kaplan S, Odacı E, Canan S & Onger ME. (2012). The dissector counting technique. *NeuroQuantology* **10,** 44-53.

Kapoor A, Dunn E, Kostaki A, Andrews MH & Matthews SG. (2006). Fetal programming of hypothalamo-pituitary-adrenal function: prenatal stress and glucocorticoids. *Journal of Physiology* **572,** 31-44.

Karbalaei N, Ghasemi A, Hedayati M, Godini A & Zahediasl S. (2014). The possible mechanisms by which maternal hypothyroidism impairs insulin secretion in adult male offspring in rats. *Experimental Physiology* **99,** 701-714.

Karvonen MJ. (1954). The diameter of foetal sheep erythrocytes. *Acta Anatomica* **20,** 53-61.

Kassem SA, Ariel I, Thornton PS, Scheimberg I & Glaser B. (2000). Beta-cell proliferation and apoptosis in the developing normal human pancreas and in hyperinsulinism of infancy. *Diabetes* **49,** 1325-1333.

Kawai M & Rosen C. (2010). The IGF-I regulatory system and its impact on skeletal and energy homeostasis. *Journal of Cellular Biochemistry* **111,** 14-19.

Keller-Wood M, von Reitzenstein M & McCartney J. (2008). Is the fetal lung a mineralcorticoid receptor target organ? Induction of cortisol-regulated genes in the ovine fetal lung, kidney and small intestine. *Neonatology* **95,** 47-60.

Kershaw EE & Flier JS. (2004). Adipose tissue as an endocrine organ. *Journal of Clinical Endocrinology and Metabolism* **89,** 2548-2556.

Kersten S. (2001). Mechanisms of nutritional and hormonal regulation of lipogenesis. *EMBO reports* **2,** 282-286.

Kester MH, Kaptein E, Van Dijk CH, Roest TJ, Tibboel D, Coughtrie MW & Visser TJ. (2002). Characterization of iodothyronine sulfatase activities in human and rat liver and placenta. *Endocrinology* **143,** 814-819.

Kido Y, Nakae J, Hribal ML, Xuan S, Efstratiadis A & Accili D. (2002). Effects of mutations in the insulin-like growth factor signaling system on embryonic pancreas development and beta-cell compensation to insulin resistance. *Journal of Biological Chemistry* **227,** 36740 –36747.

Kieffer TJ, Heller RS & Habener JF. (1996). Leptin receptors expressed on pancreatic β-cells. *Biochemical and Biophysical Research Communications* **224,** 522-527.

Kilby MD, Verhaeg J, Gittoes N, Somerset DA, Clark PMS & Franklyn JA. (1998). Circulating thyroid hormone concentrations and placental thyroid hormone receptor expression in normal human pregnancy and pregnancy complicated by intrauterine growth restriction (IUGR). *Journal of Clinical Endocrinology & Metabolism* **83,** 2964-2973.

Knapczyk K, Duda M, Szafranska B, Wolsza K, Panasiewicz G, Koziorowski M & Slomczynska M. (2008). Immunolocalisation of oestrogen receptors alpha (ERα) and beta (ERβ) in porcine embryos and fetuses at different stages of gestation. *Acta Veterinaria Hungarica* **56,** 221-233.

Kobori H, Hayashi M & Saruta T. (2001). Thyroid hormone stimulates renin gene expression through the thyroid hormone response element. *Hypertension* **37,** 99-104.

Kulkarni R. (2004). The islet β-cell. *International Journal of Biochemistry & Cell Biology* **36,** 365–371.

Kulkarni R, Brüning J, Winnay J, Postic C, Magnuson M & Kahn CR. (1999). Tissue-specific knockout of the insulin receptor in pancreatic β cells creates an insulin secretory defect similar to that in type 2 diabetes. *Cell* **96,** 329–339.

Kulkarni R, Holzenberger M, Shih D, Ozcan U, Stoffel M, Magnuson M & Kahn C. (2002). beta-cell-specific deletion of the Igf1 receptor leads to hyperinsulinemia and glucose intolerance but does not alter beta-cell mass. *Nature Genetics* **31,** 111-115.

Kulkarni R, Wang Z, Wang R, Hurley J, Smith D, Ghatei M, Withers D, Gardiner J, Bailey C & Bloom S. (1997). Leptin rapidly suppresses insulin release from insulinoma cells, rat and human islets and, in vivo, in mice. *Journal of Clinical Investigation* **100,** 2729-2736.

LaFranchi S. (2011). Approach to the diagnosis and treatment of neonatal hypothyroidism. *Journal of Clinical Endocrinology and Metabolism* **96,** 2959-2967.

Lai K-MV, Gonzalez M, Poueymirou W, Kline W, Na E, Zlotchenko E, Stitt T, Economides A, Yancopoulos G & Glass D. (2004). Conditional activation of akt in adult skeletal muscle induces rapid hypertrophy. *Molecular and Cellular Biology* **24,** 9295-9304.

Langley SC & Jackson AA. (1994). Increased systolic blood pressure in adult rats induced by fetal exposure to maternal low protein diets. *Clinical Science* **86,** 217-222.

Lanham S, Fowden A, Roberts C, Cooper C, Oreffo R & Forhead A. (2011). Effects of hypothyroidism on the structure and mechanical properties of bone in the ovine fetus. *Journal of Endocrinology* **210,** 189-198.

Latimer AM, Hausman GJ, McCusker RH & Buonomo FC. (1993). The effects of thyroxine on serum and tissue concentrations of insulin-like growth factors (IGF-I and -II) and IGF-binding proteins in the fetal pig. *Endocrinology* **133,** 1312-1319.

Lee JW, Kim NH & Milanesi A. (2014). Thyroid Hormone Signaling in Muscle Development, Repair and Metabolism. *Journal of Endocrinology, Diabetes and Obesity* **2,** 1046.

Lemmen JG, van den Brink C, Legler J, van der Saag PT & van der Burg B. (2002). Detection of oestrogenic activity of steroids present during mammalian gestation using oestrogen receptor alpha- and oestrogen receptor beta-specific in vitro assays. *Journal of Endocrinology* **174,** 435-446.

Leonardini A, Laviola L, Perrini S, Natalicchio A & Giorgino F. (2009). Cross-Talk between PPARgamma and Insulin Signaling and Modulation of Insulin Sensitivity. *PPAR Research* **2009,** 818945.

Limesand S, Jensen J, Hutton J & Hay W. (2005). Diminished beta-cell replication contributes to reduced beta-cell mass in fetal sheep with intrauterine growth restriction. *American Journal of Physiology* **288,** R1297–R1305.

Limesand SW, Rozance PJ, Zerbe GO, Hutton JC & Hay WW. (2006). Attenuated insulin release and storage in fetal sheep pancreatic islets with intrauterine growth restriction. *Endocrinology* **147,** 1488-1497.

Lin H-Y, Sun M, Tang H-Y, Lin C, Luidens MK, Mousa SA, Incerpi S, Drusano GL, Davis FB & Davis PJ. (2009). l-Thyroxine vs. 3,5,3'-triiodo-l-thyronine and cell proliferation: activation of mitogen-activated protein kinase and phosphatidylinositol 3-kinase. *American Journal of Physiology* **296,** C980-C991.

Lisboa PC, Conceicao EP, de Oliveira E & Moura EG. (2015). Postnatal overnutrition programs the thyroid hormone metabolism and function in adulthood. *Journal of Endocrinology* **226,** 219-226.

Liu J, Chen K, Valego NK, Carey LC & Rose JC. (2005). Ontogeny and effects of thyroid hormone on beta1-adrenergic receptor mRNA expression in ovine fetal kidney cortex. *Journal of the Society of Gynecologic Investigation* **12,** 563-569.

Liu P, Gan W, Inuzuka H, Lazorchak AS, Gao D, Arojo O, Liu D, Wan L, Zhai B, Yu Y, Yuan M, Kim BM, Shaik S, Menon S, Gygi SP, Lee TH, Asara JM, Manning BD, Blenis J, Su B & Wei W. (2013). Sin1 phosphorylation impairs mTORC2 complex integrity and inhibits downstream Akt signalling to suppress tumorigenesis. *Nature Cell Biology* **15,** 1340-1350.

Liu YY, Schultz JJ & Brent GA. (2003). A thyroid hormone receptor alpha gene mutation (P398H) is associated with visceral adiposity and impaired catecholamine-stimulated lipolysis in mice. *Journal of Biological Chemistry* **278,** 38913-38920.

Liu ZZ, Kumar A, Ota k, Wallner EI & Kanwar YS. (1997). Developmental regulation and the role of insulin and insulin receptor in metanephrogenesis. *PNAS* **94,** 6758-6769.

Lok F, Owens JA, Mundy L, Robinson JS & Owens PC. (1996). Insulin-like growth factor I promotes growth selectively in fetal sheep in late gestation *American Journal of Physiology* **270,** 1148-1154.

Lord APD, Martin AA, Walton PE, Ballard FJ & Read LC. (1991). Insulin-like growth factor-binding proteins in tissue fluids from the lamb. *Journal of Endocrinology* **129,** 59-68.

Loubière LS, Vasilopoulou E, Bulmer JN, Taylor PM, Stieger B, Verrey F, McCabe CJ, Franklyn JA, Kilby MD & Chan SY. (2010). Expression of thyroid hormone transporters in the human placenta and changes associated with intrauterine growth restriction. *Placenta* **31,** 295-304.

López-Espíndola D, Morales-Bastos C, Grijota-Martínez C, Liao X, Lev D, Sugo E, Verge C, Refetoff S, Bernal J & Guadaño-Ferraz A. (2014). Mutations of the thyroid hormone transporter MCT8 cause prenatal brain damage and persistent hypomyelination. *Journal of Clinical Endocrinology & Metabolism* **99,** E2799-E2804.

MacLaughlin SM, Walker SK, Kleeman DO, Tosh DN & McMillen IC. (2010). Periconceptional undernutrition and being a twin each alter kidney development in the sheep fetus during early gestation. *American Journal of Physiology* **298,** R692-R699.

Manning BD & Cantley LC. (2007). Akt/PKB signalling: Navigating downstream. *Cell* **129,** 1261-1274.

Manning J, Beutler K, Knepper MA & Vehaskari VM. (2002). Upregulation of renal BSC1 and TSC in prenatally programmed hypertension. *American Journal of Physiology* **283,** F202-206.

Manning J & Vehaskari VM. (2001). Low birth weight-associated adult hypertension in the rat. *Pediatric Nephrology* **16,** 417-422.

Marsh AC, Gibson KJ, Wu J & Owens PC. (2001). Chronic effect of insulin-like growth factor I on renin synthesis, secretion, and renal function in fetal sheep. *American Journal of Physiology* **281,** R318-R326.

Massaro D & Massaro GD. (2002). Invited Review: Pulmonary alveoli: formation, the “call for oxygen,” and other regulators. *American Journal of Physiology* **282,** L345-358.

Mastracci TL & Evans-Molina C. (2014). Pancreatic and islet development and function: The role of thyroid hormone. *Journal of Endocrinology, Diabetes and Obesity* **2,** 1044-1051.

Mathews MB, Bernstein RM, Franza Jr BR & Garrels JI. (1984). Identity of the proliferating cell nuclear antigen and cyclin. *Nature* **309,** 374-376.

McCurdy C & Klemm D. (2013). Adipose tissue insulin sensitivity and macrophage recruitment: Does PI3K pick the pathway? *Adipocyte* **2,** 135-142.

McDonough AA, Brown TA, Horowitz B, Chiu R, Schlotterbeck J, Bowen J & Schmitt CA. (1988). Thyroid hormone coordinately regulates Na+-K+-ATPase alpha- and beta-subunit mRNA levels in kidney. *American Journal of Physiology* **254,** C323-C329.

Medina M, Foseca T, Molina J, Fachado A, Castillo M, Dong L, Soares R, Hernández A, Caicedo A & Bianco AC. (2014). Maternal inheritance of an inactive type III Deiodinase gene allele affects mouse pancreatic β-cells and disrupts glucose homeostasis. *Endocrinology* **155**.

Medina M, Molina J, Gadea Y, Fachado A, Murillo M, Simovic G, Pileggi A, Hernández A, Edlund H & Bianco A. (2011). The thyroid hormone-inactivating type III deiodinase is expressed in mouse and human beta-cells and its targeted inactivation impairs insulin secretion. *Endocrinology* **152,** 3717-3727.

Mesiano S, Young IR, Baxter RC, Hintz RL, Browne CA & Thorburn GD. (1987). Effect of hypophysectomy with and without thyroxine replacement on growth and circulating concentrations of insulin-like growth factors I and II in the fetal lamb. *Endocrinology* **120,** 1821-1830.

Meyer C, Dostou J, Nadkarni V & Gerich J. (1998). Effects of physiological hyperinsulinemia on systemic, renal, and hepatic substrate metabolism. *American Journal of Physiology* **44,** F915–F921.

Meyer MM, Levin K, Grimmsmann T, Perwitz N, Eirich A, Beck-Nielsen H & Klein HH. (2002). Troglitazone treatment increases protein kinase B phosphorylation in skeletal muscle of normoglycemic subjects at risk for the development of type 2 diabetes. *Diabetes* **51,** 2691-2697.

Miell JP, Taylor AM, Zini M, Maheshwari HG, Ross RJ & Valcavi R. (1993). Effects of hypothyroidism and hyperthyroidism on insulin-like growth factors (IGFs) and growth hormone- and IGF-binding proteins. *Journal of Clinical Endocrinology & Metabolism* **76,** 950-955.

Miki Y, Nakata T, Suzuki T, Darnel AD, Moriya T, Kaneko C, Hidaka K, Shiotsu Y, Kusaka H & Sasano H. (2002). Systemic distribution of steroid sulfatase and estrogen sulfotransferase in human adult and fetal tissues. *Journal of Clinical Endocrinology & Metabolism* **87,** 5760–5768.

Mitchell EKL, Louey A, Cock ML, Harding R & Black MJ. (2004). Nephron endowment and filtration surface area in the kidney after growth restriction of fetal sheep. *Pediatric Research* **55,** 769-773.

Morioka T, Asilmaz E, Hu J, Dishinger J, Kurpad A, Elias C, Li H, Elmquist J, Kennedy R & Kulkarni R. (2007). Disruption of leptin receptor expression in the pancreas directly affects beta cell growth and function in mice. *Journal of Clinical Investigation* **117,** 2860-2868.

Moritz KM, De Matteo R, Dodic M, Jefferies AJ, Arena D, Wintour EM, Probyn ME, Bertram JF, Singh RR, Zanini S & Evans RG. (2011). Prenatal glucocorticoid exposure in the sheep alters renal development in utero: implications for adult renal function and blood pressure control. *American Journal of Physiology* **301,** R500-509.

Morreale de Escobar G, Calvo R, Obregon MJ & Escobar Del Rey F. (1990). Contribution of maternal thyroxine to fetal thyroxine pools in normal rats near term. *Endocrinology* **126,** 2765-2767.

Mostyn A, Pearce S, Budge H & Elmes M. (2003). Influence of cortisol on adipose tissue development in the fetal sheep during late gestation. *Journal of Endocrinology* **176,** 23-30.

Mulder J, Haddad MN, Vernon K, Baum M & Quigley R. (2003). Hypothyroidism increases osmotic water permeability (Pf) in the developing renal brush border membrane. *Pediatric Research* **53,** 1001-1007.

Mullur R, Liu Y-Y & Brent G. (2014). Thyroid hormone regulation of metabolism. *Physiological Reviews* **94,** 355-382.

Mühlhäusler B, Duffield JA & McMillen IC. (2007). Increased maternal nutrition stimulates peroxisome proliferator activated receptor-gamma, adiponectin, and leptin messenger ribonucleic acid expression in adipose tissue before birth. *Endocrinology* **148,** 878-885.

Mühlhäusler BS, Roberts C & McFarlane J. (2002). Fetal leptin is a signal of fat mass independent of maternal nutrition in ewes fed at or above maintenance energy requirements. *Biology of Reproduction* **67,** 493-499.

Mühlhäusler BS, Roberts C, Yuen B, Marrocco E, Budge H, Symonds M, McFarlane J, Kauter K, Stagg P, Pearse J & McMillen I. (2003). Determinants of fetal leptin synthesis, fat mass, and circulating leptin concentrations in well-nourished ewes in late pregnancy. *Endocrinology* **144,** 4947-4954.

Müller J, Mayerl S, Visser TJ, Darras VM, Boelen A, Frappart L, Mariotta L, Verrey F & Heuer H. (2014). Tissue-specific alterations in thyroid hormone homeostasis in combined Mct10 and Mct8 deficiency. *Endocrinology* **155,** 315-325

Nedergaard J, Golozoubova V, Matthias A, Asadi A, A. J & Cannon B. (2001). UCP1: the only protein able to mediate adaptive non-shivering thermogenesis and metabolic inefficiency. *Biochimica et Biophysica Acta* **1504,** 82-106.

Noorafshan A. (2014). Stereology as a valuable tool in the toolbox of testicular research. *Annals of Anatomy* **196,** 57-66.

O'Connor D, Blache D, Hoggard N, Brookes E, Wooding F, Fowden A & Forhead A. (2007). Developmental control of plasma leptin and adipose leptin messenger ribonucleic acid in the ovine fetus during late gestation: role of glucocorticoids and thyroid hormones. *Endocrinology* **148,** 3750-3757.

Offield MF, Jetton TL, Labosky PA, Ray M, Stein RW, Magnuson MA, Hogan BL & Wright CV. (1996). PDX-1 is required for pancreatic outgrowth and differentiation of the rostral duodenum. *Development* **122,** 983-995.

Otani K, Kulkarni RN, Baldwin AC, Krutzfeldt J, Ueki K, Stoffel M, Kahn CR & Polonsky KS. (2004). Reduced beta-cell mass and altered glucose sensing impair insulin-secretory function in betaIRKO mice. *American Journal of Physiology* **286,** E41-49.

Otonkoski T, Andersoon S, Knip M & Simell O. (1988). Maturation of insulin response to glucose during human fetal and neonatal development. *Diabetes* **37,** 286-291.

Pan FC & Wright C. (2011). Pancreas organogenesis: from bud to plexus to gland. *Developmental Dynamics* **240,** 530-565.

Parker CR, Falany CN, Stockard CR, Stankovic AK & Grizzle WE. (1994). Immunohistochemical localization of dehydroepiandrosterone sulfotransferase in human fetal tissues. *Journal of Clinical Endocrinology & Metabolism* **78,** 234-236.

Pende M, Kozma SC, Jaquet M, Oorschot V, Burcelin R, Le Marchand-Brustel Y, Klumperman J, Thorens B & Thomas G. (2000). Hypoinsulinaemia, glucose intolerance and diminished β-cell size in S6K1-deficient mice. *Nature* **408,** 994-997.

Peng XD, Xu PZ, Chen ML, Hahn-Windgassen A, Skeen J, Jacobs J, Sundararajan D, Chen WS, Crawford SE, Coleman KG & Hay N. (2003). Dwarfism, impaired skin development, skeletal muscle atrophy, delayed bone development, and impeded adipogenesis in mice lacking Akt1 and Akt2. *Genes and Development* **17,** 1352-1365.

Perez-Castillo A, Bernal J, Ferreiro B & Pans T. (1985). The early ontogenesis of thyroid hormone receptor in the rat fetus. *Endocrinology* **117,** 2457-2461.

Petrik J, Pell JM, Arany E, McDonald TJ, Dean WL, Reik W & Hill DJ. (1999). Overexpression of insulin-like growth factor-II in transgenic mice is associated with pancreatic islet cell hyperplasia. *Endocrinolgy* **140,** 2353-2363.

Poissonnet CM, Burdi AR & Bookstein FL. (1983). Growth and development of human adipose tissue during early gestation. *Early Human Deveopment* **8,** 1-11.

Polk DH. (1995). Thyroid hormone metabolism during development. *Reproduction, Fertility and Development* **7,** 469-477.

Polk DH, Callegari CC, Newnham J, Padbury JF, Reviczky A, Fisher DA & Klein AH. (1987). Effect of fetal thyroidectomy on newborn thermogenesis in lambs. *Pediatric Research* **21,** 453-457.

Polk DH, Cheromcha D, Reviczky A & Fisher D. (1989). Nuclear thyroid hormone receptors: ontogeny and thyroid hormone effects in sheep. *American Journal of Physiology* **256,** E543-E549.

Polk DH, Reviczky A & Wu SY. (1994). Metabolism of sulfoconjugated thyroid hormone derivatives in developing sheep. *American Journal of Physiology* **266,** E892-896.

Polk DH, Wu SY, Wright C, Reviczky AL & Fisher DA. (1988). Ontogeny of thyroid hormone effect on tissue 5'-monodeiodinase activity in fetal sheep. *American Journal of Physiology* **254,** E337-341.

Pope M, Budge H & Symonds ME. (2014). The developmental transition of ovine adipose tissue through early life. *Acta Physiologica* **21,** 20-30.

Prado CL, Pugh-Bernard AE, Elghazi L, Sosa-Pineda B & Sussel L. (2004). Ghrelin cells replace insulin-producing beta cells in two mouse models of pancreas development. *PNAS* **101,** 2924-2929.

Rabelo R, Schifman A, Rubio A, Sheng X & Silva JE. (1995). Delineation of thyroid hormone-responsive sequences within a critical enhancer in the rat uncoupling protein gene. *Endocrinology* **136,** 1003-1013.

Rachdi L, Balcazar N, Osorio-Duque F, Elghazi L, Weiss A, Gould A, Chang-Chen KJ, Gambello MJ & Bernal-Mizrachi E. (2008). Disruption of Tsc2 in pancreatic cells induces cell mass expansion and improved glucose tolerance in a TORC1-dependent manner. *PNAS* **105,** 9250-9255.

Ramos S, Goya L, Alvarez C, Martín M, Agote M, Escrivá F & Pascual-Leone A. (2001). Different role of insulin in GLUT-1 and -4 regulation in heart and skeletal muscle during perinatal hypothyroidism. *American Journal of Physiology* **281,** 1073-1081.

Ramos S, Goya L, Alvarez C & Pascual-Leone AM. (1998). Mechanism of hypothyroidism action on insulin-like growth factor-I and II from a neonatal to adult rats: Insulin mediates thyroid hormone effects in the neonatal period. *Endocrinology* **139,** 4782-4792.

Reddy RC, Estill CT, Meaker M, Stormshak F & Roselli CE. (2014). Sex differences in expression of oestrogen receptor alpha but not androgen receptor mRNAs in the foetal lamb brain. *Journal of Neuroendocrinology* **26,** 321-328.

Reddy S, Bibby N & Elliott R. (1988). An immunofluorescent study of insulin-, glucagon-, pancreatic polypeptide- and somatostatin-containing cells in the early ovine fetal pancreas. *Quarterly Journal of Experimental Physiology* **73,** 225-232.

Reddy S & Elliott RB. (1988). Ontogenic development of peptide hormones in the mammalian fetal pancreas. *Experientia* **44,** 1-9.

Reusens-Billen B, Remacle C, Daniline J & Hoet JJ. (1984). Cell proliferation in pancreatic islets of rat fetuses and neonates from normal and diabetic mothers. An in vitro and in vivo study. *Hormone and Metabolic Research* **16,** 565-571.

Rhodes C & White M. (2002). Molecular insights into insulin action and secretion. *European Journal of Clinical Investigation* **32,** 3-13.

Richard K, Hume R, Kaptein E, E.L. S, Visser TJ & Coughtrie MWH. (2001). Sulfation of thyroid hormone and dopamine during human development: Ontogeny of phenol sulfotransferases and arylsulfatase in liver, lung, and brain. *Journal of Clinical Endocrinology & Metabolism* **86,** 2734-2742.

Rieusset J, Andreelli F, Auboeuf D, Roques M, Vallier P, Riou JP, Auwerx J, Laville M & Vidal H. (1999). Insulin acutely regulates the expression of the peroxisome proliferator-activated receptor-gamma in human adipocytes. *Diabetes* **48,** 699-705.

Rodríguez-Gómez I, Banegas I, Wangensteen R, Quesada A, Jiménez R, Gómez-Morales M, O'Valle F, Duarte J & Vargas F. (2013). Influence of thyroid state on cardiac and renal capillary density and glomerular morphology in rats. *Journal of Endocrinology* **216,** 43-51.

Romero-Calvo I, Borja Ocón B, Martínez-Moya P, Suárez MD, Zarzuelo A, Martínez-Augustin O & Sánchez de Medina F. (2010). Reversible Ponceau staining as a loading control alternative to actin in Western blots. *Analytical Biochemistry* **401,** 318-320.

Rosen ED, Sarraf P, Troy AE, Bradwin G, Moore K, Milstone DS, Spiegelman BM & Mortensen RM. (1999). PPAR gamma is required for the differentiation of adipose tissue in vivo and in vitro. *Molecular Cell* **4,** 611-617.

Rosner B & Rosner R. (2010). Fundamentals of Biostatistics. 7th edn. Cengage Learning, Boston, USA.

Rozance PJ, Limesand SW & Hay Jr WW. (2006). Decreased nutrient-stimulated insulin secretion in chronically hypoglycemic late-gestation fetal sheep is due to an intrinsic islet defect. *American Journal of Physiology* **291,** E404-E411.

Rytter D, Andersen SL, Bech BH, Halldorsson TI, Henriksen TB, Laurberg P & Olsen SF. (2016). Maternal thyroid function in pregnancy may program offspring blood pressure, but not adiposity at 20y of age. *Pediatric Research* **80,** 7-13.

Salisbury RJ, Blaylock J, Berry AA, Jennings RE, De Krijger R, Piper Hanley K & Hanley NA. (2014). The window period of NEUROGENIN3 during human gestation. *Islets* **6,** e9544361-e9544365.

Saltiel A & Kahn C. (2001). Insulin signalling and the regulation of glucose and lipid metabolism. *Nature* **414,** 799-806.

Saltó C, Kindblom J, Johansson C, Wang Z, Gullberg H, Nordström K, Mansén A, Ohlsson C, Thorén P, Forrest D & Vennström B. (2001). Ablation of TRalpha2 and a concomitant overexpression of alpha1 yields a mixed hypo- and hyperthyroid phenotype in mice. *Molecular Endocrinology* **15,** 2115-2128.

Sarjeant K & Stephens JM. (2012). Adipogenesis. In *Cold Spring Harbour Perspectives in Biology*, pp. 008417.

Sarr O, Yang K & Regnault TRH. (2012). In utero programming of later adiposity: the role of fetal growth restriction. *Journal of Pregnancy* **2012,** 134758.

Schmittgen TD & Livak KJ. (2008). Analyzing real-time PCR data by the comparative C(T) method. *Nature Protocols* **3,** 1101-1108.

Seale P, Bjork B, Yang W, Kajimura S, Chin S, Kuang S, Scime A, Devarakonda S, Conroe HM, Erdjument-Bromage H, Tempst P, Rudnicki MA, Beier DR & Spiegelman BM. (2008). PRDM16 controls a brown fat/skeletal muscle switch. *Nature* **454,** 961-967.

Segar JL, Volk KA, Lipman MHB & Scholz TD. (2012). Thyroid hormone is required for growth adaptation to pressure load in the ovine fetal heart. *Experimental Physiology* **98,** 722-733.

Senese R, Cioffi F, De Lange P, Goglia F & Lanni A. (2014). Thyroid: biological actions of 'non-classical' thyroid hormones. *Journal of Endocrinology* **112,** 1-12.

Sferruzzi-Perri AN, Vaughan OR, Forhead AJ & Fowden AL. (2013). Hormonal and nutritional drivers of intrauterine growth. *Current Opinion in Clinical Nutrition and Metabolic Care* **16,** 298-309.

Sharma PK & Thakur MK. (2004). Estrogen receptor α expression in mice kidney shows sex differences during aging. *Biogerontology* **5,** 375-381.

Shepherd PR, Gnudi L, Tozzo E, Yang H, Leach F & Kahn BB. (1993). Adipose cell hyperplasia and enhanced glucose disposal in transgenic mice overexpressing GLUT4 selectively in adipose tissue. *Journal of Biological Chemistry* **268,** 22243-22246.

Shibutani M, Woo G-H, Fujimoto H, Saegusa Y, Takahashi M, Inoue K, Hirose M & Nishikawa A. (2009). Assessment of developmental effects of hypothyroidism in rats from in utero and lactation exposure to anti-thyroid agents. *Reproductive Toxicology* **28,** 297-307.

Shields BM, Knight BA, Hill A, Hattersley AT & Vaidya B. (2011). Fetal thyroid hormone level at birth is associated with fetal growth. *Journal of Clinical Endocrinology & Metabolism* **96,** E934–E938.

Song J, Hu X, Riazi S, Tiwari S, Wade JB & Ecelbarger CA. (2006). Regulation of blood pressure, the epithelial sodium channel (ENaC), and other key renal sodium transporters by chronic insulin infusion in rats. *American Journal of Physiology* **290,** F1055-F1064.

Stanley EL, Hume R & Coughtrie MWH. (2005). Expression profiling of human fetal cytosolic sulfotransferases involved in steroid and thyroid hormone metabolism and in detoxification. *Molecular and Cellular Endocrinology* **240,** 32-42.

Stephens E, Thureen PJ, Goalstone ML, Anderson MS, Leitner JW, Hay WW & Draznin B. (2001). Fetal hyperinsulinemia increases farnesylation of p21 Ras in fetal tissues. *American Journal of Physiology* **281,** E217-E223.

Stephens JM. (2012). The fat controller: adipocyte development. *PLoS Biology* **10,** e1001436.

Stevens D, Alexander G & Bell AW. (1990). Effect of prolonged glucose infusion into fetal sheep on body growth, fat deposition and gestation length. *Journal of Developmental Physiology* **13,** 277-281.

Symonds M, Mostyn A, Pearce S, Budge H & Stephenson T. (2003). Endocrine and nutritional regulation of fetal adipose tissue development. *Journal of Endocrinology* **179,** 293-299.

Symonds M, Pope M, Sharkey D & Budge H. (2012). Adipose tissue and fetal programming. *Diabetologia* **55,** 1597-1606.

Taniguchi C, Emanuelli B & Kahn C. (2006). Critical nodes in signalling pathways: insights into insulin action. *Nature Reviews Molecular Cell Biology* **7,** 85-96.

Teruel T, Valverde AM, Benito M & Lorenzo M. (1996). Insulin-like growth factor I and insulin induce adipogenic-related gene expression in fetal brown adipocyte primary cultures. *Biochemical Journal* **319,** 627-632.

Tiwari S, Nordquist L, Madala Halagappa VK & Ecelbarger CA. (2007). Trafficking of ENaC subunits in response to acute insulin in mouse kidney. *American Journal of Physiology* **293,** F178-F185.

Tontonoz P, Hu E, Graves RA, Budavari AI & Spiegelman BM. (1994). mPPAR gamma 2: tissue-specific regulator of an adipocyte enhancer. *Genes and Development* **8,** 1224-1234.

Trajkovic M, Visser T, Mittag J, Horn S, Lukas J, Darras V, Raivich G, Bauer K & Heuer H. (2007). Abnormal thyroid hormone metabolism in mice lacking the monocarboxylate transporter 8. *Journal of Clinical Investigation* **117,** 627-635.

Tsuchiya A, Kanno T & Nishizaki T. (2014). PI3 kinase directly phosphorylates Akt1/2 at Ser473/474 in the insulin signal transduction pathway. *Journal of Endocrinology* **220,** 49-59.

Tuttle RL, Gill NS, Pugh W, Lee JP, Koeberlein B, Furth EE, Polonsky KS, Naji A & Birnbaum MJ. (2001). Regulation of pancreatic beta-cell growth and survival by the serine/threonine protein kinase Akt1/PKBalpha. *Nature Medicine* **7,** 1133-1137.

Valtat B, Dupuis C, Zenaty D, Singh-Estivalet A, Tronche F, Breant B & Blondeau B. (2011). Genetic evidence of the programming of beta cell mass and function by glucocorticoids in mice. *Diabetologia* **54,** 350-359.

van Assche FA & Aerts L. (1979). The fetal endocrine pancreas. *Contributions to Gynecology and Obstetrics* **5,** 44-57.

van der Meulen T & Huising MO. (2015). Role of transcription factors in the transdifferentiation of pancreatic islet cells. *Journal of Molecular Endocrinology* **54,** R103-R117.

van Tuyl M, Blommaart PE, de Boer PA, Wert SE, Ruijter JM, Islam S, Schnitzer J, Ellison AR, Tibboel D, Moorman AF & Lamers WH. (2004). Prenatal exposure to thyroid hormone is necessary for normal postnatal development of murine heart and lungs. *Developmental Biology* **272,** 104-117.

Vandesompele J, De Preter K, Pattyn F, Poppe B, Van Roy N, De Paepe A & Speleman F. (2002). Accurate normalization of real-time quantitative RT-PCR data by geometric averaging of multiple internal control genes. *Genome Biology* **3,** 0034.0031-0034.0012.

Vehaskari VM, Aviles DH & Manning J. (2001). Prenatal programming of adult hypertension in the rat. *Kidney International* **59,** 238-245.

Verga Falzacappa C, Mangialardo C, Raffa S, Mancuso A, Piergrossi P, Moriggi G, Piro S, Stigliano A, Torrisi MR, Brunetti E, Toscano V & Misiti S. (2010). The thyroid hormone T3 improves function and survival of rat pancreatic islets during in vitro culture. *Islets* **2,** 96-103.

Verga Falzacappa C, Patriarca V, Bucci B, Mangialardo C, Michienzi S, Moriggi G, Stigliano A, Brunetti E, Toscano V & Misiti S. (2009). The TRbeta1 is essential in mediating T3 action on Akt pathway in human pancreatic insulinoma cells. *Journal of Cellular Biochemistry* **106,** 835-848.

Verga Falzacappa C, Petrucci E, Patriarca V, Michienzi S, Stigliano A, Brunetti E, Toscano V & Misiti S. (2007). Thyroid hormone receptor TRβ1 mediates Akt activation by T3 in pancreatic β-cells. *Journal of Molecular Endocrinology* **38,** 221-233.

Vidal-Puig A, Jimenez-Liñan M, Lowell BB, Hamann A, Hu E, Spiegelman B, Flier JS & Moller DE. (1996). Regulation of PPAR gamma gene expression by nutrition and obesity in rodents. *Journal of Clinical Investigation* **97,** 2553-2561.

Vidal-Puig AJ, Considine RV, Jimenez-Linan M, Werman A, Pories WJ, Caro JF & Flier JS. (1997). Peroxisome proliferator-activated receptor gene expression in human tissues. Effects of obesity, weight loss, and regulation by insulin and glucocorticoids. *Journal of Clinical Investigation* **99,** 2416-2422.

Visser TJ. (1994). Role of sulfation in thyroid hormone metabolism. *Chemico-Biological Interactions* **92,** 293-303.

Visser TJ, van Buuren JCJ, Rutgers M, Eelkman Rooda SJ & de Herder WW. (1990). The role of sulfation in thyroid hormone metabolism. *Trends in Endocrinology & Metabolism*, 211-218.

Visser W, Friesema E, Jansen J & Visser T. (2008). Thyroid hormone transport in and out of cells. *Trends in Endocrinology and Metabolism* **19,** 50-56.

Vulsma T, Gons MH & de Vijlder JJ. (1989). Maternal-fetal transfer of thyroxine in congenital hypothyroidism due to a total organification defect or thyroid agenesis. *New England Journal of Medicine* **321,** 13-16.

Wahrenberg H, Engfeldt P, Arner P, Wennlund A & Ostman J. (1986). Adrenergic regulation of lipolysis in human adipocytes: findings in hyper- and hypothyroidism. *Journal of Clinical Endocrinology and Metabolism* **63,** 631-638.

Walker DW & Schuijers JA. (1989). Effect of thyroidectomy on cardiovascular responses to hypoxia and tyramine infusion in fetal sheep. *Journal of Develpmental Physiology* **12,** 337-345.

Wallace JM, Regnault TRH, Limesand SW, Hay WW & Anthony RV. (2005). Investigating the causes of low birth weight in contrasting ovine paradigms. *Journal of Physiology* **565,** 19-26.

Wang J, Barbry P, Maiyar AC, Rozansky DJ, Bhargava A, Leong M, Firestone GL & Pearce D. (2001). SGK integrates insulin and mineralocorticoid regulation of epithelial sodium transport. *American Journal of Physiology* **280,** F303-F313.

Wang M, Wang Y, Weil B, Abarbanell A, Herrmann J, Tan J, Kelly M & Meldrum DR. (2009). Estrogen receptor β mediates increased activation of PI3K/Akt signaling and improved myocardial function in female hearts following acute ischemia. *American Journal of Physiology* **296,** R972-R978.

Wang X, Zielinski MC, Misawa R, Wen P, Wang TY, Wang CZ, Witkowski P & Hara M. (2013). Quantitative analysis of pancreatic polypeptide cell distribution in the human pancreas. *PLoS One* **8,** e55501.

Watanabe S, Matsushita K, McCray PB & Stokes JB. (1999). Developmental expression of the epithelial Na^+ channel in kidney and uroepithelia. *American Journal of Physiology* **276,** F304-F314.

Wilcox C, Terry N, Walp E, Lee R & May C. (2013). Pancreatic α-cell specific deletion of mouse Arx leads to α-cell identity loss. *PLoS One* **8,** e66214.

Wintour EM, Moritz KM, Johnson K, Ricardo S, Samuel CS & Dodic M. (2003). Reduced nephron number in adult sheep, hypertensive as a result of prenatal glucocorticoid treatment. *Journal of Physiology* **549,** 929-935.

Withers D, Gutierrez J, Towery H, Burks D, Ren J, Previs S, Zhang Y, Bernal D, Pons S, Shulman G, Bonner-Weir S & White M. (1998). Disruption of IRS-2 causes type 2 diabetes in mice. *Nature* **391,** 900-904.

Withers DJ, Burks DJ, Towery HH, Altamuro SL, Flint CL & White MF. (1999). Irs-2 coordinates Igf-1 receptor-mediated beta-cell development and peripheral insulin signalling. *Nature Genetics* **23,** 32-40.

Wu S, Polk D, Wong S, Reviczky A, Vu R & Fisher DA. (1992). Thyroxine sulfate is a major thyroid hormone metabolite and a potential intermediate in the monodeiodination pathways in fetal sheep. *Endocrinology* **131,** 1751-1756.

Wu SY, Polk DH, Huang WS, Reviczky A, Wang K & Fisher DA. (1993). Sulfate conjugates of iodothyronines in developing sheep: effect of fetal hypothyroidism. *American Journal of Physiology* **265,** E115-120.

Wu Z, Rosen ED, Brun R, Hauser S, Adelmant G, Troy AE, McKeon C, Darlington GJ & Spiegelman BM. (1999). Cross-regulation of C/EBP alpha and PPAR gamma controls the transcriptional pathway of adipogenesis and insulin sensitivity. *Molecular Cell* **3,** 151-158.

Ying H, Araki O, Furuya F, Kato Y & Cheng SY. (2007). Impaired adipogenesis caused by a mutated thyroid hormone alpha1 receptor. *Molecular and Cellular Biology* **27,** 2359-2371.

Yu F, Gothe S, Wikstrom L, Forrest D, Vennstrom B & Larsson L. (2000). Effects of thyroid hormone receptor gene disruption on myosin isoform expression in mouse skeletal muscles. *American Journal of Physiology* **278,** R1545-1554.

Yuen B, Owens P, Muhlhausler B, Roberts C, Symonds M, Keisler D, McFarlane J, Kauter K, Evens Y & McMillen I. (2003). Leptin alters the structural and functional characteristics of adipose tissue before birth. *FASEB* **17,** 1102-1104.

Zhang J & Lazar M. (2000). The mechanism of action of thyroid hormones. *Annual Review of Physiology* **62,** 439-466.

Zimanyi MA, Bertram JF & Black JM. (2000). Nephron number in the offsrpring of rats fed a low protein diet during pregnancy. *Image Analysis and Stereology* **19,** 219-222.